The Hong Kong Polytechnic University
Department of Health Technology and Informatics

DNA repair pathways: effects of SNPs on their functions and their role in drug resistance

Sau Yin, LEE

A thesis submitted in partial fulfilment of the requirements for the degree of Doctor of Philosophy

February 2010

CERTIFICATE OF ORIGINALITY

I hereby declare that this thesis is my own work and that, to the best of my knowledge and belief, it reproduces no materials previously published or written, nor material that has been accepted for the award of any other degree or diploma, except where due acknowledgment has been made in the text.

_____ (Signed)

Sau Yin, LEE (Name of student)

Abstract

DNA repair is important in maintaining genome integrity. Failure of DNA repair systems may lead to genomic instability and hence carcinogenesis. This study aimed to investigate (1) how the genetic variations affect the functions of DNA repair proteins; and (2) how DNA repair mechanisms are involved in cancer drug resistance.

The human DNA repair gene human nth endonuclease III-like 1 (*E. coli*) (*NTHL1*) is involved in base excision repair, and was chosen for investigating the effect of sequence variations on DNA repair activity. Humans and yeast have similar DNA repair mechanisms, and the *NTG2* gene is the yeast homologue of *NTHL1*. Therefore, *NTG2*-knockout *Saccharomyces cerevisiae (S. cerevisiae)* was used as the study model for examining the influence of sequence variations on NTHL1. Yeast expression vectors were constructed to express the wildtype and two mutant human NTHL1 proteins, and the mutant protein carried a frameshift mutation at 105 amino acid position (FS105) or a missense mutation at 239 amino acid position (D239Y). Yeast cells expressing the wildtype or mutant human NTHL1 protein did not demonstrate increased cytotoxicity to DNA damaging reagents. However, treatment with methyl methanesulphonate arrested the cell cycle at S phase in yeast cells carrying no recombinant plasmid or plasmid with the frameshift construct, but not in yeast cells expressing the wildtype NTHL1 protein or the D239Y mutant protein. This indicates that functional NTHL1 protein can prevent S-phase cell cycle arrest after genotoxic treatment. This finding may aid in the development of a simple protein functional assay using the *S. cerevisiae* model to detect the effects of other SNPs' on proteins, such as apoptotic proteins that are drug

targets.

In another part of the study, the involvement of DNA repair pathways in drug resistance was investigated. The comet assay was used to evaluate the relationship between DNA damage, DNA repair and Photofrin-mediated photodynamic therapy (Ph-PDT) in U87 glioma cells. Results showed that Ph-PDT prominently induced DNA damage, followed by repair being observed 24 hours after treatment with Ph-PDT in glioma cells. Quantitative reverse transcription-polymerase chain reaction, Western blotting and gene knockdown assays demonstrated that alkB, alkylation repair homolog 2 (*E. coli*) or ALKBH2 of the DNA damage reversal pathway was significantly increased at both mRNA and protein levels from 30 minutes to 48 hours post-treatment with Ph-PDT in relatively resistant glioma cells. Conversely, down-regulating ALKBH2 expression enhances Ph-PDT efficiency. Chromatin immunoprecipitation assay confirmed that TP53 may play a role in promoting the transcription of ALKBH2 after Ph-PDT. TP53 and ALKBH2-related proteins were further investigated to explore their involvement in regulating ALKBH2 expression after Ph-PDT. Quantitative RT-PCR and Western blotting showed that the expression of *c-Jun N-terminal kinases* (JNKs) and nucleophosmin (nucleolar phosphoprotein B23, numatrin) or NPM1 increased rapidly after Ph-PDT. Gene knockdown and mRNA stability assays demonstrated that the increase in NPM1 was also involved in Ph-PDT resistance by affecting TP53 mRNA stability and thus ALKBH2 expression. The identification of ALKBH2 involvement via the regulation of TP53 mRNA stability by NPM1 contributing to Ph-PDT resistance may provide insight into the development of more effective therapies for glioblastoma.

Publications

Lee, S.Y., Luk, S.K., Chuang, C.P., Yip, S.P., To, S.S.T. & Yung, Y.M.B. (2010) TP53 regulates human AlkB homologue 2 expression in glioma resistance to Photofrin-mediated photodynamic therapy. (*Br J Cancer*., **34**: 362-9)

Lee, S.Y., Yip, S.P. & To, S.S.T. Genetic studies of SNPs' effects on human DNA repair proteins using yeast model system. (in preparation)

Conference abstracts:

Oral presentations:

Lee, S.Y., Yip, S.P. & To, S.S.T. (2008) DNA repair proteins associated with Photofrin resistance in U87 glioblastoma cell line. In "*The 8th International Conference of Anticancer Research*". (Anticancer res, **28**: 3373, Kos, Greece).

Lee, S.Y., Yip, S.P., Yung, Y.M.B. & To, S.S.T. (2010) The association of NPM1/B23, TP53 and ALKBH2 in Photofrin-mediated PDT resistance. In "HTI Postgraduate symposium 2010". (Hong Kong).

Acknowledgements

I would like to express my sincere gratitude to my supervisor, Dr. Tony TO, and co-supervisor, Professor SP YIP, for their continuous guidance and invaluable advice throughout the study.

I would like to extend my gratitude to Professor Benjamin YUNG for his enthusiastic support and the insightful discussion.

I would also like to express thanks to Prof. Iris F.F.BENZIE for the acadamic support in comet assay and Dr. Ming Cheung CHOW for providing the yeast expression vector and acadamic support in the yeast study.

Grateful thanks also go to my beloved family members, especially my mother, for their love, emotional support and encouragement throughout my PhD life, my colleagues in the Department of Health Technology and Informatics and my dearest friends, especially Siu Wai Choi, Cadmon Lim, Hi Mui Tang, Connie Yuen, Nicola Cheng, Wing Tang, Ada Tse, Emily Mak, Ellie Chu, Peter Ng and Ying Wong for their concern when the going got tough.

Table of contents

List of Figures

List of Tables

Abbreviations

$2^{-\Delta\Delta Ct}$	Comparative threshold method
a.a.	Amino acid
ACT1	Actin
ACTB	Beta-actin
ALKBH2	AlkB, alkylation repair homolog 2 (*E. coli*)
ALKBH3	AlkB, alkylation repair homolog 3 (*E. coli*)
AP	Apurinic/apyrimidinic or abasic
APEX1	APEX nuclease (multifunctional DNA repair enzyme) 1
BER	Base excision repair
$CaCl_2$	Calcium chloride
cDNA	Complementary DNA
ChIP	Chromatin immunoprecipitation
CNT	No treatment controls
Ct	Thresholds
D	Aspartic acid
D239Y	A missense polymorphism at 239 amino acid position of NTHL1 protein
DC	Dark controls
DNA	Deoxyribonucleic acid
dNTPs	Deoxynucleoside triphosphates
DR	Direct reversal repair
E. coli	*Escherichia coli*
EDTA	Ethylenediaminetetraacetic acid
ERCC5	Excision repair cross-complementing rodent repair deficiency protein complex, including complementation group 5
Fapy	Formamidopyrimidine
FS105	A frameshift polymorphism of lysine at 105 amino acid position of NTHL1 protein
GAPDH	Glyceraldehyde-3-phosphate dehydrogenase
H. sapiens	Homo sapiens
H_2O_2	Hydrogen peroxide
HCl	Hydrochloric acid
HPD	Haematoporphyrin derivative
JNKs	c-Jun NH2-terminal kinases
LC	Light controls
LD	Lethal dose
LD 10	Lethal dose 10 at which 10% of cell die
LD 40	Lethal dose 40 at which 40% of cell die
LiOAc	Lithium acetate

Lipofectamine	Cells with Lipofectamine transfecting reagent
MEMα	Minimum essential medium alpha
MMS	Methyl methanesulphonate
mRNA	Messenger RNA
NaCl	Sodium Chloride
NaOH	Sodium hydroxide
Neg CNT	Cells with negative control RNA as a mock control
NF-κB	Nuclear factor of kappa light polypeptide gene enhancer in B-cells 1
NPM1	Nucleophosmin (nucleolar phosphoprotein B23, numatrin)
NTHL1	Human nth endonuclease III-like 1 (*E. coli*)
PBS	Phosphate buffered saline
PCNA	Proliferating cell nuclear antigen
PCR	Polymerase chain reaction
PDT	Photodynamic therapy
PEG	Polyethylene glycol
Ph-PDT	Photofrin-mediated Photodynamic therapy
p-TP53	phosphorylated TP53
RAD52	RAD52 homolog (*S. cerevisiae*)
REV1	REV1 homolog (*S. cerevisiae*)
RNA	Ribonucleic acid
RT	Reverse transcription
S. cerevisiae	*Saccharomyces cerevisiae*
siALKBH2	Cells with siRNA for ALKBH2 knockdown
siNPM1	Cells with RNAi plasmid for NPM1 knockdown
siRNA	Small interfering RNA
SNPs	Single nucleotide polymorphisms
SOD2	Superoxide dismutase 2, mitochondrial
Sp1	Sp1 transcription factor
TBST	Tris buffered saline buffer with Tween 20
TP53	Tumour protein p53
Tris	Tris(hydroxymethyl)aminomethane
WT	Wild-type
XRCC1	X-ray repair complementing defective repair in Chinese hamster cells 1
Y	Tyrosine
ΔCt	Differences in thresholds

Unit

n	Nano
μ	Micro
m	Milli

g	Gravity
rpm	Revolutions per minute
bp	Base pair
kb	Kilo base pair
kDa	Kilo dalton
g	Gram
L	Litre
M	Molar
mm	Millimetre
cm	Centimetre
% v/v	Volume-volume percentage
% w/v	Mass-volume percentage
°C	Degree Celsius
J	Joule
W	Watt

Chapter 1

Introduction

1.1 The deoxyribonucleic acid (DNA) damage response

Many external and internal DNA damaging agents may threaten the stability of the cell genome.[1-3] Hydrolytic reactions, non-enzymatic methylations, reactive oxygen species, ionising radiation, ultraviolet light and various chemical reagents produce DNA aberrations and damage, which are potentially cytotoxic.[1-3] In humans, highly conserved DNA damage sensor mechanisms deal with such DNA damage.[2,3]

An integrated signalling network, known as the DNA damage response may cause the damaged cells to initiate different cellular processes (Fig. 1.1).[2] These processes mainly result in (1) apoptosis, (2) transcriptional responses, (3) checkpoint activation, (4) tolerance and/or (5) DNA repair.[2,4] By activating the DNA damage response, DNA lesions are detected and the fate of the cell is determined: the cell survives or undergoes programmed cell death.[2]

The DNA damage response activates and controls diverse biological downstream effects. Therefore, failure in the DNA damage response increases the risk of several disease such as cancer.[5] DNA repair being an important component of this response and thus exploration of DNA repair pathways can further knowledge in how the cell maintains genome integrity, prevent cancers caused by DNA repair malfunction, and how to enhance the therapeutic responses of the cancer treatments that function by generating DNA damage.

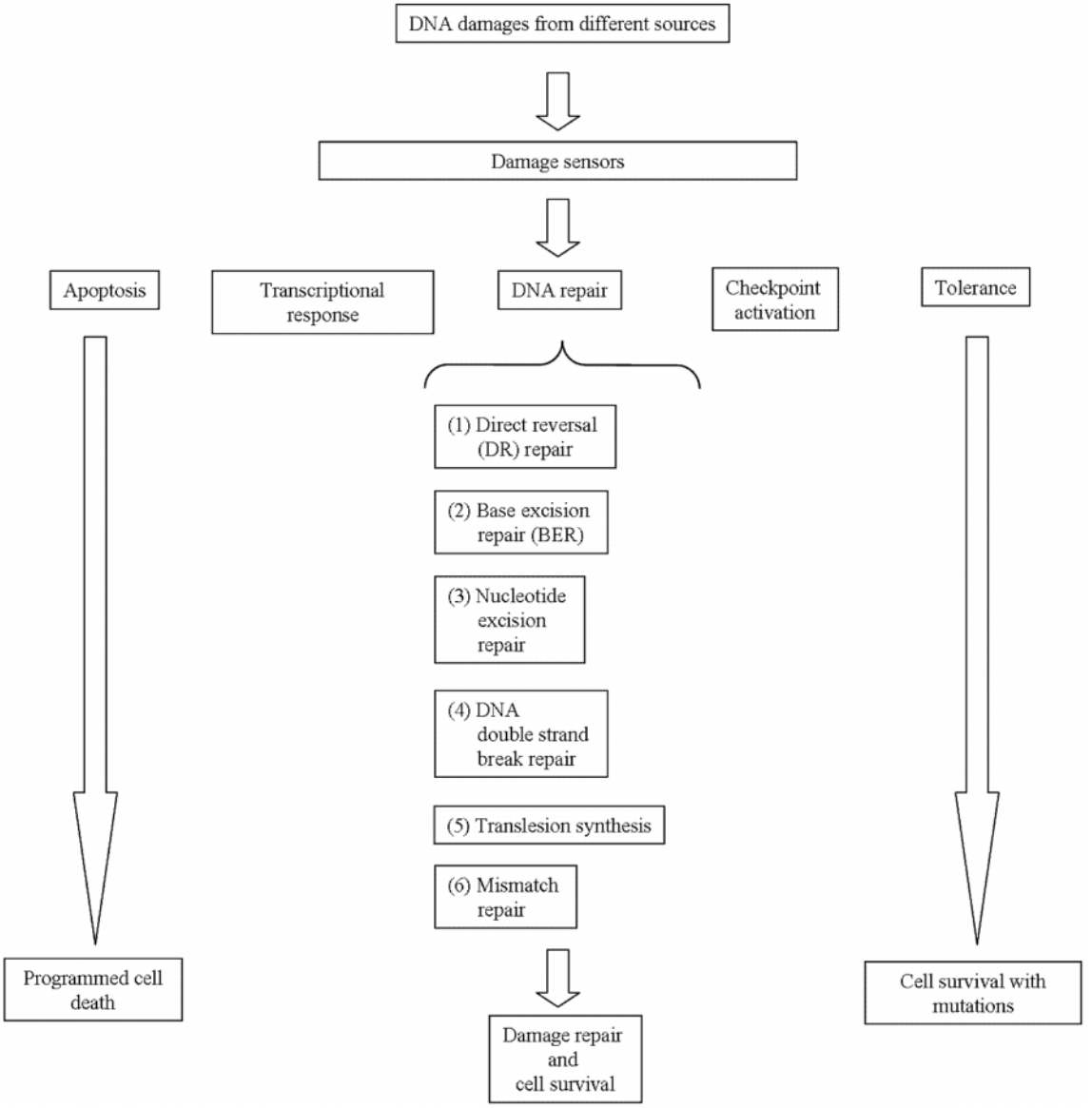

Fig. 1.1 DNA damage sensor mechanisms. (Adapted and modified from reference 2)

1.2 DNA repair pathways

A comprehensive DNA repair system is necessary for repairing DNA damage caused by different endogenous and exogenous genotoxins.[2,6,7] Ineffective or incorrect repair of these deleterious lesions may lead to serious consequences including impaired cellular function and cancer. In a cell, DNA and diverse types of DNA threats are present in both mitochondria and the nucleus. In order to maintain DNA integrity, different combinations of DNA repair pathways are adapted and used for DNA damage repair.

1.2.1 Nuclear DNA repair pathways

Various forms of DNA damage may be generated in nuclear DNA. They can be classified into four major types: base modifications, strand breaks, crosslinks and mismatches (Fig. 1.2).[8] Six major nuclear DNA repair pathways are directed to specific types of DNA damage:[6,7]

(1) Direct reversal (DR) repair for repairing bases modified with chemical groups;

(2) Base excision repair (BER) repairs DNA damage formed by alkylation, oxidation and deamination of bases;

(3) Nucleotide excision repair handles bulky DNA lesions;

(4) Double strand break repair deals with double strand breaks;

(5) Translesion synthesis is a system for tolerance of DNA damage;

(6) Mismatch repair pathway removes mismatches and small insertion/deletion loops.[1,2,6,7,9-15]

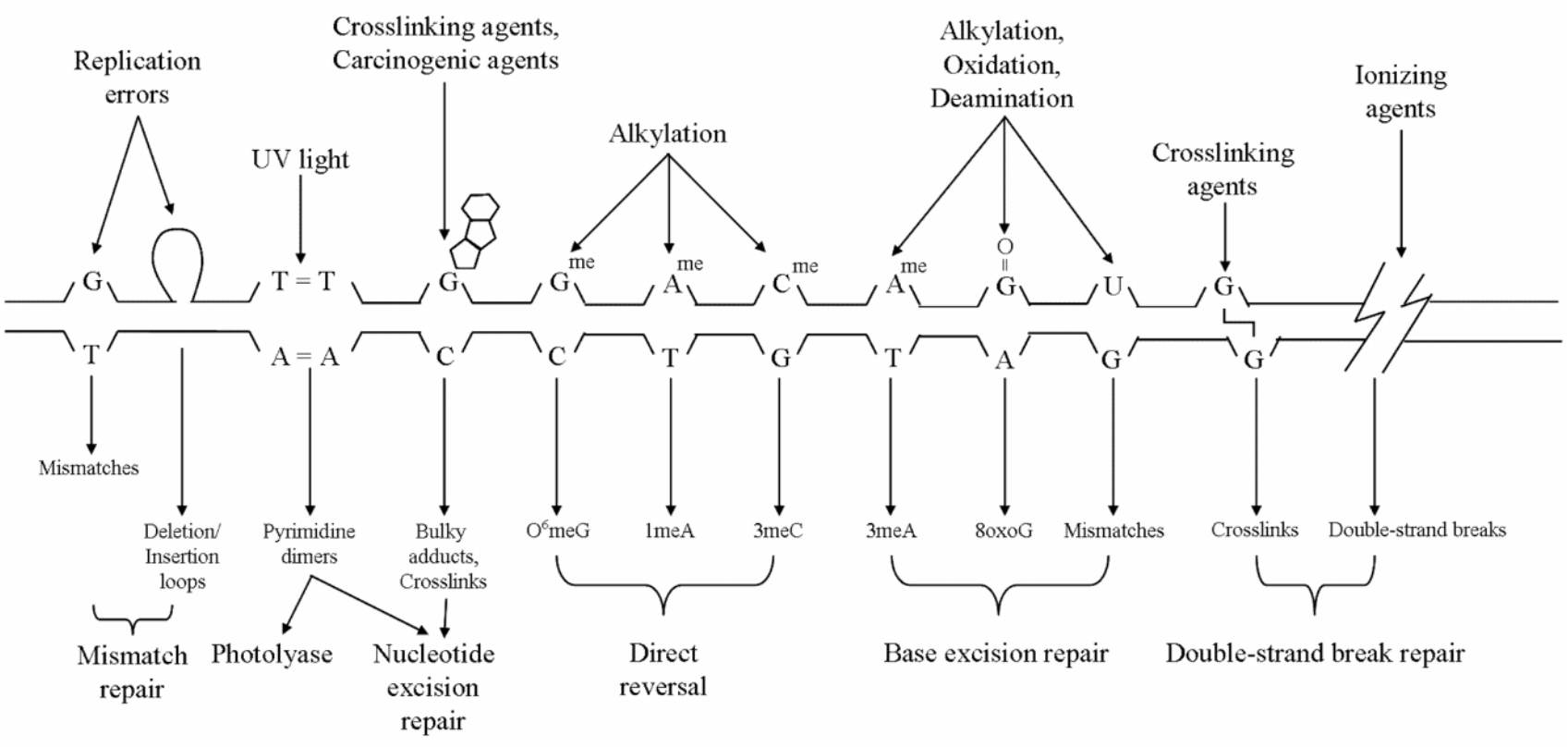

Fig. 1.2 Different types of DNA damage and their corresponding repair pathway. (Adapted and modified from reference 8)

1.2.1.1 Direct reversal pathway

In DR pathways, the modified bases can be eliminated by chemically reversing it without using a complementary DNA strand as a template and without excising the modified base, i.e. no breakage of the phosphodiester backbone by any glycosylase, lyase and exonuclease. All known DR repair proteins, except photolyase for repairing the thymine dimer, are involved in the removal of alkylated DNA damage.[16] Depending on the type of base modification, two reactions by 6-O-methylguanine-DNA methyltransferase and DNA dioxygenase are engaged in this pathway.[12]

1.2.1.1.1 O-6-methylguanine-DNA methyltransferase-mediated DR pathway

O-6-methylguanine-DNA methyltransferase is mainly responsible for the alkylation of guanine bases. This enzyme flips the damaged base into the active site and binds the alkyl groups of the base to the cysteine residue in itself. The binding of an alkyl group is irreversible and hence results in the inactivation and degradation of the O-6-methylguanine-DNA methyltransferase (Fig. 1.3).[17] Therefore, the newly synthesised O-6-methylguanine-DNA methyltransferase is essential for further repair activity.[7]

1.2.1.1.2 DNA dioxygenase-mediated DR pathway

Two nuclear DNA dioxygenases called AlkB, alkylation repair homolog 2 (*E. coli*) (ALKBH2) and AlkB, alkylation repair homolog 3 (*E. coli*) (ALKBH3) have been identified to be involved in DR pathway. These enzymes belong to the alpha ketoglutarate dioxygenase family. ALKBH2 acts on double-stranded DNA, especially the DNA located close to replication forks. Unlike ALKBH2, ALKBH3

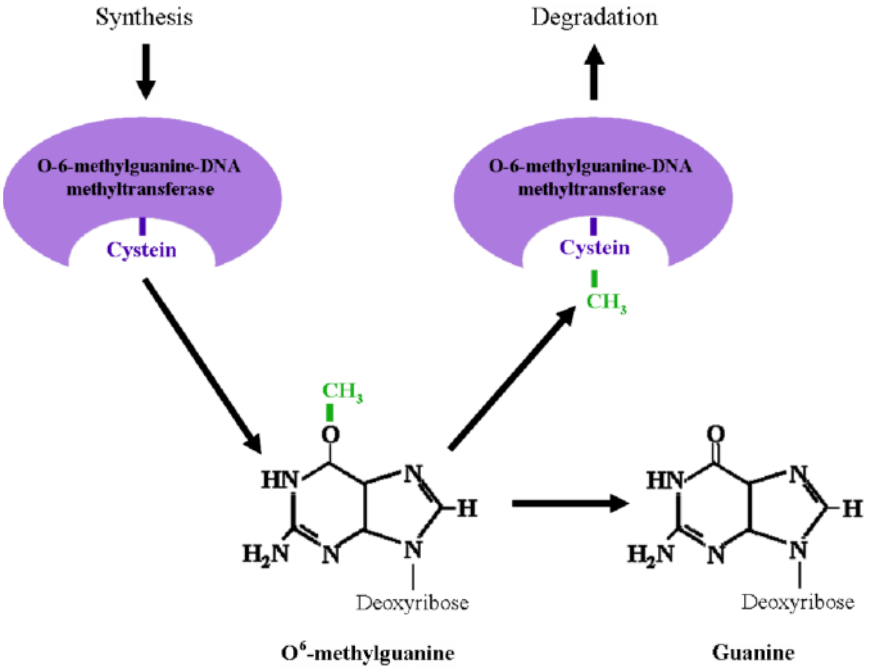

Fig. 1.3 O-6-methylguanine-DNA methyltransferase-mediated DR pathway.
(Adapted and modified from http://www.mgmt-agt.net/index.htm)

repairs nuclear single-stranded DNA and ribonucleic acid (RNA) of actively transcribing genes.[18] The preferential DNA substrates for these dioxygenases are DNA alkylation damage, particularly 1-methyladenine and 3-methylcytosine.[19]

These enzymes oxidise alkyl groups of the modified bases in a reaction dependent on oxygen, ketoglutarate and iron. The reaction finally releases formaldehyde from methylated lesions or acetaldehyde from ethylated lesions. Succinate and carbon dioxide are also produced during the reaction. As the DR pathway removes the reactive alkyl groups from modified bases without any nuclease activity, the damaged DNA can be repaired correctly (Fig. 1.4).[20]

1.2.1.2 Base excision repair pathway

The BER pathway fixes small base lesions, the most frequently occurring type of lesion in the genome, which can arise from any type of oxidation, alkylation or deamination. BER is important as front-line protection and is highly conserved among species, as incorrect repair of the small base lesions leads to mis-incorporation of DNA bases by DNA polymerases which will result in mutations. The BER pathway requires four types of enzymes for proper function. These are DNA glycosylases, apurinic/apyrimidinic or abasic (AP) endonucleases/lyases, DNA polymerases and DNA ligases.

In addition, there are various steps involved in BER and the enzymes given here work in an integrated manner (Fig. 1.5):[21]

(1) Recognition of damage by a DNA glycosylase.

(2) An AP site is generated by a DNA glycosylase.

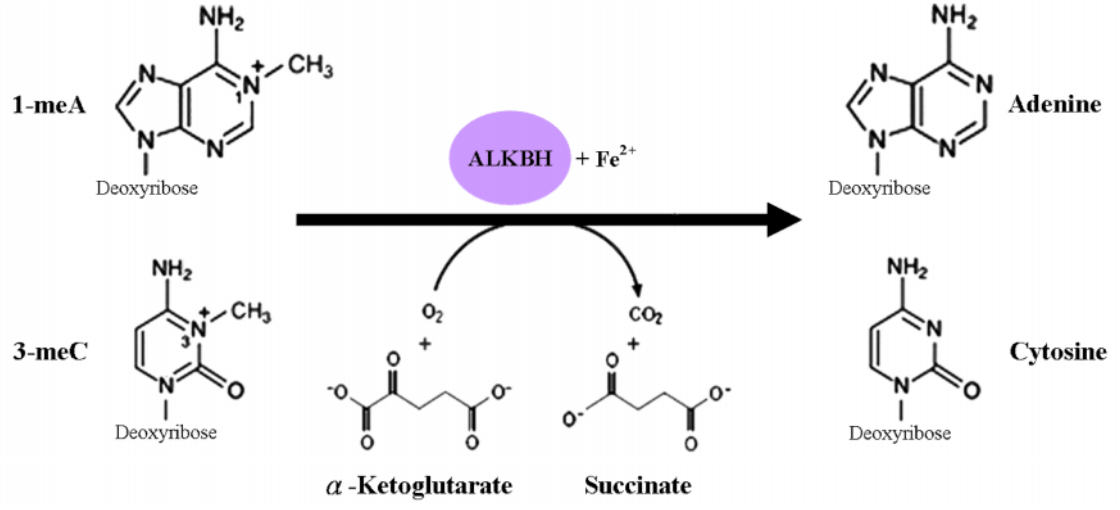

Fig. 1.4 DNA dioxygenase-mediated DR pathway. (Adapted and modified from http://www.reactome.org and reference 20)

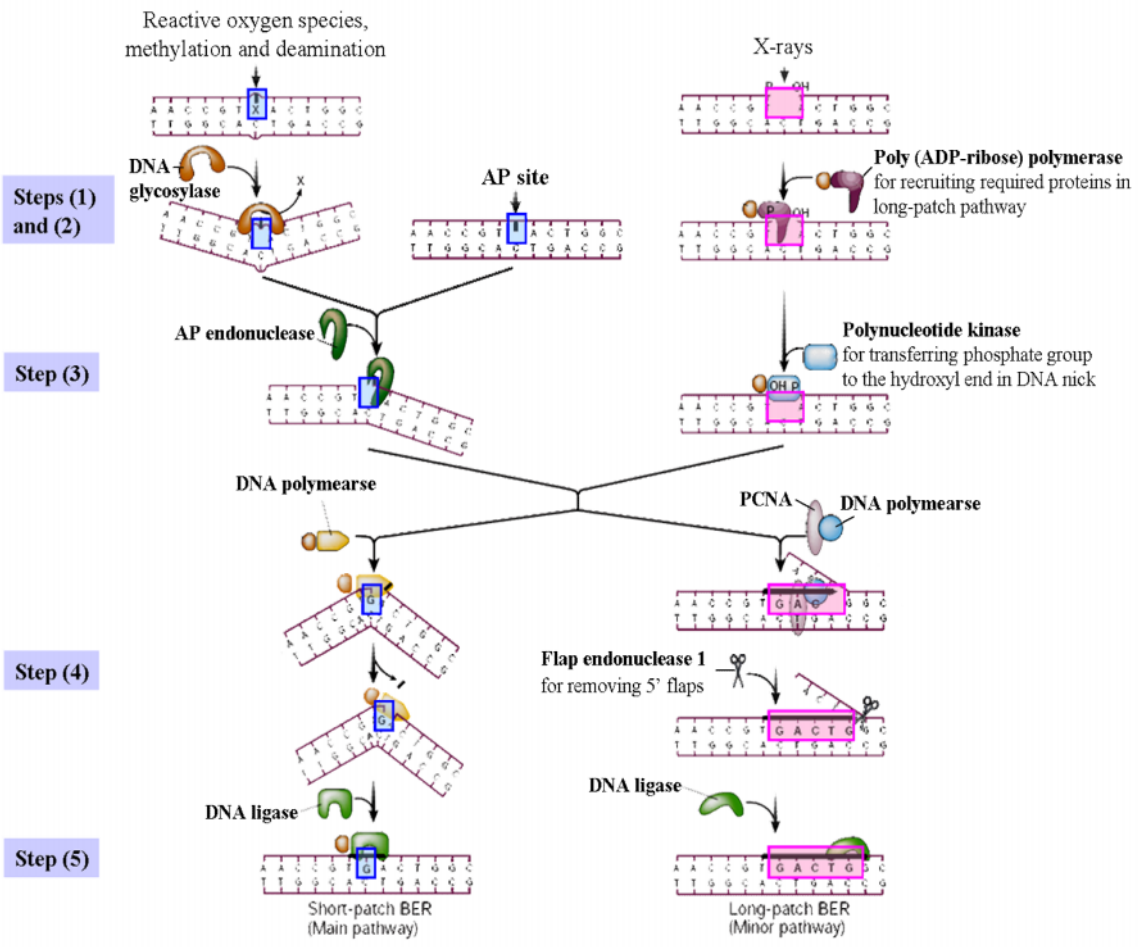

Fig. 1.5 Base excision repair pathway. (Adapted and modified from reference 21)

(3) An AP site is recognised by an AP endonuclease and the phosphodiester bond at the 5’ end of the AP site is cleaved.

(4) The deoxyribose-phosphate group at the 5’ end of the strand break is excised by a phosphodiesterase.

(5) A one-residue gap is filled by a DNA polymerase.

(6) A nick is sealed by a DNA ligase.[6,14,22,23]

In human cells, this multi-step BER process, named “short patch BER”, is the major pathway responsible for repairing base and sugar damage.[11,24,25] In contrast though, a minor “long patch BER” pathway for repairing single strand breaks is present in all organisms.[22,24,25] Long patch BER pathway leaves a fragmented sugar derivative at the 3’ end of the strand break. This derivative is a polymerase-blocking lesion and is removed by phosphodiesterases. The 5’ end of the strand break requires no additional modification. The oligonucleotide containing the 5’-incised AP site is then excised by interaction with a complex, which is formed by the combination of proliferating cell nuclear antigen (PCNA), DNA polymerase beta and DNA polymerase delta/epsilon, and flap endonuclease 1. The nick is finally sealed by DNA ligase.[6,22,24,25] The main differences between short patch and long patch BER are shown in Table 1.1.[24]

1.2.1.3 Nucleotide excision repair pathway

Nucleotide excision repair pathway repairs bulky helix-distorting lesions, e.g. ultraviolet lesions, intrastrand crosslinks and large chemically modified DNA adducts. Large multiple protein complexes are required for nucleotide excision

Table 1.1 Comparison between short patch BER and long patch BER.
(Adapted and modified from reference 24)

Properties	Short patch BER	Long patch BER
(1) Gap formation	A gap with a single nucleotide	A gap with several nucleotides
(2) Types of DNA damage	Base damage excised by bifunctional and monofunctional DNA glycosylases	Base damage excised by only monofunctional DNA glycosylase
(3) Level of cellular DNA polymerase	High level of DNA polymerase beta	Low level of DNA polymerase beta
(4) Level of cell-cycle regulated factor – PCNA	Low level of PCNA	High level of PCNA

repair activity. The nucleotide excision repair pathway initially starts from damage recognition followed by cleavage of the DNA strand with the lesions, excision of the lesions, gap filling and ligation.[26] Global genomic repair and transcription-coupled nucleotide excision repair are two distinct pathways involved in nucleotide excision repair. These pathways share most of the DNA repair proteins but differ in how repair is initiated.[27]

1.2.1.3.1 Global genomic repair pathway

Global genomic repair is transcription-independent and repairs lesions from non-transcribed regions of the genome. Many different kinds of DNA repair proteins are involved in this repair system. The basic steps of global genomic repair are (Fig. 1.6A):[12,28]

(1) Damage recognition by several protein complexes consisting of
   (a) xeroderma pigmentosum, complementation group C with RAD23 homolog B (*S. cerevisiae*) complex,
   (b) replication protein A1 with xeroderma pigmentosum, complementation group A complex and
   (c) damage-specific DNA binding protein 1 with damage-specific DNA binding protein 2 complex.
(2) DNA unwinding by general transcription factor IIH.
(3) Lesion excision by excision repair cross-complementing rodent repair deficiency protein complex, including complementation group 5 (ERCC5), 4 and 1.
(4) Resynthesis of the DNA strand by DNA polymerase delta and epsilon.
(5) Ligation of the newly synthesised DNA strand to the original strand by DNA ligase I.[29]

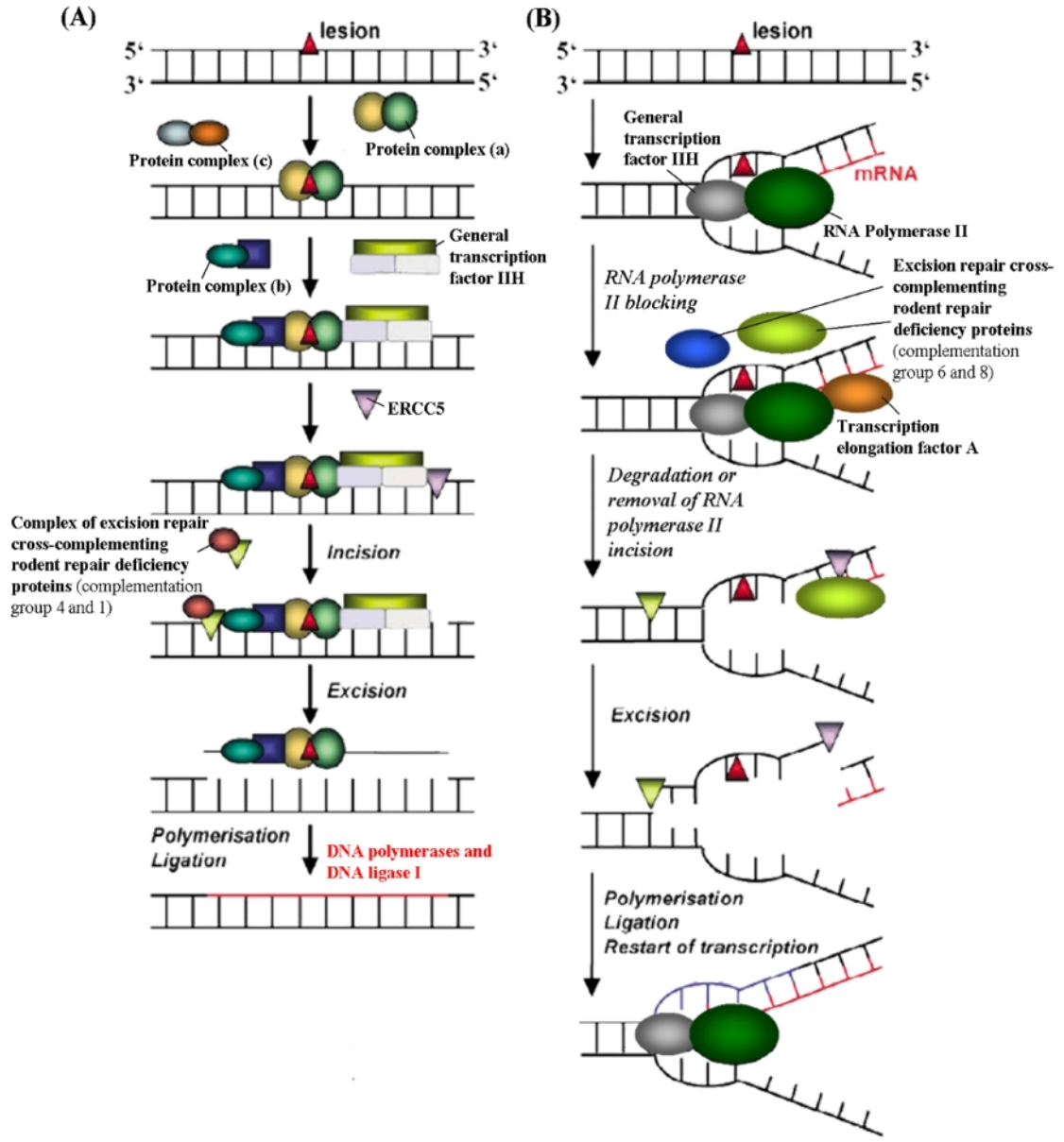

Protein complex (a): xeroderma pigmentosum, complementation group C with RAD23 homolog B (*S. cerevisiae*) complex;

Protein complex (b): replication protein A1 with xeroderma pigmentosum, complementation group A complex and

Protein complex (c): damage-specific DNA binding protein 1 with damage-specific DNA binding protein 2 complex

Fig. 1.6 **Nucleotide excision repair pathway.** (A) Global genomic repair pathway. (B) Transcription-coupled nucleotide excision repair pathway. (Adapted and modified from reference 12)

1.2.1.3.2 Transcription-coupled nucleotide excision repair pathway

Transcription-coupled nucleotide excision repair acts on DNA damage in the transcription region of active genes triggered by RNA Polymerase II stalling. The two nucleotide excision repair pathways are similar and the difference lies only in the initiation step. Transcription-coupled nucleotide excision repair starts with the assembly of a protein complex which degrades RNA Polymerase II. The protein complex is a combination of excision repair cross-complementing rodent repair deficiency, complementation group 8 and 6. Another difference between the repair pathways is that the DNA damage is verified only by a protein – xeroderma pigmentosum, complementation group A – in transcription-coupled nucleotide excision repair whereas different protein complexes are used to verify the DNA damage in global genomic repair (Fig. 1.6B).[12,30]

1.2.1.4 Double strand break repair pathway

Double strand break repair pathway is used to repair double strand breaks produced from ionising radiation, reactive oxygen species and replication errors. Double strand breaks are especially dangerous to genomic integrity because no complementary DNA template can be used for accurate repair. Therefore, a complicated repair system with two discrete pathways is necessary for handling this type of DNA damage. The associated pathways are non-homologous end-joining pathway and homologous recombination repair pathway.[31]

1.2.1.4.1 Non-homologous end-joining pathway

Non-homologous end-joining pathway is error-prone but predominant in repairing double strand breaks in mammals. Since more than 90% of DNA in

mammalian cells is non-coding, simple non-homologous end-joining is tolerated in cells.[32] This end-joining pathway repairs double strand breaks according to the following steps (Fig. 1.7A):[33]

(1) A heterodimer of two proteins, which are X-ray repair complementing defective repair in Chinese hamster cells 6 and 5, binds to the ends of the double strand breaks.

(2) DNA-dependent protein kinase is a catalytic subunit. It combines with the heterodimer to form the holoenzyme.

(3) Two ends of the break are brought together to form a DNA synapsis.

(4) A complex, which is formed by polynucleotide kinase and Artemis (a nuclease), process the ends to remove DNA.

(5) The recruited proteins and protein complexes for processing of the DNA ends are removed by autophosphorylation of DNA-dependent protein kinase before end-joining.

(6) DNA ends are ligated and the DNA is restored.

1.2.1.4.2 Homologous recombination repair pathway

Compared to the non-homologous end-joining pathway, homologous recombination repair pathway is error-free and more complex. Homologous recombination repair deals with double strand breaks within replicated DNA or those generated at the broken replication forks.[32,34] As the homologous recombination repair process is complicated, a general description is given below (Fig. 1.7B).[33]

(1) The repair pathway is triggered by a MRN complex, consisting of MRE11 meiotic recombination 11 homolog A (*S. cerevisiae*), RAD50 homolog (*S. cerevisiae*) and nibrin.

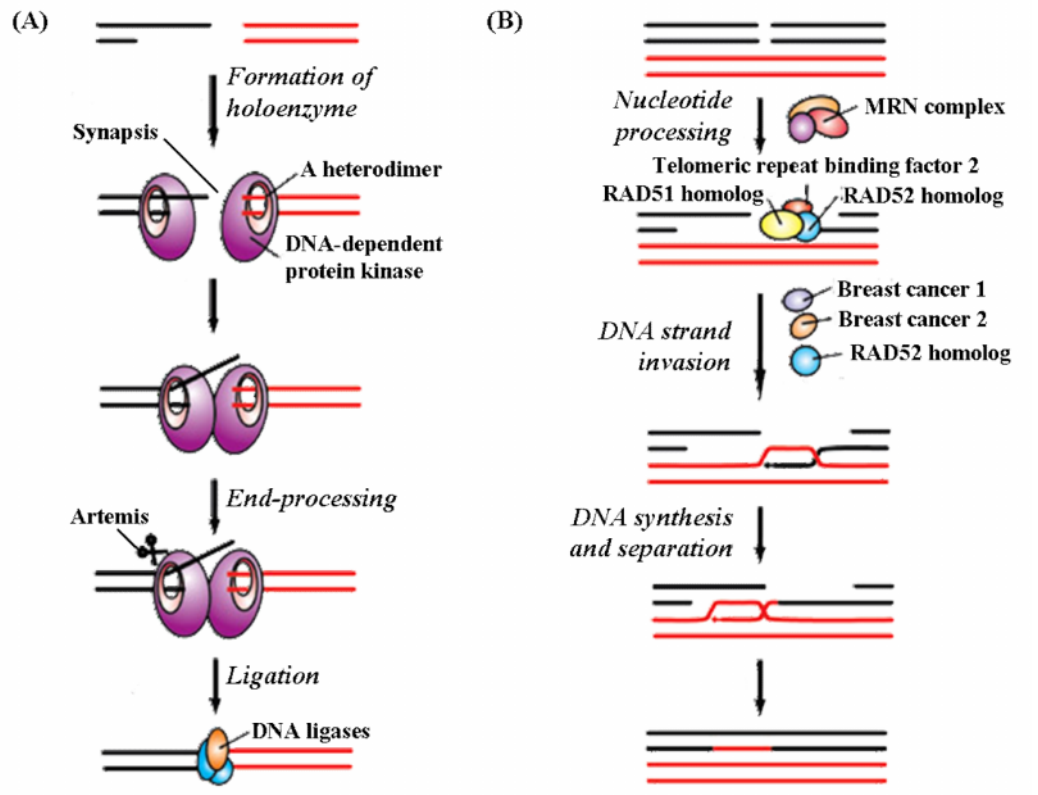

A heterodimer: X-ray repair complementing defective repair in Chinese hamster cells 6 and 5

MRN complex: MRE11 meiotic recombination 11 homolog A (*S. cerevisiae*), RAD50 homolog (*S. cerevisiae*) and nibrin

Fig. 1.7 Double strand break repair pathway. (A) NHEJ pathway. (B) HR pathway. (Adapted and modified from reference 33)

(2) The ends of the break are then processed by meiotic recombination 11 homolog A (*S. cerevisiae*) and telomeric repeat binding factor 2, interacting protein and the homologous DNA template is recognised by RAD52 homolog (*S. cerevisiae*) (RAD52), a mediator protein.

(3) The homologous recombination is initiated by loading the 3' end of the strand with the break and the DNA template into the recombinase machinery, including RAD51 homolog (RecA homolog, *E. coli*) (*S. cerevisiae*), breast cancer 1, early onset and breast cancer 2, early onset proteins.

(4) The joint proteins and the DNA strands are stabilised by "Holliday junctions" or strand exchange. DNA strands are finally synthesised and separated by alpha thalassemia/mental retardation syndrome X-linked protein.

1.2.1.5 Translesion synthesis

Although translesion synthesis is classified as a DNA repair pathway, it is inherently different from the others described so far as it is error-prone and can tolerate a certain degree of DNA damage. This then allows the damaged cell to tolerate, temporarily, the unexcised damaged DNA and thus prevent cell cycle arrest. This pathway involves DNA synthesis from the distorted DNA template using Y-family polymerases that lack 3' to 5' exonuclease activity.[35] The low fidelity and weak processivity of these enzymes allow DNA to be synthesised from DNA strands containing pyrimidine dimers induced by ultraviolet light, oxidative DNA lesions and AP sites. Mutations may be introduced to the newly synthesised DNA, but it can prevent cell death by limiting the formation of double strand breaks when the DNA is seriously damaged.[36] Five important proteins, which are DNA polymerases zeta, eta, lota, kappa and REV1 homolog (*S. cerevisiae*) (REV1), carry out the

processes of translesion synthesis.[37] From the genetic and biochemical data of these proteins, both the polymerase-switching model and the gap-filling model have been used to elucidate the mechanism of translesion synthesis.

The polymerase-switching model is specific for DNA lesion bypass at the primer-template terminus of the replication fork. It allows forward progression of DNA replication. Recruitment of translesion synthesis polymerases to the DNA lesion begins with the PCNA monoubiquitination by ubiquitin-conjugating enzyme E2 (RAD6 homolog)/RAD18 homolog (*S. cerevisiae*) heterodimer and the loading of 9-1-1 complex onto the lesion. An interchange of the replicative polymerase to the translesion synthesis polymerases is then mediated and DNA synthesis continues past the distorting lesion, finally restarting the stalled replication fork (Fig. 1.8A).[37,38]

The polymerase-switching model is used to explain the DNA repair at the replication fork and in the S phase of the cell cycle, whereas the gap-filling model is used to understand the translesion synthesis-assisted DNA lesion bypass in the regions containing ssDNA gap opposite the blocking lesion. The translesion synthesis polymerases, PCNA, 9-1-1 clamp and REV1 are recruited to the region with a gap. These proteins then fill the single-stranded DNA gap with the newly synthesised nucleotide chain with the help of polymerase while the lesion opposite the gap is ignored during this gap-filling. This chain is then ligated onto the original DNA chain. Ultimately, the lesion on double-stranded DNA can be repaired by other DNA repair pathways before the next round of replication (Fig. 1.8B).[37,39]

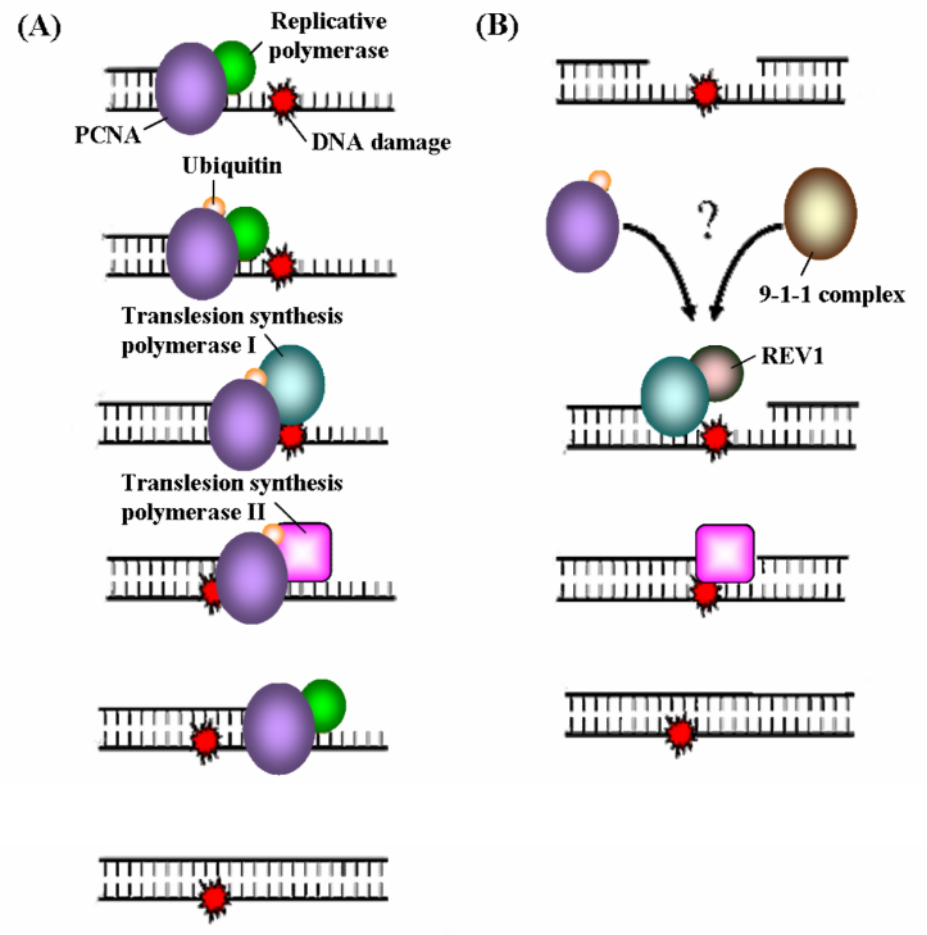

Fig. 1.8 **Translesion synthesis.** (A) The polymerase-switching model. (B) The gap-filling model. (Adapted and modified from reference 37)

When the translesion synthesis polymerases are recruited to the DNA lesions, they will take over the job of the highly stringent replicative DNA polymerases, such as DNA polymerase beta, which are already present. How this exchange occurs remains to be clarified.[37]

1.2.1.6 Mismatch repair

Mismatch repair removes base mismatches formed by deamination, oxidation, methylation and replication errors. Mismatch repair is a simple and conserved pathway and involves just 3 steps (Fig. 1.9):[40]

(1) Mismatch recognition. The base-base mismatches and small insertion/deletion mispairs are recognised and localised by a complex, which is composed of mutS homolog 2, colon cancer, nonpolyposis type 1 (*E. coli*) and mutS homolog 6 (*E. coli*) proteins, or the large insertion/deletion mispairs by another complex, which is composed of mutS homolog 2, colon cancer, nonpolyposis type 1 (*E. coli*) and mutS homolog 3 (*E. coli*);

(2) Strand discrimination and excision. The heterodimers of MutS homologues with adenosine triphosphatase activity, post-meiotic segregation 2 and exonulcease I interact with PCNA to facilitate strand discrimination near the mismatches and remove errors by excision; and

(3) DNA replication and ligation.[41,42]

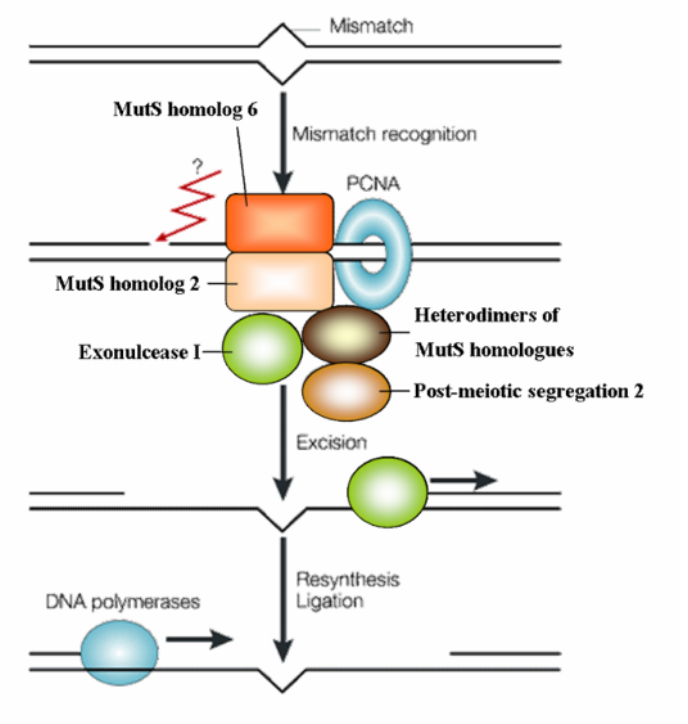

Fig. 1.9 Mismatch repair pathway. (Adapted and modified from reference 40)

1.2.2 Mitochondrial DNA repair pathways

In contrast to the nucleus, the mitochondria accumulate large amounts of reactive oxygen species, since they are the centre for oxidative phosphorylation and close to the free-radical producing electron transport chain. In mitochondria, the dominant type of DNA damage is therefore reactive oxygen species-generated oxidative damage. Therefore, mitochondrial DNA repair pathways are more adapted to deal with DNA damage from oxidative stress when compared to their nuclear counterparts.

Although it is clear that DNA repair exists in the mitochondria, it still remains unclear how DNA repair pathways work in combination in the mitochondria. DR, BER and DSB, but not NER repair pathways, were found to exist in the mitochondria. The absence of nucleotide excision repair in the mitochondria may be due to the lack of large multiprotein complexes required for nucleotide excision repair activity. Although mismatch repair and translesion synthesis proteins have been found to be present in the mitochondria, their role in mitochondrial DNA repair is still under investigation.

In principle, mitochondrial DNA repair is similar to nuclear DNA repair with the exception that nuclear DNA repair requires more proteins. Mitochondrial DNA repair mechanisms is still not fully understood, and yeast may be a good model for study based on the similarity between human and yeast DNA repair systems.

DNA repair pathways and DNA repair proteins are highly conserved. In particular, the homology between yeast and human genes is around 80%.[22] Since

most of the DNA repair proteins are similar in structure and function between human and yeast, human DNA repair pathways can be extrapolated from the analysis of yeast systems.

1.2.3 Conservation of DNA repair pathways

DNA repair pathways show a high degree of evolutionary conservation. It is useful to study simple organisms to learn the fundamentals about the critical pathways in complex organisms. Many human DNA repair genes were first discovered by characterising their homologues in prokaryotes and yeast.[43,44] The sequence homology of DNA repair genes between prokaryotes and eukaryotes may be not high, but the structural and functional homology of DNA repair proteins involved in various of DNA repair mechanisms is.[45]

BER is the focus of this section and the budding yeast *Saccharomyces cerevisiae* (*S. cerevisiae*) is used as the model as described in Chapter 2, therefore a more detailed comparison for BER in *S. cerevisiae* and Homo sapiens (*H. sapiens*) is illustrated in the following section.

1.2.3.1 Similarities of human and yeast BER

Since DNA repair pathways and proteins are well conserved among eukaryotes, the functions of most DNA repair proteins in human and budding yeast are similar.[22,46,47] Both human and budding yeast have five important DNA repair pathways, although the budding yeast repair pathways are more simple than the human ones.[4,6,47] Fewer DNA repair proteins are present in budding yeast.[4,47]

BER pathways in humans and budding yeast are found to show marked conservation.[22,46-48] For example, seven DNA glycosylases have been identified in human BER and at least five of these glycosylases can also be found in *S. cerevisiae*.[22] The BER genes and proteins in humans and budding yeast are summarised in Table 1.2 and their differences are summarised below.[4,22,25,46,48]

1.2.3.2 Differences between human and yeast BER

These differences are summarised as follows:

(1) Differences between the function of APEX nuclease (multifunctional DNA repair enzyme) 1 (APEX1) in *H. sapiens* and Apn1 in *S. cerevisiae*. They share similar substrates but they are different in structure.[48]

(2) *S. cerevisiae* does not have a homologue to ligase III.[48]

(3) The Pol β and X-ray repair complementing defective repair in Chinese hamster cells 1 (XRCC1) of *H. sapiens* operate in BER pathways. However, in *S. cerevisiae*, Pol β contributes to the DNA end-joining pathway and XRCCI-like is responsible for S phase onset and M phase restraint.[48]

(4) Although both *H. sapiens* and *S. cerevisiae* contain 8-oxoguanine DNA glycosylase, they handle oxidative damage using different mechanisms.[48]

In summary, BER pathways in humans and budding yeast consists of different steps and involve different DNA repair proteins, although both of these pathways deal with DNA base damage using similar mechanisms. A few of the DNA repair proteins mentioned above are significantly different between humans and budding yeast, while other DNA repair proteins involved in BER pathways have functions conserved in both humans and budding yeast. Because of these conserved

Table 1.2 **Homologues of BER genes in *H. sapiens* and *S. cerevisiae*.** (Adapted and modified from reference 22)

Enzymes	*H. sapiens*	*S. cerevisiae*
DNA glycosylase		
Uracil DNA glycosylase	*UNG*	*UNG1*
3MeA DNA glycosylase	*MPG*	*MAG1*
8-oxoguanine DNA glycosylase/AP lyase	*OGG1*	*OGG1*
8-oxoguanine DNA glycosylase/AP lyase	*NEIL1*	Absent
Thymine glycol DNA glycosylase/AP lyase	*NTHL1*	*NTG1/OGG2 NTG2*
Mut Y G:A mismatch glycosylase/AP lyase	*MYH*	Absent
TDG T:G mismatch DNA glycosylase	*TDG*	Absent
AP endonuclease		
Endonuclease III	*APEX1*	Absent
Endonuclease III	*APEX2*	*APN2*
Endonuclease IV	Absent	*APN1*
Additional factors		
Flap endonuclease	*FEN1*	*RTH1/RAD27*
8-oxo-dGTPase	*NUDT1*	Absent
Proliferating cell nuclear antigens	*PCNA*	*POL30*
Replication Factor C	*RFC1*	*RFC*
XRCC1	*XRCC1*	Absent
DNA polymerase	*POLB*	*POL4*
	POLD	*POL3*
	POLE	*POL2*
DNA ligase	*LIG1/LIG3*	*CDC9*

Abrreviations:
UNG: uracil-DNA glycosylase; *MPG*: N-methylpurine-DNA glycosylase; *OGG1*: 8-oxoguanine DNA glycosylase (*H. sapiens*); *NEIL1*: nei endonuclease VIII-like 1 (*E. coli*); *NTHL1*: nth endonuclease III-like 1 (*E. coli*); *MYH*: mutY homolog (*E. coli*); *TDG*: thymine-DNA glycosylase; *APEX1*: APEX nuclease (multifunctional DNA repair enzyme) 1; *APEX2*: APEX nuclease (apurinic/apyrimidinic endonuclease) 2; *FEN1*: flap structure-specific endonuclease 1; *NUDT1*: nudix (nucleoside diphosphate linked moiety X)-type motif 1; *PCNA*: proliferating cell nuclear antigen; *RFC1*: replication factor C (activator 1) 1, 145 kDa; *XRCC1*: X-ray repair complementing defective repair in Chinese hamster cells 1; *POLB*: polymerase (DNA directed), beta; *POLD*: polymerase (DNA directed), delta 1, catalytic subunit 125 kDa; *POLE*: polymerase (DNA directed), epsilon; *LIG1*: ligase I, DNA, ATP-dependent; *LIG3*: ligase III, DNA, ATP-dependent.

functions and the relative simplicity in handling *S. cerevisiae*, it is the model of choice for investigating the functions of polymorphic BER proteins.

1.3 DNA repair and cell cycle checkpoints

The DNA repair genes and their related mechanistic pathways play a critical role in the cell cycle.[11] The cell cycle is divided into four phases:[49-53]

(1) G1 phase — Rapid biosynthesis and cell growth;

(2) S phase — DNA synthesis;

(3) G2 phase — Continued cell growth and synthesis of mitotic proteins; and

(4) M phase — Mitosis.

Cell cycle checkpoints occur at the G1/S boundary, G2/M boundary and metaphase/anaphase boundary in M phase.[49-51,53-59] Different DNA repair genes are involved in different cell cycle checkpoints. Ataxia telangiectasia mutated, tumour protein p53 (*TP53*) and cyclin-dependent kinase inhibitor 1A (p21, Cip1) genes have been identified to be essential for G1/S checkpoint arrest.[49,53-55,57-68] Cells deficient in any of these genes can bypass the G1/S arrest.[66,68-71] For controlling the G2/M checkpoint, ataxia telangiectasia mutated, ataxia telangiectasia and Rad3 related, cyclin-dependent kinase inhibitor 1A (p21, Cip1), *TP53*, growth arrest and DNA-damage-inducible, alpha and breast cancer 1, early onset genes are necessary.[49,53,55,57-62,64-67,72-75] RAD51-like genes X-ray repair complementing defective repair in Chinese hamster cells 2 and 3 have been shown to regulate the

metaphase/anaphase checkpoint. Their main function is to reduce chromosome mis-segregation.[76]

Cell cycle checkpoints are the key events in cell cycle progression/control and in carcinogenesis. When DNA is damaged, the cell cycle will halt in order to allow for DNA repair through different DNA repair pathways and thus the damaged cell remains in a checkpoint status. Failure or reduced efficiency in DNA repair mechanisms may allow the cell to continue with the cell cycle.[77] The consequences may include uncontrolled cell growth, adverse drug responses of some anti-cancer drugs (e.g. chemotherapy drug -- 6-thioguanine), birth defects, accelerated ageing and other diseases, such as ataxia telangiectasia.[78-82] Abnormal checkpoint functions have been demonstrated in cancer cells.[55,77,83]

The above evidence indicates that DNA repair genes are closely related to cell cycle and carcinogenesis because they take part in the control of cell growth. Defects in DNA repair genes such as breast cancer 1, early onset, breast cancer 2, early onset, mutS homolog 2, colon cancer, nonpolyposis type 1 (*E. coli*), excision repair cross-complementing rodent repair deficiency, complementation group 2 and XRCC1 have been proved to induce various cancers.[84-89] Their importance in carcinogenesis has been confirmed by the yeast homologues of human DNA repair genes, transgenic studies and gene targeting studies. Many studies have also demonstrated that cancer cells exhibit down-regulation or altered function of these proteins encoded by DNA repair genes.[87,90-95]

1.4 DNA repair genes and functional single nucleotide polymorphisms (SNPs)

In addition to mutations, SNPs are also major factors affecting DNA repair capacity, carcinogenesis and efficacy of cancer treatments.[96-99] SNPs in DNA repair genes have been found to be associated with cancers in many clinical epidemiological studies.[100,101] For instance, breast cancer 2, early onset 372 HH genotype is significantly associated with breast cancer risk and prenatal viability.[102] The polymorphism Ser326Cys in the 8-oxoguanine DNA glycosylase protein is associated with lung cancer development.[103] Moreover, T allele in exon 7 (position 18067) of the X-ray repair complementing defective repair in Chinese hamster cells 3 gene has been found to be associated with skin cancer.[104]

The results of these epidemiological studies warrant investigation of DNA repair genes with the corresponding SNPs by functional studies. The effect of SNPs on DNA repair genes have been explored using cell culture models. Ataxia telangiectasia mutated gene is a good example in that it has been extensively studied using lymphoblastoid cell lines. It was found that the presence of ataxia telangiectasia mutated haplotypes correlated with high breast cancer risk and adverse radiotherapy responses due to low levels of ataxia telangiectasia mutated messenger RNA (mRNA) transcripts.[105] Another example is mismatch repair gene deficiency in HeLa cells, which causes resistance to 6-thioguanine by shortening G2/M checkpoint arrest.[82]

DNA repair genes with functional SNPs may encode deleterious proteins, so functional data about the expressed proteins are important. An example is the highly abnormal protein expression of ataxia telangiectasia mutated, breast cancer 1, early onset and TP53 in high-grade breast tumours, which may be involved in breast cancer pathogenesis.[106] Another example is the importance of the protein from xeroderma pigmentosum, complementation group C gene in cancer prevention. The xeroderma pigmentosum, complementation group C protein initiates the cisplatin DNA damaging treatment-mediated signal transduction process and hence results in activation of the TP53 pathway and cell cycle arrest. This in turn allows DNA repair and apoptosis to take place.[107]

In addition, functional data about the expressed proteins may help develop a new drug and prevent drug resistance. For example, a recent study revealed that Simaomicin α works against cancer via abrogating bleomycin-induced G2 checkpoint.[108] If the compound is studied in relation to the interaction of different DNA repair genes with functional SNPs, new information may become available on the best way to prescribe drugs and prevent drug resistance.

As the DNA repair capacity of the cells very much depends on DNA repair protein activity, it is worth studying how SNPs affect the functions of DNA repair proteins and therefore may aid to prevent cancer drug resistance. In the following sections, some background regarding the work covered in Chapter 2, which is to examine the effects of SNPs on DNA repair protein's functions, is introduced.

1.5 Human nth endonuclease III-like 1 (*E. coli*) (NTHL1)

1.5.1 DNA repair and NTHL1

The structure of human NTHL1 protein has been predicted and confirmed from its orthology. The NTHL1 protein contains five conserved domains near the C-terminal: (1) active sites, which are the catalytic sites, including Lys 212 and Asp 239; (2) substrate binding pocket; (3) minor groove reading motif, which stabilises holes in the DNA base stack; (4) helix-hairpin-helix signature motif, which may interact with the DNA backbone and (5) iron-sulphur binding domain in DNA-(apurinic or apyrimidinic site) lyase, which locates conserved basic residues for interaction with the DNA phosphate backbone (Fig. 1.10).[109-115] At the N-terminal tail, NTHL1 possesses a unique sequence with an inhibitory role. This regulatory N-terminal tail inhibits the release rate of this enzyme from the multi-step DNA repair reaction mediated by NTHL1. As a result, human NTHL1 has a relatively low activity when compared with its *E. coli* counterpart.

The NTHL1 protein is a DNA repair enzyme that is involved in the BER pathway.[116-118] It is a bifunctional enzyme, which can act as a DNA N-glycosylase for removing oxidised pyrimidines, or an AP lyase for introducing a single strand nick at the AP site. Enzymes with homology to NTHL1 are also found in bacteria and yeast. All these conserved proteins found in bacteria, yeast and humans have a similar specificity for the types of DNA damage.[116-118]

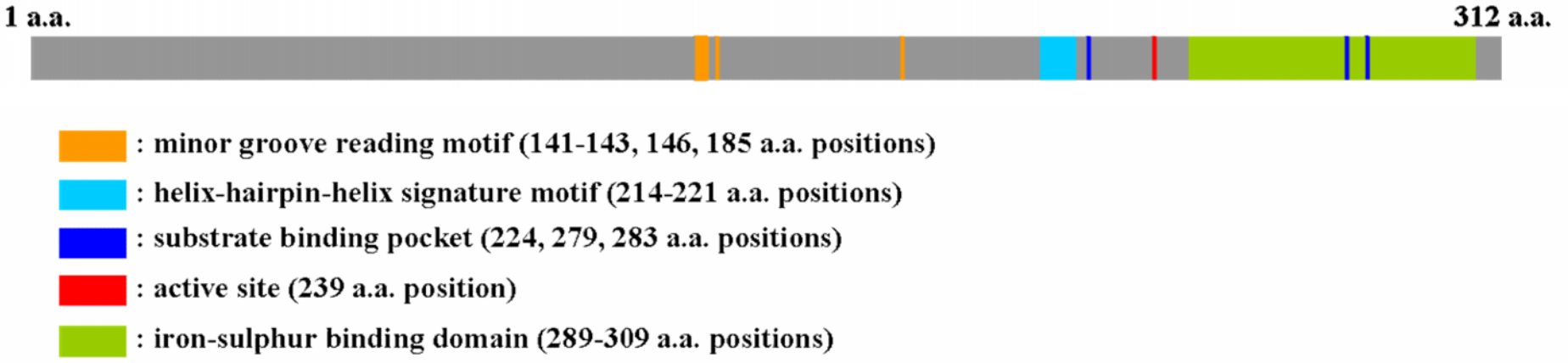

Fig. 1.10 NTHL1 protein structure. (Adapted and modified from reference 115.)

This highly conserved NTHL1 protein is also related to cancer pathogenesis. Goto *et al.'s* study showed that reduced NTHL1 expression and abnormal distribution in the cytoplasm of primary gastric cancer tissue contribute to the pathogenesis of gastric cancer.[119] The expression level of the NTHL1 protein is also closely related to the pathogenesis of astrocytomas and colorectal cancer.[120,121] This protein is also involved in cancer drug resistance and additional details are given in Chapter 1.5.3.

1.5.2 Comparison of human NTHL1 and yeast homologue NTG2

In yeast, two homologues of the human NTHL1 exist: NTG1 and NTG2. Two encoded proteins from the yeast genes show significant similarity to human NTHL1; only NTG2, but not NTG1, contains both important conserved domains as their human homologues. The domains are a putative active site helix-hairpin-helix domain and an iron-sulphur cluster located near the C-terminus.[122-124] Since there is no iron-sulphur cluster, and a putative mitochondrial transit sequence is formed in the NTG1 protein, the protein may be more likely involved in mitochondrial DNA repair.[124,125] On the other hand, NTG2 is defined as a yeast homologue of human NTHL1 due to its highly conserved sequence and protein structure (http://www.ncbi.nlm.nih.gov/homologene/?term=NTHL1).

Both NTHL1 and NTG2 proteins have similar binding specificity and recognition for a spectrum of base damage products. The specific DNA substrates processed by the enzymes are listed in Table 1.3.[48,117,126]

Table 1.3 The DNA substrates for NTHL1 and NTG2.
(Adapted and modified from references 48, 116 and 125)

NTHL1	NTG2
Abasic sites, Dihydrouracil, Formamidopyrimidine (fapy), 5-hydroxycytosine, 5-hydroxyuracil and Thymine glycol	
Dihydrothymine, 5-hydroxy-dihydrothymine, 6-hydroxy-dihydrothymine, Uracil glycol, Urea and β-ureidoisobutyric acid	5-hydroxy-6-hydrothymine, 5-hydroxy-6-hydrouracil and 5-hydroxy-5-methylhydantoin

1.5.3 NTHL1 and cancer treatment

Human NTHL1 protein has been proposed to be a target gene for cancer therapy.[127] However, studies have revealed a relationship between NTHL1 protein and cancer treatment resistance. A review from Ide *et al.* concluded that the efficacy of anticancer drugs and radiotherapy can be potentiated by depletion of DNA glycosylases resulting from reduced BER activity.[128]

Another study on Y-box-binding protein 1 indicated that it stimulates NTHL1 activity by forming a Y-box-binding protein 1/NTHL1 complex, and the cytotoxicity of cisplatin in mammary adenocarcinoma MCF7 cell line was intensified after knockdown of NTHL1.[129] The association of NTHL1 with Y-box-binding protein 1 may provide a clue about the role of NTHL1 in resistance to cisplatin and as a marker for predicting the drug responses and patient prognosis in different cancers, including breast and ovarian cancers.

In addition to Y-box-binding protein 1, NTHL1 also interacts with a mismatched repair enzyme, mutS homolog 2, colon cancer, nonpolyposis type 1 (*E. coli*). Knockdown of mutS homolog 2, colon cancer, nonpolyposis type 1 (*E. coli*) results in resistance to 6-thioguanine and temozolomide in NTHL1 proficient and/or deficient cells. Both 6-thioguanine and temozolomide are used in the treatment of glioblastomas and other cancers. Therefore, interaction between NTHL1 and mutS homolog 2, colon cancer, nonpolyposis type 1 (*E. coli*) may affect the DNA repair pathways involved in 6-thioguanine or temozolomide treated glioma cells and thus treatment outcomes.[130] Therefore, it is worthwhile to investigate the role of NTHL1.

Taken together, these pieces of evidence, the SNPs' effects on the function of NTHL1 should be investigated to prevent failure in cancer treatment. NTHL1 is just one example in which genes or proteins can affect the efficacy of cancer treatment. Other DNA repair genes have also been shown to be involved in determining cancer treatment outcome.

1.6 DNA repair genes and cancer treatment

The DNA repair genes and their related mechanistic pathways play a critical role in the treatment outcome of chemotherapy.[11] DNA repair is activated in order to reduce cell death caused by different cancer therapies, including radiotherapy and chemotherapy using a platinum agent.[131-133] In addition, DNA repair pathways repair the DNA damage generated by anticancer agents, and may therefore influence the treatment outcome of chemotherapy.[11,96,134,135] For example, O^6-benzylguanine and its derivatives have been developed to inactivate the DNA repair protein O-6-methylguanine-DNA methyltransferase, and thus to re-sensitise the O^6-alkylating anticancer drugs used. However, an American study showed that the O-6-methylguanine-DNA methyltransferase polymorphism Gly160Arg reduced the inactivation of this enzyme by the drug and hence resulted in resistance to cancer chemotherapy to this anticancer agent.[136] In this polymorphism, the amino acid at position 160 is glycine in the wildtype protein, but is replaced by arginine in the mutant protein. The mutant protein is more resistant to inactivation by the drug. Therefore, the role of DNA repair genes and their influence on the chemotherapeutic outcomes and hence drug development is an important area of research.

Photodynamic therapy (PDT) is now increasingly used in the treatment of

cancers and has been reported to induce obvious DNA damage but also repair in different cancer cells.[137-140] The associated DNA repair after PDT may affect PDT efficacy. In the following sections, PDT and its association with DNA repair are described in detail.

1.7 Photodynamic therapy

PDT is an emerging adjuvant therapy used in the treatment of different tumours, macula degeneration and psoriasis.[141-144] PDT has several advantages over traditional treatment regimens. Compared with surgery and radiotherapy, PDT causes less severe long-term morbidity with comparable treatment outcomes.[145] In a clinical study by Zhao *et al*., it was shown that PDT can be effectively used on patients with nasopharyngeal carcinomas (8 out of 10 had complete responses, meaning that all signs of cancer of the patients disappeared, to PDT) and this treatment caused few major side effects.[146] Mild generalised skin photosensitive reactions were seen.[146] In another study by Lou *et al*., PDT provided good cosmetic outcomes and minimised the disease-associated symptoms without reduction of the patients' physical abilities, e.g. swallowing.[147] Photodynamic therapy can also be the re-treatment of choice in cases of recurrence and incomplete tumour responses after standard therapies and/or PDT as PDT does not compromise re-treatment effectiveness. For example, in the research study conducted by Hornung *et al.* in 1998, meso-tetrahydroxyphenylchlorin-mediated PDT did not induce resistance or interfere with the treatment outcomes of conventional therapies or PDT in breast cancer cells.[148]

1.7.1 Working principle of PDT

The basic mechanism of PDT utilises (1) the preferential accumulation of photosensitisers in tumour cells, (2) oxygen in tissues and (3) light, to kill the tumour cells.[149] After tumour cells have taken up the photosensitiser, light is applied to excite the photosensitising molecules to a higher energy level. A small portion of the excited molecules then return to the ground state with the release of energy in the form of fluorescence, but most of the molecules go through intersystem crossing to a longer-lived triplet state. These longer-lived molecules release their energy subsequently by reacting with organic cellular substrates and reacting with ground state oxygen by mediating the Type I (a redox reaction) and II (an energy transfer process) photo-oxidative reactions. These reactions result in the generation of several chemically reactive molecular species including radical ions, reactive oxygen species and singlet oxygen (Fig. 1.11).[150,151]

At the cellular level, these reactive molecular species, especially singlet oxygen, destroy different cellular organelles, with DNA being one of the targets. If this damage is not repaired, the tumour cells would be killed via apoptosis and/or necrosis.[149,152,153] As singlet oxygen can only diffuse within a short distance, the concentration and distribution of photosensitisers is important in killing tumour cells. However, different animal and clinical studies have demonstrated that concentration is not an essential determinant for PDT responses.[154-156] Therefore, other killing mechanisms must also be present for tumour destruction by PDT.

Targeting the vascular systems surrounding the tumour is an indirect method of killing the tumour at the tissue level. Since the blood vessels are destroyed, the

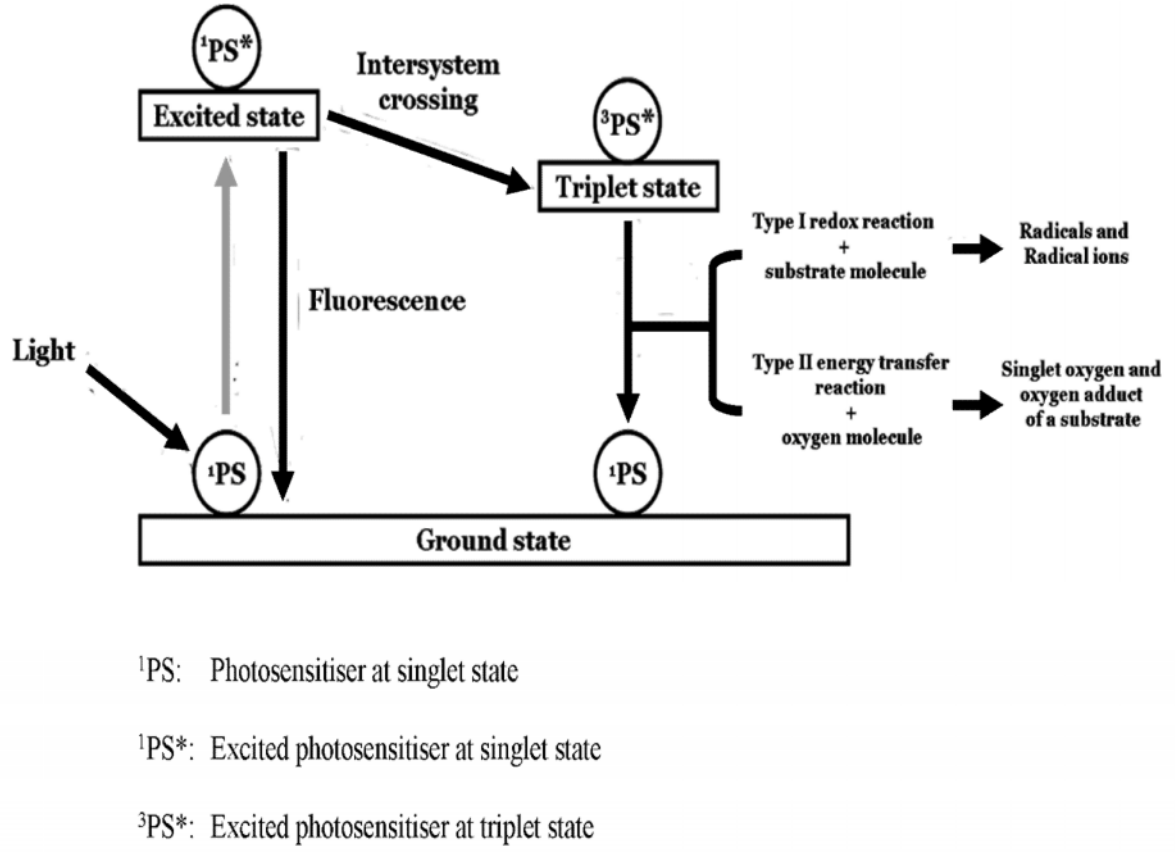

Fig. 1.11 The working principle of PDT. (Adapted and modified from reference 150)

tumour cells die because of hypoxia and/or starvation.[152,157] Significant tumour cell death can also be a consequence of immunological effects triggered by PDT.[150,158]

1.7.2 Localisation of photosensitisers

The distribution of photosensitisers in a cell depends mostly on their hydrophobicity with hydrophobic molecules binding onto membranes. However, photosensitisers may re-distribute to other cellular organelles after light irradiation. Several target sites of photosensitiser binding have been investigated.[159] The target sites are:

1. Membrane: Plasma memebrane is the first target site of PDT. Some photosensitisers also locate in the nuclear membrane or other intracellular membranes. The disruption of the plasma membrane causes cell death by necrosis.[160]
2. Lysosomes: Lysis of lysosomes may cause inactivation of cellular compartments and thus is responsible partially for tumour cell death after PDT.[161]
3. Mitochondria: Most types of photosensitisers used are localised in the mitochondria, for example, Photofrin and 5-aminolevulinic acid. Mitochondria are the critical sites as release of cytochrome c from mitochondria leads to apoptosis.[162]
4. Nucleus: The nucleus is not a usual PDT target, but hydrophobic PDT sensitisers may bind onto the nuclear membrane. Finally, DNA damage occurs in PDT-treated cells because the nuclear membrane is immediately broken down after light illumination.[163]
5. Endoplasmic reticulum.
6. Golgi apparatus.

1.7.3 Photosensitiser classifications

Photosensitisers can be classified into 3 groups: (1) Porphyrin; (2) Chlorophyll and (3) Dyes.[164] Examples of photosensitisers belonging to these 3 groups are listed in Table 1.4.[164]

Photosensitising drugs can also be grouped into different generations according to the year of discovery as well as the modifications on the photosensitisers. The photosensitisers developed in the 1970s to early 1980s are called “First generation”, e.g. Photofrin, and in the late 1980s “Second generation”, e.g. 5-aminolevulinic acid. The “Third generation” photosensitisers refer to those photosensitising drugs with modifications, such as biological conjugates. These terms are still used, but may cause confusion as the new generation photosensitisers may not be better than the old ones.[165]

1.8 Photofrin-mediated Photodynamic therapy (Ph-PDT)

1.8.1 Photofrin

Photofrin, also known as porfimer sodium, is a first generation photosensitiser. Photofrin-mediated PDT is most commonly used for cancer treatment and has already been approved for the treatment of different solid tumours by the U.S. Food and Drug Administration.[166,167]

The chemical structure of Photofrin is illustrated in Fig. 1.12. Photofrin is a mixture of oligomers formed by haematoporphyrin units.

Table 1.4 Photosensitiser classifications. (Adapted from reference 163)

Generation	Porphyrin	Chlorophyll platform	Dyes
First	Photofrin		
Second	Benzoporphyrin derivative; 5-aminolevulinic acid; Texaphyrins	Chlorins; Purpurins; Bacteriochlorins	Phtalocyanine; Napthalocyanine

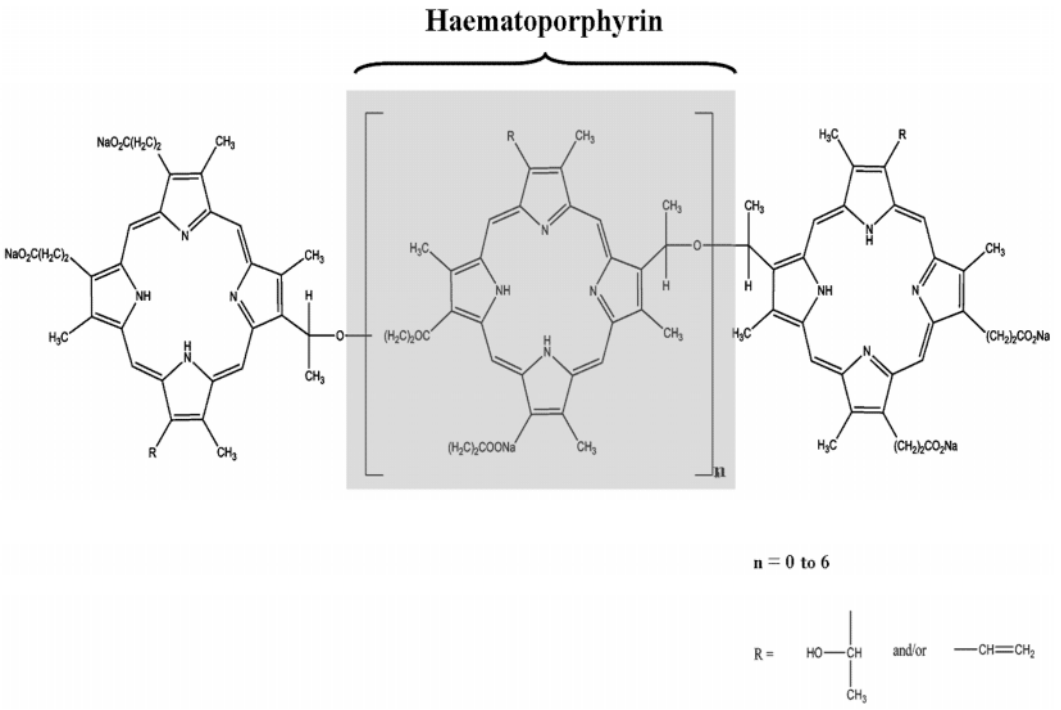

Fig. 1.12 The structure of Photofrin. (Adapted and modified from http://en.wikipedia.org/wiki/Porfimer_sodium)

1.8.2 Applications of Ph-PDT

Photofrin is recommended for use in high-grade dysplasia in Barrett's oesophagus and different cancers. The uses of Photofrin are listed in Table 1.5.[158]

1.8.3 The association of DNA repair with Ph-PDT resistance

DNA repair activity has been observed in different cell types after Ph-PDT.[137-140] In the study of DiProspero and her colleagues, enhanced recovery from Ph-PDT induced DNA damage was found in PDT resistant mouse fibrosarcoma cells and Chinese hamster ovary multi-drug resistant mutant cells.[168] This result implies that DNA repair is related to Ph-PDT resistance. Although different mechanisms have been suggested to explain the causes of resistance in Ph-PDT, the role of DNA repair mechanisms has not been investigated extensively.

1.8.4 Ph-PDT resistance in glioma treatment

1.8.4.1 Glioblastoma multiforme and treatment resistance

Glioblastoma multiforme is one of the most common tumours affecting the brain and is notoriously difficult to cure. The median survival of patients with glioma is 12 to 15 months with the survival rate being less than 5% at 5 years.[169,170]

The common therapeutic modalities used for other tumours are also applied to glioblastomas, namely, chemotherapy, radiotherapy and surgery.[171] However, glioma cells are particularly resistant to therapy, and coupled with the problem of the blood-brain-barrier and the susceptibility of healthy brain tissue to damage during

Table 1.5 Applications of Photofrin. (Adapted and modified from reference 157)

Approved indications	Pending for regulatory approval	Adjuvant therapy
High-grade dysplasia in Barrett's oesophagus, Advanced stage oesophageal tumours, Prophylatic treatment for bladder cancers, Advanced non-small-cell lung cancer and Early stage lung cancer	Early stage oesophageal cancer, Head and neck cancers and Superficial bladder cancer	Brain tumour, Head and neck cancers, Intrathoracic tumours and Intraperitoneal tumours

treatment, new adjuvant therapies are clearly needed to tackle this treatment-resistant tumour.[172,173]

1.8.4.2 Glioblastoma multiforme and Ph-PDT

Clinical trials using Ph-PDT for treating gliomas are underway and reports are emerging about resistance in and/or no responses to Ph-PDT *in vitro* or *in vivo*.[174-177] The situation was seen in Rigual *et al.'s* study of head and neck dysplasia or cancer, where some patients failed to respond or only partially responded to Ph-PDT.[178-180] The underlying cellular mechanisms leading to failure to respond to Ph-PDT are not fully understood. Several proteins and signalling pathways have been shown to play significant roles in resistance to Ph-PDT by various suggested mechanisms. One of these is cellular antioxidant defence mechanisms which help to cope with the oxidative stress-induced damage of Ph-PDT, such as increased expression of Heme oxygenase-1 and superoxide dismutase.[181-183] Activation of anti-apoptotic proteins and pathways is another proposed protective mechanism against Ph-PDT.[177,184] Prostaglandin-endoperoxide synthase 2 is an anti-apoptotic protein that can be up-regulated by Ph-PDT and initiates treatment resistance.[185,186] In addition, the changes in the microenvironment of the area adjacent to the tumour may account for the resistance observed.[187,188] PDT uses oxygen and destroys the capillaries in the PDT-treated and adjacent areas. Hypoxia in these areas causes the induction of "ADAM17-EGFR-PI3K-Akt" pathway and other responsive genes, e.g. epidermal growth factor receptor, that facilitate the tumour invasiveness and minimise the efficacy of Ph-PDT.[189,190] The interactions of these different pathways and proteins will enhance tumour cell proliferation and differentiation, promote invasion, and prevent apoptosis, leading to the decreased cytotoxicity of Ph-PDT.

As Ph-PDT has been reported to induce obvious DNA damage and repair in different cancer cells, different DNA repair pathways may be also related to Ph-PDT resistance in glioblastoma multiforme.[137-140] Thus, DNA repair genes, which belong to individual repair pathways and do not participate in other biochemical pathways, and DNA repair-related genes should be studied to understand the relationship between DNA repair mechanisms and the development of resistance in Ph-PDT. The following genes were investigated in Chapter 3.

1.9 DNA repair and DNA repair-related genes and proteins

1.9.1 AlkB, alkylation repair homolog 2 (*E. coli*) of DNA direct reversal repair pathway

ALKBH2 is the *E. coli* AlkB homologue. It is involved in DNA dioxygenase -mediated DNA repair pathway and its function is to remove 1-methyladenine and 3-methylcytosine. This protein prefers to repair double-stranded DNA.[19] Therefore, ALKBH2 has been found to locate in the nucleus and redistribute to replication foci during S-phase of the cell cycle.[20] Research has shown that ALKBH2 couples with PCNA to accumulate in the replication foci by a new PCNA-binding motif.[191]

The structure of ALKBH2 includes two binding sites for the co-factors and active site pocket for flipping the bases.[192,193] The function of ALKBH2 protein depends on the binding of two co-factors, α-ketoglutarate and ferrous ion, onto the binding sites of ALKBH2 protein.[194]

The detailed repair mechanism performed by ALKBH2 is explained in Section 1.2.1.1.2. As ALKBH2 is a new gene and its role has not yet been confirmed in DNA repair, the association of this gene and Ph-PDT or cancer treatment responses still awaits further investigation.

1.9.2 REV1 homolog (*S. cerevisiae*) of translesion synthesis

The role of REV1 DNA repair protein is to recruit DNA polymerases involved in translesion synthesis. Two alternative splicing transcripts, which encode REV1 protein of different sizes, have been found, but their biological significance has not yet been defined. These proteins are around 138 kDa and 43 kDa.

The REV1 protein has a BRCA1 C-terminal domain, which is a domain for protein-protein interactions, e.g. with PCNA, and an interacting motif for polymerase (DNA directed) kappa. REV1 has also been associated with cytotoxicity and mutagenicity in cisplatin-treated ovarian cancer cells but the relationship between translesion synthesis or REV1 and Ph-PDT remains to be investigated.

1.9.3 RAD52 homolog (*S. cerevisiae*) of double strand break repair pathway

Rad52 is involved in double strand break repair. It binds to the ends of single-stranded DNA and mediates the annealing of the complementary strands. It has been found to interact with RAD51 homolog (RecA homolog, *E. coli*) (*S. cerevisiae*), a DNA recombination protein.[195,196] Evans *et al.*'s study showed that B

lymphoblastic cells deficient in double strand break repair demonstrated low mutatation frequency and some of these mutations may be generated from intergenic mutations produced by double strand break repair.[197] The latter has been shown to be associated with the mutagenicity of Ph-PDT. Therefore, it is worth examining how this repair is related to Ph-PDT resistance because mutations in cancer cells caused by Ph-PDT may affect its responsiveness.

1.9.4 APEX nuclease (multifunctional DNA repair enzyme) I of BER pathway

The APEX1 gene encodes the major AP endonuclease to repair abasic sites, which is caused by hydrolysis, DNA damaging agents or DNA glycosylases. APEX1 cleaves the phosphodiester backbone of damaged DNA in abasic sites and initiates the BER pathway.[198]

PDT using different photosensitisers produce base modifications and oxidative DNA damage, which are the substrates for BER, on DNA by PDT-generated reactive oxygen species.[138,199,200] Another study showed that when APEX1 was silenced, an improvement in the cytotoxicity of haematoporphyrin-mediated PDT was seen.[201] These results imply that BER efficiency may affect the cytotoxicity of PDT and result in PDT resistance.

1.9.5 X-ray repair complementing defective repair in Chinese hamster cells 1 of short-patch BER pathway

XRCC1 protein plays a role in short-patch BER pathway and complexes with

DNA ligase III, polymerase (DNA directed), beta and poly (ADP-ribose) polymerase.[202] It may be involved in DNA manipulation during meiosis and recombination in gametes.[203] Some polymorphic variations in this gene are associated with radiotherapy resistance.[204,205] BER, which proceeds through either short-patch or long-patch or both subpathways, may also be responsible for reactive oxygen species induced base damage after PDT as described in section 1.9.4.

1.9.6 Excision repair cross-complementing rodent repair deficiency, complementation group 5 of nucleotide excision repair pathway

ERCC5 protein participates in the nucleotide excision repair pathway, which is mainly responsible for repairing ultraviolet-induced DNA damage, to prevent the development of genetic instability and thus cancer.[206] Mutations in ERCC5 cause Cockayne syndrome, which is characterised by severe growth defects and mental retardation.[207] This protein has several variants, but their biological validity has not been determined. Finlan *et al*. found that 5-aminolevulinic acid-mediated PDT did not induce nucleotide excision repair in skin tissues, but no studies about the effect of Ph-PDT on nucleotide excision repair have been found.[208]

1.9.7 Tumour protein p53 (TP53) and phosphorylated TP53 (p-TP53)

The TP53 protein is defective in most human cancers. This suggests that TP53 has an important role in cancer prevention. Activation of TP53 is related to various signalling processes from DNA damage, abnormal proliferation, hypoxia and loss of

cell adhesion.[209,210] In the study of Donehower *et al*., TP53-deficient mice was found to have a higher risk of developing multiple tumours. This finding implies that TP53 is a critical functional protein.[211,212]

The functions of TP53 include inhibition of the abnormal growth of cells and angiogenesis, involvement in programmed cell death, DNA repair and cell cycle, regulation of other genes via transcriptional activation and modulation of other protein activities.[213-216] Impairment of TP53 may also cause adverse drug responses and ageing.[217,218] The involvement of different TP53 forms, including mutant TP53 and wildtype TP53, in PDT with various photosensitisers and cell types have been extensively investigated, although results are inconsistent. For example, fibroblast cells with mutant TP53 were shown to be more resistant to Ph-PDT than the cells with wildtype TP53.[219] In contrast, colon cancer cells with abrogated TP53 has no effect in sensitivity to Ph-PDT.[220] Therefore, the participation of TP53 in Ph-PDT may be cell type-dependent.

1.9.8 Proliferating cell nuclear antigen

PCNA as a cell regulator determines the eukaryotic cell fate since it affects the cell cycle arrest, cell death and DNA repair. It also influences the processivity of DNA polymerase Delta involved in DNA synthesis.[31] The transcription of PCNA is induced by TP53 as shown by promoter-reporter gene assay in Kannabiran and her colleagues' study.[221] In 2006, Banks *et al*. further showed that PCNA will cooperate with TP53's negative regulator, i.e Mdm2 p53 binding protein homolog (mouse), to ubiquitinate TP53 protein followed by degradation resulting in decreased TP53 stability.[222]

PCNA was demonstrated to stimulate and interact with different DNA repair proteins of excision repair pathways, mismatch repair, double strand break repair and translesion synthesis, and another important regulator—TP53—via PCNA-interacting peptide.[223] Under genotoxic stress, PCNA may bind proteins via a newly discovered motif called AlkB homologue 2 PCNA-interacting motif. One of the examples is ALKBH2, which co-localises with PCNA in the replication foci during DNA repair.[191] In several reports of PDT using haematoporphyrin and Photofrin, the increase in PCNA expression level was suggested to be caused by DNA damage and the related cellular responses, e.g. induction of DNA repair proteins.[224-226] Thus, PCNA-involved DNA repair may affect PDT effectiveness.

1.9.9 c-Jun NH2-terminal kinases (JNKs)

c-Jun NH2-terminal kinases (JNKs) is a group of mitogen activated protein kinases. There are 3 isoforms (JNK1, JNK2 and JNK3) which are responsible for stress sensing, for example, oxidative stress, inflammation and ultraviolet insult. Activation of JNKs is via phosphorylation by mitogen activated protein kinases.[227]

JNKs can activate different proteins, including TP53. Different isoforms of JNKs have different roles including phosphorylation, complex formation and TP53 regulation.[228] The relationship between TP53 and JNKs is suggested to be a negative feedback mechanism. Expression of TP53 is increased if there is a decrease in JNK1 and an increase in JNK2 expression, but overexpression of TP53 limits the phosphorylation of JNKs.[229]

Since JNKs phosphorylate TP53, and is therefore involved in TP53-dependent

DNA repair, they should also play a part in DNA repair activities. JNKs enhance DNA repair in cells through various mechanisms, for instance, transcriptional activation of the activating transcription factor 2 or TP53 multimerisation by dissociating TP53 from an E2 ubiquitin-conjugating enzyme.[230,231]

DNA repair elicited by JNKs' activation after treatment contributes to treatment resistance.[232] In the study of Assefa *et al.*, HeLa cells were protected from Hypericin-PDT due to activation of JNKs whereas, in another study, Photofrin treated human epidermoid carcinoma cells were found to be killed by Ph-PDT and the activation of JNKs.[233,234] These contrasting results may be caused by the presence of wild type or mutant TP53.[230]

1.9.10 Nucleophosmin (nucleolar phosphoprotein B23, numatrin) (NPM1)

NPM1 is a multifunctional nucleolar protein, which is abundant in proliferating cells. This protein is a "chaperone" and thus has many biochemical activities, including processing RNA, ribosome biogenesis and transport and anti-apoptotic activity.[235]

NPM1 is associated with DNA repair activity. Under ultraviolet irradiating conditions, NPM1 interacted with PCNA to enhance nucleotide excision repair.[236] The participation of NPM1 in DNA repair is also via interaction with TP53.[237]

Many proteins work with NPM1, and TP53 is a well-documented NPM1 partner.

NPM1 increases the stability and transcriptional activity of TP53.[238,239] The stabilisation of TP53 may be due to the formation of a NPM1-Mdm2 p53 binding protein homolog (mouse) complex to prevent ubiquitination and degradation of TP53.[240] However, in contrast to previous reports, no co-immunoprecipitation of NPM1 and Mdm2 was observed in the study of Bertwistle and his colleagues.[241]

Li *et al*. found that an increase in NPM1 expression enhances cell survival in hypoxia by inhibition of TP53 phosphorylation at Serine 15 position and interaction with TP53. Therefore, overexpression of NPM1 is characterised to promote hypoxia-driven cancer progression.[242] This finding may relate NPM1 to PDT resistance as PDT causes hypoxia in cancer cells after the treatment.

1.10 Scope of project

This project consists of two parts. Firstly, a detection method using a yeast model was developed to evaluate the SNPs' effects on the function of DNA repair protein. In the second part, the expression of DNA repair genes were examined in relatively resistant glioma cells after Ph-PDT to investigate the involvement of DNA repair in Ph-PDT resistance. The general outline of this thesis is as follows:

Chapter 2 To evaluate two SNPs' effects on human NTHL1 DNA repair gene using the yeast expression vectors and flow cytometry.

Chapter 3 To investigate the expression of six DNA repair genes and their co-operating molecules in relatively resistant glioma cells after Ph-PDT.

Chapter 4 General discussion and suggestions for future research.

Chapter 2

SNPs’ effects on DNA repair proteins

2.1 Introduction

As the *NTHL1* gene is important for chemotherapy of glioblastoma, and different polymorphisms may affect the DNA repair activity of the NTHL1 protein, this gene has been targeted for the development of a simple, and rapid detection method for analysing the effects of SNPs on the protein. Two SNPs of the *NTHL1* gene, which include deletion of an adenine to cause a frameshift polymorphism of lysine at 105 amino acid position (FS105), and substitution of thymine for guanine to cause a missense polymorphism with a change of amino acid from aspartic acid to tyrosine (D239Y) at 239 amino acid position, were examined because different degrees in protein function and structural damage may be caused by these SNPs.

Two different DNA damaging reagents, methyl methanesulphonate (MMS) and hydrogen peroxide (H_2O_2), were used to generate different types of DNA damage. MMS is an alkylating agent used in cancer treatment (http://www.mondofacto.com/facts/dictionary?methyl+methanesulfonate). This agent is also commonly used in research to study the mechanisms involved in drug resistance, for example, alkylating drug resistance in glioblastoma.[243] MMS produces mainly N-methylpurines in DNA.[244] Hydrogen peroxide is a well-known genotoxic agent that oxidises DNA bases via reactive oxygen species.[245]

Specific questions to be addressed in this chapter are as follows:

1. **What are the SNPs' effects on the NTHL1 protein in response to different genotoxic reagents?**
2. **Is it possible to examine the SNPs' effects by means of yeast expression vector coupled with cell cycle analysis?**

2.2 Experimental design

The experimental design in this chapter is shown in Fig. 2.1. The human *NTHL1* complementary DNA (cDNA) was reverse-transcribed and amplified by conventional polymerase chain reaction (PCR) from a human RNA sample. The PCR product of human *NTHL1* cDNA was digested by the restriction enzymes EcoRI and HindIII. The digested human *NTHL1* PCR product was then ligated into pYX113 vector digested by the same restriction enzymes, to form the pYX113-NTHL1 plasmid. By *Escherichia coli* (*E. coli*) transformation, the pYX113-NTHL1 plasmid was separated from other products, i.e. non-ligated plasmids and PCR products, and the amount of pYX113-NTHL1 plasmid was multiplied. The size and sequence of pYX113-NTHL1 plasmid were confirmed by PCR and sequencing respectively. The verified pYX113-NTHL1 plasmid was further used to introduce two particular SNPs individually by site-directed mutagenesis. Two plasmids, pYX113-FS105 and pYX113-D239Y, were generated. All plasmids, including the pYX113 vector, were finally transformed into the mutant *NTG2*-knockout yeast cells and then treated with different genotoxic agents. Finally, cell survival assay, Western blotting and cell cycle analysis were performed.

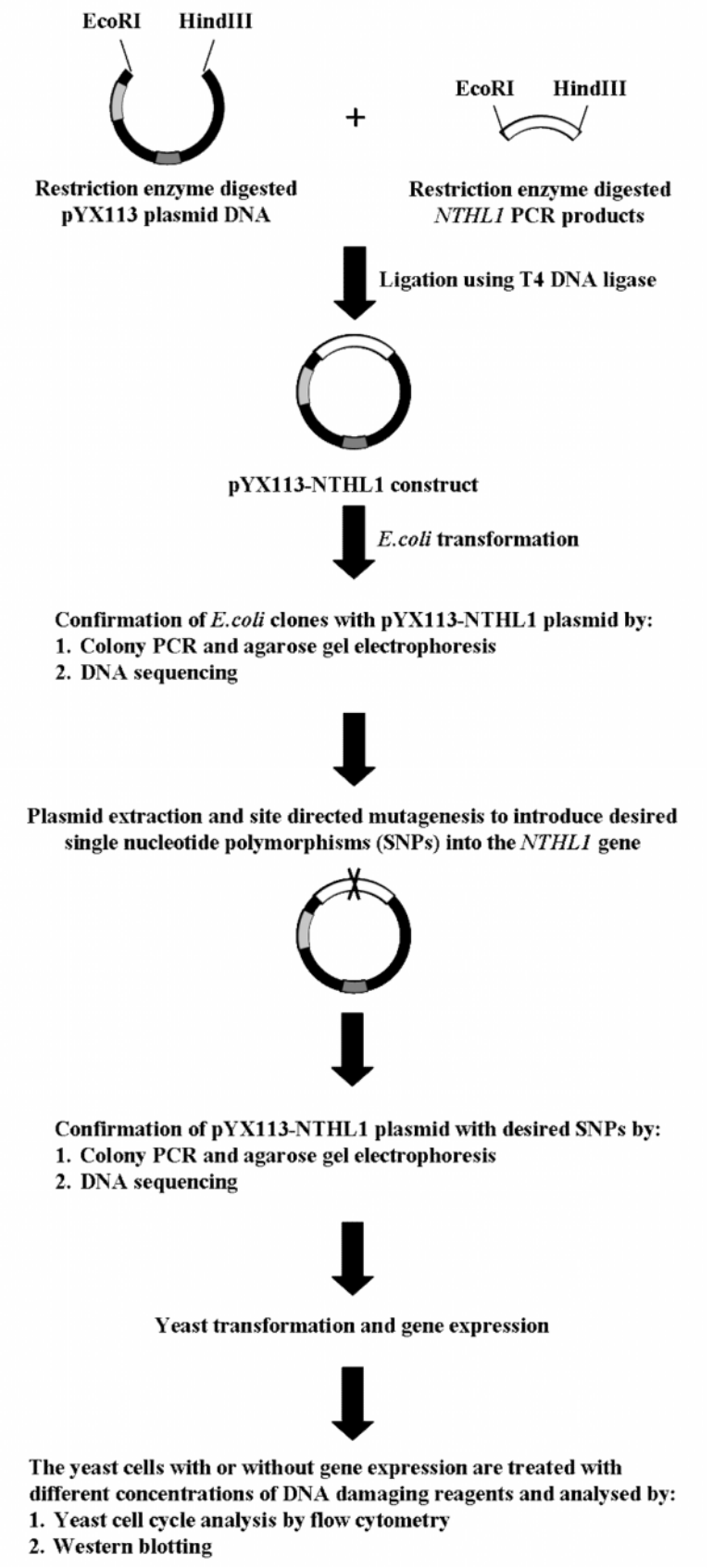

Fig. 2.1 Schematic diagram of workflow in Chapter 2.

2.3 Methodology (The materials and reagents are listed in appendices.)

2.3.1 Construction of plasmid

2.3.1.1 Amplification of *NTHL1* by reverse transcription – polymerase chain reaction (RT-PCR)

Principle

Reverse transcription

RNA is reverse-transcribed into cDNA using a reverse transcriptase and primers. RT is an RNA-dependent DNA polymerase to transcribe, initially, the single-stranded RNA into single-stranded cDNA and subsequently forms double helix DNA. The cDNA formed is used as the template for real-time polymerase chain reaction.

Conventional PCR

PCR is a molecular biology technique for DNA amplification to generate many copies of a particular DNA sequence. The product is obtained by the repeated heating and cooling of the reaction mixture, i.e. thermal cycling. It provides suitable temperatures for DNA melting and enzymatic replication of the DNA. In PCR, there are two main components: (1) primers, which are short DNA fragments, are designed to be complementary to the target region; and (2) a thermostable DNA polymerase used in repeated amplification. During the progression of PCR, the generated PCR products themselves are used as templates for amplication, so a chain reaction occurs and the DNA template is exponentially amplified.

Melting temperature of the primers is predicted by the following equation:[246]

$$\mathbf{69.3°C + (GC\% \times 0.41 - \frac{650}{Primer\ Length\ (bp)})}$$

The final annealing temperature and cycle number are optimised experimentally. The time of extension depends on the PCR product size.

Procedures

Reverse transcription

Briefly, 5 µg total RNA extracted from human U87 glioma cells was added to the RT mixture, which contained 1X reaction buffer, 5 µM oligo $(dT)_{18}$ primer, 1 mM dNTPs, 20 units RiboLock™ RNase Inhibitor and 200 units of RevertAid™ M-MuLV Reverse Transcriptase. The sample was mixed, centrifuged and incubated for 60 minutes at 42°C. The RT reaction was stopped by heating at 70°C for 5 minutes. The cDNA products were stored at -20°C until use.

Conventional PCR for NTHL1 amplification

Conventional PCR were performed in GeneAmp® PCR System 9700 (Applied Biosystems, Carlsbad, CA, USA). Fifty nanograms of cDNA (one bacterial/yeast colony in case of colony PCR) were amplified by 0.5 µM of primers in 25 µL PCR master mix with 0.5 units of FastStart high fidelity enzyme, 0.2 mM dNTPs and 3.5 mM of $MgCl_2$. The amplification cycle was carried out as follows: 1 cycle for denaturation (95°C/5 minutes) followed by 35 cycles for amplification (95°C/15 seconds, 60°C/1 minute and 72°C/1 minute) and final extension of 10 minutes at 72°C. The PCR products were subjected to agarose gel electrophoresis and sequencing for examination. The primers used for amplifying *NTHL1* genes are listed in Table 2.1.

Table 2.1 Primers used in *NTHL1* amplification for construction of plasmid.

Primers	Sequences (5' to 3')[a-c]	Positions in *NTHL1* mRNA sequence[d]
(1) N1exppF1	ATATAAGAATTCATTATGGATGTGTA GTCCGCAGGAGTCC	20-40
(2) N1exppR1	CAATATAAGCTTTCAGAGACCCTGGG CGGC	941-958

a. The sequences highlighted in grey are the restriction enzyme sites of EcoRI in N1exppF1 and HindIII in N1exppR1.
b. The underlined sequence of N1exppF1 is the Kozak sequence for yeast cell protein expression.
c. The boxed sequences in both primers are additional sequences to enhance restriction enzyme digestion
d. The primers were designed from Homo sapiens *NTHL1* mRNA sequence (Accession no.: NM_002528) by using Oligo program version 6.57 (Molecular Biology Insights, Cascade, CO, USA).

2.3.1.2 Restriction enzyme digestion

Principle

This is a molecular biology method using restriction endonucleases to cleave the double-stranded DNA at a specific nucleotide sequence, the restriction site. The cleaved DNA fragments can be used for fingerprinting, plasmid construction and the determination of restriction fragment length polymorphism.

Procedures

Two restriction enzymes and pYX113 vector were used for constructing the plasmid. They are: (1) EcoRI recognises “GAATTC” DNA sequence and (2) HindIII recognises “AAGCTT” DNA sequence.

First restriction enzyme digestion using EcoRI:

Ten microlitres of PCR products from *NTHL1* PCR amplification or 0.4 µg plasmid DNA (pYX113) were added to 20 µL of restriction enzyme digestion mixture containing 1X buffer and 10 units of EcoRI. The mixture was incubated for 16 hours at 37°C and the reaction was stopped by incubating for 20 minutes at 65°C.

Second restriction enzyme digestion using HindIII:

Ten microlitres of EcoRI digested product (both PCR products and plasmid DNA) were added to 20 µL of restriction enzyme digestion mixture containing 1X Buffer R and 10 units of HindIII. The mixture was incubated for 16 hours at 37°C and the enzyme reaction was inactivated by incubating for 20 minutes at 80°C.

2.3.1.3 Ligation

Principle

This enzymatic method makes use of T4 DNA ligase to link up two DNA strands that have a break in both complementary strands of DNA (double strand break). In this project, EcoRI and HindIII produce sticky ends in the PCR products and plasmid DNA for linkage.

Procedures

The procedures were performed according to the manufacturer's manual. Briefly, 0.1 µg of restriction enzyme digested pYX113 vector and about 5.5 ng restriction enzyme- digested *NTHL1* PCR product (insert) (3:1 molar ratio over vector calculated by equation 1[*]) were added to 20 µL of DNA ligation mixture containing 1X T4 DNA ligase Buffer and 1 unit of T4 DNA ligase. The mixture was incubated for 10 minutes at 22°C and the reaction was stopped by incubating for 5 minutes at 70°C. Five microlitres of the mixture containing pYX113 vector with *NTHL1* coding sequence (pYX113-NTHL1 plasmid) were used for transformation of 50 µL of chemically competent *E. coli* cells. The schematic diagram of pYX113-NTHL1 plasmid is shown in Fig. 2.2.

[*]**Equation 1:**

$$\frac{\text{Amount of vector (ng) x Size of insert (kb)}}{\text{Size of vector (kb) x (Molar ratio of } \frac{\text{insert}}{\text{vector}}\text{)}} = \text{Amount of insert (ng)}$$

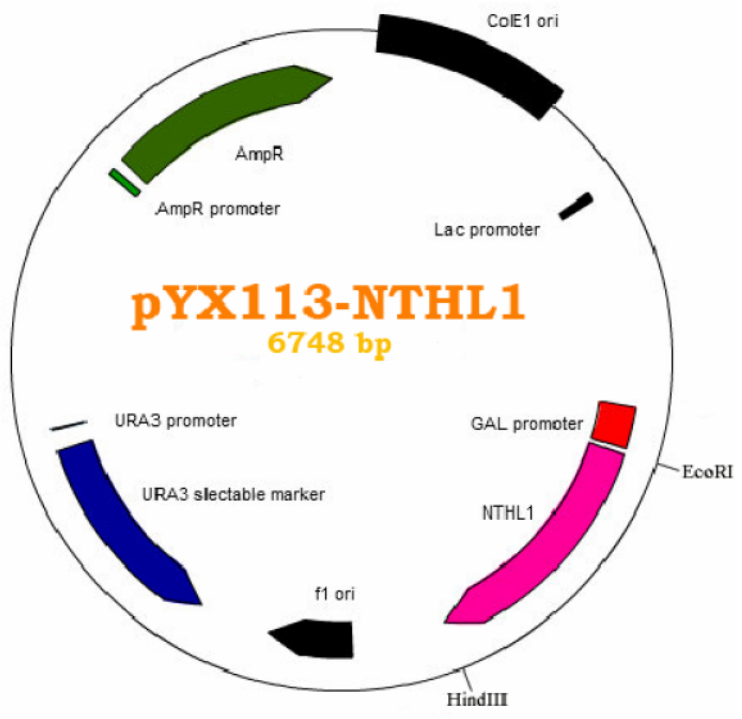

Fig. 2.2 The schematic diagram of pYX113-NTHL1 construct.

2.3.2 *E. coli* transformation

Principle

Transformation is a molecular biological method to transfer foreign genetic material (plasmid DNA) into bacterial cells. Two procedures can be used to make the bacterial cells permeable to plasmid DNA: (1) chilling cells in the presence of divalent cations, e.g. Ca^{2+}, and then heat shock at 42°C (chemical competence) or (2) shocking them with an electric field (electro-competence). In this section, *E. coli* transformation by the chemical method was used to select the *E. coli* cells with pYX113-NTHL1 plasmid and increase the plasmid amount as bacterial cells propagate very quickly.

Procedures

Preparation of chemical competent *E. coli* cells:

One colony of One Shot® TOP10 Chemically Competent *E. coli* cell was inoculated from LB agar plate into 2 mL LB broth and incubated at 37°C overnight with shaking at 250 rpm. One millilitre of cells cultured overnight was inoculated into 100 mL LB broth and incubated for about 3 hours at 37 °C with shaking at 250 rpm to obtain an OD600 reading of approximately 0.2 to 0.4 (log phase of *E. coli*). The culture was then chilled on ice for 15 minutes and centrifuged for 10 minutes at 4000 rpm at 4°C. The supernatant was discarded and the cell pellet was resuspended in 40 mL cold 0.1 M $CaCl_2$. The cells were kept on ice for 30 minutes and centrifuged for 10 minutes at 4000 rpm at 4°C. The supernatant was removed and the cell pellet was resuspended in 6 mL 0.1 M $CaCl_2$ plus 15% glycerol solution. One hundred microlitres of the cell suspension were aliquoted into sterile eppendorf tubes and stored at -80°C.

E. coli transformation:

The cells were thawed on ice and 1 μL of pYX113-NTHL1 plasmid DNA was added to the cells for each transformation. The cells were mixed gently and incubated on ice for 30 minutes. After incubation, the cells were heat-shocked for 30 seconds at 42°C followed by incubation on ice for 2 minutes. The cells were recovered by adding 250 μL pre-warmed SOC broth and shaken at 37°C for 1 hour at 225 rpm. Ten microlitres and 100 μL from each transformation were spread on a pre-warmed LB agar plate containing 100 μg/mL ampicillin and incubated overnight at 37°C to select successfully transformed clones. The identity of the clones was confirmed by analysing PCR products using agarose gel electrophoresis and sequencing.

2.3.3 Isolation of plasmid DNA

Principle

Plasmid DNA extraction is achieved in 3 parts: (1) bacterial cell growth, (2) lysis of bacterial cells and (3) plasmid DNA purification. In this project, QIAprep spin miniprep kit was used for plasmid DNA extraction. The principle of this kit is based on a modified alkaline lysis method to lyse bacterial cells, followed by adsorption of DNA onto silica in the presence of high salt. Ribonucleic acids, proteins and different impurities are removed in the washing steps and optimised buffers are used to prevent these impurities from being retained on the silica membrane. Purified plasmid DNA is finally eluted with elution buffer or DNase/RNase-free distilled water, and is ready for immediate use in downstream applications.

Procedures

Plasmid DNA extraction using QIAprep spin miniprep kit was carried out according to the manufacturer's protocol. In brief, overnight culture of *E. coli* with pYX113-NTHL1 plasmids in 5 mL LB broth was centrifuged for 15 minutes at 6000 *g* at 4°C. The pelleted bacterial cells were resuspended and lysed using different buffers. After centrifugation, the plasmid DNA was released into the supernatant, and the supernatant was then loaded onto the silica column for binding of plasmid DNA. The plasmid DNA was purified by a series of washing steps and eluted out from the column by elution buffer for further applications.

2.3.4 Sequencing

Principle

The nucleotide order of a given DNA fragment can be determined by DNA sequencing. The commonest sequencing method is the dye terminator method. In dye terminator sequencing, low concentrations of chain terminating nucleotides (called di-deoxynucleotides) labelled with different fluorescent dyes are incorporated during the extension of DNA synthesis at a specific site on the template DNA. Different DNA fragments are terminated at the positions where a di-deoxynucleotide is incorporated. These fragments are then separated according to size by capillary electrophoresis in a viscous polymer using a DNA sequencer.

Procedures

Purification of PCR products:

Seven microlitres of PCR product amplified from pYX113-NTHL1 plasmid were purified by 10 units of exonuclease I and 2 units of shrimp alkaline phosphatase.

The mixture of PCR products and enzymes was incubated for 30 minutes at 37°C and inactivated for 10 minutes at 80°C.

Cycle sequencing:

Three microlitres of purified PCR product were added in 10 µL of cycle sequencing mixture containing 2 µL of BigDye® Terminator v3.1 ready reaction mix and 1.6 pmol of primer. The cycle sequencing was carried out as follows: 1 cycle for denaturation (96°C/1 minute) followed by 25 cycles for amplification (96°C/10 seconds, 50°C/5 seconds and 60°C/4 minutes). After cycle sequencing, the final volume of the product was made up to 20 µL with sterilised MilliQ H_2O.

The primers used for determination of the DNA sequence of pYX113-NTHL1 plasmid are listed in Table 2.2.

Purification and precipitation of extension products:

Twenty microlitres of cycle sequencing product were added to 80 µL of ethanol/sodium acetate solution containing 90 mM sodium acetate, pH 4.6 and 60% ethanol. The mixture was incubated for 30 minutes at room temperature and then centrifuged for 20 minutes at maximum speed (~ 14000 rpm) in a microcentrifuge. The supernatant was removed and 250 µL 70% ethanol was added to wash the pellet. After washing, the mixture was centrifuged for 5 minutes at maximum speed and dried in SpeedVac for 10 to 15 minutes. The products were protected from light.

Table 2.2 Primers used for DNA sequencing of *NTHL1* gene-containing plasmids with or without SNPs.

Primers	Sequences (5' to 3')	Positions in *NTHL1* mRNA sequence[a]
(1) N1exppF1	ATATAAGAATTCATTATGGATGTG TAGTCCGCAGGAGTCC	20-40
(2) N1exppR1	CAATATAAGCTTTCAGAGACCCTG GGCGGC	941-958
(3) N1R2	TGTGGCTTTTCCTCGCTTCT	176-157
(4) N1F2	AGCTGTGGCACGAGATCAAT	837-856
(5) M13 forward	GTAAAACGACGGCCAG	---

a. The primers were designed from Homo sapiens *NTHL1* mRNA sequence (Accession no.: NM_002528) by using Oligo program version 6.57 (Molecular Biology Insights).

Sample resuspension:

The purified extension product was resuspended in 10 µL Hi-Di™ Formamide and incubated for 30 minutes at room temperature. Before loading, the sample was heated for 2 minutes at 95°C and placed on ice immediately. Finally, the sample was loaded into 3130 Genetic Analyser (Applied Biosystems) for size separation in polymer by capillary electrophoresis.

2.3.5 Site-directed mutagenesis

Principle

Site-directed mutagenesis is a technique to create a mutation at a specific site in a DNA molecule. The GeneTailor method used in this chapter is based on PCR with the overlapping primers. Before the mutagenesis step, the DNA (the plasmid with gene of interest) is methylated using DNA methylase and then linear PCR amplicons carrying the desired mutation are produced. The amplicons are transformed directly to *E. coli* and circularised by the host cell repair enzymes. The *Mcr*BC endonuclease is used to digest the original unmutated methylated DNA plasmid templates. The principle is illustrated in Fig. 2.3.

Procedures

The procedures were carried out following the GeneTailor™ site-directed mutagenesis system manufacturer's manual and is only briefly described here.

Methylation reaction:

One hundred microlitres pYX113-NTHL1 plasmid DNA were added to the

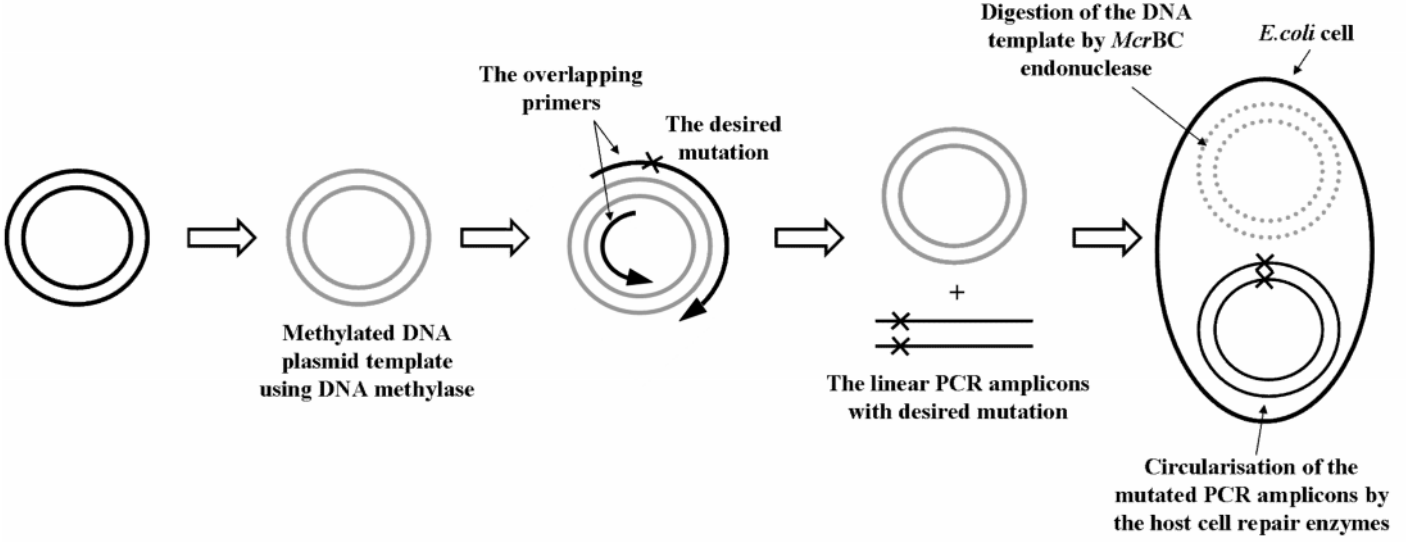

Fig. 2.3 The principle of site-directed mutagenesis. (Adapted and modified from http://www.invitrogen.com/site/us/en/home/Products-and-Services/Applications/Cloning/Mutagenesis/GeneTailor/How-Gene-Tailor-Works.html)

methylation mixture, which contains methylation buffer, 1X SAM buffer and 4 units of DNA methylase. The sample was mixed and incubated for 1 hour at 37°C.

Mutagenesis reaction:

The linear mutated amplicons were amplified from the methylated plasmid DNA templates using the overlapping primers with the desired mutations (FS105 or D239Y). In brief, 12.5 ng of methylated plasmid DNA was amplified by 0.5 µM of primers listed in Table 2.3 in 25 µL PCR master mix with 2 mM of $MgCl_2$ and 0.5 units of Phusion high-fidelity DNA polymerase. The amplification cycle was carried out as follows: 1 cycle for denaturation (98°C/30 seconds) followed by 35 cycles for amplification (98°C/30 seconds, 60°C/1 minute and 72°C/4 minutes) and final extension of 10 minutes at 72°C.

E. coli transformation:

The linear amplicons and the methylated plasmid DNA were transformed into the One-Shot® MAX Efficiency® DH5α™-T1R competent cells.

Clone confirmation:

The selected colonies from the LB agar plates were examined and analysed by sequencing to confirm the presence of mutated plasmids with desired SNPs, pYX113-FS105 and pYX113-D239Y, using the primers listed in Table 2.2. The clones with mutated plasmids were then selected and the mutated plamids were extracted for yeast transformation.

Table 2.3 Primers used in site-directed mutagenesis of pYX113-NTHL1 plasmid.

Primers	Sequences (5' to 3')[a,b]	Positions in *NTHL1* mRNA sequence[c]
(1) NTH1FS105_ MpF1M	AACATACGTGCCATGAGGA AC[AAAA]GGATGCACC	311-345 (deletion of A base at 332)
(2) NTH1FS105_ pR1M	TCCTCATGGCACGTATGTTG ACGAGCTGTT	300-329
(3) D239Y_ MpF1M	ACTGTGTCTGGCATAGCAG TG[T]ACACGCATGTGCAC	713-748 (G → T at 734)
(4) D239Y_ pR1M	ACTGCTATGCCAGACACAG TGCCCCAGGCCAC	701-732

a. The boxed sequences are the sites for site-directed mutagenesis of the desired SNPs.
b. The underlined bases are the desired mutated bases without changing the translated amino acids.
c. The primers were designed from Homo sapiens *NTHL1* mRNA sequence (Accession no.: NM_002528) by using Oligo program version 6.57 (Molecular Biology Insights).

2.3.6 Yeast transformation and gene expression

Principle

The modified lithium acetate method was used for yeast transformation in this project.[247-249] In this method, a lithium acetate solution with the plasmid DNA to be transformed and excess carrier DNA is added to yeast chemical competent cells. The introduced plasmid DNA is allowed to enter the cells by heat shocking and the transformants containing the introduced DNA are selected on the selective agar, i.e. appropriate synthetic dropout medium. The pYX113 vector used in this chapter is a low-copy number plasmid with *GAL1* promoter, so the target protein can only be expressed from the introduced plasmid in yeast cells under galactose induction, i.e. culturing the yeast cells in galactose-containing medium as the *GAL1* promoter is repressed in the presence of glucose.[250,251]

Procedures

Preparation of chemical competent yeast cells:

Several colonies were inoculated into 50 mL of yeast peptone dextrose broth and vortexed vigorously for 5 minutes to disperse any clumps. The yeast cell culture was incubated at 30°C for 16-18 hours with shaking at 250 rpm to stationary phase (OD_{600}>1.5). Ten millilitres of the yeast cells cultured overnight were then transferred to 100 mL of yeast peptone dextrose broth and incubated at 30°C for 3 hours with shaking (230 rpm) until the log phase (OD_{600} ~0.4-0.6) was reached. The culture was centrifuged at 1000 *g* for 5 minutes at room temperature. The supernatants were discarded and the cell pellets were resuspended in 15 mL sterile distilled H_2O. The centrifugation step was repeated and the supernatant discarded. The cells were finally resuspended in 500 µL freshly prepared sterile

Tris-EDTA/lithium acetate solution.

Yeast transformation:

Plasmid DNA pYX113-NTHL1, pYX113-FS105 and pYX113-D239Y were transformed individually to *NTG2*-knockout yeast cells; *NTG2* is the yeast homologue to human *NTHL1*. One hundred nanograms each of these plasmid DNA and 100 μg of DNA sodium salt from salmon testes were added to 100 μL of yeast competent cells with 600 μL of polyethylene glycol 3350/lithium acetate solution. The cell mixture was mixed by vortexing at high speed for 10 seconds and incubated at 30°C for 30 minutes with shaking at 200 rpm. Seventy microlitres of dimethyl sulphoxide were added to the cell mixture and mixed by gentle inversion. The cell mixture was heat-shocked for 15 minutes at 42°C and chilled on ice for 2 minutes. The cells were collected by centrifugation for 5 seconds at 14000 rpm at room temperature. The supernatant was removed and the cells were resuspended in 500 μL of 1X Tris-EDTA buffer. One hundred microlitres of the resuspended cells were plated on yeast synthetic dropout agar, which contains no uracil for selection of colonies with desired plasmids, and incubated at 30°C until colonies were seen. The colonies were selected and confirmed by analysing PCR products using agarose gel electrophoresis and sequencing using N1exppF1 and N1exppR1 (Table 2.2).

Gene expression in yeast cells:

The selected clone with introduced plasmid DNA was incubated in yeast synthetic dropout medium at 30°C with shaking at 200 rpm for 16-18 hours in shaking incubator. The selected clone in glucose-containing broth was centrifuged at 1500 *g* for 5 minutes at room temperature and the broth was discarded. The cell

pellet was then sub-cultured into 50 mL galactose induction medium, which contains galactose for gene expression from the pYX113 plasmids, until an optical density of 0.4 at 600 nm was obtained. The cells were incubated at 30°C with shaking at 200 rpm and were collected at different time points. The cell lysates from different time points were analysed by Western blotting and the yeast cells with pYX113-NTHL1, pYX113-FS105 and pYX113-D239Y plasmids were finally subjected to DNA-damaging reagents.

2.3.7 Treatment with hydrogen peroxide and methyl methanesulphonate

Principle

H_2O_2 and MMS are oxidising and alkylating agents respectively. H_2O_2 produces oxidised bases and MMS methylases both guanine (7-methylguanine) and adenine (3-methyladenine) to cause base mispairing and replication blocks.[252] DNA damage caused by these agents is repaired by the BER pathway. NTHL1 functions both as a BER glycosylase and as a AP lyase. NTHL1 is also responsible for repairing BER DNA damage induced by both DNA-damaging agents.

Procedures

Selected yeast cells were inoculated in 5 mL of yeast synthetic dropout medium overnight. Approximately 2.5×10^7 cells were sub-cultured to 5 mL of fresh yeast synthetic dropout or galactose induction medium. Cells were incubated until approximately $2–3 \times 10^7$ cells/mL was obtained, which were determined by a haematocytometer using trypan-blue exclusion assay. The yeast cell samples were

mixed with MMS at 0.02% or 0.2%, and H_2O_2 at 0.05 mM or 0.5 mM and incubated for 20 minutes and 30 minutes respectively. The samples treated with MMS were neutralised by 5% w/v sodium thiosulphate. All samples were then washed twice with sterile distilled water and centrifuged. The samples were used immediately for cell survival assay or recovered in yeast synthetic dropout medium for 2 hours and fixed for cell cycle analysis by flow cytometry to investigate the SNPs' effects on the NTHL1 protein.

2.3.8 Cell survival assay

Principle

Cell survival was determined using the trypan blue exclusion method. The number of viable cells present in a cell suspension was determined. The principle of this assay is based on the exclusion of trypan blue dye by live cells, which possess an intact cell membrane and is impermeable to trypan blue dye, whereas dead cells with compromised membranes absorb the dye. Therefore, a clear cytoplasm is seen in viable cells, but a blue cytoplasm would be observed in nonviable cells under microscopic examination. In this study, the yeast cell suspensions after treating with DNA-damaging agents were mixed with trypan blue dye and subjected to improved Neubauer Chamber for counting the number of viable cells.

The percentage (%) of cell viability is calculated as follows:

$$\% \text{ of cell viability} = \left(\frac{\text{mean number of viable cells of sample}}{\text{mean number of viable cells of control}}\right) \text{ x } 100$$

Procedures

For yeast cell survival test, yeast cell suspensions of each DNA-damaging reagent treated samples were diluted in 1:10 in 1 mL distilled water. Fifty

microlitres of the diluted sample were mixed with 50 µL 0.4% w/v trypan-blue. Ten microlitres of the stained samples were loaded into each side of the improved Neubauer Chamber (Hausser Scientific, Horsham, PA, USA). The number of unstained yeast cells was counted in five 1 x 1 mm^2 squares. The number of unstained yeast cells, which is the number of viable cells of the counted yeast suspension sample, was calculated by the following equation 2* and finally the percentage of viable cells of the different sampels were calculated.

***Equation 2:**

$$\text{Number of yeast cells (cells/mL)} = \text{Number of cells counted in 5 squares x 5 x dilution factor x } 10^4$$

2.3.9 Western blotting

Principle

Western blotting is a gel electrophoresis technique to detect specific proteins. Denatured proteins are separated in the gel according to the length of the polypeptide. The proteins on the gel are transferred onto a membrane. Finally, the target protein is probed by its specific antibody on the membrane and detected by chemiluminescence.

Procedure

Yeast cell lysate preparation:

Yeast cell samples treated by different DNA-damaging agents were collected, washed in ice-cold PBS and concentrations were adjusted by measuring the optical density at 600 nm so that each sample had a similar cell density. The samples were then lysed in 100 µL yeast cell sample buffer and boiled for 5 minutes at 95°C. The boiled samples were centrifuged at 14000 *g* for 5 minutes and the supernatants

were collected.

Gel electrophoresis:

Fifteen microlitres of each supernatant and Novex sharp pre-stained protein standard were separated by sodium dodecyl sulphate polyacrylamide gel electrophoresis. The gel consisted of 4% stacking gel and 10% separating gel. The samples and the marker were electrophoresed at 80V in stacking gel and at 100V in separating gel using mini-PROTEAN 3 system (Bio-Rad laboratories, Hercules, CA, USA) with running buffer at room temperature. The time of electrophoresis was 2 hours for separating the NTHL1 protein (~34.4 kDa), or actin (ACT1, 41.7 kDa), from other proteins.

Gel blotting:

The separated proteins were transferred onto polyvinylidene fluoride membranes in transfer buffer for 2 hours at 70V and 4°C using Mini Trans-Blot cell (Bio-Rad laboratories).

Membrane blocking and primary antibody staining:

The membrane was blocked with 10 mL 5% w/v non-fat milk in 1X Tris buffered saline with Tween 20 (TBST) buffer with shaking for 1 hour at room temperature. To examine protein expression, NTHL1 protein was detected by probing with 1:1000 human NTH1 MAb (Clone 208521), mouse IgG antibody in 5 mL 2% w/v bovine serum albumin and ACT1 protein by 1:1000 actin (C-11) antibody in 5 mL 2% w/v bovine serum albumin. The membranes were incubated with shaking for 16 hours at 4°C.

Washing, secondary antibody staining and signal detection:

Before secondary antibody staining, the membrane was washed with shaking in 10 mL 1X TBST buffer (3 x 10 minutes) at room temperature. Corresponding horseradish peroxide-labelled scondary mouse antibody in 5 mL 5% w/v non-fat milk for NTHL1 primary antibody-stained membranes or rabbit antibody in 5 mL 5% w/v non-fat milk for ACTB primary stained-membranes were then used. The membranes were incubated with secondary antibodies for 1 hour at room temperature. The final complexes on membranes were visualised by enhanced chemiluminescence autoradiography.

2.3.10 Yeast cell cycle analysis by flow cytometry

Principle

The improved flow cytometric analysis of the budding yeast cell cycle by Haase & Reed was used in this experiment.[253] SYTOX Green, which is a nucleic acid-specific stain, is widely used for cell cycle analysis as the stain can increase the fluorescence signal more than 500 fold after binding to nucleic acids. It is necessary to use RNAse to eliminate the RNA, which is not of interest in cell cycle analysis, since SYTOX Green can bind both DNA and RNA.[254] In this project, the cell cycle stages of yeast cell cultures were monitored to investigate the yeast cells' ability to pass cell cycle checkpoints after DNA-damaging treatments.[255] This ability can indirectly reflect the DNA repair ability of the yeast cells.

Procedure

Yeast cell fixation:

Ten million cells from an exponentially growing yeast culture (optical density of

0.4 at 600 nm) were centrifuged for 5 minutes at 2000 rpm and the supernatant was removed. One millilitre of 70% ethanol was added to the cells and resuspended by vortexing (cells can be stored at 4°C indefinitely). Three millilitres of 50 mM sodium citrate were added to 3×10^6 cells, i.e 300 µL of the cell suspension, mixed and centrifuged for 5 minutes at 2000 rpm. Sodium citrate chelates divalent ions to prevent DNA degradation by DNases in the samples and thus the resolution of flow cytometry analysis is improved.

RNA digestion:

The supernatant of each fixed yeast sample was discarded and the fixed yeast cell pellet was resuspended in 500 µL of 50 mM sodium citrate containing 0.1 mg/mL RNase A. The fixed cell samples were incubated for 2 hours at 37°C.

DNA staining:

Five hundred microlitres of 50 mM sodium citrate containing 2 µM SYTOX Green were added to the RNA digested sample, thus the final concentration of SYTOX Green nucleic acid stain in the sample was 1 µM. The sample was sonicated for 45 seconds before being analysed by flow cytometry (Beckman Coulter, Brea, CA, USA).

Flow cytometry setting for yeast cell cycle analysis

Forward scatter, side scatter, AUX and FL1 channel were used in the settings for yeast cell cycle analysis. The volts and gains of the channels were set respectively as follows: FS were 674 and 5, SS were 490 and 20, AUX were 227 and 1, and FL1 were 391 and 2. One million cells were counted and different scatter plots of

different channels based on measurements of different parameters were plotted for analysis.

2.4 Results

2.4.1 Confirmation of the human *NTHL1* cDNA (insert) and pYX113 vector sequences

2.4.1.1 Using agarose gel electrophoresis

The human *NTHL1* cDNA was reverse-transcribed from an anonymous human RNA sample and amplified by PCR. The pYX113 vector was extracted from *E. coli* bacterial colonies after transformation. The sizes of the *NTHL1* cDNA PCR product (the predicted size is 939 bp) and the linearised pYX113 vector (the predicted size is 5806 bp after linearisation using EcoRI and HindIII) were then confirmed by agarose gel electrophoresis. As expected, the gel images show the ~950 bp DNA band from the *NTHL1* RT-PCR product and ~5000 bp DNA band from the plasmid DNA sample of *E. coli* cells transformed with pYX113 vector (Fig. 2.4).

2.4.1.2 Using sequencing analysis

The whole sequence of the human *NTHL1* cDNA and part of the pYX113 vector sequence were further verified by sequencing using different primers listed in Table 2.2. The *NTHL1* cDNA sequence was identical to the coding sequence of *NTHL1* mRNA reference sequence (accession no.: NM_002528), as indicated by alignment using the Kalign (2.0) alignment tool (http://www.ebi.ac.uk/Tools/kalign/). The partial sequences of the pYX113 vector were also identical to the manufacturer's vector map.

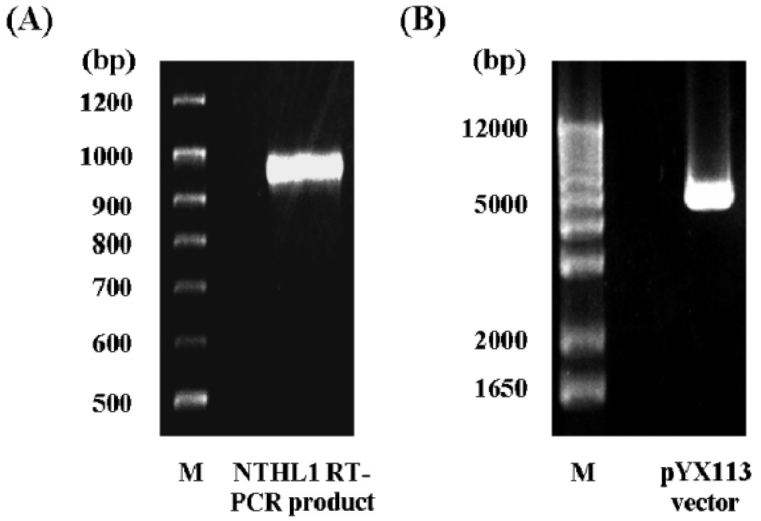

Fig. 2.4 Examination of the sizes of *NTHL1* RT-PCR product and pYX113 vector by agarose gel electrophoresis. (A) The size of the *NTHL1* RT-PCR product (~939 bp). Lane M: Fermentas GeneRuler DNA ladder mix. (B) The size of the pYX113 vector after linearisation (~5806 bp). Lane M: Invitrogen 1 kb plus DNA ladder.

2.4.2 Confirmation of the sequence of the pYX113-NTHL1 plasmid

Clones with the pYX113 vector are ampicillin resistant, and several bacterial clones which grew on LB agar with ampicillin were selected for plasmid DNA preparation. The presence of the human *NTHL1* cDNA insert in the extracted plasmid DNA samples were then confirmed by PCR. The *NTHL1* PCR product from the extracted plasmid DNA samples (~939 bp) and the extracted plasmid after linearisation using HindIII (~6745 bp) are shown in Fig. 2.5. Four out of 5 plasmid samples contained the *NTHL1* cDNA sequence, and the ligation efficiency of the insert and vector was about 80%.

The sequence of the selected pYX113-NTHL1 plasmid was further confirmed by sequencing using M13 forward primer, N1exppF1, N1exppR1, N1F2 and N1R2 primers. The sequencing results are attached in Appendix 1. Multiple alignment was performed and the result showed that all obtained sequences were identical to their corresponding parts of the predicted pYX113-NTHL1 plasmid sequence.

2.4.3 The presence of the desired SNPs in the pYX113-NTHL1 plasmid

FS105 and D239Y of *NTHL1* were individually introduced using site-directed mutagenesis reactions into the human *NTHL1* cDNA region in the pYX113-NTHL1 plasmids. The pYX113-NTHL1 plasmids with the introduced SNPs, i.e. pYX113-FS105 and pYX113-D239Y plasmids, were examined by sequencing and confirmed to carry the SNPs at the correct positions in the plasmids (Fig. 2.6).

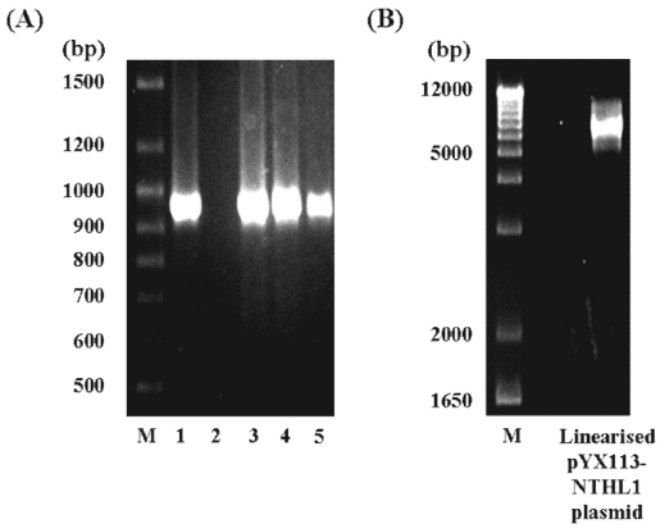

Fig. 2.5 **Examination of the plasmid DNA samples by agarose gel electrophoresis.** (A) The amplification of *NTHL1* cDNA sequence from the extracted plasmid DNA samples of different bacterial clones. Lane M: Fermentas GeneRuler DNA ladder mix; Lane 1 to Lane 5: The *NTHL1* cDNA PCR products (~939 bp) from the extracted plasmid DNA samples of Clone 1 to 5. Clone 2 contains pYX113 vector without *NTHL1* cDNA sequence and other clones contain pYX113 vector with the cDNA sequence (the desired plasmid). (B) The extracted pYX113-NTHL1 plasmid after HindIII linearisation with expected size (~6745 bp). Lane M: Invitrogen 1 kb plus DNA ladder.

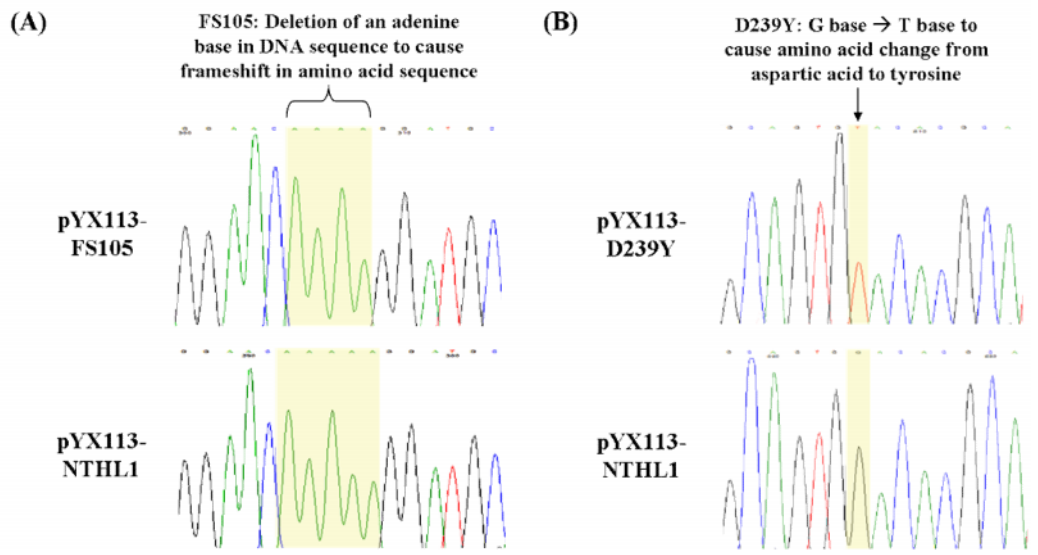

Fig. 2.6 **Confirmation of desired SNPs in the plasmids by sequence analysis.** (A) Amino acid position 105 in pYX113-FS105 and pYX113-NTHL1 plasmids sequenced with N1exppF1 primer. (B) Amino acid position 239 in pYX113-D239Y and pYX113-NTHL1 plasmids sequenced with N1exppR1 primer.

The DNA sequences obtained from sequence analysis were translated and aligned with the human NTHL1 protein reference sequence (accession no.: NP_002519.1) and the desired changes in amino acid are observed in the alignment results (Fig. 2.7 and Fig. 2.8).

2.4.4 Selection of the yeast clones containing desired plasmids (pYX113-NTHL1, -FS105 and -D239Y)

Several yeast colonies, which grew on yeast synthetic dropout agar, were selected for colony PCR to confirm the presence of the desired plasmids in the yeast cells. The *NTHL1* PCR products with correct size from the yeast clones 1 to 5 are shown in Fig. 2.9 and the plasmid contained in each of the yeast clones were further verified by sequencing. Yeast clones with pYX113 vector, pYX113-NTHL1, pYX113-FS105 and pYX113-D239Y plasmids were individually stored in yeast synthetic dropout agar plates at 4°C and labelled as “control yeast cells”, “y+hsNTHL1”, “y+hsFS105” and “y+hsD239Y” respectively. The yeast cells were sub-cultured at regular intervals until use.

2.4.5 SNPs’ predicted effects on the human NTHL1 protein

It is predicted that the FS105 SNP of the *NTHL1* gene results in a premature stop codon at the 136 amino acid position (by Transeq DNA sequence translation tool: http://www.ebi.ac.uk/Tools/emboss/transeq/) (Fig. 2.7). The early termination of *NTHL1* coding sequence leads to the loss of five conserved protein domains: (1) active sites, (2) substrate binding pocket, (3) minor groove reading motif,

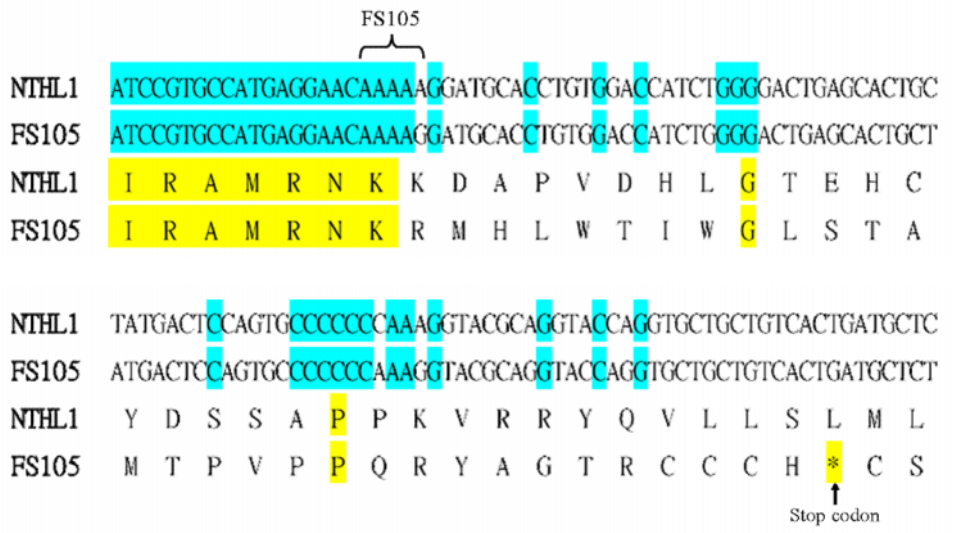

Fig. 2.7 **Alignment result of the NTHL1 protein reference sequence (accession no.: NP_002519.1) and the DNA sequence of the pYX113-FS105 plasmid.**

Fig. 2.8 **Alignment result of the NTHL1 protein reference sequence (accession no.: NP_002519.1) and the DNA sequence of the pYX113-D239Y plasmid.**

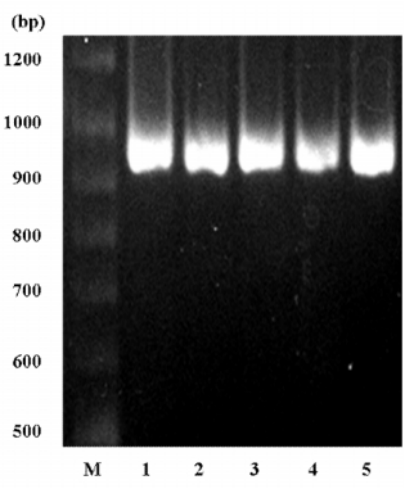

Fig. 2.9 The *NTHL1* PCR products (~939 bp) from yeast clones 1-5.

(4) helix-hairpin-helix signature motif and (5) iron-sulphur binding domain in DNA-(apurinic or apyrimidinic site) lyase. As a result, a truncated NTHL1 protein would be produced.

Another SNP – D239Y causes the change from aspartic acid to tyrosine. Asp239 of NTHL1 protein is one of the conserved active sites and inside a structural residue from the prediction of a ConSeq tool (http://conseq.tau.ac.il/index.html) (Fig. 2.10).[256] From the study of human 8-oxoguanine DNA glycosylase and its orthologues, the invariant aspartic acid residue is suggested to activate a catalytic nucleophile, a lysine residue (K), and assist in glycosylase or AP-lyase activity.[257] In addition, this SNP is predicted to be "damaging" and was proposed as an excellent candidate for disease-predisposition investigations in Savas *et al.'s* study.[258] Since aspartic acid carries a negative charge but tyrosine is a neutral molecule with a bulky side chain, the D239Y polymorphism may affect both the structure and DNA repair activity of the NTHL1 protein. The characteristics of aspartic acid and tyrosine are summarised in Table 2.4.[259,260]

2.4.6 Expression of human NTHL1 protein expression at different time points after galactose induction

The human NTHL1 protein was expressed in y+hsNTHL1 cells from 2 hours to 8 hours after the GAL promoter of the plasmid was induced by adding galactose in yeast culture medium, i.e. the galactose induction. No expression of the protein was seen in the cells without galactose induction (Fig. 2.11).

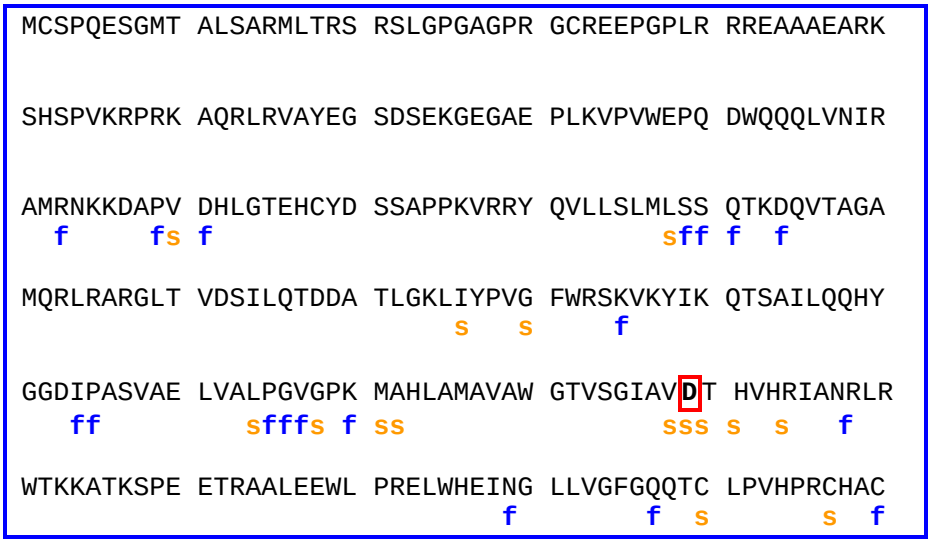

Legend:

f - A predicted functional residue (highly conserved and exposed).

s - A predicted structural residue (highly conserved and buried).

D - Amino acid position 239

Fig. 2.10 Identification of functionally and structurally important residues in NTHL1 protein sequence from the ConSeq tool.

Table 2.4 **Characteristics of aspartic acid and tyrosine.** (Adapted and modified from reference 258 and 259)

Amino acid	Side chain polarity	Side chain charge at pH 7.4	Hydropathy index[a]	Structure
(1) Aspartic acid (D)	Polar	Negative	-3.5	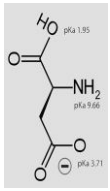
(2) Tyrosine (Y)	Polar	Neutral	-1.3	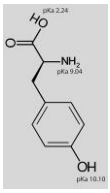

a. The hydropathy index is calculated using Kyte and Doolittle's method.

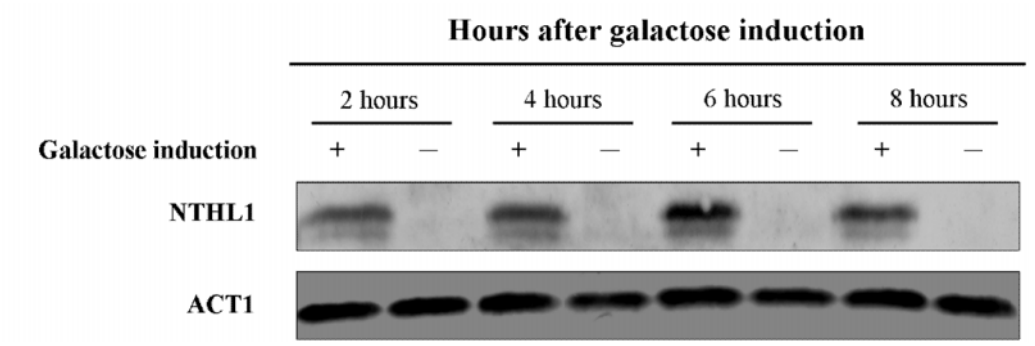

Fig. 2.11 Detection of human NTHL1 proteins in y+hsNTHL1 cells at different time points after galactose induction. NTHL1 protein is ~35 kDa. ACT1 is actin (~42 kDa), a structural protein involved in cell polarisation, endocytosis, and other cytoskeletal functions, which acts as loading control for the Western blotting of *S. cerevisiae* cell lysates.

2.4.7 The cell growth curves of yeast cells with different plasmids

The amount of starting yeast cell numbers was optimised to obtain 2-3 $\times$ 10^7 cells/mL after 6 hours of sub-culturing from overnight culture. Yeast cells with galactose induction grew much slower than the cells without the induction (Fig. 2.12).

2.4.8 The human NTHL1 protein expression in yeast cells after galactose induction

Different forms of human NTHL1 proteins are expressed in the y+hsNTHL1, y+hsFS105 and y+hsD239Y cells in low-copy numbers when induced with galactose. In Fig. 2.13, the Western blot shows that no human NTHL1 proteins were expressed in any cells under normal culturing conditions. After galactose induction for 6 hours, no NTHL1 protein expression was present in the control yeast cells and y+hsFS105 cells. However, the NTHL1 protein was detected in y+hsNTHL1 and y+hsD239Y cells by Western blotting.

2.4.9 Yeast cell viability after treatment with DNA damaging agents

All yeast cells with different plasmids had similar viability after treatment with DNA damaging agents (Fig. 2.14). Yeast cells treated with MMS had a higher survival rate when compared to cells treated with H_2O_2.

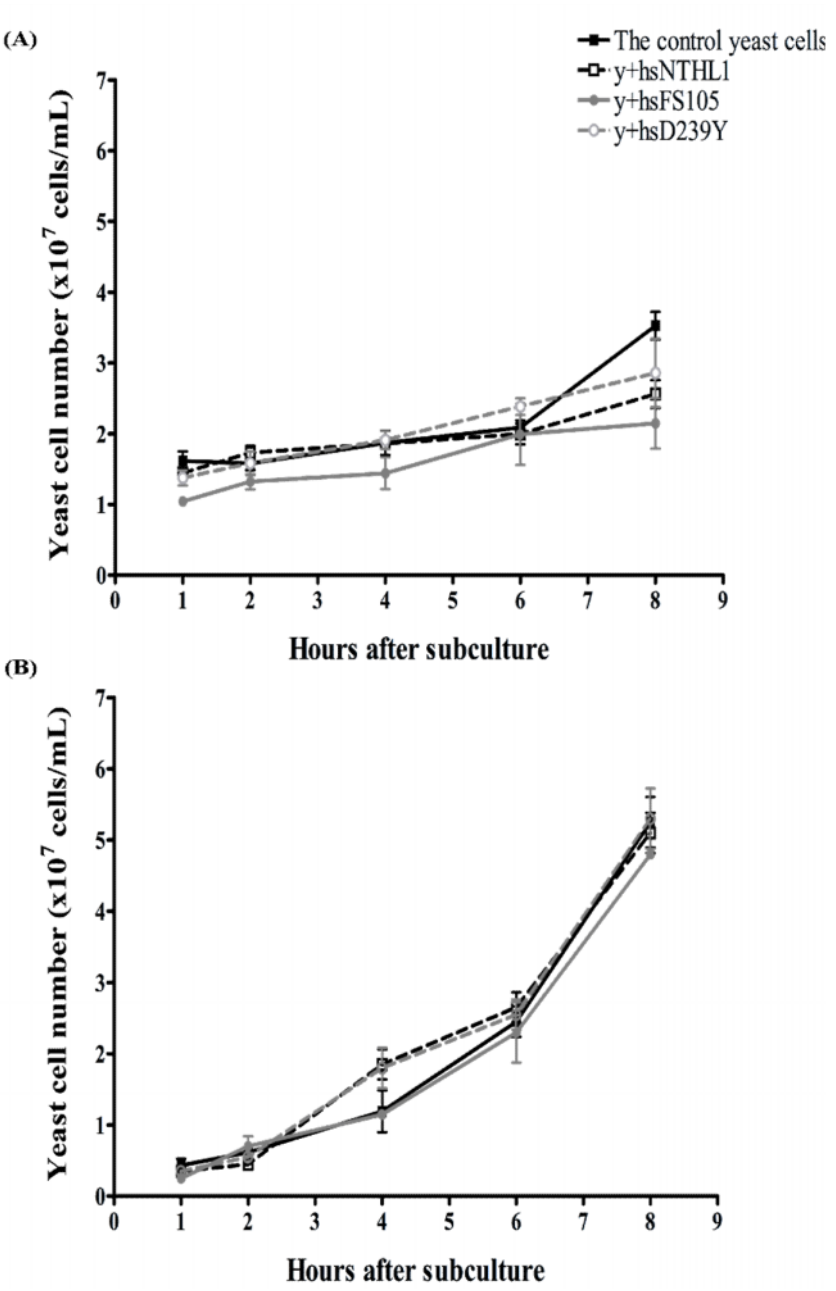

Fig. 2.12 **The yeast cell growth curves with or without galactose induction.** (A) The yeast cells were incubated in galactose induction medium. (B) The yeast cells were incubated in glucose-containing yeast synthetic dropout medium. Yeast cells without the plasmid are the control yeast cells, with pYX113-NTHL1 plasmid are y+hsNTHL1, with pYX113-FS105 plasmid are y+hsFS105 and with pYX113-D239Y are y+hsD239Y. Data are expressed as mean±SD of three independent experiments.

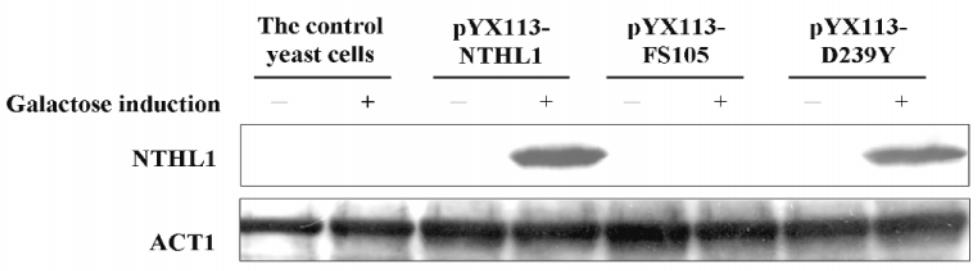

Fig. 2.13 Detection of human NTHL1 proteins in yeast cells with different plasmids before and after 6-hour galactose induction. ACT1 acts as loading control for the Western blotting of *S. cerevisiae* cell lysates.

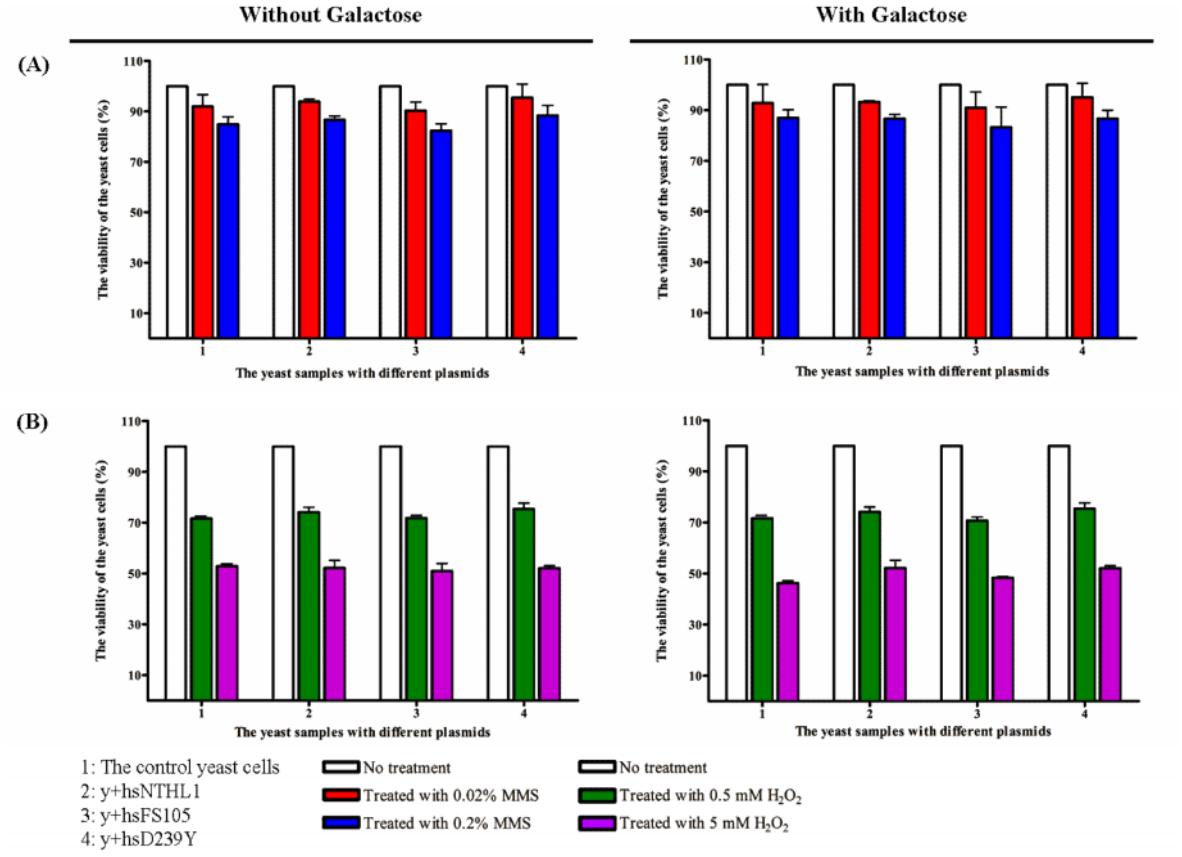

Fig. 2.14 **Yeast cell viability after treatment with DNA damaging agents (with or without galactose induction).** (A) Yeast cells with different plasmids treated with MMS. (B) Yeast cells with different plasmids treated with H_2O_2. The data are presented as mean + SD of two independent experiments. Yeast cells without the plasmid are the control yeast cells, with pYX113-NTHL1 plasmid are y+hsNTHL1, with pYX113-FS105 plasmid are y+hsFS105 and with pYX113-D239Y are y+hsD239Y.

2.4.10 Yeast cell cycle analysis

2.4.10.1 Treatment with low-dose methyl methanesulphonate

When yeast cells were cultured without galactose induction, it was found that there was a slight increase in the number of cells in the G1 phase. Cells cultured with galactose induction showed similar cell cycle patterns as their untreated control after 2 hours of 0.02% MMS treatment (red lines in Fig. 2.15 and Fig. 2.16).

2.4.10.2 Treatment with high-dose methyl methanesulphonate

Two hours after removal from 0.2% MMS, the cell cycle patterns of all yeast cells were shown to be arrested in the S phase if they had not received galactose induction. Some yeast cells, including y+hsNTHL1 and y+hsD239Y, were also arrested in the G1 phase. In contrast, the cell cycle patterns of the yeast cells were different if the cells were induced with galactose. The control and y+hsFS105 yeast cells showed obvious S phase arrest, but both the y+hsNTHL1 and y+hsD239Y cells escaped from cell cycle arrest and show the same cell cycle patterns as untreated cells (blue lines in Fig. 2.15 and Fig. 2.16).

2.4.10.3 Treatment with low-dose hydrogen peroxide

Without galactose induction, different yeast cells were all arrested in S phase and an increase in G2/M phase was observed in the control yeast cells after 2 hours of 0.5 mM H_2O_2 treatment. In contrast, the cell cycle patterns remained unchanged in all yeast cells. These results are shown in Fig. 2.17 (green lines).

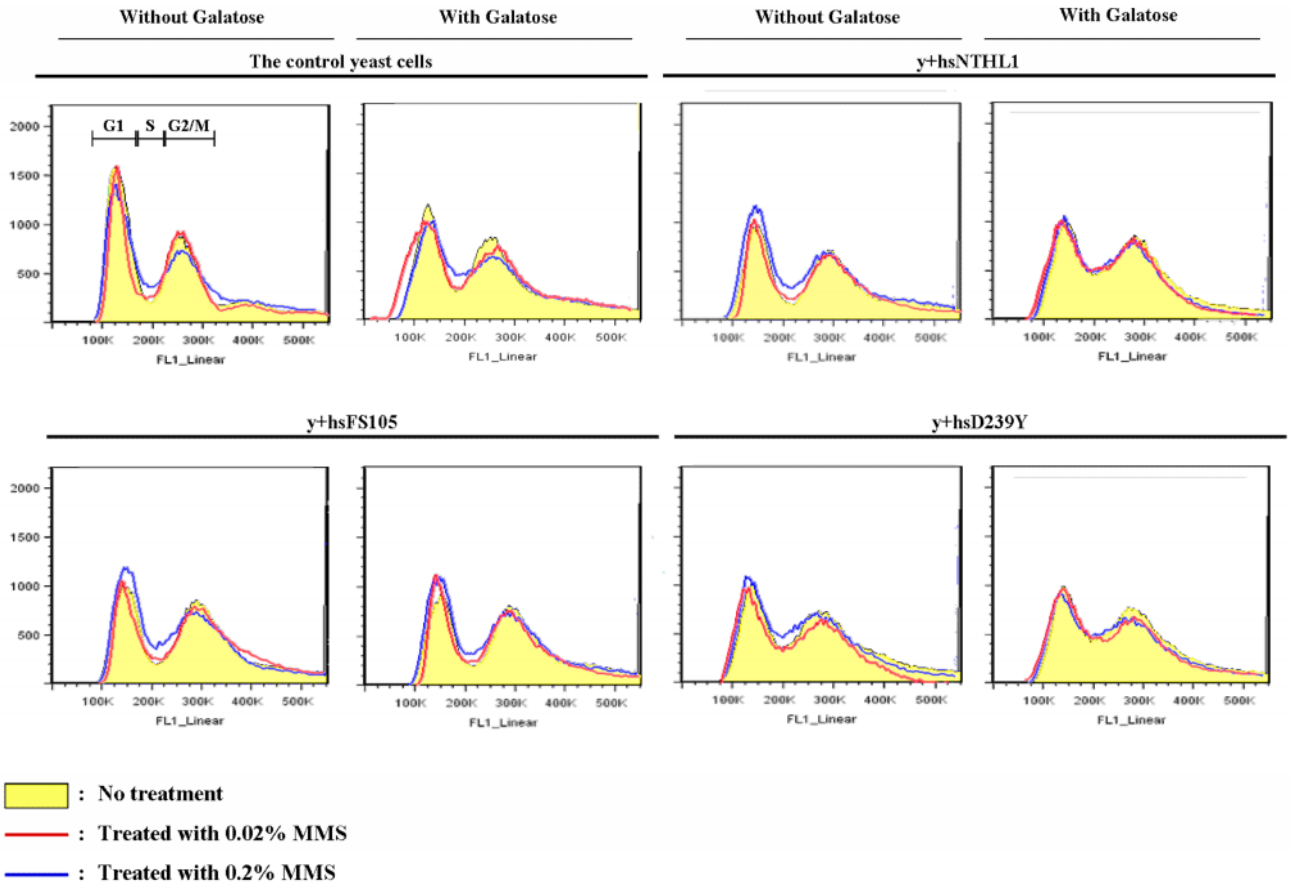

Fig. 2.15 **Cell cycle patterns after 2 hours of treatment with 0.02% and 0.2% MMS.** Yeast cells without the plasmid are the control yeast cells, with pYX113-NTHL1 plasmid are y+hsNTHL1, with pYX113-FS105 plasmid are y+hsFS105 and with pYX113-D239Y are y+hsD239Y. The distribution of cells in G1, S and G2/M phases of the cell cycle are indicated.

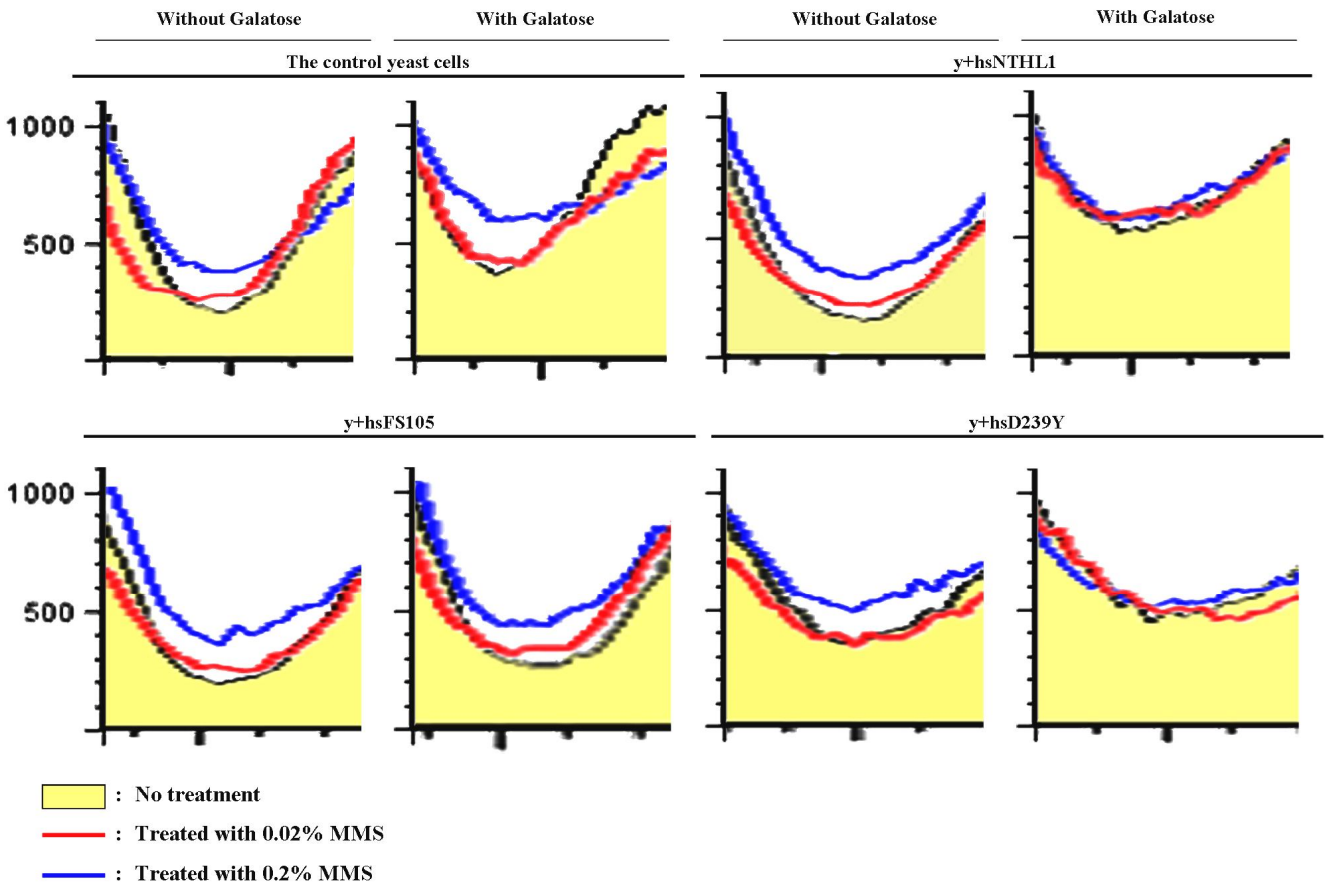

Fig. 2.16 **S-phase patterns after 2 hours of 0.02% and 0.2% MMS treatment.** Yeast cells without the plasmid are the control yeast cells, with pYX113-NTHL1 plasmid are y+hsNTHL1, with pYX113-FS105 plasmid are y+hsFS105 and with pYX113-D239Y are y+hsD239Y.

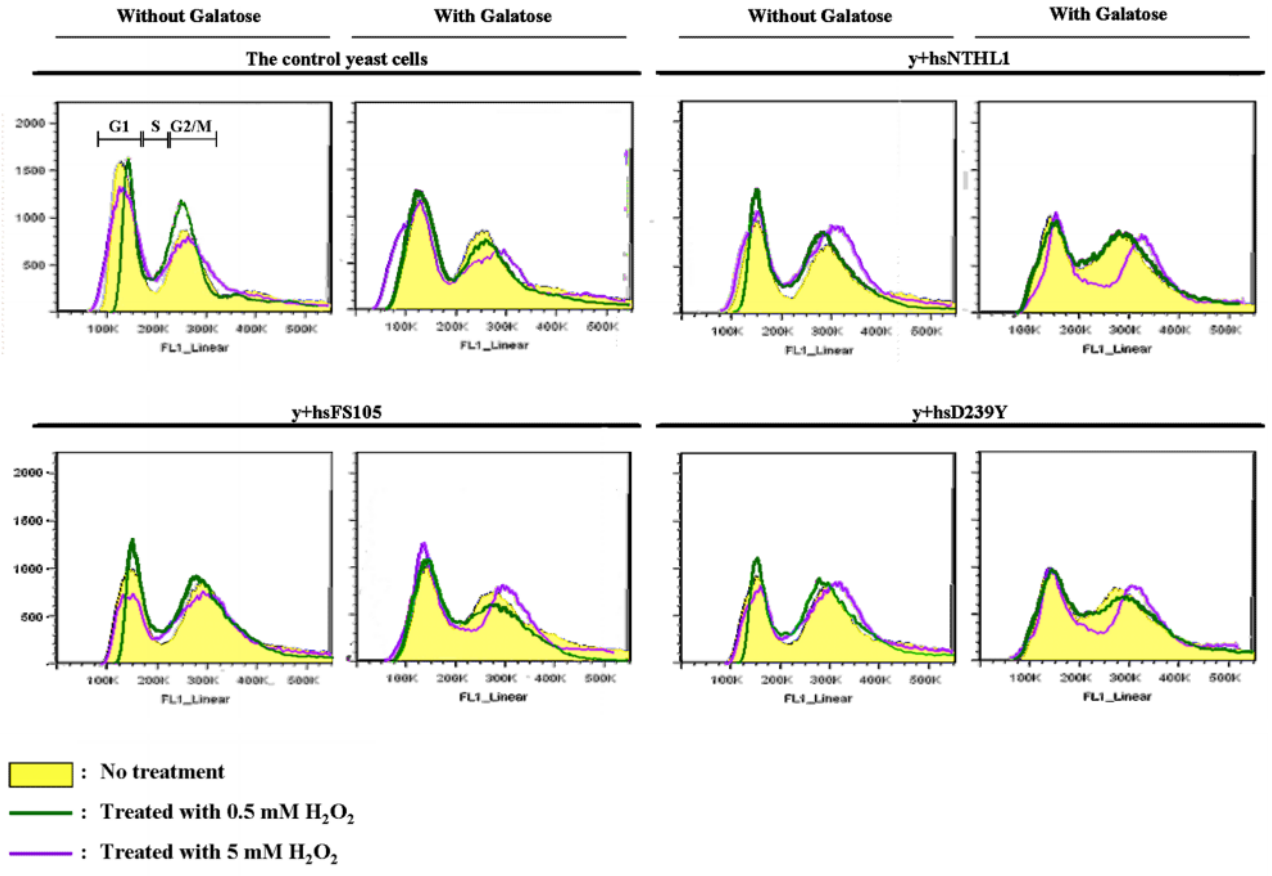

Fig. 2.17 **Cell cycle patterns after 2 hours of treatment with 0.5 mM and 5 mM H_2O_2.** Yeast cells without the plasmid are the control yeast cells, with pYX113-NTHL1 plasmid are y+hsNTHL1, with pYX113-FS105 plasmid are y+hsFS105 and with pYX113-D239Y are y+hsD239Y. The distribution of cells in G1, S and G2/M phases of the cell cycle are indicated.

2.4.10.4 Treatment with high-dose hydrogen peroxide

After 2 hours of the genotoxic treatment, the yeast cells without galactose induction were found to be slightly more in the S phase. A shift in the G2/M peaks was observed in the yeast cells that were induced with galactose (purple lines in Fig. 2.17).

2.5 Discussion

In this part of study, two SNPs of human *NTHL1* were examined for their effects on the cytotoxicity and cell cycle pattern after MMS and H_2O_2 treatments in *NTG2*- knockout *S. cerevisiae*. *NTHL1* is the human homologue of yeast *NTG2* and these enzymes repair similar DNA adducts (Table 1.2 and Table 1.3).[261] The examination of SNPs' effects was achieved by the transformation of yeast expression vectors containing wild-type (WT) and mutated *NTHL1* coding sequence. The introduced plasmids included pYX113-NTHL1 (WT), pYX113-FS105 (mutated) and pYX113-D239Y (mutated). The NTHL1 expression in y+hsNTHL1 yeast cells was maximal after 6 hours of galactose induction (Fig. 2.11). Yeast cells in galactose-containing induction medium grew slower than those in glucose-containing yeast synthetic dropout medium as galactose is a "non-conventional" carbon source for yeast growth and therefore adaptation time in an induction medium is required.[262,263] The starting numbers of yeast cells were optimised to ensure sufficient cells after 6 hours of subculture for MMS and H_2O_2 treatments.

The NTHL1 expression from different plasmids after 6 hours of subculture with

or without galactose induction was also confirmed by Western blotting (Fig. 2.13). From the Western blot, human NTHL1 identified by the NTHL1 antibody was shown to be expressed in y+hsNTHL1 and y+hsD239Y yeast cells. However, no NTHL1 expression was seen in the control and y+hsFS105 yeast cells. It was an expected result since pYX113 vector of the control cells contains no *NTHL1* coding sequence and pYX113-FS105 plasmid encodes a truncated NTHL1 protein. This truncated protein has a shorter peptide sequence (Fig. 2.7) and thus cannot be recognised by the antibody. It is also possible that the truncated protein may not be produced at all because of "nonsense-mediated mRNA decay".[264]

The yeast cells with or without human NTHL1 expression did not show different survival rates after MMS and H_2O_2 treatments (Fig. 2.14). This observation indicates that there were no significant effects of human NTHL1 on the sensitivity of the *NTG2*-knockout yeast cells to MMS and H_2O_2. No studies have yet reported the relationship between MMS cytotoxicity and human NTHL1 protein expression. However, results seen after MMS treatment is in agreement with similar studies showing no effects on survival rate after treating the *NTG2*-knockout yeast with MMS.[126,265] In contrast, protection against H_2O_2 damage in the NTHL1 overexpressing-TK6 cells was reported by Yang *et al.*[266] The discrepancy in the cell survival rate may be explained by low expression of NTHL1 protein from the low copy number plasmids used in our study. The reduced DNA repair capacity seen in the *NTG2*-knockout yeast cells caused by the lost in NTG2 activity, is compensated partly by the expressed NTHL1 protein. As a result, no "extra" NTHL1 protein can cause "additional" DNA repair activity and contribute to the protection from H_2O_2 challenge in the yeast cells. Another possible reason is that

other glycosylases/AP lyases of yeast, such as OGG1 and APN1, also participate in repairing the DNA lesions produced by MMS and H_2O_2. These repair activities will affect the survival rate of yeast.

In cell cycle analysis, y+hsNTHL1 and y+hsD239Y cells were shown to escape from S-phase cell cycle arrest after the release from high-dose MMS (0.2%) treatment, but no obvious difference was seen in cells treated with low-dose MMS (0.02%) (Fig. 2.16). This effect demonstrates that the extra human NTHL1 protein can effectively eliminate the DNA adducts formed after MMS treatment in yeast. MMS is an alkylating agent used in cancer treatment, and produces N-methylpurines, especially 7-methylguanines, which can be converted to formamidopyrimidine (fapy) and abasic sites produced from the DNA adducts.[244,265] Therefore, DNA synthesis is blocked and cells are arrested in S-phase.[267] As fapy is the preferential substrate removed by yeast NTG2 and human NTHL1, *NTG2*-knockout yeast cells with additional NTHL1 protein increase the effectiveness in removing fapy generated by MMS. DNA synthesis continues after recovery from treatment with genotoxic substances and the yeast cells are not arrested in S-phase.[268,269] Little fapy DNA damage produced by 0.02% MMS may be a reason for there being no effect on cell cycle patterns as the damage may be effectively removed by the compensating DNA repair enzymes of yeast in a short period of time.

Hydrogen peroxide predominantly produces oxidation of purines and pyrimidines, including thymine glycol and 8-oxo-7,8-dihydrodeoxyguanine. Thymine glycol is another main DNA substrate of human NTHL1.[270] No improved protective effect is observed in NTHL1 expressing-yeast cells after 2 hours of

0.5 mM and 5 mM H_2O_2 treatments (Fig. 2.17). These observations suggest that alternative DNA repair mechanisms, rather than BER initiated by NTHL1 play an important role in repairing the H_2O_2 induced damage in *S. cerevisiae* cells. The most probable pathways responsible for this observation are NTG1- and OGG1-induced BER since the budding yeast mutants with either *NTG1*- or *OGG1*-knockout showed elevated sensitivity to H_2O_2 agents.[271] Hydrogen peroxide has been reported to induce G2/M block in different types of cells.[272-274] However, G2/M phase arrest was not seen in yeast cells with galactose induction after 0.5 mM H_2O_2 treatment probably because a different carbon source is used and different gene expression is induced in the cells with/without induction. Different gene expression in yeast cells may affect the cell proliferating rate and trigger different DNA repair mechanisms against oxidative stress. Consequently, the cells were mildly arrested in G1 phase or remained unchanged in cell cycle patterns in our experiments. Significant arrest in G2/M phase was observed when cells were treated with 5 mM H_2O_2. An explanation for the shift in G2/M peaks may be due to extra-nuclear DNA resulting from inhibition in mitosis. The inhibition of mitosis in the yeast cells may be related to massive cell death. This theory is supported by our results which shows that about 40-50% of cells died instantly after the high-dose H_2O_2 treatment (Fig. 2.14).

The wild type and Asp 239 mutated NTHL1 proteins showed no difference in the ability to prevent the cell cycle arrest in yeast cells after genotoxic treatments. Thus, it may imply that D239Y polymorphism may not affect the glycosylase/AP lyase activity of the NTHL1 protein even though amino acid position 239 is an active site. The change of amino acids of a protein may result in 3 outcomes:

(1) inactivation of the protein; (2) decrease in the recognition and binding of substrates and (3) decrease in specificity of binding.[260] In our case, the D239Y mutated NTHL1 protein was active under cell cycle analysis since different cell cycle patterns were obtained in yeast cells compared to that of full-length NTHL1 and with FS105 mutated proteins. However, the possibility that D239Y reduces a protein's binding and binding specificity on DNA lesions cannot be excluded from our experiments. The indistinguishable result might also be attributable to the end-point detection (2 hours after release from MMS/H_2O_2 treatments) used in cell cycle analysis, which may not be a suitable time point to discriminate the differences in repair capacity between wild type and mutated proteins. Further work to optimise the time points for examination is needed.

To date, studies on the effect of SNPs on protein function rely on prediction from computational programs/databases and epidemiology studies on the diseases/drug responses. Few functional tests for proteins with polymorphisms have been conducted because the effects of SNPs may be quite small in terms of protein function and therefore difficult to detect. However, determining the effects of polymorphisms on DNA repair activity is important for cancer treatment with DNA-damaging agents since it may affect the therapeutic outcomes. Compared to other methods in detecting the DNA repair activity using radioactive substances, our method is safer and easier to handle. The only limitation is that the sensitivity is not good enough to detect the SNPs with insignificant changes in protein function and thus further improvement is required by optimising the time-points and adjusting the dosage of genotoxic agents.

In this study, yeast was used as a screening model. Several advantages of yeast system make this a more favourable eukaryotic screening model (Table 2.5).[275] First, human proteins can be expressed, modified and function properly in yeast as there is a high degree of conservation between yeast and human in fundamental cellular processes, such as DNA repair and protein metabolism, and around 40% of yeast proteins have similar amino acid sequences to their human homologues.[276-279] The biological function of human protein can be conserved in yeast, this can be illustrated by the example of human *Ras* gene.[280] Viability was restored in *Ras*-knockout nonviable yeast by expressing human Ras protein.[281] Second, genetic mutant yeasts are obtained easily since the desired genes can be intergrated or deleted in the yeast genome by homologous recombination.[282] Third, the yeast system is simple, fast growing and inexpensive, so it is suitable for high throughput screening, e.g. SNP effects of different genes. This is in contrast to the mammalian system which is not amenable for high throughput screening due to expensive culture and slow propagation.[275]

2.6 Conclusion

In conclusion, human NTHL1 protein is shown to be more sensitive in DNA damage caused by MMS than H_2O_2 treatment in yeast cell cycle analysis. Detection of SNPs' effect by using the yeast cell expression vector followed by cell cycle analysis is a cheap and simple method to perform. This method is successfully used here to differentiate the SNPs in genes that produce seriously damaged proteins, such as NTHL1 protein with FS105, from the wild type protein. As mentioned above, alternative DNA repair mechanisms, culturing conditions and the dosages of DNA-damaging agent may interfere with the outcomes, thoughtful

Table 2.5 Comparison between Yeast and Human cell systems for SNP effect screening. (Adapted and modified from reference 274)

Technology	Yeast cell system	Human cell system
Advantages	The expressed proteins can maintain native conformation Eukaryotic environment Easy for genetic manipulation Null-background without other human homologous proteins and simple steps in biological pathways enhances easy detection of the effect on a specific target human protein Simple culture and fast growing Inexpensive culture	The expressed proteins can maintain native conformation Eukaryotic environment Physiologically relevant environments
Disadvantages	It is not physiologically relevant environment No well-established protocol for yeast screening of human proteins	Difficult to culture and slow growing The detection is influenced by redundant pathway and other homology proteins Expensive culture Difficult for genetic manipulation

planning and optimisation are needed. Systematic development in this method can provide a simple means for protein functional analysis and prediction in the responses to different cancer drugs, especially those targeting DNA.

Chapter 3

Relationship between DNA repair mechanisms and glioma cell resistance to Photofrin-mediated photodynamic therapy

3.1 Introduction

Although Ph-PDT has been successful when used in combination with conventional therapies to treat cancers, there has been recent reports of patients who have not responded to Ph-PDT treatment. Different mechanisms have been suggested to explain the cause of Ph-PDT non-responsiveness, e.g. induced expression of survivine, an antiapototic gene, and increase in angiogenesis after Ph-PDT. In this study, the role of DNA repair mechanism in Ph-PDT resistance was investigated as Ph-PDT had been demonstrated to cause significant DNA damage in different cell or animal models. Since several different DNA repair pathways may be involved in the reduction of the therapeutic effect, the specific genes representative of the main DNA repair pathways in humans were examined. The six specific genes were (1) AlkB, alkylation repair homolog 2 (*E. coli*) (*ALKBH2*) of direct DNA damage reversal; (2) APEX nuclease (multifunctional DNA repair enzyme) 1 (*APEX1*) of base excision repair, which removes small base lesions; (3) X-ray repair complementing defective repair in Chinese hamster cells 1 (*XRCC1*) of short-patch BER, which is responsible for repairing single base damage; (4) Excision repair cross-complementing rodent repair deficiency, complementation group 5 (*ERCC5*) of nucleotide excision repair that repairs bulky, helix-distorting lesions; (5) RAD52 homolog (*S. cerevisiae*) (*RAD52*) of double-strand break repair; and (6) *REV1* of translesion synthesis, which is a DNA damage tolerance machinery.[12,283,284] Another two main repair pathways including O-6-methylguanine-DNA methyltransferase direct repair and mismatch repair pathways were not investigated in this study as the U87 cell line is O-6-methylguanine-DNA methyltransferase-deficient and mismatch repair-proficient making the effects of Ph-PDT on these pathways difficult to

examine. A glioma cell line was selected for study as the application of Ph-PDT in treating gliomas is still under clinical trial. Gliomas are multiresistant to cancer treatment and difficult to cure, therefore, the understanding of how gliomas develop resistance to Ph-PDT may help enhance the therapeutic efficacy of Ph-PDT against gliomas by targeting the causes of resistance.

To explore the influence of DNA repair on the responsiveness of Ph-PDT, specific questions addressed in this chapter are as follows:

1. **Will Ph-PDT cause DNA damage and repair?**
2. **Which DNA repair pathways will be involved in repairing Ph-PDT induced DNA damage and thus affect the cytotoxicity of Ph-PDT?**
3. **How the DNA repair protein(s) interact with other proteins to develop Ph-PDT resistance in cells?**

3.2 Methodology (The materials and reagents are listed in appendices.)

3.2.1 Cell Culture

Principle

Cell culture is the process by which cells derived from multicellular eukaryotes are grown under controlled conditions.

Procedures

The human glioblastoma U87 cell line was obtained from American Type Culture Collection. The cells were maintained in complete MEMα medium and grown to a monolayer in a humidified atmosphere at 37°C and 5% CO_2. The U87 cells were frozen and kept in liquid nitrogen to maintain the "age" and passage number of the cells for the experiments throughout the study. Confluent U87 cells were washed with phosphate buffered saline (PBS) solution and trypsinised with 0.05% Trypsin-EDTA solution for 5 minutes at 37°C. The cells were then centrifuged and resuspended in freezing medium, i.e. 90% v/v complete MEMα medium with 10% v/v cell culture grade dimethyl sulphoxide at 0°C. The resuspended cells were aliquoted into cryotubes (1.5 mL per tube). The cryotubes were stored in an alcohol freezer box filled with 100% isopropanol that allows slow freezing at approximately -1°C/minute and left at -70°C overnight. The cryotubes were then stored in liquid nitrogen until required for experiments. When required, the cryopreserved cells were thawed quickly in a 37°C water bath. One vial of cells was then washed with 10 mL PBS solution and the cell suspension was centrifuged at 1200 rpm for 5 minutes. The supernatant was discarded and the cell pellet was resuspended in a small volume of complete MEMα medium. The cells in flasks

with the appropriate cell number, (depending on the sizes of culture flask/dish), was finally transferred to the culture flask/dish and incubated in a humidified atmosphere at 37°C and 5% CO_2 to allow growth until an adequate cell number was reached for the experiments.

3.2.2 Cell survival assay

Principle

The detailed principle is given on p.76. In brief, the trypan-blue dye can enter dead cells but not live cells, therefore allowing live cells to be differentiated from ones which have died.

Procedures

Human U87 glioma cells were diluted 1:9 in 500 µL PBS followed by staining with 500 µL 0.4% w/v trypan-blue. The number of viable and dead cells were counted in fifty images taken by an automated Vi-CELL cell viability analyser (Beckman Coulter), which is an automated cell counter, and calculated with the dilution factor taken into account. Three replicates were performed on each sample.

3.2.3 Photofrin-mediated photodynamic therapy

Principle

Photodynamic therapy utilises (1) the preferential accumulation of photosensitisers in tumour cells versus normal cells, (2) oxygen in tissues and (3) light, to kill the tumour cells.[149] Photofrin was used as the photosensitiser in this study because Photofrin is an approved drug for cancer therapy and clinical trials on

glioma cases is still on-going.[285] When tumour cells take up Photofrin, Photofrin molecules are excited to a higher energy level by light irradiation. After reacting with organic cellular substrates and ground state oxygen, the excited molecules release their energy. These reactions generate several chemically reactive molecular species, including radical ions, reactive oxygen species and singlet oxygen.[150] DNA is destroyed by these reactive molecular species. If this damage is not repaired, apoptosis and/or necrosis may result.[286]

Procedures

The U87 glioma cells (2×10^5) were seeded onto 60 mm culture dishes with 3 mL complete MEMα medium and incubated overnight. For gene knockdown experiments, 2×10^5 or 1×10^5 cells were seeded onto 35 mm culture dishes with 2 mL complete medium. Cells were then incubated in serum-free MEMα medium containing 1 μg/mL Photofrin in 5% w/v dextrose for at least 18 hours prior to illumination. This concentration of Photofrin and time for incubation were optimised in a previous study, which showed maximum Photofrin uptake by glioma cells after 18 hours.[287] A quartz-halogen lamp coupled with a 500 nm long pass filter (Newport, Irvine, CA, USA) was used for illumination. The energy fluence rate was 33.5 mW/cm^2 at a wavelength of 630 nm. The energy fluence rate was measured by ILT70 OEM radiometer with detector for 400-800nm visble light (Gigahertz-Optik Inc.). Different lethal doses (LD) of Ph-PDT were adjusted using different light doses by changing illumination time. The light doses were calculated by the following equation: Fluence rate (W/cm^2) x time (seconds) = Light doses (J/cm^2). Two light doses, 0.8 J/cm^2 to obtain LD10 of Ph-PDT and 1.3 J/cm^2 to LD40, were used in this study. Various controls were included in the study,

which includes cell cultures without Photofrin and light illumination [no treatment controls (CNT)], without Photofrin but illuminated [light controls (LC)], and with Photofrin but not illuminated [dark controls (DC)]. Three hours after light irradiation, the cells were used directly for cell survival analysis and alkaline comet assay (for examining DNA damage) or allowed to recover in complete medium for various times before being analysed by (1) Chromatin immunoprecipitation, (2) Western blotting, (3) real-time quantitative RT-PCR, and (4) alkaline comet assay (for examining DNA repair). The significantly expressed gene(s) in the glioma cells, which is(are) relatively resistance to Ph-PDT, and the gene of interest were chosen for the gene knockdown experiments. The procedures are summarised in Fig. 3.1. Glioma cells were recovered in complete medium 3 hours after Ph-PDT and cells that remained attached to the culture dish were collected at different times and used for examination. The cells that had recovered and remained alive are considered to be relatively resistant to Ph-PDT.

3.2.4 Alkaline comet assay

Principle

Comet assay is a microgel electrophoresis technique to evaluate DNA damage at the level of individual cells.[288,289] It can also be used to determine the DNA repair ability of individual cells after recovering from damage.[290,291] Cells are embedded in a thin layer of agarose set on a pre-coated microscopic slide. The cells are then lysed, electrophoresed and then stained with ethidium bromide. The migration of chromosomal DNA from the nucleus towards the anode increases with the increase of DNA damage. The extent of migration depends on the size of the DNA and the amount of DNA breakage. Thus, the shape of a cell is similar to a comet with a tail

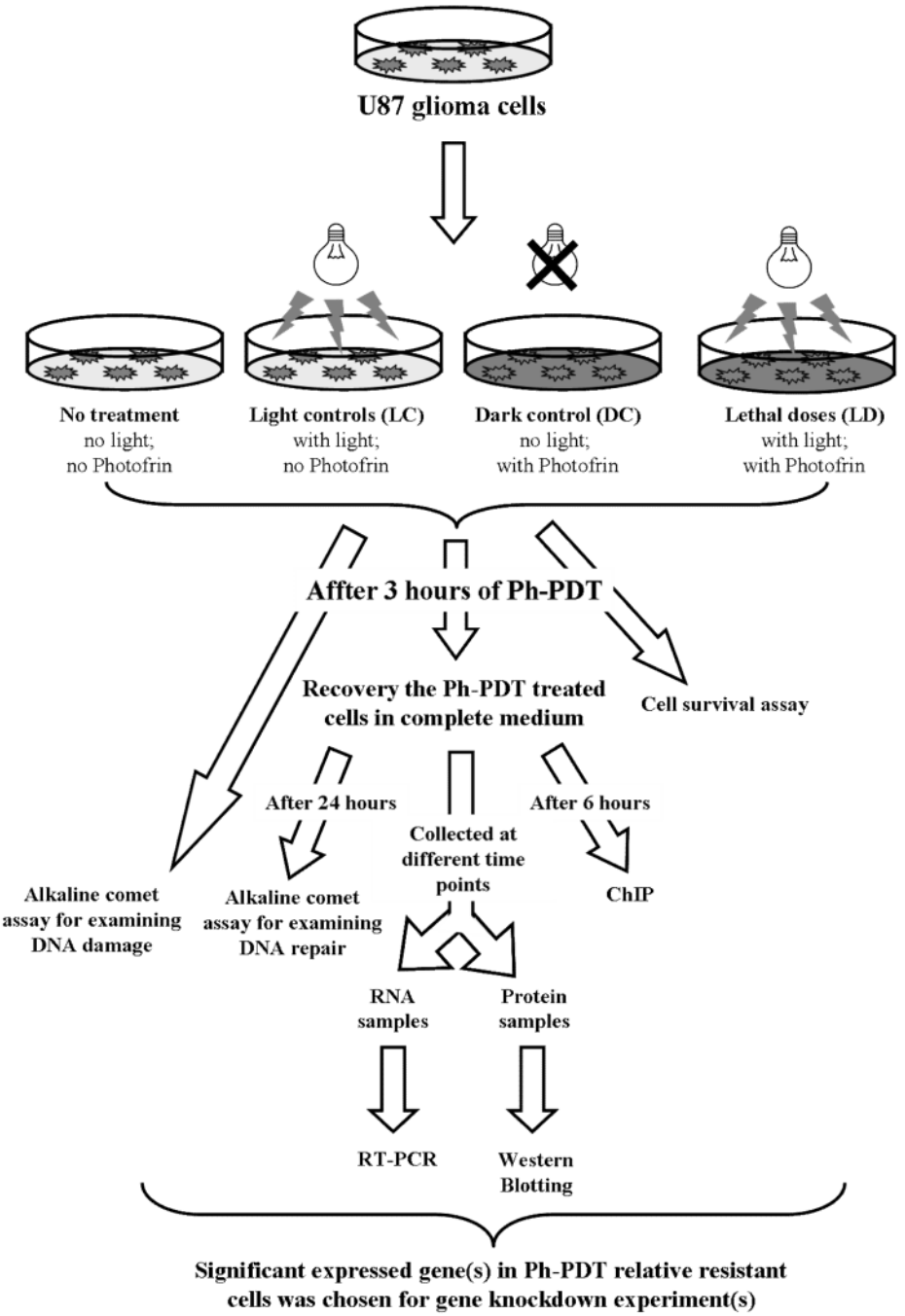

Fig. 3.1 Schematic workflow of Photofrin-mediated photodynamic therapy.

and can be visualised by fluorescence microscopy after ethidium bromide staining.[292,293] Although the length and intensity of comet tail increases with DNA damage, saturation in length and intensity may occur due to the electrophoretic conditions. Therefore, both visual scoring and DNA % in comet tail should be used in the analysis of DNA damage.[294,295] As the relative intensity of fluorescence in the comet tail is positively associated with DNA breaks, it can be expressed as DNA % in comet tail using an image analysis software.[293,296]

$$\text{DNA \% in comet tail} = \left(\frac{\text{The integrated tail intensity}}{\text{The total integrated cell intensity}} \right) \text{ x } 100$$

Procedures

The assay was performed according to the procedure of Collins *et al.*[293,297] After the U87 glioma cells were treated with Ph-PDT or 30% v/v hydrogen peroxide, which was used as positive control, 4×10^4 were washed in PBS and mixed with 60 µL of 1% w/v low melting point agarose in PBS (37°C). The cells were then embedded on a 1% w/v standard agarose pre-coated microscope slide. The slides were immersed in working lysis buffer for 1 hour to denature the cellular proteins and transferred to the alkaline electrophoresis buffer for 30 minutes for DNA unwinding at 4°C in the dark. After DNA unwinding, electrophoresis was conducted for 30 minutes at 25V and 300mA in a Sub-Cell GT electrophoresis tank (Bio-Rad laboratories). The slides were then neutralised with 3 changes of neutralising buffer for 5 minutes each and stained with 30 µL ethidium bromide (20 µg/mL). Individual comets were viewed at a final magnification of 400X using an Eclipse E600 fluorescent microscope (Nikon, Tokyo, Japan) equipped with 590 nm long pass emission filter and Komet 5.5 software (Kinetic Imaging Ltd., Nottingham, UK). Comets from three microgels on two slides of each sample were analysed and

150 individual comets were counted.

3.2.5 Isolation of RNA

Two RNA isolation methods were used in this study, they were: (1) PureLink™ Micro-to-Midi™ Total RNA Purification Kit for real-time RT-PCR, as this method yields high quality of RNA; and (2) a modified guanidinium isothiocyanate-phenol -chloroform extraction method.

3.2.5.1 PureLink™ Micro-to-Midi™ Total RNA Purification Kit

Principle

This method is based on an improved guanidinium isothiocyanate extraction method using an extraction column to isolate the RNA.[298] After RNA precipitation using 70% (v/v) ethanol, RNA binds to the silica-based membrane in the spin cartridge, and impurities are effectively removed by washing. RNA adsorption on the solid phase, i.e. silica, relies on the pH and the salt content of the buffers used.

Procedures

The procedures used were according to the manufacturer's manual. In brief, the U87 glioma cells were lysed directly in a culture dish by adding 300 µL of RNA lysis buffer and the cells were resuspended by pipetting up and down. Three hundred microlitres of 70% v/v ethanol were then added to the homogenised sample and mixed thoroughly by vortexing. Then, the sample was transferred to the column, centrifuged and washed using washing buffers. Finally, 30 µL of RNase-free water were used to elute the RNA. The RNA samples were quantified

by NanoDrop 1000 spectrophotometer (Thermo Fisher Scientific, MA, USA) and stored at -70°C.

3.2.5.2 Modified guanidinium isothiocyanate-phenol-chloroform extraction

Principle

Modified guanidinium isothiocyanate-phenol-chloroform extraction makes use of TRIZOL LS reagent, which is an improved single-step RNA isolation method originally developed by Chomczynski & Sacchi.[298] TRIZOL LS reagent is a mono-phasic solution of phenol and guanidine isothiocyanate which maintains the integrity of the RNA, but disrupts cells and dissolves cell components. This method is dependent upon the phase separation of the aqueous sample and TRIZOL LS reagent. RNA remains in the aqueous phase and is precipitated out by isopropanol.

Procedures

Homogenisation and phase separation

The U87 glioma cells were lysed directly in a 35 mm or 60 mm diameter culture dish by adding 300 µL or 750 µL TRIZOL LS reagent respectively. The homogenised sample was collected into an eppendorf tube and incubated for 5 minutes at room temperature to allow complete dissociation of nucleoprotein complexes. Eighty microlitres (for 35 mm dish) or 200 µL (for 60 mm dish) of Phenol:Chloroform: Isoamyl Alcohol (25:24:1) were added to the sample and then shaken vigorously for 15 seconds. After 15 minutes' incubation at room temperature, the sample was centrifuged at 12000 *g* for 15 minutes at 4°C.

Following centrifugation, the mixture was separated into a lower pink phenol-chloroform phase, an interphase and a colourless upper aqueous phase where the RNA is.

RNA precipitation and wash

The aqueous phase was transferred to a clean eppendorf tube. RNA precipitation was carried out by adding isopropanol: 200 µL were added into 35 mm dish or 500 µL into 60 mm dish. Incubation was then performed at room temperature for 10 minutes. The sample was centrifuged at 12000 *g* for 10 minutes at 4°C. After centrifugation, the supernatant was removed. The remaining RNA pellet was washed with at least 1 mL cold 75% ethanol. The sample was mixed and centrifuged at 7500 *g* for 5 minutes at 4°C.

Dissolution of RNA

The supernatant was removed and the RNA pellet was dried in air. The RNA pellet was then re-dissolved in 30 µL diethyl pyrocarbonate-treated water and then the RNA were quantified by NanoDrop 1000 spectrophotometer (Thermo Fisher Scientific) and stored at -70°C.

3.2.6 Reverse transcription-polymerase chain reaction

Principle

Real-time PCR using TaqMan assay

TaqMan assay was used to measure the relative quantification of gene expression. The principle of TaqMan assay is based on the 5' to 3' exonuclease activity of Taq DNA polymerase to cleave the dual-labelled TaqMan probe. The TaqMan probe is

labelled with fluorescent dye at 5' end and a quencher at 3' end. The quencher is a dye molecule, which may convert the fluorescent light into heat or other light with a wavelength undetected by the real-time instrument. During the amplification step of PCR, i.e. the primers and probe is sitting on the complementary target sequence (the PCR products), Taq DNA polymerase extends the primers and cleaves the probe simultaneously. A fluorescent signal is produced after the probe cleavage because the fluorescent dye is released and separated from the quencher.[299,300] The principle is illustrated in Fig. 3.2. Therefore, the accumulative fluorescent signals in the amplification stages of PCR are detected by sensors of real-time thermocyclers. The relative changes in gene expression can be calculated based on the comparative threshold ($2^{-\Delta\Delta Ct}$) method.[301] This is a relative quantification method calculated by mathematical equations without the use of a standard curve. First, differences in thresholds (ΔCt) are obtained by normalising the amounts of a target gene in the sample (Ct_{TARGET}) and a calibrator ($Ct_{CAL.}$), such as untreated sample, to the housekeeping gene (Ct_{HKG}), i.e.

$$\Delta Ct_{TARGET} = Ct_{TARGET} - Ct_{HKG} \quad \text{and} \quad \Delta Ct_{CAL.} = Ct_{CAL.} - Ct_{HKG}.$$

Second, the normalised amount of the taget gene is relative to that of the calibrator, i.e (ΔΔCt), by subtraction: $\Delta\Delta Ct = \Delta Ct_{TARGET} - \Delta Ct_{CAL}$. Since it is hypothesised that the amount of target DNA is doubling in each PCR amplification cycle, the relative quantitation of a target gene in a sample is finally calculated by the following equation:

$$\text{Relative quantitation of a target gene} = 2^{-\Delta\Delta Ct}$$

The mathematical equations used in this method are derived based on the criteria that the amplification efficiencies of both target gene and housekeeping gene are nearly equal and the efficiencies should be around 90 to 100%.[302,303]

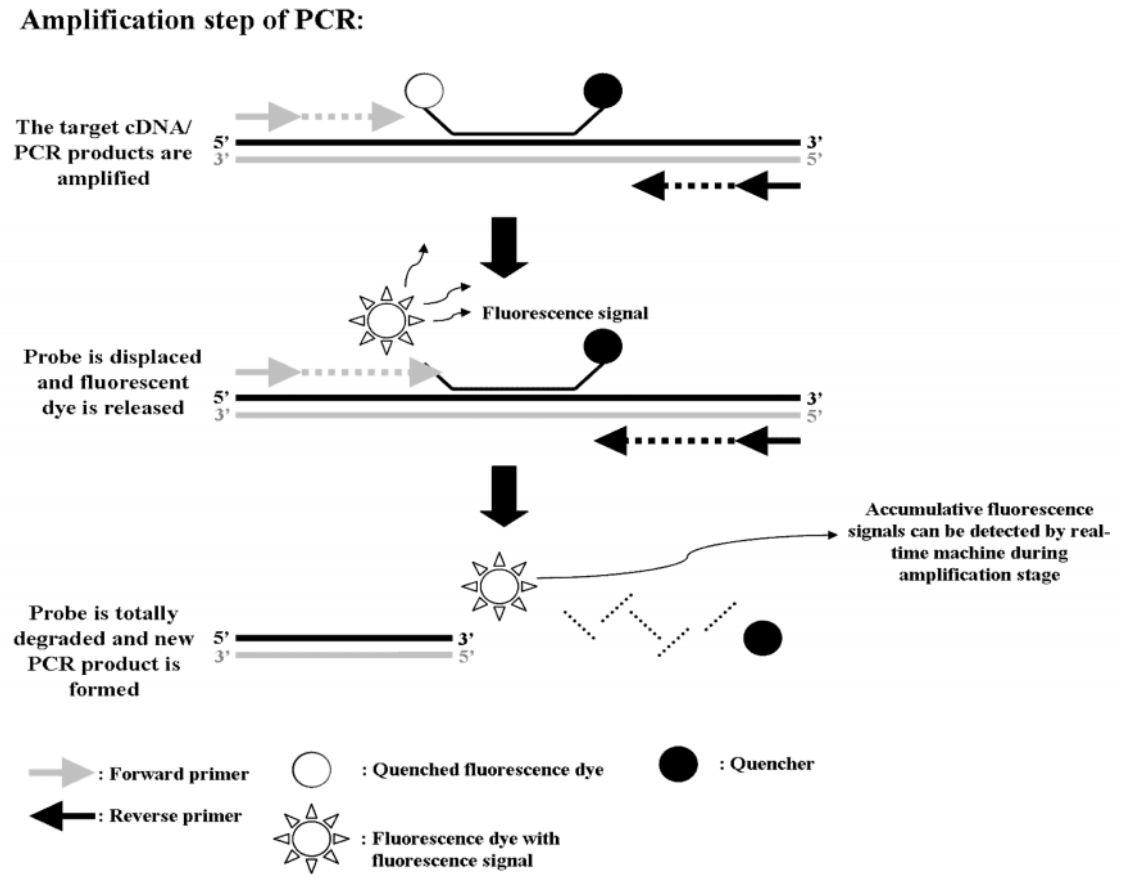

Fig. 3.2 **The principle of TaqMan assay.** (Adapted and modified from http://en.wikipedia.org/wiki/File:Taqman.png#filelinks)

Procedures

Reverse transcription

Briefly, 5 µg total RNA extracted from U87 glioma cells was added to the RT mixture, which contained 1X reaction buffer, 5 µM oligo $(dT)_{18}$ primer, 1 mM dNTPs, 20 units RiboLock™ RNase Inhibitor and 200 units of RevertAid™ M-MuLV Reverse Transcriptase. The sample was mixed, centrifuged and incubated for 60 minutes at 42°C. The RT reaction was stopped by heating at 70°C for 5 minutes. The cDNA products were stored at -20°C until use.

Conventional PCR for *TP53* and *NPM1* amplification

Conventional PCR was performed in GeneAmp® PCR System 9700 (Applied Biosystems). Fifty nanograms of cDNA were added to 25 µL of standard PCR master mix containing 1X PCR buffer, 0.2 mM of each dNTPs, 2.5 mM of $MgCl_2$, 0.3 µM of primers and 0.5 units of AmpliTaq Gold DNA polymerase. The cycling conditions were carried out as follows: 1 cycle for denaturation of 95°C/5 minutes. Amplification was carried out for 25 cycles of 95°C/30 seconds; 55°C/ 1 minute and 72°C/1 minute followed by a final extension step at 72°C/10 minutes. The PCR products were subjected to agarose gel electrophoresis for examination. The primers used for amplifying *TP53* and *NPM1* genes are listed in Table 3.1. Glyceraldehyde-3-phosphate dehydrogenase (*GAPDH*) was used as the housekeeping gene.

Real-time PCR

To quantify the relative gene expression, cDNA was then subjected to TaqMan-based real-time quantitative PCR. Briefly, 7.5 ng cDNA was added to 20 µL PCR

Table 3.1 Primers used in RT-PCR.

Primers	Sequences (5' to 3')	Positions in reference mRNA sequence[a]
(1) p53_rtpF1	TGTTCCGAGAGCTGAATGAG	1216-1235
(2) p53_rtpR1	CCCTTCTGTCTTGAACATGAG	1344-1364
(3) NPM1_pF1	TTGCTGCTGATGAAGATGATG	628-648
(4) NPM1-PR1	CCACTTTGGGAAGAGAACCA	929-948

a. The *TP53* and *NPM1* primers were designed from Homo sapiens tumor protein *p53* (*TP53*), transcript variant 1, mRNA (Accession no.: NM_000546) and nucleophosmin (nucleolar phosphoprotein B23, numatrin) (*NPM1*), transcript variant 1, mRNA (Accession no.: NM_002520) by using Oligo program version 6.57 (Molecular Biology Insights) respectively.

mix containing 1X Universal PCR Master Mix and 1µL validated TaqMan® gene expression assay mix. The amplification cycle used was as follows: 1 cycle for denaturation (95°C/10 minutes) followed by 40 cycles for amplification (95°C/15 seconds and 60°C/1 minute). The fluorescent signal was measured continuously during the repetitive cycles with an Applied Biosystems 7500 Real-Time PCR system (Applied Biosystems). The relative change in gene expression was calculated based on the $2^{-\Delta\Delta CT}$ method. The validated TaqMan® gene expression assays used in this study are listed in Table 3.2. *GAPDH* was used as the housekeeping gene for normalisation.

3.2.7 Western blotting

Principle

The detailed principle is given on p.77. In brief, target proteins are separated by electrophoresis on an acrylamide gel for detection.

Procedure

Cell lysate preparation

Cells were collected, washed in ice-cold PBS and lysed in 20 µL whole cell extraction buffer. The protein concentration of the lysate was then quantified based on the method of Bradford. In brief, 10 µL of the protein lysate sample were added to 200 µL of diluted Bradford reagent (1 part reagent with 4 parts distilled water) in a microtiter plate. Five dilutions of bovine serum albumin from 50 µg/mL to 500 µg/mL were used as protein standards. All samples and standards were assayed in duplicates and mixed thoroughly. Finally, the samples were incubated at room

Table 3.2 The validated TaqMan® gene expression assays. (Adapted and modified from http://www.appliedbiosystems.com.hk/)

Gene	Assay ID	Interrogated Sequence	Exon Boundary	Assay Location	Amplicon length (bp)
(1) *ALKBH2*	Hs00419572_m1	NM_001001655.1	2-3	478	86
(2) *REV1*	Hs00249411_m1	NM_001037872.1	2-3	268	63
(3) *RAD52*	Hs00172536_m1	NM_134424.2	2-3	197	65
(4) *APEX1*	Hs00172396_m1	NM_080648.1	3-4	510	81
(5) *XRCC1*	Hs00959834_m1	NM_006297.2	4-5	536	75
(6) *ERCC5*	Hs00164482_m1	NM_000123.2	14-15	3407	118
(7) *GAPDH*	Hs99999905_m1	NM_002046.3	2-3	156	122

temperature for 5 minutes and the absorbance was measured at 595nm. After quantitation, the lysate was diluted to 4 μg/μL with buffer, mixed with equal volume of 2X sodium dodecyl sulphate sample buffer and boiled for 3 minutes at 99°C. Thus, the final protein concentration of the lysate was 2 μg/μL.

Gel electrophoresis and gel blotting

Fifteen microlitres of each diluted sample were separated by sodium dodecyl sulphate-polyacrylamide gel electrophoresis. The gel consisted of 4% stacking gel and 10% separating gel. The samples and pre-stained protein marker were electrophoresed at 80V in stacking gel and at 100V in separating gel using mini-PROTEAN 3 system (Bio-Rad laboratories) with running buffer at room temperature. The time of electrophoresis was 1.5 to 2 hours depending on the molecular weights of the proteins under investigation. The separated proteins were then transferred onto PVDF membranes in transfer buffer for 2 hours at 70V and 4°C using Mini Trans-Blot cell (Bio-Rad laboratories).

Membrane blocking and primary antibody staining

The membrane was blocked with either 10 mL 5% non-fat milk or 5% bovine serum albumin in TBST buffer, depending on the primary antibody (see Table 3.3), with shaking for 1 hour at room temperature. The proteins of interest were detected by probing different primary antibodies listed in Table 3.3 and incubated with shaking for 16 hours at 4°C. ACTB was used as loading control.

Secondary antibody staining and detection

The membrane was then washed with shaking in 10 mL TBST (3 x 10 minutes)

Table 3.3 Antibodies used in Western blotting.

Primary (1°) antibodies	1° antibody dilutions	Blocking agent	Secondary (2°) antibodies	2° antibody dilutions
(1) ABH2 antibody [hABH2-7]	1:1000 in 2% BSA, 1X TBST buffer	5% milk in 1X TBST buffer	**Anti-mouse IgG, HRP-linked antibody**	1:10000 in 5% milk, 1X TBST buffer
(2) REV1 antibody	1:500 in 2% BSA, 1X TBST buffer	5% milk in 1X TBST buffer	**Anti-mouse IgG, HRP-linked antibody**	1:10000 in 5% milk, 1X TBST buffer
(3) p53 (FL-393) antibody	1:200 in 2% BSA, 1X TBST buffer	5% milk in 1X TBST buffer	**Anti-rabbit IgG, HRP-linked antibody**	1:10000 in 5% milk, 1X TBST buffer
(4) Phospho-p53 (Ser15) antibody	1:1000 in 2% BSA, 1X TBST buffer	5% BSA in 1X TBST buffer	**Anti-rabbit IgG, HRP-linked antibody**	1:10000 in 2% BSA, 1X TBST buffer
(5) NPM antibody	1:1000 in 2% BSA, 1X TBST buffer	5% milk in 1X TBST buffer	**Anti-rabbit IgG, HRP-linked antibody**	1:10000 in 5% milk, 1X TBST buffer
(6) SAPK/JNK (56G8) Rabbit mAb	1:1000 in 2% BSA, 1X TBST buffer	5% milk in 1X TBST buffer	**Anti-rabbit IgG, HRP-linked antibody**	1:10000 in 5% milk, 1X TBST buffer
(7) Phospho-SAPK/JNK (Thr183/ Thy185) antibody	1:1000 in 2% BSA, 1X TBST buffer	5% BSA in 1X TBST buffer	**Anti-rabbit IgG, HRP-linked antibody**	1:10000 in 2% BSA, 1X TBST buffer
(8) PCNA antibody	1:1000 in 2% BSA, 1X TBST buffer	5% milk in 1X TBST buffer	**Anti-rabbit IgG, HRP-linked antibody**	1:10000 in 5% milk, 1X TBST buffer
(9) β-Actin (C4) Antibody	1:1000 in 2% BSA, 1X TBST buffer	5% milk in 1X TBST buffer	**Anti-mouse IgG, HRP-linked antibody**	1:10000 in 5% milk, 1X TBST buffer

at room temperature. Corresponding horseradish peroxide-labelled anti-rabbit or anti-mouse antibodies were used as secondary antibodies and incubated with shaking for 1 hour at room temperature. The final complex was visualised by enhanced chemiluminescence autoradiography.

3.2.8 Gene knockdown

Principle

Small interfering RNA (siRNA) is one type of double-stranded RNA molecule, 20-25 nucleotides in length, involved in RNA interference pathways. siRNA is intently engineered to downregulate a complementary mRNA, i.e. target mRNA. When siRNA is introduced into the cell, it will associate with RNA-induced silencing complex. This complex contains an endonulease called argonaute, which digests double stranded RNA. Subsequently, siRNA binds to the target mRNA with this complex. Therefore, double stranded RNA is formed by siRNA with mRNA and argonaute degrades the RNA.[304,305]

There are two methods to introduce siRNA into the cells for gene knockdown. They are: (1) by directly transfecting with synthetic oligonucleotides and (2) by transfecting with RNAi plasmid. Synthetic oligonucleotides provide a convenient way to knockdown the target gene, but the knockdown effect is short-lived. Thus, this problem is solved by utilising RNAi plasmid, because the plasmid can consistently express siRNA in the cells. However, the design and construction of the plasmid is time-consuming and complicated.[306-308]

Procedures

For *ALKBH2* knockdown by transfecting synthetic oligonucleotides

Fifty percent confluent density of U87 glioma cells (1 X 10^5) were seeded in 2 mL complete MEMα medium onto 35 mm dishes and left overnight. One hundred picomolar *ALKBH2* siRNA oligomers and 5 µL Lipofectamine 2000 transfection reagent were diluted in 250 µL incomplete MEMα medium and mixed together for 5 minutes. The mixture was incubated for 20 minutes at room temperature and 500 µL oligomer-Lipofectamine 2000 complexes were added to each dish of cells that had been washed and maintained in 1.5 mL incomplete MEMα medium. In mock controls, the negative control RNA was used instead of siRNA. After 6 hours' incubation, the cells were allowed to recover in 2 mL complete MEMα medium for 16 hours. Cultures were incubated as follows: (1) with Lipofectamine reagent alone as a blank to examine the effect of Lipofectamine on Ph-PDT (Lipofectamine); (2) with negative control RNA as a mock control (Neg CNT) and (3) with siRNA (siALKBH2). After transfection and Ph-PDT treatment, cells were examined by cell survival assay, RT-PCR using TaqMan assay and Western blotting. The workflow of ALKBH2 knockdown is shown in Fig. 3.3.

For *NPM1* knockdown by transfecting RNAi plasmid

Ninety percent confluent density of U87 glioma cells (2 X 10^5) were seeded in 2 mL complete MEMα medium. Two micrograms of *NPM1* RNAi plasmid (pSilencer 2.0 vector with 5' GGACAAGAAUCCUUCAAGA 3') and 5 µL Lipofectamine 2000 transfection reagent were diluted in 125 µL incomplete MEMα medium and mixed together for 5 minutes. Therefore, the ratio of *NPM1* RNAi plasmid to Lipofectamine 2000 is 1:2.5 (µg:µL). This ratio was optimised

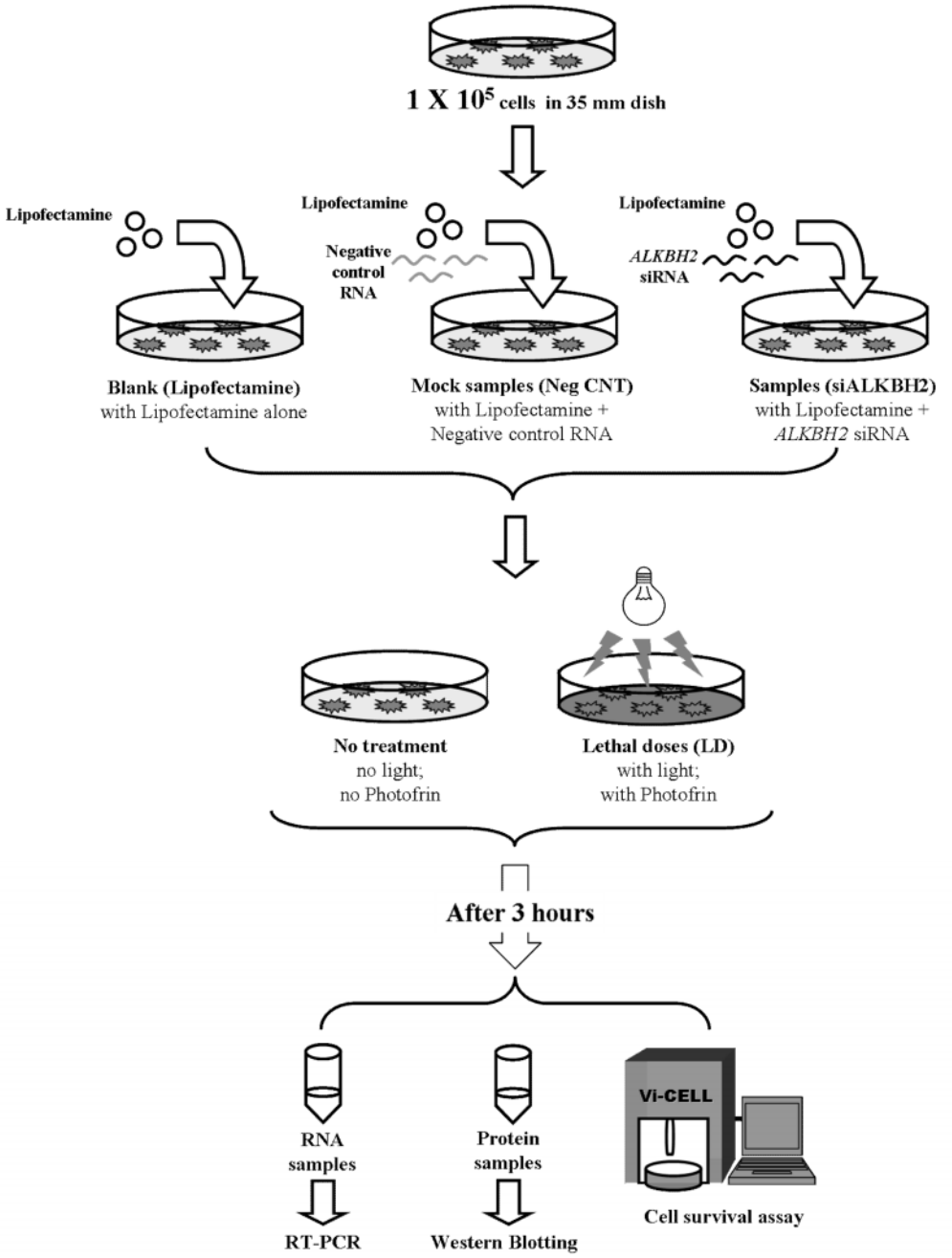

Fig. 3.3 Schematic workflow of *ALKBH2* knockdown.

experimentally for efficient *NPM1* knockdown in U87 glioma cells. The mixture was incubated for 20 minutes at room temperature and 250 μL NPM1 RNAi plasmid-Lipofectamine 2000 complexes were added to each dish containing 750 μL incomplete MEMα medium. In mock controls, the non-specific dsRNAi control plasmid was used instead of NPM1 RNAi plasmid. After 6 hours, the cells were allowed to recover in 2 mL complete MEMα medium for 16 hours. Cultures were incubated as follows: (1) with Lipofectamine reagent alone as a blank to examine the effect of Lipofectamine on Ph-PDT (Lipofectamine); (2) with pSilencer 2.0 vector, which containing negative control siRNA template, as a mock control (vector) and (3) with *NPM1* RNAi plasmid (siNPM1). After transfection and PDT treatment, cells were examined by cell survival assay, conventional RT-PCR and Western blotting. The workflow of *ALKBH2* knockdown is shown in Fig. 3.4.

3.2.9 Chromatin immunoprecipitation (ChIP) assay

Principle

Chromatin immunoprecipitation

ChIP is used to illustrate the DNA-protein interactions by determining the protein binding sites, e.g. transcription binding sites, on the target genome region in cells or tissues. This method works by crosslinking the protein and DNA to form a complex. The protein-DNA complex is then sonicated to fragment DNA into shorter lengths. After sonication, this complex is immunoprecipitated out by an antibody against the protein of interest. As a result, the DNA fragments, which initially bound with the target protein, are dissociated from the complex and can be examined by PCR.[309]

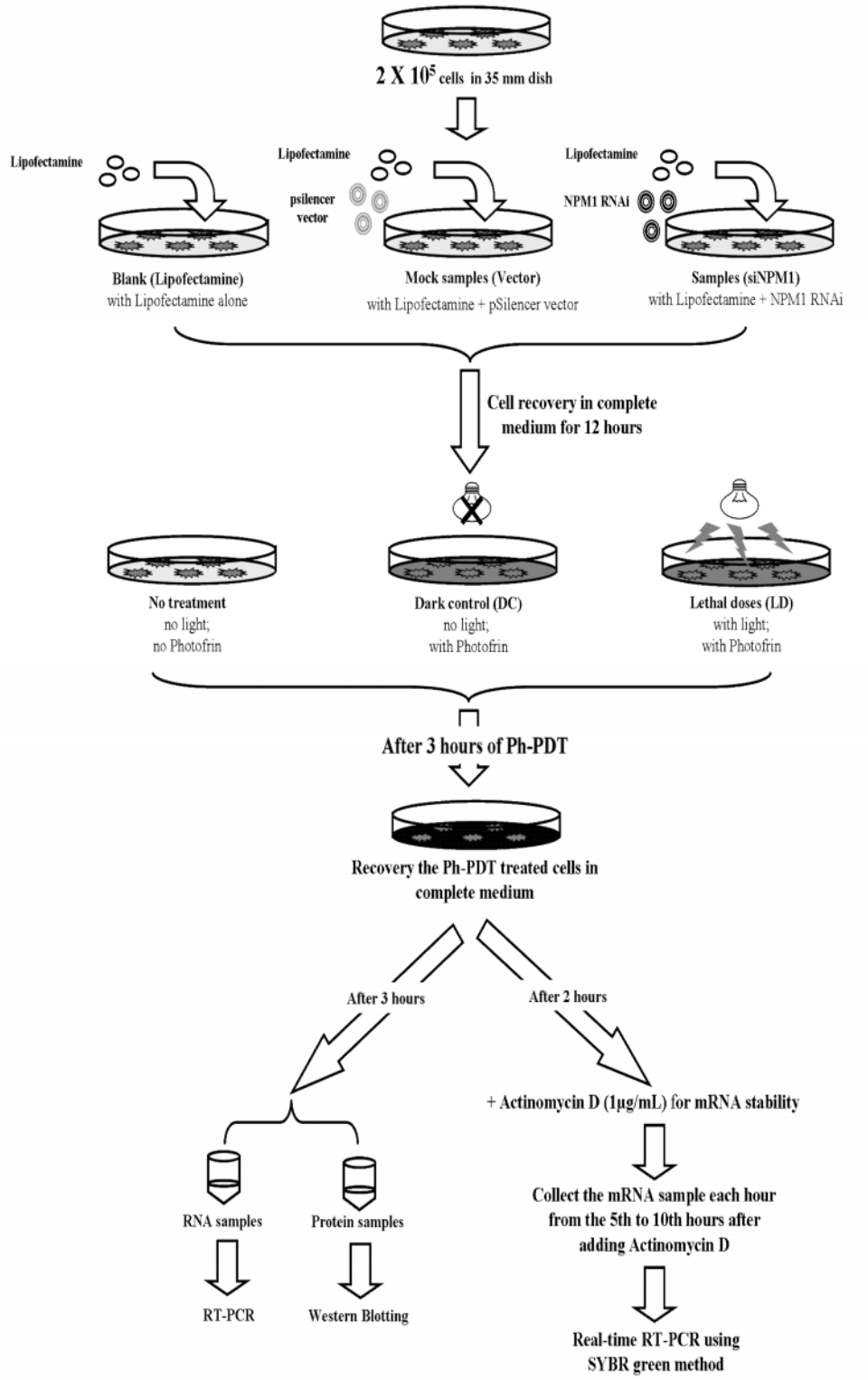

Fig. 3.4 Schematic workflow of *NPM1* knockdown.

Real-time PCR using SYBR green

SYBR Green I is a cyanine dye, which binds to the minor groove of double stranded DNA. At the beginning of PCR, the fluorescent signal from SYBR green is minimal since little double-stranded DNA is present in the PCR mixture. However, the fluorescent signal increases dramatically during annealing and amplification since SYBR green dye binds to the newly synthesised PCR products. The fluorescence signal is measured by real-time instruments.[302,310]

Procedures

Cross-linking, quenching and collecting cells

U87 glioma cells were cross-linked using formaldehyde to a final concentration of 1% at room temperature for 10 minutes in 35 mm dish. The fixation was then quenched by the addition of glycine at a final concentration of 0.125 M. The cells were washed with cold PBS with protease inhibitors and collected by scraping.

ChIP for TP53 and NPM1 proteins

ChIP was performed using MAGnify™ chromatin immunoprecipitation system according to the manufacturer's protocol and is only briefly described here. The cells were lysed and chromatin was released from the nuclei. The released chromatin was sheared to around 200 to 500 bp fragment sizes by sonication in the Sonicator 4000 ultrasonic liquid processor (Qsonica, LLC, Newton, CT, USA). The cross-linked protein-protein and protein-DNA fragments were then immunoprecipitated by anti-TP53, anti-NPM1 or anti-IgG antibodies conjugated to Dynabeads® Protein A/G. Anti-IgG was used as negative control as IgG protein should not bind to DNA. Finally, the crosslinking was reversed by heat treatment

and DNA associated with TP53 was isolated by DNA purification magnetic beads. The isolated DNA was analysed by both conventional and real-time PCR using SYBR green quantitative PCR. The primers used for investigating the binding of TP53 and NPM1-related transcription factors, which includes Sp1 transcription factor (Sp1) and nuclear factor of kappa light polypeptide gene enhancer in B-cells 1 (NF-κB), on *ALKBH2* promoter region are listed in Table 3.4 and 3.5 respectively. The locations of these primers on *ALKBH2* promoter are illustrated in Fig. 3.5.

Conventional PCR examination:

Five microlitres of the DNA samples from ChIP assay were added to 25 µL of conventional PCR master mix containing 1X PCR buffer, 0.2 mM of each dNTPs, 2.5 mM $MgCl_2$, 0.3 µM primers and 0.5 units of AmpliTaq Gold DNA polymerase. The cycling conditions were as follows: 1 cycle for denaturation at 95°C/5 minutes; amplification for 25 cycles of 95°C/30 seconds; annealing temperature (Table 3.4 and 3.5)/1 minute and 72°C/1 minute followed by a final extension step at 72°C/10 minutes. The PCR products were subjected to agarose gel electrophoresis for examination.

Quantification of binding by real-time PCR using SYBR green:

Five microlitres of the DNA samples from ChIP assay were added to 25 µL PCR mix containing Maxima™ SYBR Green/ROX qPCR Master Mix and 0.3 µM forward and reverse primers of the target gene. The amplification cycle used was as follows: 1 cycle for denaturation (95°C/10 minutes) followed by 40 cycles of amplification (95°C/15 seconds and 60°C/1 minute). Fluorescence signal was detected using an Applied Biosystems 7500 Real-Time PCR system and the relative

Table 3.4 Primers used in PCR for ChIP assay of TP53 binding on *ALKBH2* promoter region.

Primers	Sequences (5' to 3')	Positions in *ALKBH2* reference sequence[a]	Annealing temperature (°C)	Applications
(1) p53_F1	TGCTCCCACTC GTGACAATA	-257 to -238	60	For conventional PCR and real-time PCR of position 1 binding site
(2) p53_R1	AACCGCACGC AAAATTCTGA TAT	+147 to +125	60	For conventional PCR and real-time PCR of position 2 binding site
(3) p53_F2	CAGCCGTGAT TCTCGACA	-143 to -160	60	For real-time PCR of position 2 binding site
(4) p53_R2	GCCACTGTCG AGAATCAC	-138 to -155	60	For real-time PCR of position 1 binding site

a. The primers were designed from selected region (109530294 to 109533293) of Homo sapiens chromosome 12, GRCh37 primary reference assembly sequence (Accession no.: NC_000012), which is -2000 and +1000 of *ALKBH2* promoter region, by using Oligo program version 6.57 (Molecular Biology Insights). +1 position is the transcription start site.

Table 3.5 Primers used in PCR for ChIP assay of NPM1-related transcription factors binding on *ALKBH2* promoter region.

Primers	Sequences (5' to 3')[a]	Positions in *ALKBH2* reference sequence	Annealing temperature (°C)	Applications
(1) Sp1_NFkBpF1	TAACCCCTGAGCCCATTAATCTA	-1223 to -1201	55	Used in conventional PCR
(2) Sp1_NFkBpR1	CACCACCACAATCAAGATCTAAG	-911 to -933	55	Used in conventional PCR
(3) Sp1pF1	CATTGAGGGGAGACAGAGTAAA	-841 to -820	55	Used in conventional PCR
(4) Sp1pR1	GAACTCCTGGGTTAGAGCGAT	-590 to -610	55	Used in conventional PCR
(5) Sp1_NFkBpF2	ACCCCAGCCGTGATTCTC	-163 to -146	55	Used in conventional PCR
(6) Sp1_NFkBpR2	TAAACCGCACGCAAAATTCTGATAT	+149 to +125	55	Used in conventional PCR
(7) NFkBpF1	CCTTAAAGGGGTGGACAGTTG	+263 to +283	55	Used in conventional PCR
(8) NFkBpR1	CACCTGTGCATCAGAATCAGC	+479 to +459	55	Used in conventional PCR
(9) Sp1pF2	GGGGACAGGATGGACAGATT	+694 to +713	55	Used in conventional PCR
(10) Sp1pR2	TTTGCCAAACAGGACTGTGTAACT	+927 to +904	55	Used in conventional PCR

The primers were designed from selected region (109530294 to 109533293) of Homo sapiens chromosome 12, GRCh37 primary reference assembly sequence (Accession no.: NC_000012), which is -2000 and +1000 of *ALKBH2* promoter region, using Oligo program version 6.57 (Molecular Biology Insights, Cascade, CO, USA). +1 position is transcription start site.

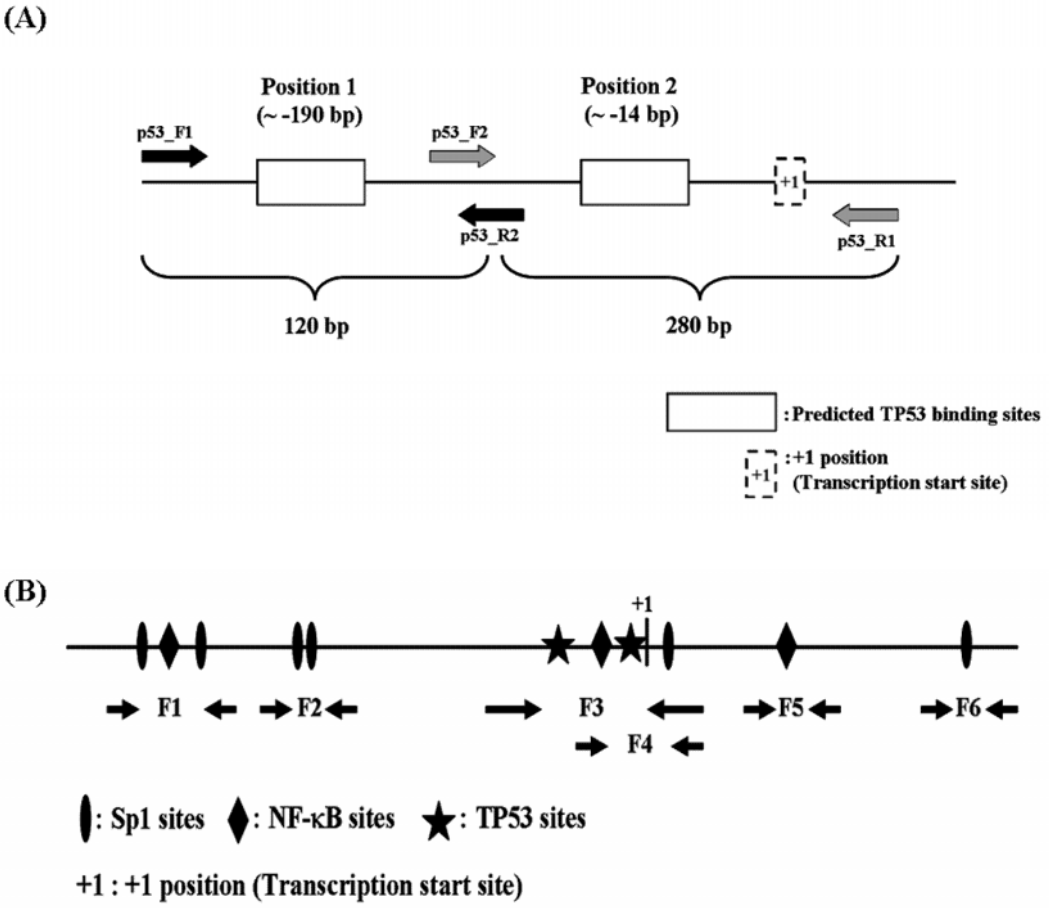

Fig. 3.5 The schematic diagrams of primer locations on *ALKBH2* promoter region for ChIP assays. (A) PCR for amplifying TP53 binding sites. (B) PCR for amplifying NPM1-related transcription factors binding sites. The arrows shown in this figure are primer locations on the promoter.

gene expression levels were calculated by the $2^{-\Delta\Delta CT}$ method. *GAPDH* is used as the housekeeping gene for normalisation.

3.2.10 mRNA stability

Principle

The influence of mRNA stability on gene expression can be examined using actinomycin D, which is a transcription inhibitor.[311] The transcription of the target gene is stopped at the time when actinomycin D is added (Time 0), so the subsequent reduction in mRNA amount is an indication of mRNA stability.[312] Actinomycin D inhibits transcription by binding onto the transcription initiation complex of DNA. This binding prevents the transcription by RNA polymerase.[313]

Procedures

U87 glioma cells (2×10^5) were seeded onto 60 mm culture dishes with 3 mL complete MEMα medium and left to incubate for more than 16 hours. The cells were subjected to two conditions, i.e. with or without NPM1 knockdown, before Ph-PDT. They were then incubated in serum-free MEMα medium containing 1 μg/mL Photofrin for at least 18 hours prior to illumination. Light irradiation of cells was carried out using light dose of 1.3 J/cm^2 and cells were allowed to recover for 5 hours after Ph-PDT in complete MEMα medium. Then, 2 μL of actinomycin D were added into each dish (final concentration, 1 μg/mL) and incubated at 37°C. A dish of cells was collected every hour for 5 hours. Consequently, total RNA was extracted from the cells and analysed by RT-real time PCR. Primers p53_rtpF1 and p53_rtpR1 (Table 3.1) were used to amplify the *TP53* PCR product and SYBR green was used for signal detection (Chapter 3.2.9).

3.2.11 Statistics

Data are presented as mean + SD except for the data on cytotoxicity, quantitation of RNA levels at different time-points using real-time RT-PCR and mRNA stability, which are presented as mean ± SD. Statistical difference was determined by paired *t*-test for Comet and ChIP assays, one-way ANOVA with Tukey post-test for mRNA quantification and cytotoxicity after gene knockdown, and two-way ANOVA with Bonferroni post-test for mRNA stability.

3.3 Results

3.3.1 Ph-PDT cytotoxic effect on U87 glioma cells

Photofrin-treated U87 cells were exposed to white light passing through a 500 nm long-pass filter with the energy fluence rate of 33.5 mW/cm^2 at a wavelength of 630 nm. The selected light doses for the cell survival test were 0 J/cm^2 to 2.1 J/cm^2. Cell viability was determined 3 hours after illumination using the trypan-blue exclusion method. Figure 3.6 shows the cytotoxicity of Ph-PDT on U87 glioma cells at 1 μg/mL Photofrin. The toxicities in light controls (LC) were negligible. However, increase in cytotoxicity was observed in Ph-PDT treated cells with increased light doses, i.e. illumination time, from as low as a 0.8 J/cm^2 light dose. The light doses 0.8 J/cm^2 and 1.3 J/cm^2 were chosen to obtain a lethal dose (LD) of 10, i.e. 10% cell death, and LD 40, i.e 40% cell death, after Ph-PDT for the subsequent experiments.

3.3.2 Effects of Ph-PDT on DNA damage

U87 glioma cells were exposed to different light doses, CNT at 0 J/cm^2, LC 1 at

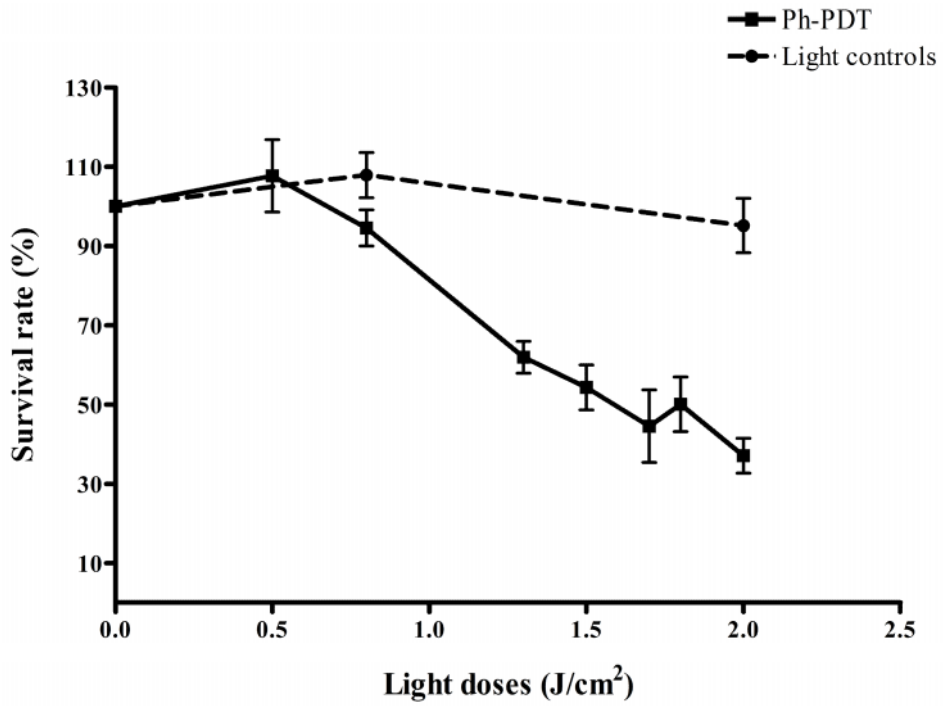

Fig. 3.6 **Cytotoxicity of U87 glioma cells after Ph-PDT.** The cells were treated with or without 1 μg/mL Photofrin and different light doses, i.e. Ph-PDT and light controls, respectively.

0.8 J/cm^2 and LC 2 at 1.3 J/cm^2 respectively. LC 1 and LC 2 were used to mimic the light doses used in LD 10 and LD 40 samples respectively. In Fig. 3.7, the comet images of U87 glioma cells 3 hours after Ph-PDT show that no comet tail, an indication of DNA damage, was visible in untreated control (CNT) and LCs, but different degrees in tail intensity were observed in dark control (DC) and Ph-PDT treated cells after exposure to different light doses. By quantifying the mean DNA percentages in the comet tails, the DNA percentage, and therefore DNA damage of LCs (~2%) were not significantly different from the CNT at 3hrs or 24hrs after illumination (Fig. 3.8A). In contrast, glioma cells treated with Photofrin (1 μg/mL) had noticeable DNA damage even in the dark control (DC) 3 hours after treatment (8.1%, $p<0.001$ when compared with CNT). Light illumination further enhanced the DNA damage to 13.9% in LD 10 and 33.2% in LD 40 ($p<0.001$ when compared with CNT).

3.3.3 Involvement of DNA repair in relatively resistant glioma cells after recovery from Ph-PDT

Since DNA damage increased rapidly 3hrs after Ph-PDT, experiments were carried out to determine if DNA repair took place in those relatively resistant glioma cells that survived after 24 hours. The comet assay showed that the comet tails in DC, LD 10 and LD 40 were shortened after 24-hour recovery from Ph-PDT (Fig. 3.7). The mean comet tail DNA percentage in DC (3.3%), LD 10 (10.3%) and LD 40 (20.3%) were also significantly decreased when compared with those 3 hours after PDT (grey bars compared with black bars in Fig. 3.8A).

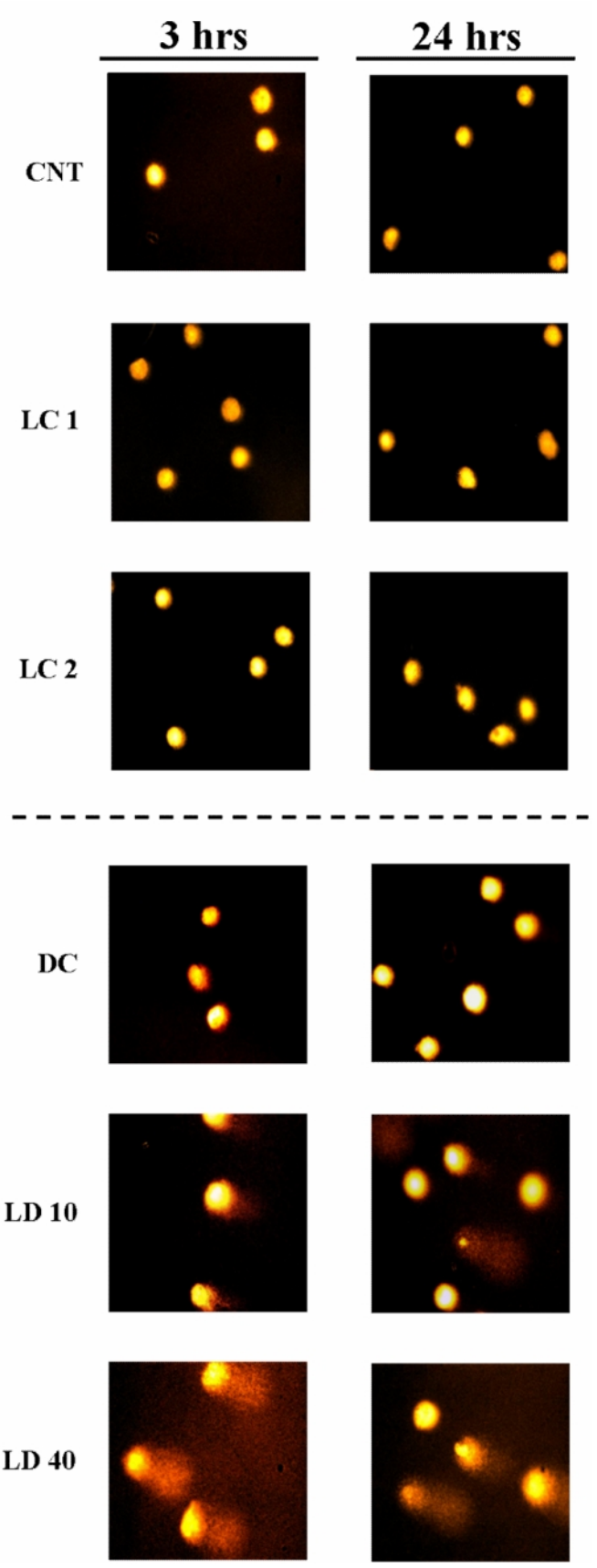

Fig. 3.7 **The comet images of U87 glioma cells 3 hours and 24 hours after Ph-PDT.**

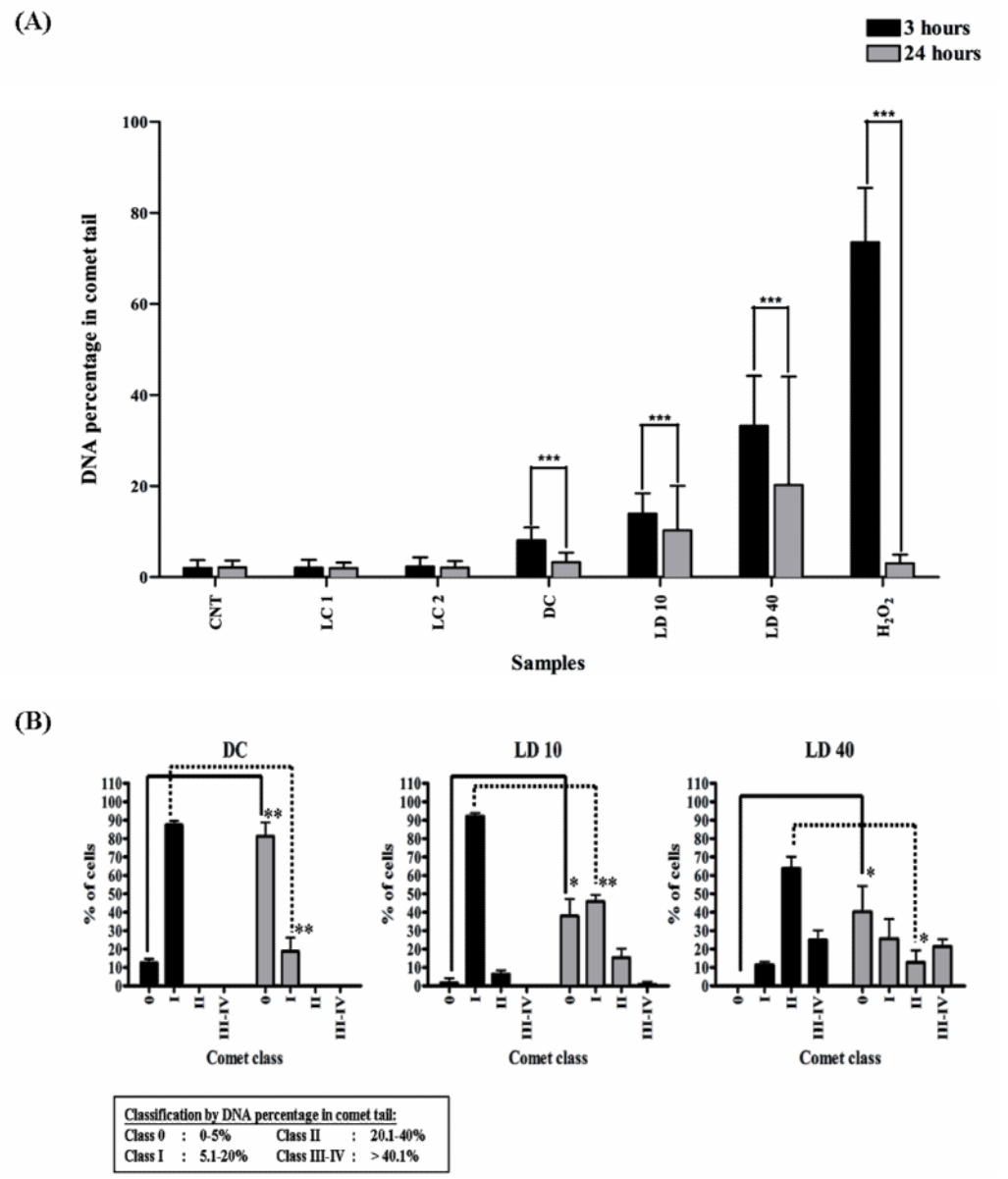

Fig. 3.8 **DNA damage and repair in U87 glioma cells after Ph-PDT.** DNA damage was detected by the alkaline comet assay and quantified as DNA percentage in tail. Cells were collected 3 hours (black bars) and 24 hours (grey bars) after the treatment. Hydrogen peroxide was used as positive control in the comet assay. (A) DC, LD 10 and LD 40 cells were significantly damaged when compared with the CNT, LC1 and LC2 cells. DC, LD 10 and LD 40 were also significantly repaired after 24 hours of recovery. Data from three independent experiments are expressed as mean+SD and analysed using paired t-test (*** indicates $p<0.001$). (B) Distribution of different comet classes at 3 hours (black bars) and 24 hours (grey bars) after treatment. Significant increase of Class 0 in DC and LD 10, and increase of Class 0 and Class I in LD 40 are indicative of DNA repair 24 hours after treatment. Data from three independent experiments are expressed as mean+SD and analysed using paired t-test (* indicates $p<0.05$ and ** indicates $p<0.01$).

The DNA repair of the relatively resistant glioma cells could be further illustrated by classifying the comet tails into an arbitrary scale of 0-IV according to Zhao *et al.*'s study, as shown in Fig. 3.8B.[314] The classification is based on the DNA percentages in comet tails: 0 represents no DNA damage and III-IV represents extensive DNA damage. After 24 hours of recovery from PDT, the fractions of heavily DNA-damaged cells, i.e. class III-IV, in different light doses were prominently decreased and the fractions of less DNA-damaged cells, i.e. class 0-I, were increased.

3.3.4 ALKBH2 significantly expressed after Ph-PDT

The involvement of the six selected DNA repair pathways were evaluated by determining the relative mRNA expression levels ($2^{-\Delta\Delta Ct}$) of their major DNA repair genes in the relatively resistant glioma cells, i.e. cells survived 48 hours after Ph-PDT. The six major DNA repair genes include: (1) *ALKBH2* of direct reversal, (2) *APEX1* of base excision repair, (3) *XRCC1* of short-patch BER, (4) *ERCC5* of nucleotide excision repair, (5) *RAD52* of double strand break repair, and (6) *REV1* of translesion synthesis. Most of the target genes were expressed equally in both the controls (i.e. CNT and DC) and Ph-PDT treated cells. Interestingly, *ALKBH2* and *REV1* were significantly over-expressed in the cells which were recovering and therefore less responsive to PDT. These cells showed 3-fold and 1.4-fold increases in *ALKBH2* and *REV1* mRNA expression levels respectively when compared with the controls ($p<0.05$) (Fig. 3.9A). The mRNA expressions of *ALKBH2* and *REV1* were evidently induced from 0.5 hours and remained high until 12 hours (Fig. 3.9B). *ALKBH2* was maintained at 2 to 3-fold increase after 0.5 hours of Ph-PDT, which is comparable to the mRNA level at 48 hours. However, *REV1* was highly expressed

(A)

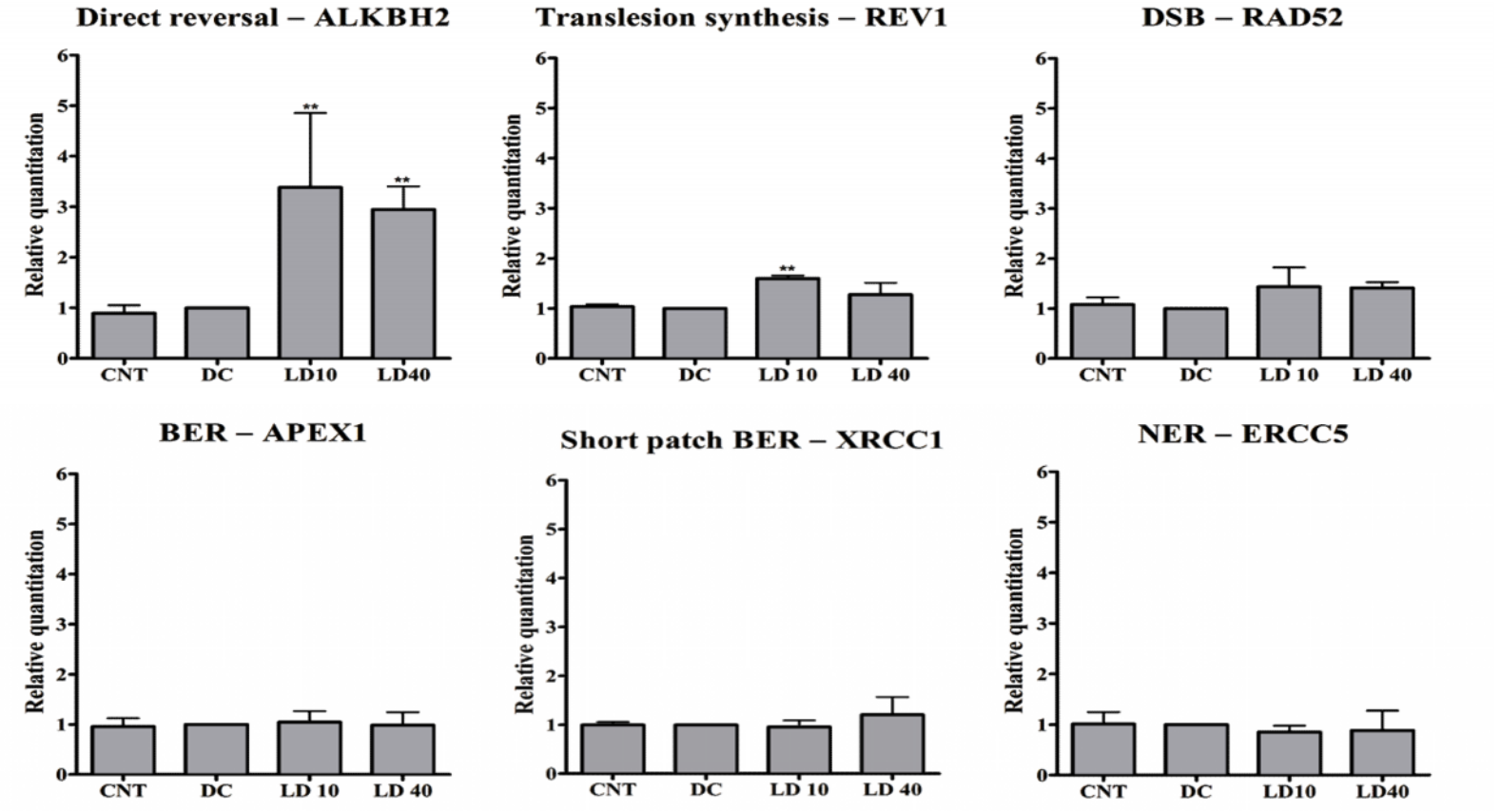

Fig. 3.9 Relative mRNA expression of DNA repair genes after Ph-PDT. (see page 150 for legend)

(B)

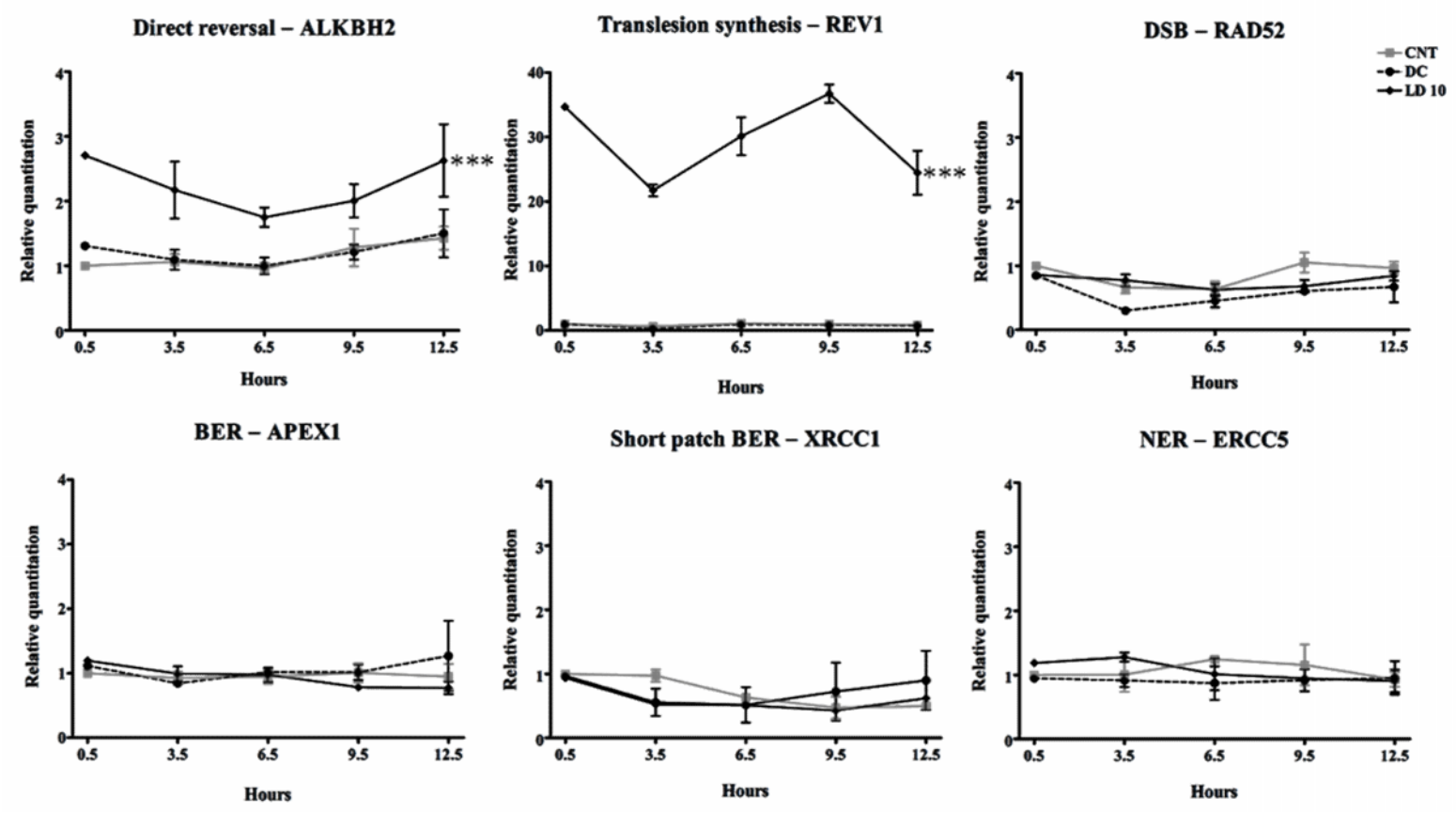

Fig. 3.9 Relative mRNA expression of DNA repair genes after Ph-PDT. (see page 150 for legend)

Fig. 3.9 **Relative mRNA expression of DNA repair genes after Ph-PDT.** (A) The mRNA levels of different DNA repair genes in cells 48 hours after Ph-PDT were determinated by quantitative real time RT-PCR. *ALKBH2* was significantly expressed in both LD 10 and LD 40 and *REV1* was significantly expressed in LD 10 when compared with dark control. Data are expressed as mean+SD and analysed using one-way ANOVA with Tukey's multiple comparison post-test of three independent experiments (** indicates $p<0.01$). (B) Quantitative real-time PCR of DNA repair genes at different time points after Ph-PDT with LD 10. *ALKBH2* and *REV1* mRNA expression of LD 10 was significantly increased when compared to that of CNT and DC. Note that the relative quantitation scale of all mRNA expression graphs are 0-4 except *REV1* is 0-40 as *REV1* mRNA was expressed at high levels. Data are expressed as mean+SD and analysed by using repeated measures one-way ANOVA with Tukey's multiple comparison post-test of three independent experiments (*** indicates the whole curve of LD 10 group is significant compared with both DC and CNT with $p<0.001$). *GAPDH* was used as housekeeping gene for normalisation.

at the mRNA level, with 20 to 35-fold increase at different time points after Ph-PDT when compared to that at 48 hours. This highly expressed mRNA level may indicate that the PDT-treated cells contained a large amount of unrepaired damage as REV1 is responsible for DNA replication to bypass the damage and to aid the cell in survival.

Sufficient time was required for the U87 glioma cells to recover and become resistant: the cell number decreased gradually from 3 hours to 24 hours and this cell number was maintained at 24-48 hours after Ph-PDT (data not shown). Therefore, the time point at 48 hours was selected to be a starting point in this study. Two lethal doses were also used at the beginning of this study to compare the differences in DNA repair gene expression under a low lethal dose condition, which produces cells with lower resistant ability to PDT, and a high lethal dose condition, which results in cells with higher resistant ability to PDT. The study was then followed by investigating the time course expression to further understand (1) when the genes were expressed, especially those genes that were significantly expressed at 48 hours, and (2) any other DNA repair gene expression was notably changed before 48 hours after Ph-PDT, which might also be a sign of their involvement. Western blotting was used to further examine ALKBH2 and REV1 protein expression (~29 kDa and 138 kDa respectively) 48 hours and at different time points after Ph-PDT. A slight increase was seen in REV1 protein expression at 48 hours (Fig. 3.10A) but no significant changes were observed for different time points (Fig3.11A). In contrast, ALKBH2 protein expression was up-regulated, in a time-dependent manner, in the cells less responsive to Ph-PDT (Fig. 3.10B and 3.11B) but not in the control cells.

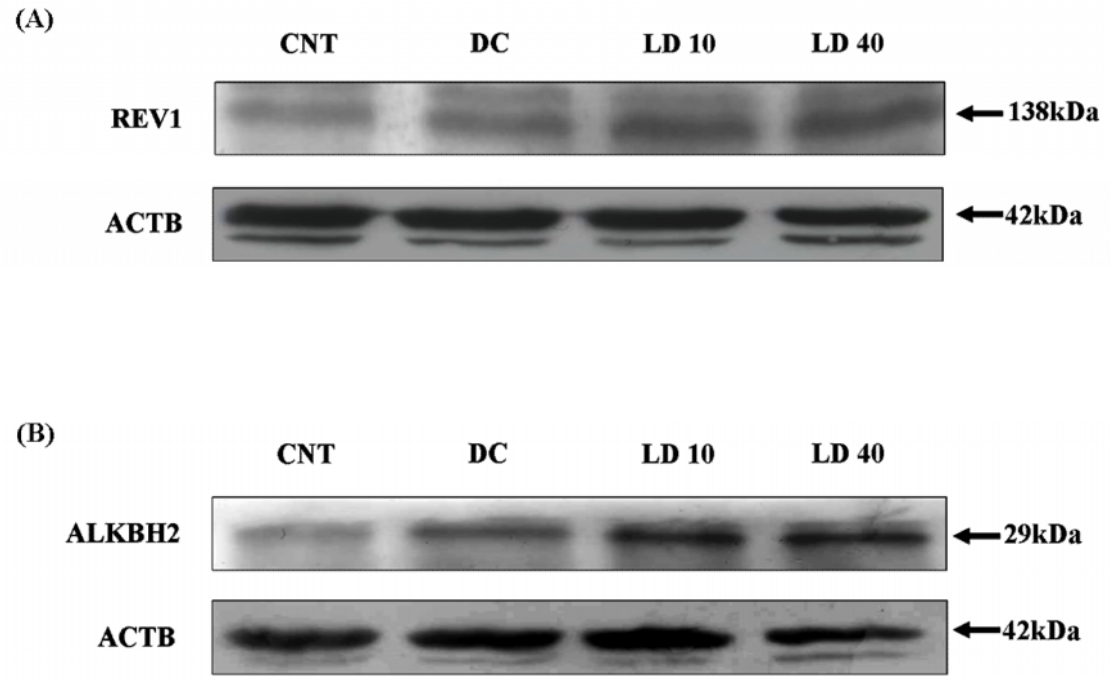

Fig. 3.10 REV1 and ALKBH2 protein expression 48 hours after Ph-PDT. (A) REV1 protein expression. (B) ALKBH2 protein expression. ACTB is beta-actin, which acted as loading control. These are the representative results from three independent experiments.

(A)

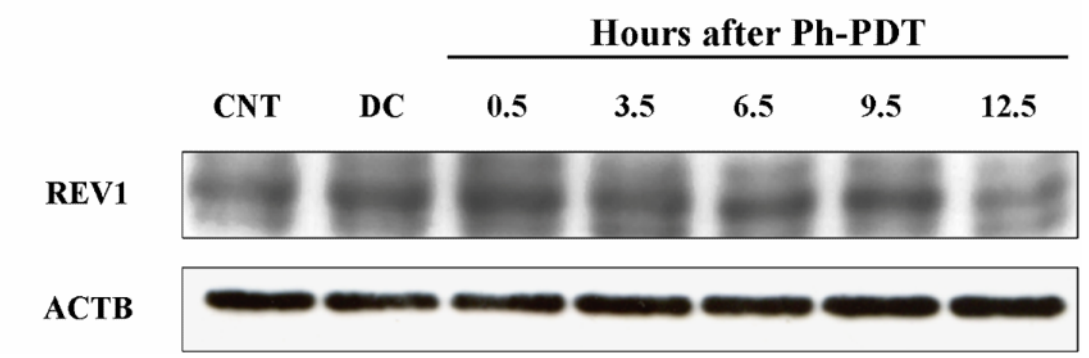

(B)

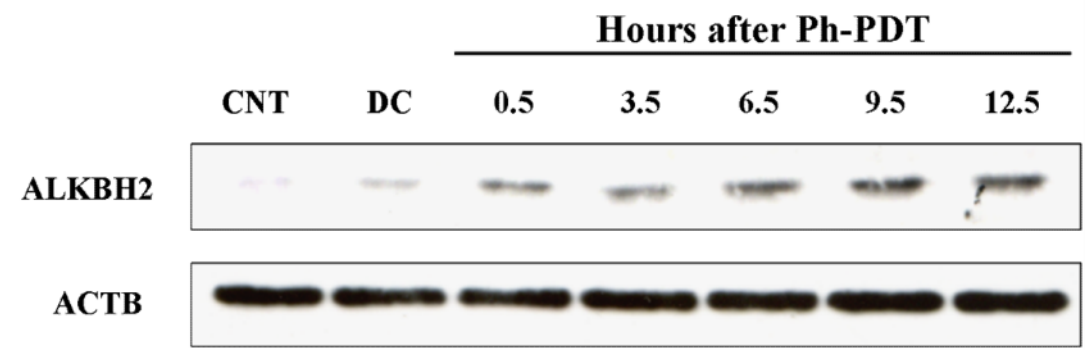

Fig. 3.11 REV1 and ALKBH2 protein expression after different time points of Ph-PDT with LD 10. (A) REV1 protein expression. (B) ALKBH2 protein expression. ACTB acts as loading control for Western blotting of human cell lysates. The time course is started at 0.5 hours because the time for Ph-PDT experiment was 0.5 hours. The CNT and DC samples were collected at 0.5 hour and the Ph-PDT treated cells were then collected every 3 hours until 12.5 hours after Ph-PDT experiment. These are the representative results from three independent experiments.

3.3.5 *ALKBH2* knockdown significantly increases the cytotoxic effect of Ph-PDT

Introducing siALKBH2 into cells can effectively knock down the mRNA and protein expression [Lipofectamine alone and cells with negative control RNA (Neg CNT)], as shown in Fig. 3.12A and B. Increased cell death was then seen in ALKBH2 under-expressing cells following Ph-PDT (Fig. 3.13). The sensitising effect was more evident with increasing light doses of the PDT, cytotoxicity was ~ 10% at low light dose (0.8 J/cm^2) and increased to ~ 25% at high light dose (1.3 J/cm^2). ALKBH2 under-expressing cells were more sensitive to Ph-PDT induced cell death when compared with the Neg CNT (Fig. 3.13).

3.3.6 Ph-PDT increases expression of TP53

According to the transcription element search system (TESS) web tool (http://www.cbil.upenn.edu/cgi-bin/tess/tess?RQ=WELCOME), TP53 is a potential transcription factor that binds to the promoter of *ALKBH2*. Therefore, the role of TP53 in Ph-PDT was first examined by RT-PCR and Western blotting. The mRNA and protein expression of TP53 in U87 glioma cells increased after 0.5 hours of PDT. At the mRNA level, TP53 expression was maximum at 0.5 hour (Fig. 3.14A). However, TP53 protein expression was maximum at 3 hours (Fig. 3.14B). The protein expression of the activated phosphorylated TP53 at Ser15 amino acid position [pTP53 (Ser15)] was then investigated. It is because the phosphorylation at Ser15 amino acid position of TP53 is an indication of DNA damage and lead to DNA repair in cells.[315,316] pTP53 (Ser15) was also found to increase from 3.5 hours, reach a maximum at 6.5 hours and then decline thereafter in relatively

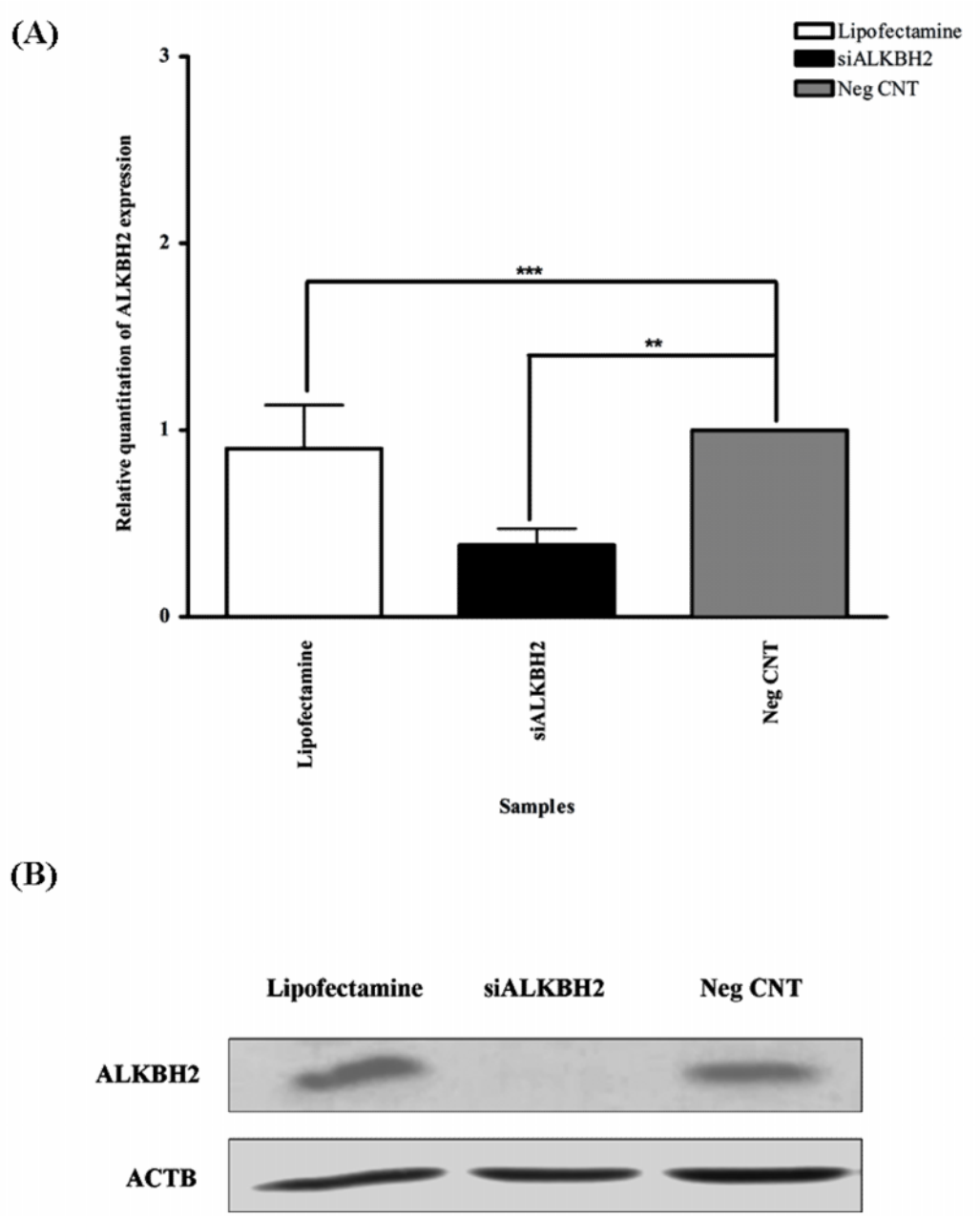

Fig. 3.12 **Effect of siRNA on ALKBH2.** The experiments were performed 22 hours after *ALKBH2* knockdown. (A) Relative mRNA expression of *ALKBH2*. Cells were transfected with the antisense oligonucleotide (siRNA) for knockdown and unrelated oligonucleotide as Neg CNT. mRNA expression is relative to Neg CNT as Lipofectamine control is just used to evaluate the effect of this transfecting reagent in target gene expression. Data are expressed as mean+SD and analysed by using one-way ANOVA with Tukey's multiple comparison post-test of three independent experiments (** indicates $p<0.05$ and *** indicates $p<0.001$). *GAPDH* was used as housekeeping gene for normalisation. (B) Protein expression of ALKBH2. ACTB acts as loading control for Western blotting. These are the representative results from three independent experiments.

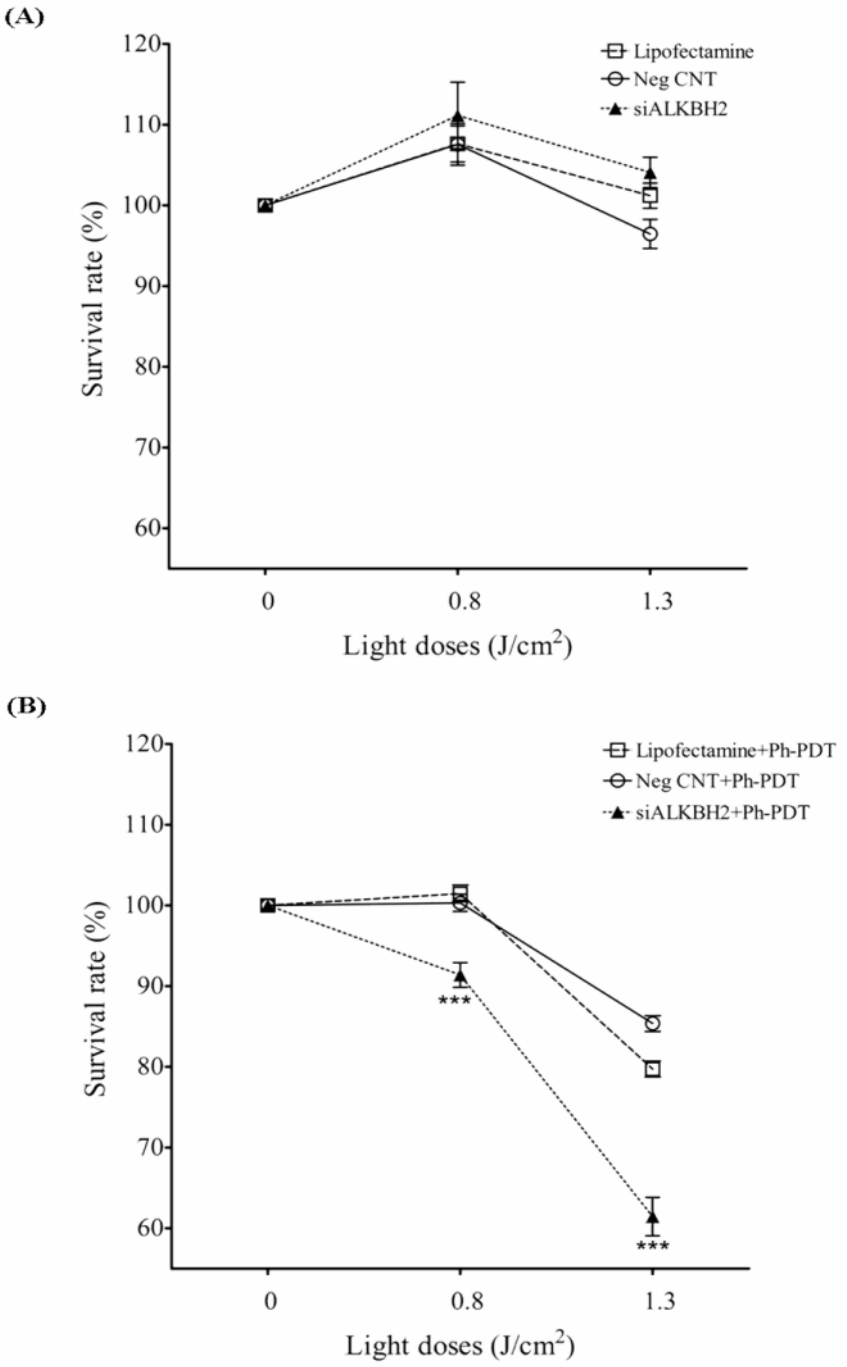

Fig. 3.13 **Effect of siRNA on cytotoxicity.** Survival rate (%) of cells treated with Lipofectamine alone (Lipofectamine) (dashed line with squares), siALKBH2 (dotted line with triangles) and Neg CNT (solid line with circles) was assessed using the trypan blue assay. (A) Cells were exposed to different light doses alone and (B) cells treated with Ph-PDT (1ug/mL). Data are expressed as mean±SD and analysed by using one-way ANOVA with Tukey's multiple comparison post-test of three independent experiments (** indicates $p<0.05$ and *** indicates $p<0.001$).

(A)

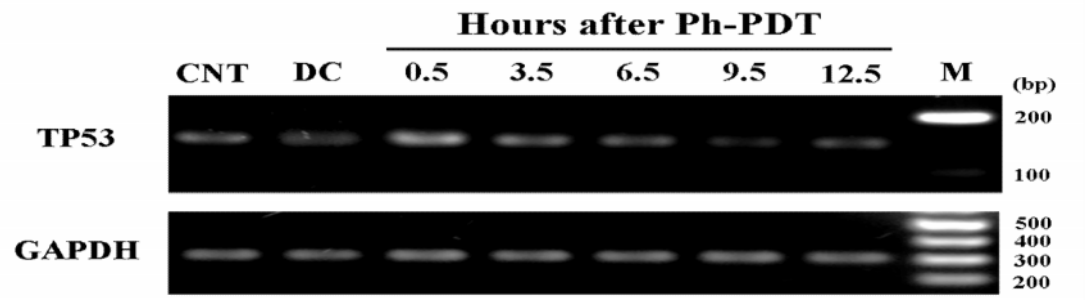

(B)

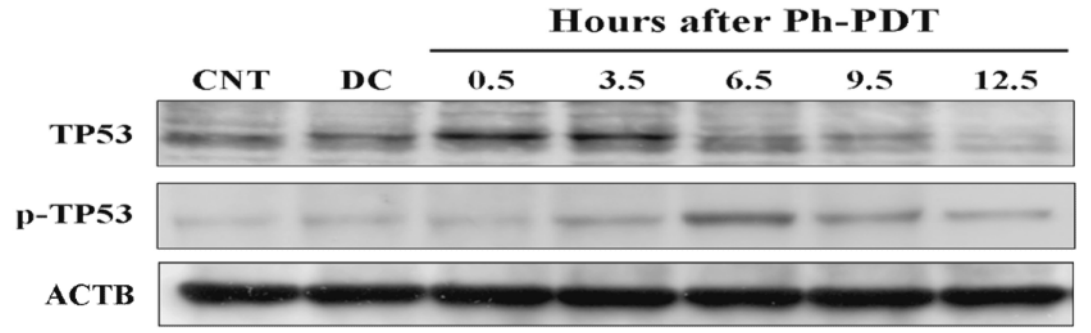

Fig. 3.14 Expression of TP53 and p-TP53 at different time points after Ph-PDT. (A) TP53 mRNA expression increased rapidly (0.5 hour) and declined gradually over time. Lane M is the DNA marker ladder. (B) TP53 protein expression (~53 kDa) also increased rapidly and maintained up to 3.5 hours, then declined with time. p-TP53 protein expression (~53 kDa) was significant increased from 3.5 hours, reached a maximum at 6.5 hours and declined with time. *GAPDH* and ACTB acted as loading controls for RT-PCR and Western blotting respectively. These are the representative results from three independent experiments.

resistant glioma cells (Fig. 3.14B).

3.3.7 Increased TP53 binding on *ALKBH2* after Ph-PDT

3.3.7.1 Optimisation of DNA shearing

The sonication conditions of U87 cells were optimised for generating DNA fragments of 200-500 bp, which is the most suitable DNA fragment size range for the ChIP assay (Fig.3.15). The U87 cell suspension was sonicated for 10 seconds on ice, then paused for 30 seconds. Eleven cycles was determined to be optimum for generating the most 200-500 bp fragments by software (data not shown).

3.3.7.2 ChIP assay on *ALKBH2* promoter region

The participation of TP53 in the transcription of *ALKBH2* during Ph-PDT was explored using the ChIP assay. Two TP53 binding sites were predicted by TESS at-190 bp and -14 bp from +1 transcription start site of *ALKBH2* (Fig. 3.5). The U87 glioma cells with or without Ph-PDT were treated as follows: (1) Input controls, i.e. no immunoprecipitation, were used as positive control for determining the amount of chromatin present and used in each reaction; (2) IP with IgG, i.e. immuno-precipitated by IgG antibody, was a negative control for indicating the amount of background signal formed during ChIP assay procedures; and (3) IP with TP53, i.e. immunoprecipitated by TP53 antibody. The conventional PCR result showed that a PCR product could be amplified in the DNA sample extracted from cells treated with Ph-PDT. This PCR product was amplified from -257 bp to +147 bp promoter region of *ALKBH2*, where the predicted TP53 binding sites were. This result implied that the binding of TP53 was increased after Ph-PDT on the promoter region of *ALKBH2* (Fig. 3.16A). Real-time PCR was then used to confirm and quantify

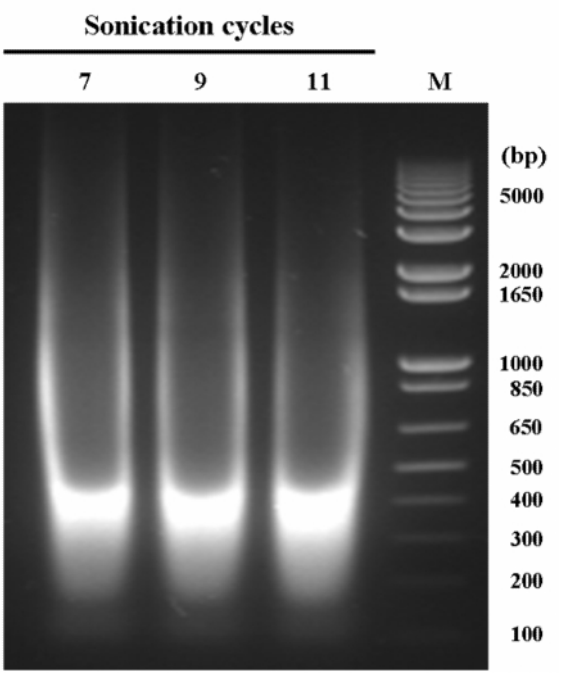

Fig. 3.15 **Optimisation of the sonication cycles of U87 for ChIP assay.** The optimised sonication condition is 11 cycles since more DNA fragments are in 200 to 500 bp after the sonication. The intensities of each DNA band were quantified by KODAK Image Station 4000 (Carestream Health, Inc, Rochester, NY, USA) and highest intensity was obtained in the DNA band with 11 cycles of sonication (data not shown). Lane M is the 1 kb DNA ladder.

(A)

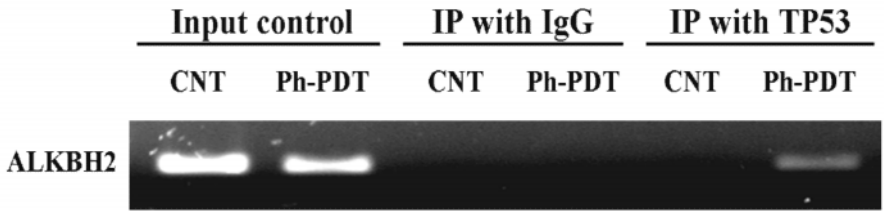

(B)

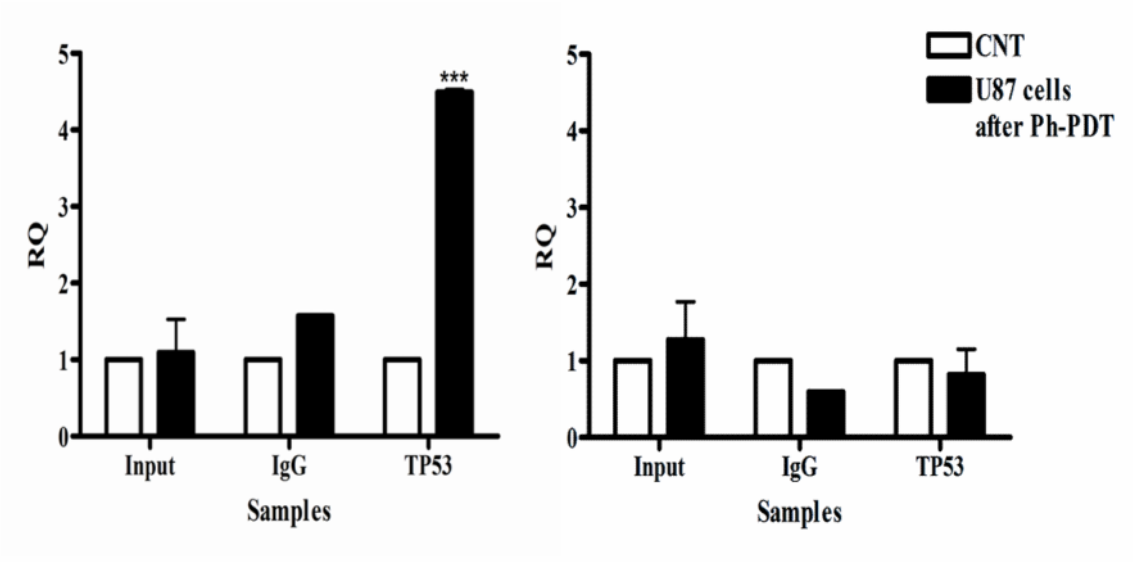

Fig. 3.16 **Interaction of TP53 with the *ALKBH2* promoter.** (A) ChIPs were performed using anti-rabbit IgG or anti-TP53 antibodies. Immunoprecipitated DNA was analysed by conventional PCR for the presence of *ALKBH2* gene. These are the representative results from three independent experiments. (B) ChIP samples analysed and quantified by real-time PCR. The left panel is for the predicted TP53 binding site (Position 1) and the right panel for the predicted TP53 binding site (Position 2). Data are expressed as mean+SD of three independent experiments and analysed using paired t-test (*** indicates $p<0.001$). *GAPDH* was used as housekeeping gene for normalisation.

the binding position of TP53 on *ALKBH2* promoter. The result demonstrated that more PCR products were amplified from the -257 bp to -138 bp of ALKBH2 promoter region in the Ph-PDT sample. This region contains a TP53 binding site at -190 bp, i.e. Position 1 shown in Fig 3.5. Therefore, it can be concluded that TP53 binding increased at position 1 (4.5-fold increase) after Ph-PDT (Fig. 3.16B).

3.3.8 TP53/ALKBH2 related protein expression at different time points after Ph-PDT

To understand the mechanism of Ph-PDT resistance caused jointly by TP53 and ALKBH2, for example, how TP53 is regulated to bind on the *ALKBH2* promoter, different TP53 and ALKBH2 related proteins were examined to link up the existing known protein interactions with the findings in this study. The proteins of interest include the following: (1) PCNA, which may reduce the DNA repair capacity of ALKBH2 through binding; (2) JNKs, which activates TP53 by phosphorylation; and (3) NPM1, which stabilises TP53 protein. These proteins may be involved in Ph-PDT resistance by interacting with TP53 and ALKBH2.

3.3.8.1 PCNA and JNKs

Little effect on the expressions of PCNA and total JNKs were found after Ph-PDT (Fig. 3.17). However, a high level of p-JNKs was found in relatively resistant glioma cells (Fig. 3.17B). The phosphorylation of JNKs was sharply increased and peaked at 0.5 hours after Ph-PDT. Both JNK1 and JNK2/3 were phosphorylated, but the latter one to a greater extent after Ph-PDT. The levels of phosphorylated JNKs decreased rapidly within 3 hours and remained at a low level

(A)

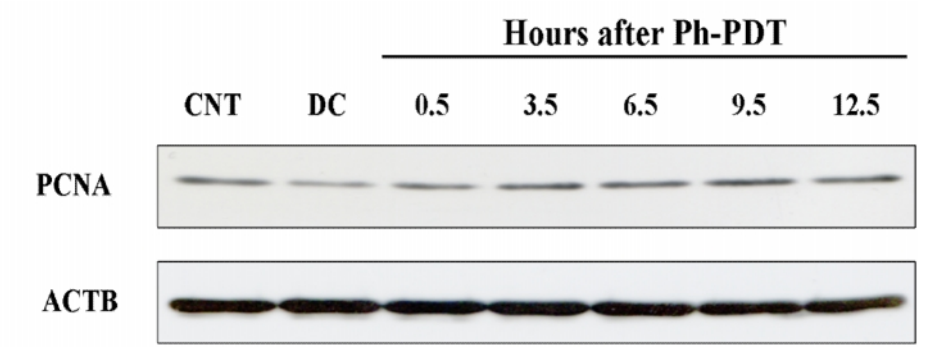

(B)

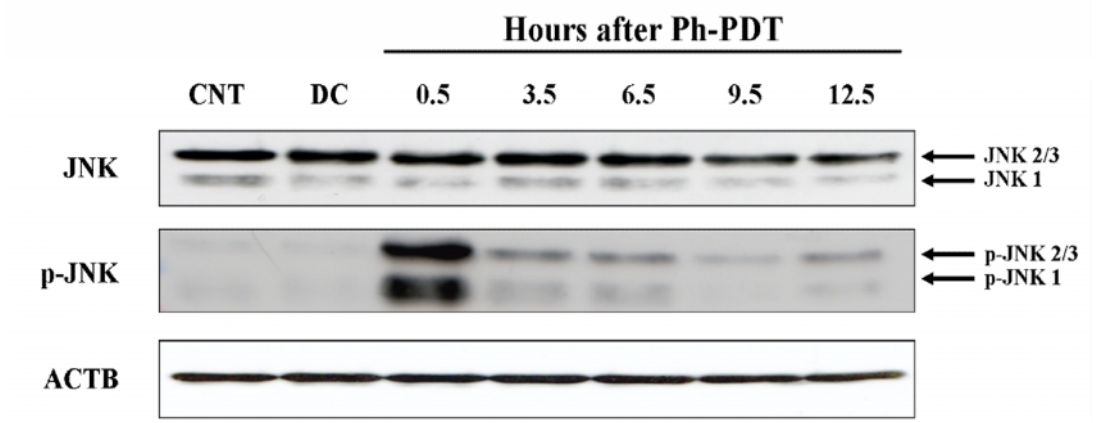

Fig. 3.17 **Effect of Ph-PDT on PCNA, JNK and p-JNK protein levels.** (A) PCNA protein expression at different time points after Ph-PDT but no difference observed. (B) JNK protein decreased slightly in expression 9.5 hours after Ph-PDT and p-JNK protein increased significantly and reached a maximum at 0.5 hours. ACTB acts as loading control for Western blotting and these are the representative results from three independent experiments.

up to 12.5 hours after Ph-PDT.

3.3.8.2 NPM1

The protein level of NPM1 rapidly increased at 0.5 hours after Ph-PDT, then declined gradually over the next 6 hours (Fig. 3.18). The corresponding mRNA level was also slightly increased, compared with control, 0.5 hours after Ph-PDT and decreased to an undetectable level when analysed using SYBR safe DNA gel stain in agarose gel electrophoresis at 6.5 hours after Ph-PDT. As there was an increase in NPM1 after Ph-PDT with a similar expression pattern as TP53, it is worth determining the role of NPM1 in Ph-PDT and its contribution to Ph-PDT resistance.

3.3.9 *NPM1* knockdown significantly increases the cytotoxicity of Ph-PDT

Compared with the controls (Lipofectamine alone and Lipofectamine plus Vector), increased cell death was seen in NPM1 knockdown cells after Ph-PDT (Fig. 3.19). Approximately 45% of these cells died as compared with the vector-transfected cells. In addition, these cells were more sensitive to Photofrin alone. Under DC conditions, NPM1 knockdown cells experienced 25% more cell death when compared with the cells with vector only.

3.3.10 Significant decrease in TP53 and ALKBH2 expression after *NPM1* knockdown

As can be seen in Fig. 3.20, the mRNA and protein expression of TP53 and ALKBH2 were suppressed after NPM1 knockdown. Compared with the cells

(A)

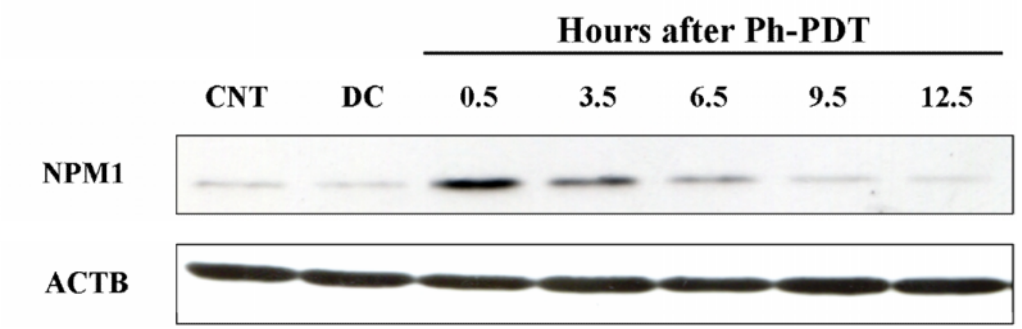

(B)

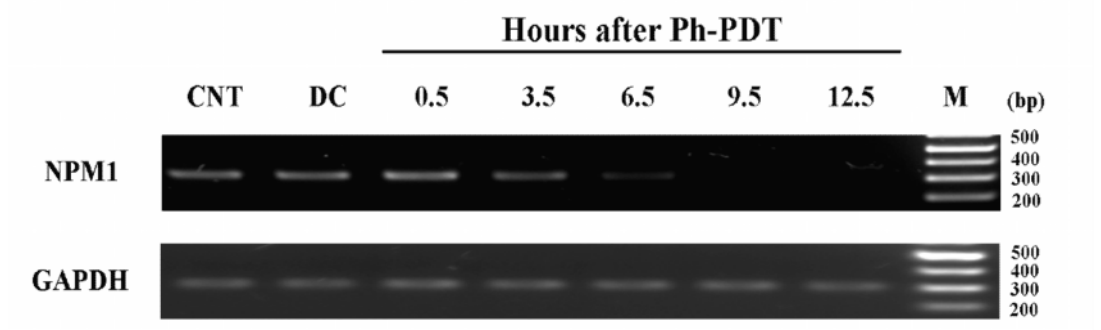

Fig. 3.18 Protein and mRNA expression of NPM1 at different time points after Ph-PDT. (A) NPM1 protein expression increased sharply and reached a maximum at 0.5 hours and declined back to control levels after 9.5 hours. (B) NPM1 mRNA expression was increased only slightly at 0.5 hours when compared with the controls. Lane M is Invitrogen 1 kb plus DNA ladder. ACTB and *GAPDH* act as loading controls for Western blotting and RT-PCR respectively. These are the representative results from three independent experiments.

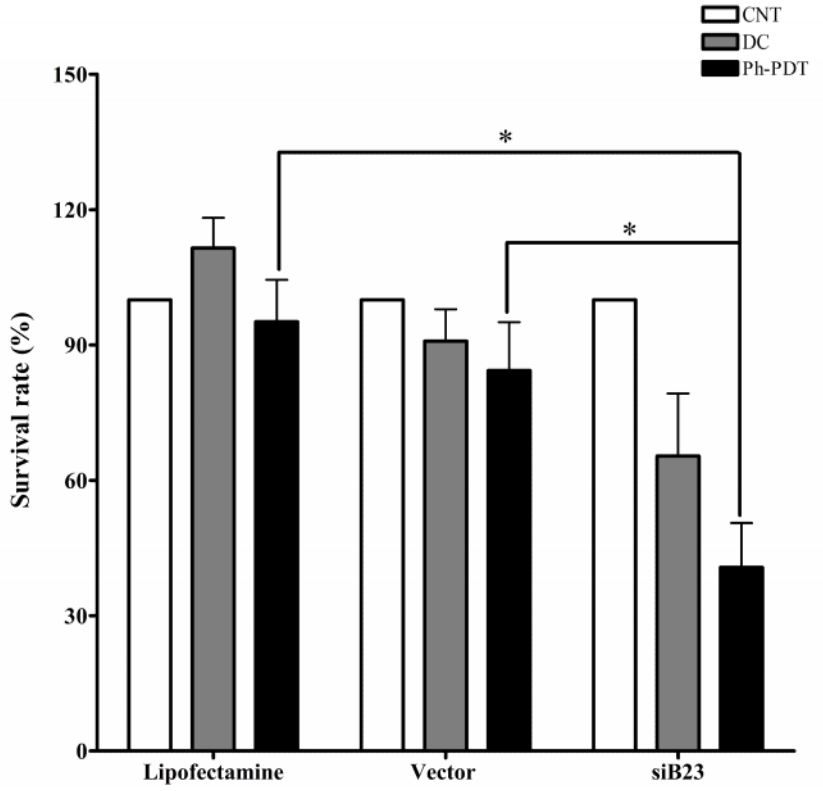

Fig. 3.19 Cytotoxicity of Ph-PDT on U87 glioma cells after *NPM1* knockdown. The cells were treated with 1 μg/mL Photofrin and 0.5 J/cm^2 light dose. Data are expressed as mean+SD of three independent experiments and analysed using one-way ANOVA with Tukey's post-test (* indicate $p<0.05$).

(A)

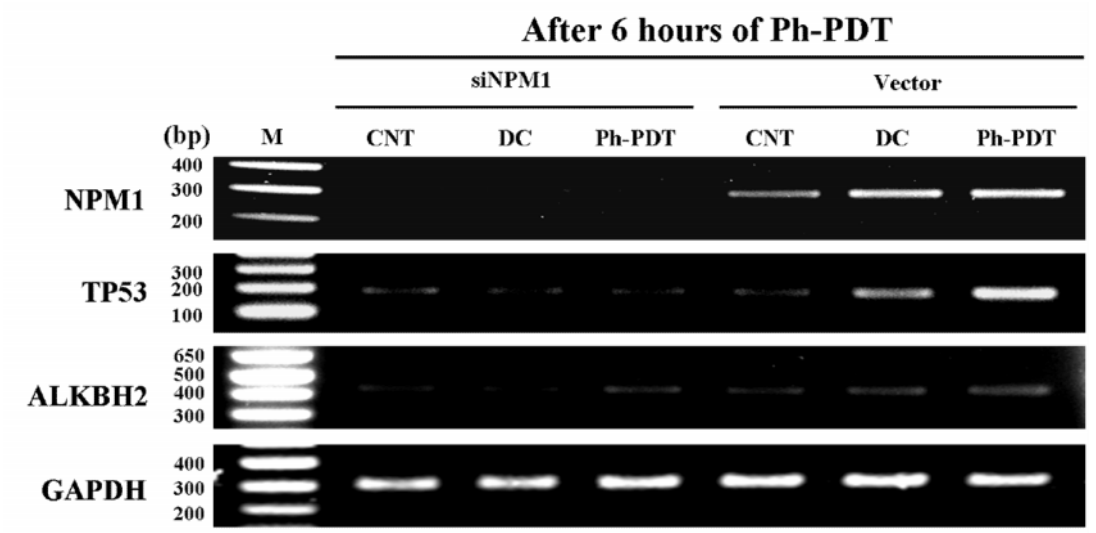

(B)

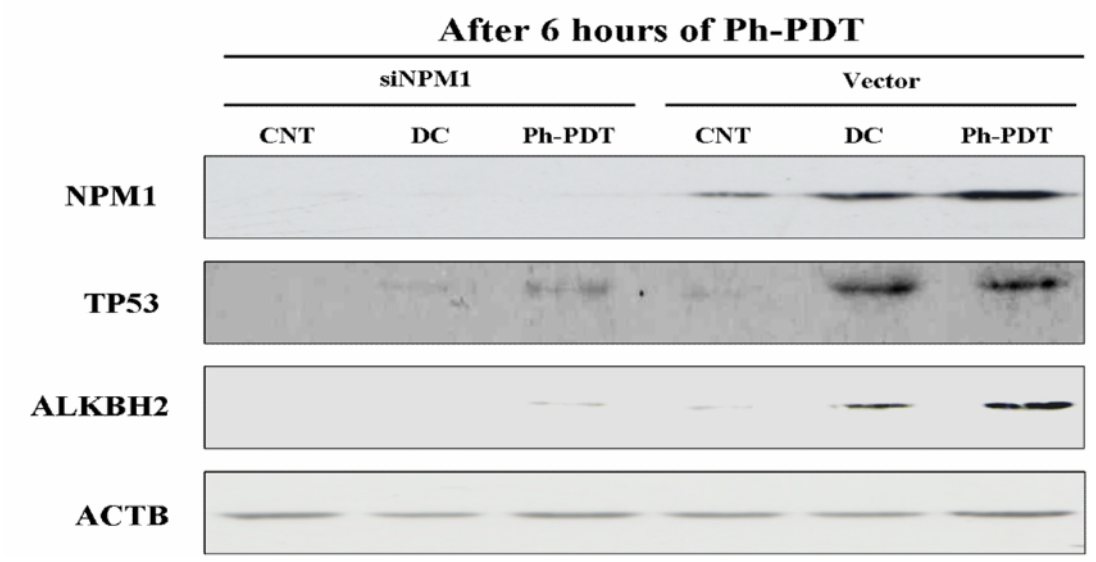

Fig. 3.20 The effects on TP53 and ALKBH2 expression after *NPM1* knockdown. Both mRNA (A) and protein expression (B) of TP53 and ALKBH2 decreased significantly in CNT, DC and Ph-PDT treated cells after the NPM1 knockdown compared with those cells with vector alone. Lane M in (A) is Invitrogen 1 kb plus DNA ladder. *GAPDH* and ACTB act as loading controls for RT-PCR and Western blotting respectively. These are the representative results from three independent experiments.

under-expressing NPM1, the mRNA and protein levels of NPM1, TP53 and ALKBH2 in vector-transfected cells were higher in DC and more so in Ph-PDT treated cells. The same expression trends at very low levels were observed in the cells under-expressing NPM1 in DC and after Ph-PDT.

3.3.11 Interaction of NPM1 with different transcription factors on *ALKBH2* promoter

To further study how NPM1 affected ALKBH2 expression and thus the cytotoxicity of Ph-PDT, ChIP assay was performed to investigate NPM1 binding on *ALKBH2* promoter region. As NPM1 is not a transcription factor, it has to bind proteins through other transcription factors. TP53, Sp1 and NF-κB are three transcription factors that may bind NPM1. Therefore, TP53, Sp1 and NF-κB binding sites on *ALKBH2* promoter region were predicted by TESS. Different primers were designed to amplify the promoter region of *ALKBH2* from -2000 bp to +1000 bp, this region contains two TP53, six Sp1 binding sites and three NF-κB binding sites (Fig. 3.5). However, no PCR product was amplified in the samples of IP with IgG and IP with NPM1, i.e. immunoprecipitated with NPM1. This result indicated that no binding of NPM1 via TP53, Sp1 and NF-κB binding sites on *ALKBH2* promoter from -2000 bp to +1000 bp region will occur. ChIP assay results using NPM1 antibody are shown in Fig 3.21.

3.3.12 Nucleophosmin affects TP53 mRNA stability after Ph-PDT

As no NPM1 binding via the transcription factors on *ALKBH2* promoter were

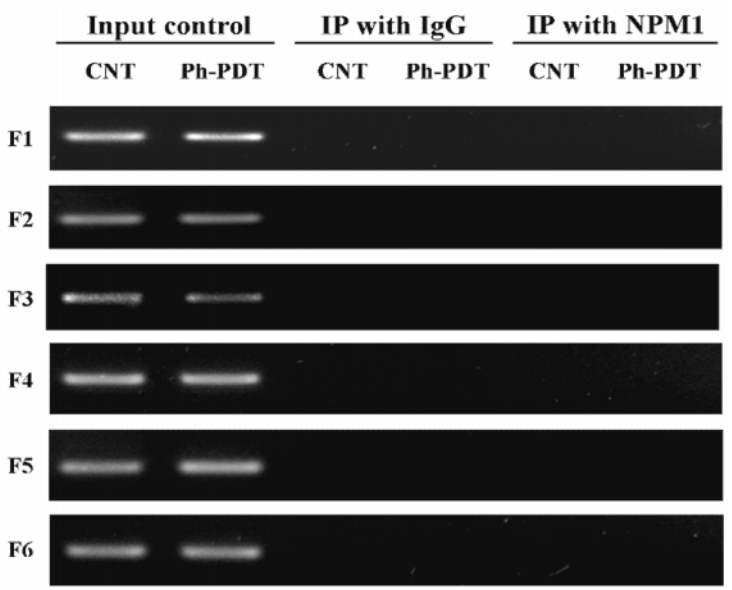

Fig. 3.21 ChIP assay result for studying the binding of NPM1 on *ALKBH2* promoter region. ChIPs were performed using anti-rabbit IgG or anti-NPM1 antibodies and the immunoprecipitated DNA was analysed by conventional PCR. PCR products were amplified from six regions of DNA (the locations of these regions are indicated as F1 to F6 in Fig. 3.5), which contains different NPM1-related transcription factors. The result is representative of two independent experiments.

observed in the experiment mentioned above, the decrease in ALKBH2 expression after *NPM1* knockdown may be explained by the decrease in TP53 expression, which may be affected by NPM1. To illustrate the relationship between NPM1, TP53 and ALKBH2, mRNA stability assay was performed because NPM1 can stabilise TP53 mRNA.[238] The U87 cells with or without Ph-PDT after NPM1 knockdown showed a more rapid decrease in the amount of TP53 mRNA than the cells without *NPM1* knockdown (Fig. 3.22). This result indicates that NPM1 help in TP53 mRNA stabilisation. However, in the Ph-PDT treated cells with *NPM1* knockdown the decrease in TP53 mRNA was reduced from 7 hours to 10 hours after Ph-PDT when compared with the untreated cells with *NPM1* knockdown. This result means that Ph-PDT may help stabilise TP53 mRNA via other proteins or mechanisms. The comparisons were made with the vector controls at different time points.

The research questions and main results are summarised in Fig. 3.23.

3.4 Discussion

Numerous reports have shown that Ph-PDT induces significant DNA damage.[137-140] Different types of DNA damage may be observed, including double strand breaks, single strand breaks, DNA base oxidation and cross-links.[138,139,286,317,318] As DNA damage is not directly linked to the cell death caused by PDT, little research has been conducted to investigate the involvement of DNA repair in PDT. However, Penning *et al*. showed that the inhibition of a DNA repair enzyme (poly(ADP-ribose)polymerase) activity and the formation of irreversible DNA damage were correlated to the killing effect of haematoporphyrin

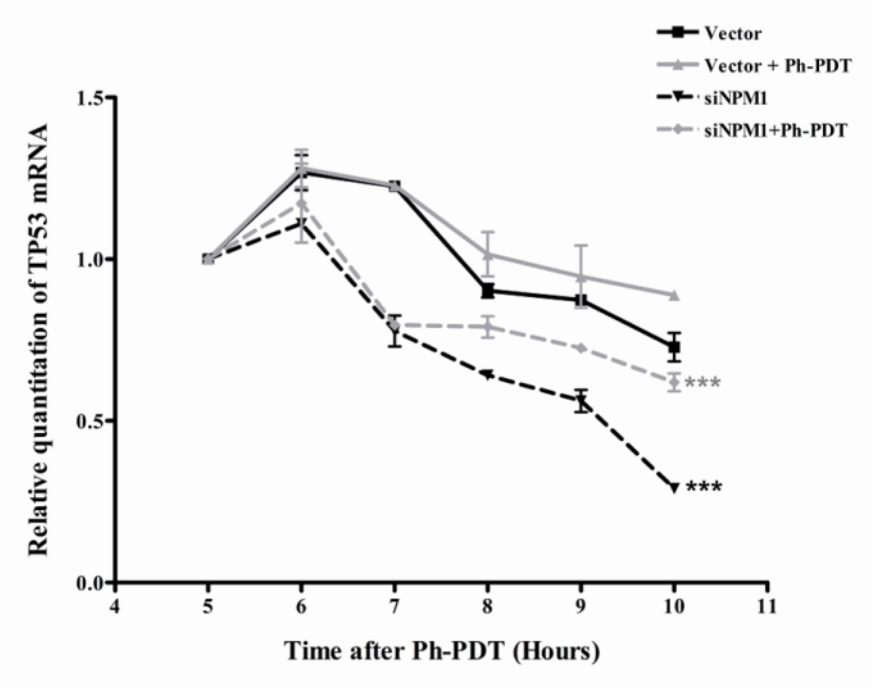

Fig. 3.22 mRNA stability of TP53 after *NPM1* knockdown and Ph-PDT. Data are expressed as mean+SD of three independent experiments and analysed using two-way ANOVA with Bonferroni post-test. *** represent TP53 mRNA stability of siNPM1 when compared with that of Vector and siNPM1+Ph-PDT when compared with Vector+Ph-PDT are significantly decreased with $p<0.001$ from 6 to 10 hours. *GAPDH* was used as housekeeping gene for normalisation.

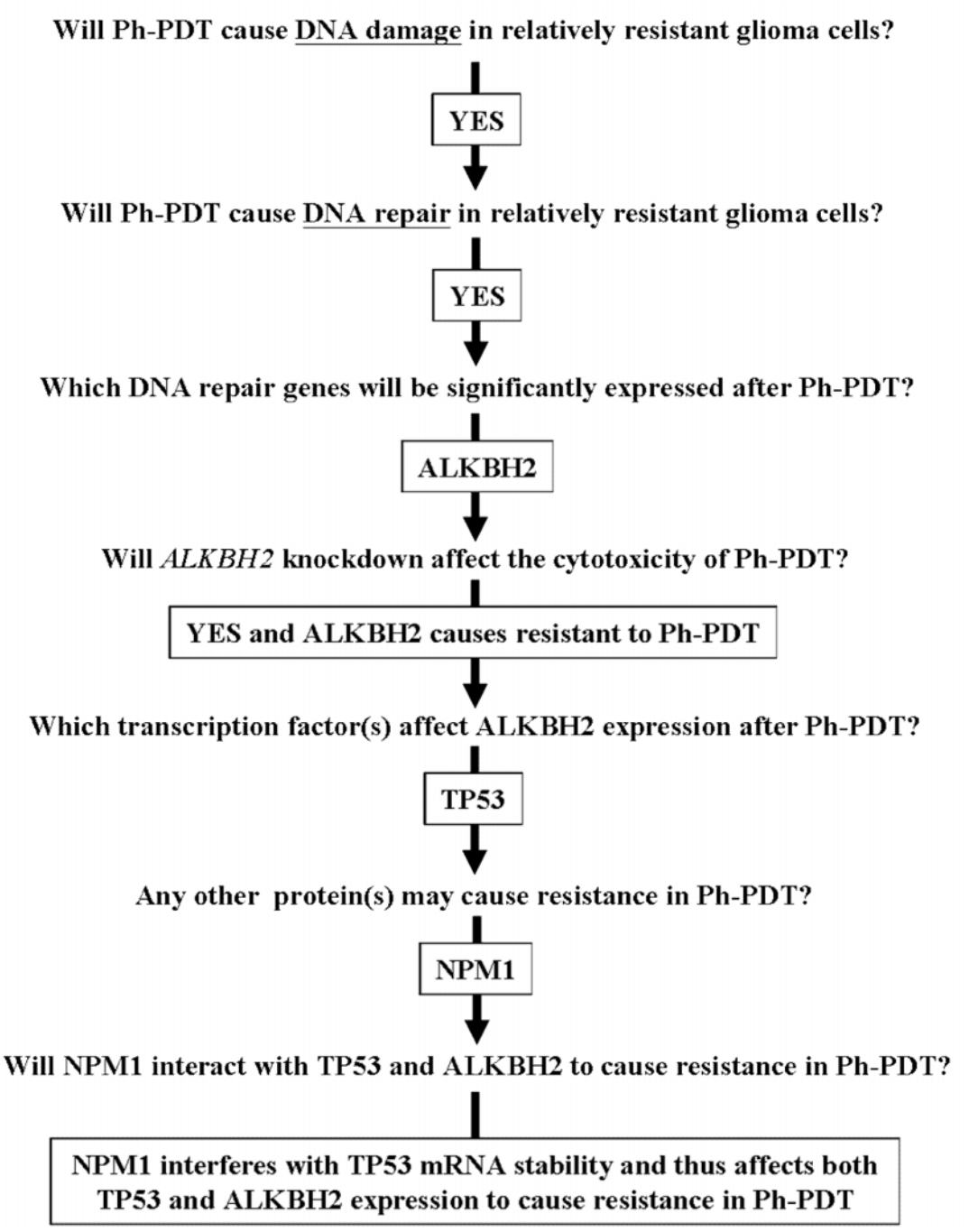

Fig. 3.23 The flow of research questions and main results in Chapter 3.

derivative (HPD)-PDT in a murine fibroblast cell line; note that Photofrin is purified form of HPD.[319] This research article suggested that the involvement of DNA damage and repair in PDT is cell type dependent. Another study by Gupta *et al*. illustrated that enhanced DNA repair reduced the micronuclei formation, which is an indication of cytogenetic damage, in the glioma cells and this damage caused the cells to be relatively resistant to HPD-PDT.[320] The DNA repair capacity is determined not only by cell type, but also oxygen concentration and subcellular localisation of Photofrin. Since glioma treatment using Ph-PDT is still under clinical trial, the detailed DNA repair mechanism involved in Ph-PDT for glioma treatment should be studied so that the efficacy of Ph-PDT can be enhanced by preventing DNA repair-induced resistance.

Based on the knowledge gained from previous studies mentioned above, our preliminary focus was to examine the participation of DNA damage and repair in a glioma cell line after Ph-PDT. Our results are consistent with other reports in that the amount of DNA damage is positively associated with PDT light dosage.[138,321] DNA damage is increased in Ph-PDT treatment groups (i.e. LD 10 and LD 40) when the PDT light dose was increased (Fig. 3.8A). The DNA damage in treatment groups are significantly different from that of the control groups (light control and dark control). It is clear from the results presented here that light alone will not cause significant DNA damage. As seen in the DC group, DNA was damaged to a lesser extent when compared with that of the treatment groups. This effect may be due to the low dose of light such as low ambient lighting affecting the cells during the course of the experiments. As Photofrin itself cannot localise to the nucleus and cause DNA damage, the increased DNA damage in treatment groups could be

explained by the impairment of the nuclear membrane after light irradiation.[159,322-325] Consequently, sensitised reactive molecules, including photoproducts, can enter the nucleus and damage DNA.[324,326]

The level of DNA damage in treatment groups was reduced (Fig. 3.8A) and the number of Class 0 and I cells were increased (Fig. 3.8B) after the cells were allowed to recover for 24 hours. The DNA repair efficiency was less effective in the low light dose (LD 10) treatment group than that in the high light dose (LD 40). Since the DNA repair capacity of the cells should be the same, the difference in the efficiency may be due to different DNA repair kinetics being activated by different light intensities. These findings indicate that DNA damage and repair were induced in the relativly resistant glioma cells after the cells were allowed to recover post Ph-PDT treatment. Although DNA damage was also seen in DCs, the damage seen was completely recovered after 24 hours. This may be because little DNA damage was present in DC cells, but the participation of another DNA repair mechanism cannot be excluded.

Our data demonstrate that DNA repair mechanisms are triggered in relatively resistant glioma cells. However, it is not known which DNA repair pathways are involved. To address this question, we used real-time quantitative PCR to quantify the gene expression of six specific DNA repair genes and used Western blotting to semi-quantify the target proteins. As shown in Fig. 3.9, the *ALKBH2* gene of DNA damage reversal and the *REV1* gene of translesion synthesis were expressed. Their mRNA transcripts were expressed at a significantly higher level in Ph-PDT treated glioma cells when compared with that of the control cells. This indicates that both

DNA damage reversal and translesion synthesis mechanisms may play important roles in conferring resistance to glioma cells against Ph-PDT.

Some interesting findings are observed in Fig. 3.9. Compared to Fig. 3.11, the protein expression of ALKBH2 did not show a U-shaped trend with a trough at 6.5 hr (Fig. 3.11) as shown in mRNA expression data (Fig. 3.9). It was probable that the relative differences in mRNA expression between each time point are not large enough to affect the expression of protein and be detected by Western blotting, which is a semi- quantitative method. The figures also show that *REV1* mRNA expression is "abnormally" high after Ph-PDT. The *REV1* gene is involved in translesion synthesis, and allows damaged DNA to be tolerated by replicative bypass. When translesion synthesis is triggered, DNA replicates with mutations or errors and thus DNA damage-induced mutagenesis occurs.[327] Therefore, large amounts of DNA damage may be introduced by Ph-PDT and thus increase in REV1 expression is required to maintain cell survival. Although REV1 mRNA expression level was very high but its protein expression level showed inconsistent results. This may be due to the poor sensitivity of the REV1 antibody, and therefore we further focused on how ALKBH2 involved in Ph-PDT responsiveness as both mRNA and protein expression levels of ALKBH2 are significantly higher in relatively resistant glioma cells.

The *ALKBH2* gene is not significantly expressed in normal brain cells but high levels are found in liver and sex organs.[19,328] It is responsible for repairing 1-methyladenine, 3-methylcytosine and 1,N^6-ethenoadenine on double stranded DNA by oxidative demethylation.[328,329] Cetica *et al*. showed that *ALKBH2* was

highly expressed in gliomas and suggested that aberrant ALKBH2 expression played a part in tumour cell resistance to cancer treatments.[330] We also found an up-regulation of ALKBH2 in glioma cells from 30 minutes to 48 hours post Ph-PDT treatment. This observation may imply that the photosensitised reactive products in Ph-PDT produce 1-methyladenine, 3-methylcytosine and/or 1,N^6-ethenoadenine on DNA. Most DNA damage studies on Ph-PDT targeted DNA damage caused by oxidation. Here, we suggest that the photosensitised reactive products may also cause DNA methylation and lipid peroxidation to produce methylated DNA damage and ethenoadenine DNA lesions respectively. Prolonged high expression of ALKBH2 also indicates that its expression may modulate the cell's responsiveness to Ph-PDT. To confirm a specific role of ALKBH2 in affecting Ph-PDT response, we used a gene-knockdown approach. As illustrated in Fig. 3.13, cytotoxicity of Ph-PDT is enhanced after silencing the *ALKBH2* gene expression. Lower cytotoxicity of Ph-PDT was seen at two light doses in blank (Lipofectamine) and mock (Neg CNT) samples as compared with the knockdown untreated U87 cells. This may be due to the fact that lipofectamine may affect Photofrin uptake by U87 cells through alterations in the cell membrane.

The transcription factor(s) involved in *ALKBH2* transcription remains unknown. We have observed increased TP53 binding on the *ALKBH2* promoter region and the expression of p-TP53 was rapidly increased after Ph-PDT. Therefore, TP53 is critical for the regulation of *ALKBH2* gene expression after Ph-PDT. TP53 is involved in Ph-PDT, but the exact relationship of TP53 to Ph-PDT responsiveness is controversial. Some *in vitro* studies of human colon carcinoma, immortalised Li-Fraumeni syndrome and promyelocytic leukaemia found that the cell lines with

mutant TP53 have lower sensitivity to Ph-PDT than those with wild-type TP53.[219,331,332] This may be due to a decrease in TP53-dependent apoptosis after Ph-PDT. However, Evans *et al*. found that the Ph-PDT induced apoptosis was higher in the lymphoblastic cell line with mutant TP53 although the cytotoxic effects of Ph-PDT on both cell lines were not different.[197] Another important finding of the Evans' group was that the mutagenicity induced by Ph-PDT in the cell line with mutant TP53 was higher. Therefore, the relationship between TP53 and Ph-PDT responsiveness seems to be cell-type dependent. In our case, U87 glioma cell line has a wild-type TP53 and we found that wild-type TP53 was also involved in relative resistance to Ph-PDT via activation of the *ALKBH2* DNA repair gene. These results suggest that the resistance to Ph-PDT in cells with wild-type TP53 or mutant TP53 may act via different mechanisms.

Ph-PDT resistance can be induced through interactions of diverse proteins, which may lead to the changes in microenvironement of the cancer cells. In this study, three proteins, namely PCNA, JNKs and NPM1, were selected for investigating their roles in TP53-ALKBH2-involved Ph-PDT resistance as these proteins can interact with TP53 and/or ALKBH2.

PCNA

Xie *et al*. showed that PCNA expression remained unchanged in nasopharyngeal carcinoma bearing-nude mice examined after 14 days of 5-ALA-PDT.[333] The authors suggested that it may be because of no significant DNA damage being induced by PDT. Consistent with their findings, unchanged PCNA protein expression in relatively resistant glioma cells after Ph-PDT was also found in our

study (Fig. 3.17A). However, another study conducted by Akramiene *et al*. indicated that PCNA is significantly expressed in lung cancer-bearing mice within 7 days after Ph-PDT, and so the authors concluded that DNA repair mechanism was triggered in lung cancer cells after Ph-PDT.[224] The contradictory results may be due to downstream tests being performed at different time points after Ph-PDT. Although total PCNA protein expression is unaltered, the active form of PCNA, phosphorylated PCNA, is not detected in this study. Therefore, whether PCNA participates in Ph-PDT resistance and Ph-PDT induced DNA damage repair cannot be determined.

JNKs

JNKs have been shown to be up-regulated quickly after PDT in many studies.[186,334,335] This rapid up-regulation of p-JNKs may be required for the subsequent activation of TP53 [Phosphorylation (Ser15) of TP53 occurs at 6.5 hours after Ph-PDT in this study (Fig. 3.14)] and hence DNA repair to prevent cell death after PDT.[232] Conversely, some studies have shown that the cytotoxicity of Ph-PDT in other cell lines was not affected by the JNK inhibitor and concluded that JNKs are not the cause of Ph-PDT resistance.[233,336] These contradictory results may be explained by the differences in TP53 expression or status (wild type or mutant type), distribution of Photofrin in different cell types, DNA repair capacity of the cells and initiation of different JNK-related pathways.[232,337,338] JNKs may also be directly related to ALKBH2. p-JNKs level was shown to decrease after knockdown of another human AlkB homologue, ALKBH8, and this lead to an increase in cell death of bladder cancer cells by apoptosis.[339] This is consistent with our findings that ALKBH2 was increased when p-JNKs are decreased after

Ph-PDT. Therefore, further study on the contribution of JNKs in glioma resistance to Ph-PDT is needed.

NPM1

To investigate the role of the inductive response of NPM1 in Ph-PDT, the Ph-PDT induced cell death in NPM1 under-expressing glioma cells was analysed using cell survival assay. After Ph-PDT, the cell survival rate of glioma cells with *NPM1* knockdown was reduced by nearly 2-fold as compared with lipofectamine and vector controls (Fig. 3.19). The reduction in survival rate indicates that NPM1 protects glioma cells from Ph-PDT induced cell death and therefore may confer Ph-PDT resistance. The light dose used in this experiment was lower than in other experiments in order to enhance the observation of the differences in cell survival rate after gene knockdown.

As NPM1 was found to affect the cytotoxicity of Ph-PDT, its possible role in protecting glioma cells against Ph-PDT induced cell death via TP53 and ALKBH2 was investigated. Strikingly, both TP53 and ALKBH2 expression were significantly down-regulated after *NPM1* knockdown (Fig. 3.20). Two potential hypotheses of Ph-PDT resistance are proposed: (1) NPM1 acts on *ALKBH2* promoter via binding with transcription factors to regulate *ALKBH2* transcription and (2) NPM1 interferes in TP53 stability and thus ALKBH2 expression is affected.

To test the first hypothesis, different NPM1-related transcription factors were studied as NPM1 does not bind to the ALKBH2 gene promoter directly. TP53, SP1 and NF-κB were chosen because these factors have been shown to interact with

NPM1 in the promoter of a DNA repair gene called superoxide dismutase 2, mitochondrial (*SOD2*).[340-342] Furthermore, the ALKBH2 promoter contains a similar distribution of these sites, predicted from TESS, as the *SOD2* promoter (data not shown). However, no binding of NPM1 with any of these NPM1-related transcription factors was found and, therefore, the second hypothesis was subsequently tested. The results in Fig. 3.22 clearly show that NPM1 affects TP53 mRNA stability, thus suggesting that its main function may be through stabilisation of TP53 mRNA, leading to increased binding of TP53 on the *ALKBH2* promoter. It is worth noting that TP53 mRNA stability increases after Ph-PDT. This implies that there are other proteins or factors induced by Ph-PDT that can stabilise TP53 mRNA.

3.5 Conclusion

DNA direct reversal pathway is important in Ph-PDT efficacy in treating gliomas. The induction of *ALKBH2* transcription after Ph-PDT is related to the binding of TP53 on the promoter region of *ALKBH2*. Together with the participation of p-JNKs and NPM1 as upstream activators of TP53, these findings may explain, at least in part, the mechanisms leading to glioma cell resistance to Ph-PDT.

Chapter 4

General Discussion and suggestions for further study

4.1 Introduction

Intact genetic materials, especially DNA, are vitally important in maintaining and developing cells. However, DNA can be damaged by different exogenous and endogenous DNA-damaging agents. If DNA damage is not repaired or if it is repaired incorrectly, the lesions become mutations and may initiate genome instability. The latter can lead to cancer and cancer treatment resistance.[5,343] Therefore, DNA repair is essential for guarding the cells from cancer and maintaining responsiveness to cancer treatment. Numerous DNA repair proteins, which are mainly enzymes, are involved in the six main DNA repair pathways that determine the repair capacity in mammals. Many investigations have proved that individuals with reduced DNA repair capacity are associated with increased risks of various cancers and resistance to cancer treatment.[344,345] Sequence variants, especially SNPs, in DNA repair genes may explain the alterations in DNA repair proteins leading to a decrease in DNA repair capacity.[346]

4.2 Single nucleotide polymorphisms in DNA repair genes affect their protein functions

There are studies investigating the relationship between different SNPs in DNA repair genes, cancer susceptibility and/or clinical resistance to cancer therapy. For example, SNPs in genes of mismatch repair and translesion synthesis pathways have been identified to have a strong association with the risks of lung cancer and head and neck cancer.[347] Another epidemiological study has shown that SNPs in DNA repair genes may be related to the better prognosis of lung cancer patients treated with cisplatin.[348-350] In different association and pharmacogenomics studies, SNPs

or haplotypes [i.e. a set of associated SNPs on a chromatid] in DNA repair genes have been shown to be associated with (International HapMap Consortium, 2005) high cancer risks and cancer treatment responses.[351-353] SNPs in DNA repair genes can affect the DNA repair capacity by several means, including (1) gene expression, (2) RNA splicing, (3) protein translation and (4) protein functions.[354] Non-synonymous SNPs, which is a type of SNPs resulting in amino acid substitutions, mainly act via altering the structures and functions of the proteins. However, only about 30% of non-synonymous SNPs have an effect on their proteins.[354-356] Most of the structure-function studies of DNA repair genes are still based on computational tools, such as SIFT, to predict the biological significance of the non-synonymous SNPs.[258,357,358] In this thesis, two non-synonymous SNPs in *NTHL1* were selected for investigation based on the study of Savas *et al*. and the predicted result from SIFT and ConSeq computational tools.[258] FS105 in the *NTHL1* gene was predicted to have a premature stop codon and shown to affect DNA repair capacity by ceasing NTHL1 protein translation and cause protein loss. This result implies that the DNA repair capacity of a cell can vary depending on the presence of SNPs in DNA repair genes. In contrast, D239Y of the *NTHL1* gene was predicted to cause protein inactivation via structural alteration although this alteration was shown to have no effects on protein functions in terms of cell cycle arrest and cytotoxicity after the cellular DNA had been damaged. As structural alteration may not completely terminate the protein's function, this may explain the failure to detect the structural alteration of NTHL1 by the system in this thesis.[359] Another possible reason is that this SNP may produce an effect too small to be detected by this yeast-based system due to inadequate sensitivity. Taken together, the functional effects of SNPs on DNA repair proteins should not simply be

predicted by computational tools, but that confirmation by simple functional assays are needed.

4.3 Functional study of SNPs in DNA repair genes

There are limited number of functional analysis assays that have been developed to evaluate how SNPs in DNA repair genes affect their protein functions because the vast majority of SNPs may not have any profound effects.[360] Other reasons for the lack of functional studies include laborious experimental steps and complicated human gene knock-out experiments.[361] The heterozygous genetic background of individuals/human cells may also render interpretations on the significance of SNPs and their biological effects on the protein functions invalid because other unknown or not investigated SNPs may also contribute to the observed effects.[362] Therefore, it is necessary to develop a convenient method, which without the disturbance of the confounding factors in humans/human cells, in assessing the functional effects of SNPs. Yeast cells provide a suitable environment because they have highly conserved DNA repair proteins as in humans at the structural level. In addition yeast knock-out mutants can be easily obtained.[363,364] Results from this study shows that the yeast-based assay can distinguish a protein which has completely abrogated BER activity, because of variations due to SNPs. This result confirms the usefulness of the simple yeast assay as reported by Jeong *et al*. and Takahashi *et al*. to screen and analyse many SNPs of DNA repair genes without complicated steps.[362,365] One major problem in using this assay is that the duration of cell cycle arrest cannot linearly determine the drug responses in those with this particular SNP. However, the assay can provide more information about the function of DNA repair proteins affected by the variations, which is due to SNPs and, therefore, aid in the

understanding of therapeutic responses in combination with epigenetic data.

4.4 The roles of DNA repair in cancer treatment resistance

SNPs in DNA repair genes may affect an individual's predisposition to cancer risk and subsequent therapy. In addition, the interactions between DNA repair proteins and DNA also play a role in cancer treatment responsiveness.

DNA repair pathways have been correlated to the chemotherapy and radiotherapy resistance in clinical and *in vitro* studies.[284,366] The main reason is that most of the chemotherapeutic agents and ionising radiation kill cancer cells by introducing DNA damage.[133,284,367] The DNA damage produced by anticancer treatments can be classified into double and single strand breaks, base modifications and DNA strand crosslinks.[368-370] The damage stalls the replication forks during DNA replication/transcription and thus leads to cancer cell death.[371] However, DNA repair mechanisms repair the DNA damage induced by cancer treatment leading to therapeutic resistance.[372] Photodynamic therapy has been used in the treatment of cancer and resistance to PDT has been reported.[188,189,373] Compared with other anti-cancer therapies, resistance to PDT occurs to a lesser extent. However many studies have been conducted to explore the possible causes of resistance based on different mechanisms, including microenvironment changes and expression of anti-apoptotic proteins. The study described here is the first of its kind to investigate the role of DNA repair mechanisms in the development of PDT resistance in cancer cells[177,374,375] Unlike other cancer therapies, PDT does not induce cancer

cell death by causing DNA damage.[159,286] Instead PDT destroys cancer cells by damaging the target organelles, but notably, not the nucleus and eliciting apoptosis via the caspase cascade.[334,376] But interestingly, DNA damage, the types of which are similar to that in other cancer treatments, and DNA repair were seen in different cell models after PDT.[138,321,324,377] Regarding these results, DNA damage and repair pathways have been proposed to be involved in cellular responses to PDT and development of PDT resistance.[224] In agreement with recent findings, DNA damage and repair was observed in the Ph-PDT glioma cell model used in this study. Yang *et al.*'s study demonstrated that silencing apurinic⁄apyrimidinic endonuclease, which is a DNA repair enzyme involved in the base excision repair pathway, enhances the therapeutic efficacy and prevents resistance of haematoporphrphyrin derivative-PDT in lung cancer cell and mouse models.[201] In contrast, apurinic⁄apyrimidinic endonuclease was proved to have no response after Ph-PDT in this study, the contradictory results may be due to different photosensitisers and PDT conditions. However, ALKBH2, another DNA repair protein participated in direct reversal pathway, is involved in Ph-PDT resistance. Based on the findings from this present study and other studies, it can be concluded that DNA repair plays a critical role in cellular responses to PDT and may initiate PDT resistance.

4.5 Regulation of DNA repair in cancer treatment resistance

DNA dioxygenase-mediated direct reversal DNA repair pathway has been for the first time discovered to be associated with PDT resistance. Nevertheless, another pathway of direct reversal DNA repair mechanism is well-known to participate in

other chemoresistance.[378,379] The O-6-methylguanine-DNA methyltransferase-mediated direct reversal pathway has been confirmed to link up with alkylating drug resistance, particularly temozolomide for treating gliomas.[380] Temozolomide cytotoxicity is mediated by production of O^6-methylated guanine lesions in the DNA, but O-6-methylguanine-DNA methyltransferase converts these toxic lesions into non-toxic guanine to prevent cancer cell death.[381] Recently, a DNA dioxygenase, ALKBH2, has been recognised to be involved in the direct reversal DNA repair pathway and removes alkylated bases on DNA by simple chemical reversion similar to the O-6-methylguanine-DNA methyltransferase action.[382] Therefore, it is suggested that ALKBH2 causes PDT resistance in a way similar to O-6-methylguanine-DNA methyltransferase by eliminating the toxic DNA lesions in PDT. However, the biological effects of ALKBH2 in PDT are still not fully understood and further investigations are required. Involvement of different DNA repair pathways in resistance to PDT and cancer therapy, including the direct reversal DNA repair pathway shown in this thesis, indicates that precise regulation of DNA repair is taking place in the cancer resistant cells.[168,201]

TP53, named “the guardian of the genome”, is a key sensor of DNA damage and initiator of subsequent biological processes.[383] It functions as a transcription factor to control target gene expression and triggers either DNA repair or apoptosis, depending on the extent of DNA damage.[384,385] This key protein has been demonstrated to be a determining factor in cancer treatment outcomes through the regulation of DNA repair mechanisms.[386-388] Naumann *et al*. showed that the cells with wild-type TP53 are more resistant to temozolomide than those with the mutant TP53.[388] Similarly, in this present study, wild-type TP53 has been shown to be

associated with Ph-PDT resistance. These results are contrary to the general findings which shows that cells containing mutant TP53 are more resistant to chemotherapy and PDT.[389,390] For instance, immortalised Li-Fraumeni syndrome fibroblasts with mutant TP53 are more resistant to PDT because of impaired TP53-dependent apoptosis.[219] These opposite observations may be clarified by determining the mechanism/role of TP53 in DNA repair and apoptosis in different cancer cells after various cancer therapies.[388] According to this study, wild-type TP53 may be involved in the transcription of ALKBH2 DNA repair gene. This finding may help explain the development of PDT resistance caused by ALKBH2-mediated DNA repair. TP53 is responsible for a variety of cancer treatment resistance. Therefore, the regulation of TP53 expression is important. The expression of TP53 can be governed at both post-translational and post-transcriptional levels using different approaches: (1) TP53 protein degradation by ubiquitination; Mdm2 p53 binding protein homolog (mouse) is the main protein that causes proteolytic degradation of TP53; (2) Covalent modification, such as phosphorylation, to stabilise TP53 protein; (3) mRNA degradation by micro-RNAs, which facilitate endonucleases to digest the TP53 mRNA followed by a decrease in TP53 protein expression; and (4) mRNA stabilisation/destabilisation by binding with different proteins, e.g. zinc finger, matrin type 3 protein, which binds at U-rich region to prevent deadenylation of mRNA.[391,392] In this present study, NPM1 was found to stabilise TP53 mRNA in PDT. In Palaniswamy *et al.*'s study NPM1 was shown to take part in the polyadenylation process, which increases mRNA stability.[393] Thus, NPM1 is possibly one of factors causing Ph-PDT resistance through stabilisation of TP53 to transcribe ALKBH2.

4.6 Limitations and significance of the study

Limitations

There are some limitations in this study. First, the DNA glycosylase activity assay using radioactive substances has not been developed in our laboratory, and so the activity and substrate specificity of the expressed NTHL1 protein could not at present be measured. However, human NTHL1 protein expressed in yeast and bacteria was shown to have normal glycosylase activity for its specific substrates in other studies.[123,394] Second, only two SNPs were tested in the yeast-based systems because of time and resource limitations. Third, Ph-PDT resistant glioma cells are not available and so relatively resistant U87 glioma cells collected after recovery from Ph-PDT were used. The resistant cells and other glioma cell lines may be different in cellular responses after Ph-PDT.

Significance

This study describes a simple yeast-based method for detecting the effects of SNPs on protein functions. This method can eliminate the complicated procedures for traditional functional assays for DNA repair activity, such as using radioactive substances. This simplified method can ”speed up” the investigation on SNPs’ effects and identify the possible target SNPs that may be involved in carcinogenesis and drug responses for further investigation. The study of DNA repair has led to a better understanding of the causes of PDT resistance. By knowing the relationship between regulation of DNA repair and PDT resistance, a new therapeutic strategy may be developed to improve PDT efficacy. The problem of glioma resistance to PDT may be minimised by inhibiting DNA repair activity using DNA repair inhibitors targeting different DNA repair enzymes.[395] DNA repair inhibitors are

used with DNA-damaging cancer therapy.[396] However, back-up DNA repair pathways may compensate for the inhibited pathway and reduce the therapeutic effects of DNA repair inhibitors.[371] By understanding its regulators and the pathway involved after PDT in this study, ALKBH2 may become a specific target for developing DNA repair inhibitor, which can be used in combination with PDT.

4.7 Suggestions for further investigation

Studying the SNPs' effects on DNA repair proteins, a newly developed functional assay using a yeast-based system was established. However, it requires to be validated by other fully developed functional assays, such as DNA glycosylase activity assay for determining the activity of expressed proteins or nicking assay for determining the function of the examined human proteins. The cell cycle assay should also be performed on a time-point basis to examine the cell cycle arrest patterns of yeast cells with different plasmids to increase the accuracy of the results.

In the second part of this project on the involvement of DNA repair in Ph-PDT resistance, the cell line model is good for the basic investigation on how DNA repair is involved in developing drug resistance. However, further investigation using animal models is required to confirm that DNA repair is involved in Ph-PDT resistance *in vivo*. As ALKBH2 is identified as a key player in Ph-PDT resistance, the interactions between ALKBH2 and other molecules should be further examined in detail. The molecules or pathways required for further investigation are illustrated in Fig. 4.1. By recognising the signalling partners of ALKBH2, it would help understand the biological and physiological role of ALKBH2 and assist in developing targeted therapy against PDT resistance.

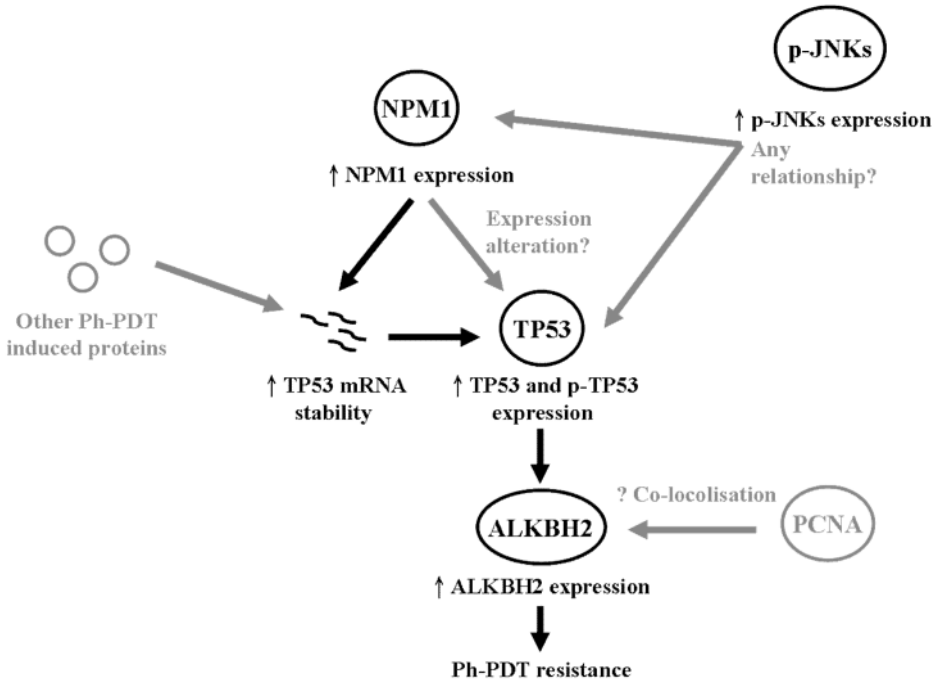

Fig. 4.1 **The biochemical pathways for future study.** The pathways highlighted in grey is suggested for future study and the black ones are the confirmed results in this study.

Appendix I Sequencing results of pYX113-NTHL1 plasmid

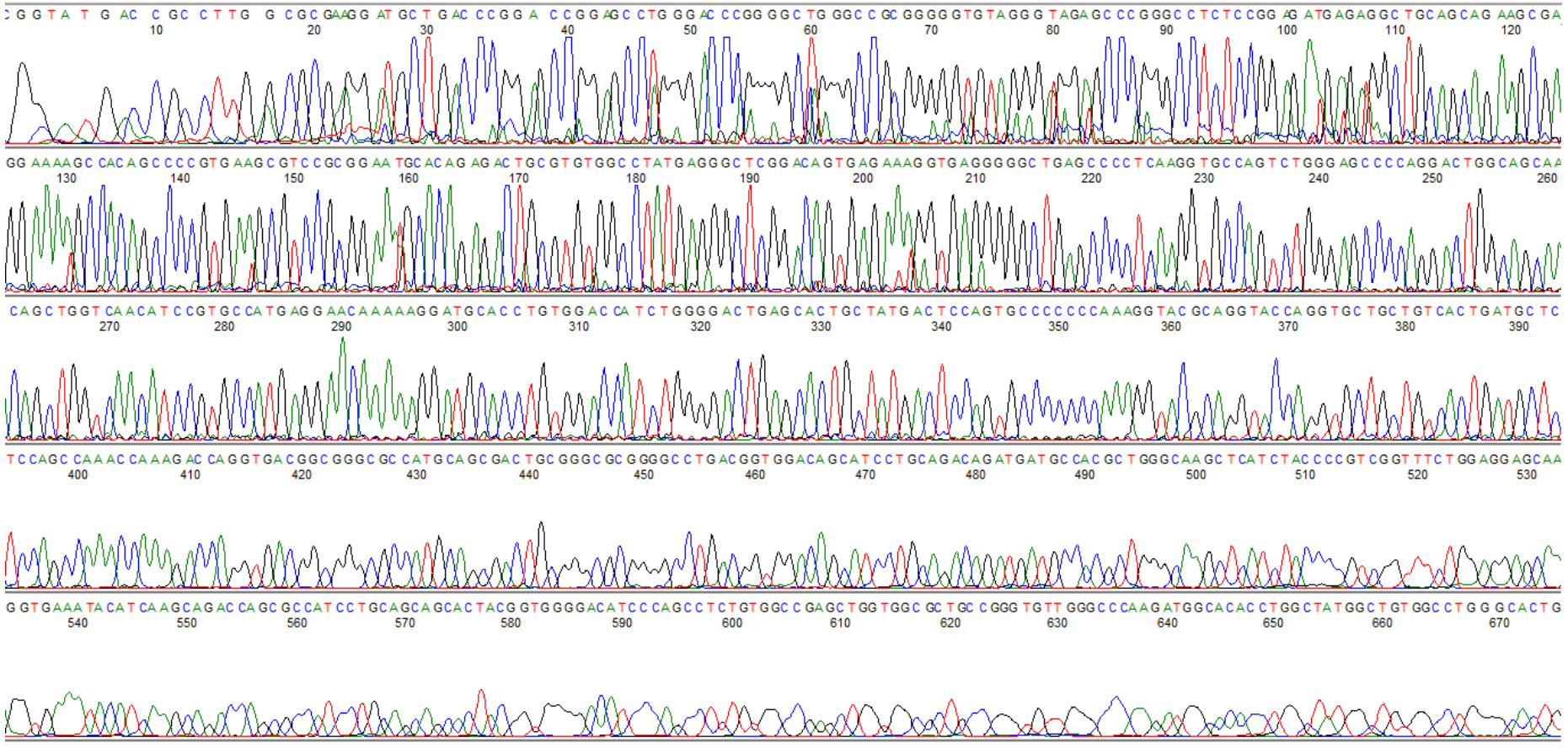

Sequencing results of pYX113-NTHL1 plasmid using N1exppF1 primer.

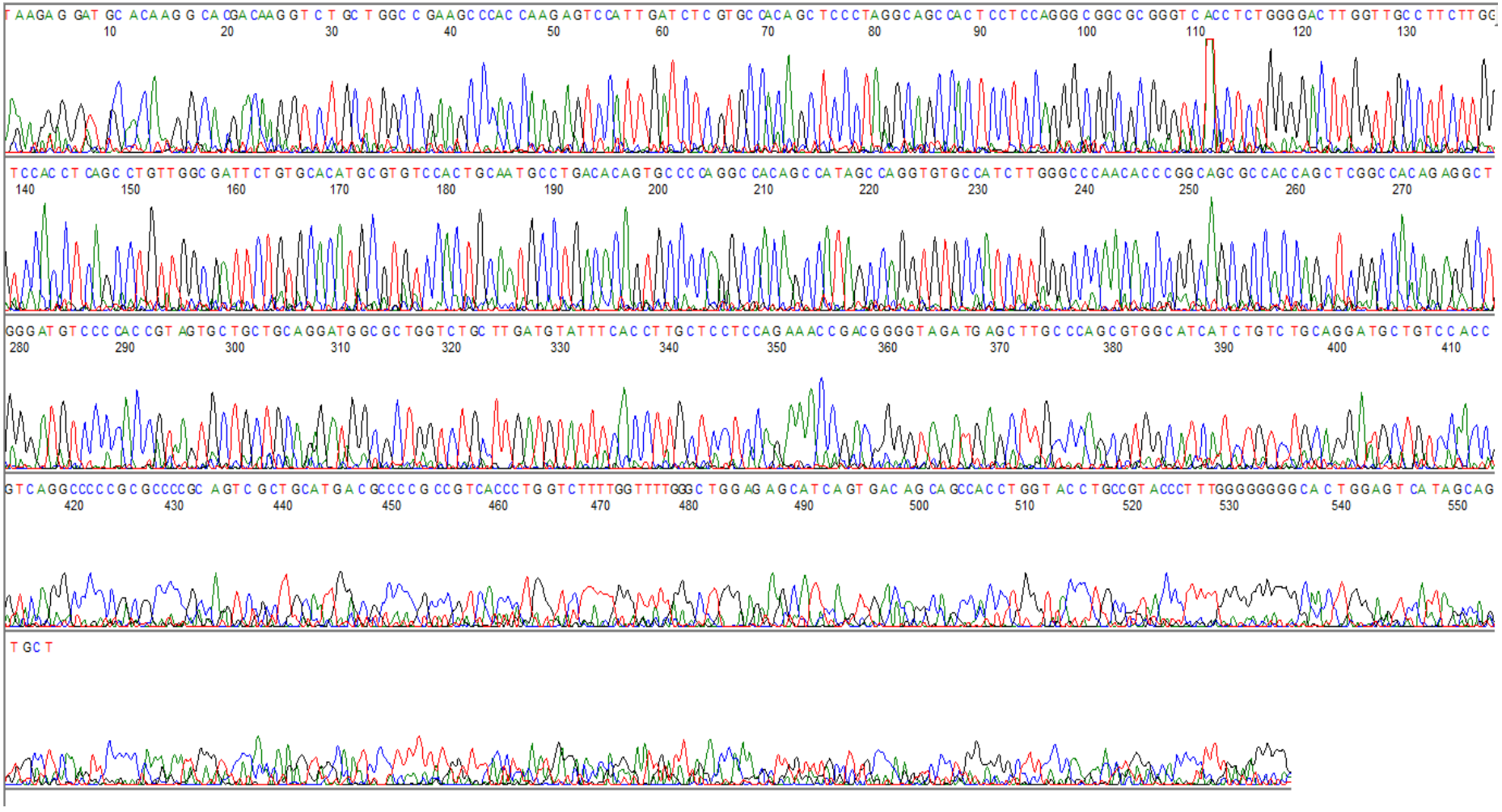

Sequencing results of pYX113-NTHL1 plasmid using N1exppR1 primer.

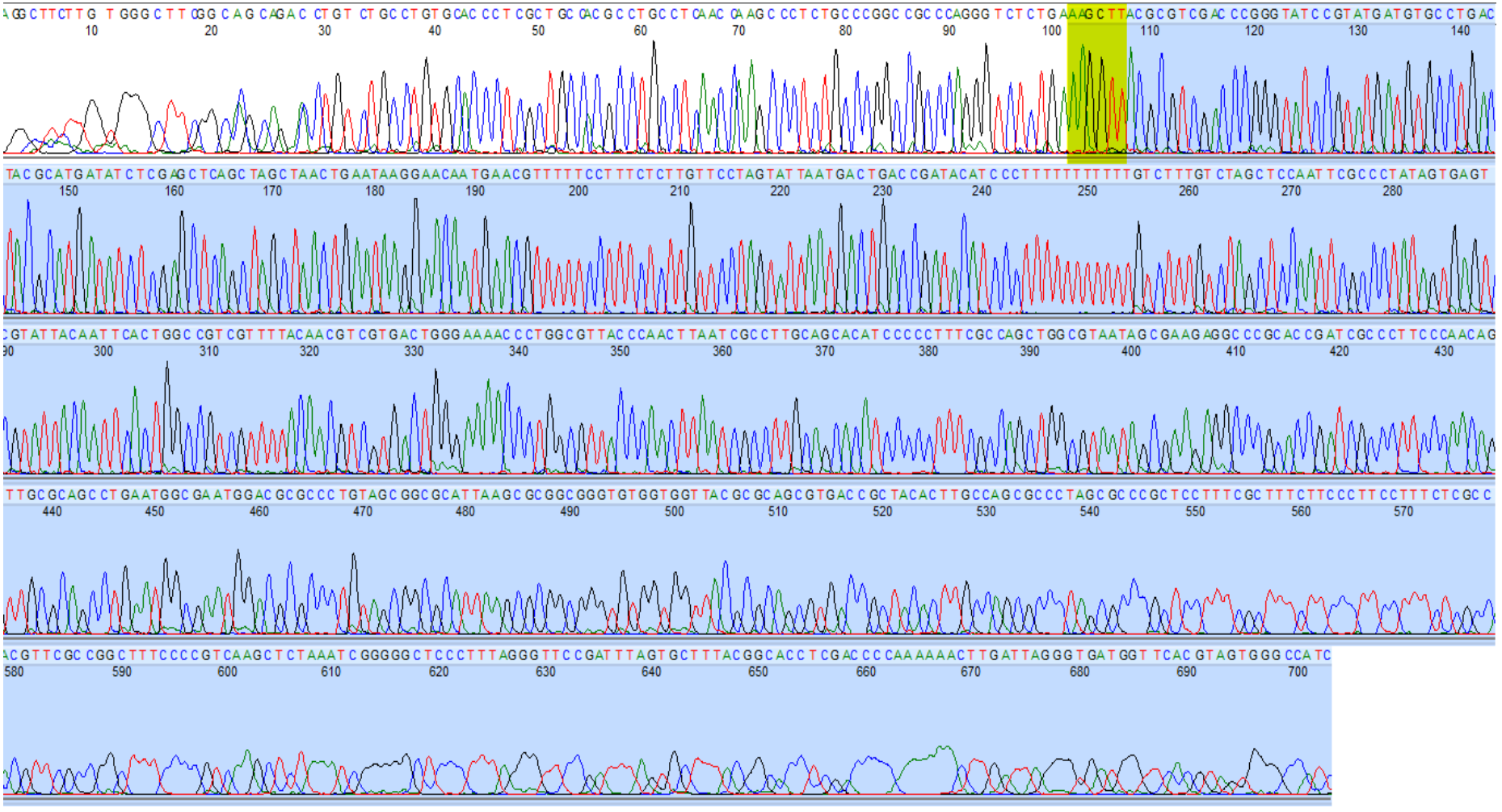

Sequencing results of pYX113-NTHL1 plasmid using N1F2 primer. The yellow highlighted part is HindIII enzyme digestion site.

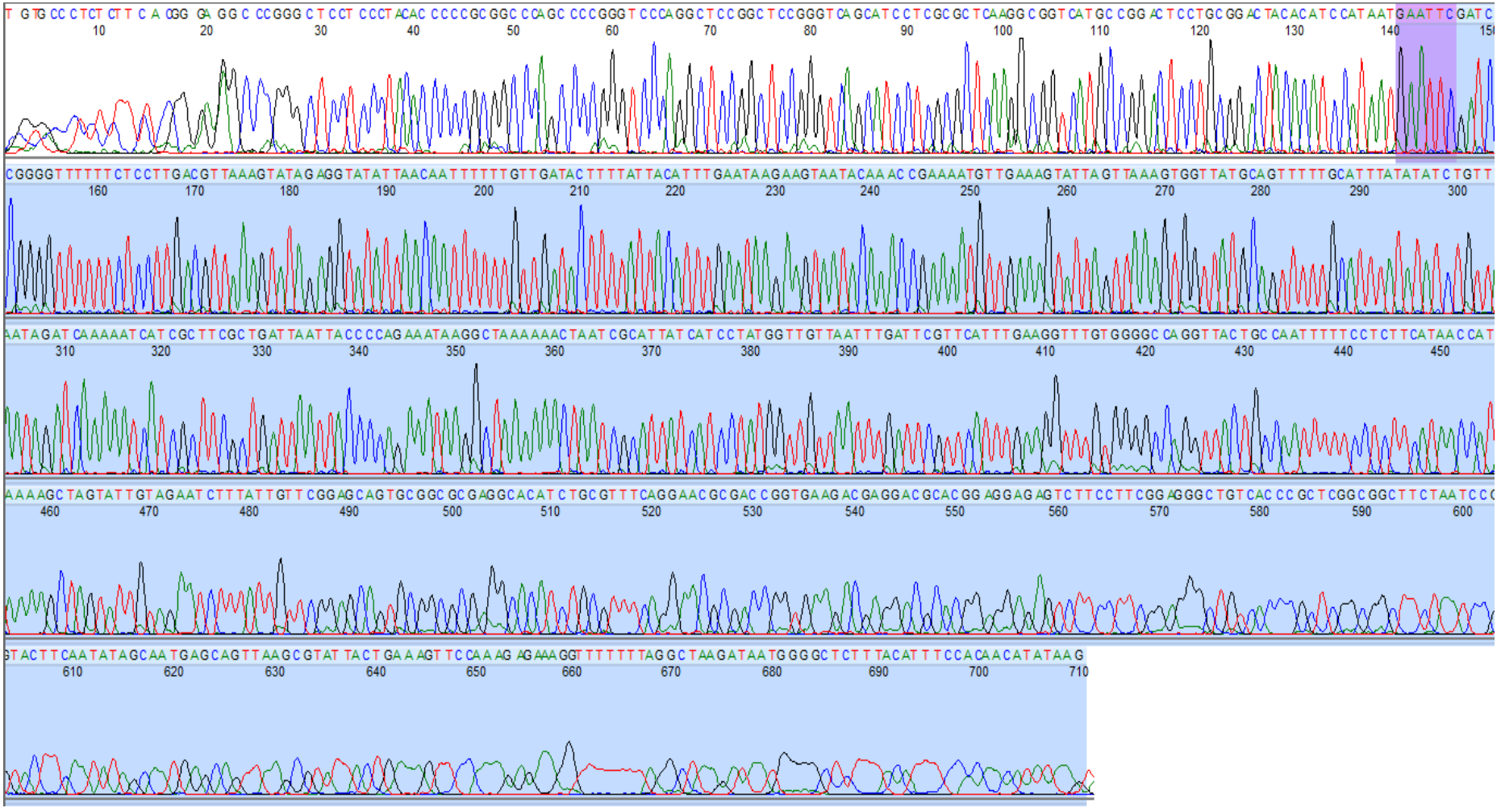

Sequencing results of pYX113-NTHL1 plasmid using N1R2 primer. The purple highlighted part is EcoRI enzyme digestion site.

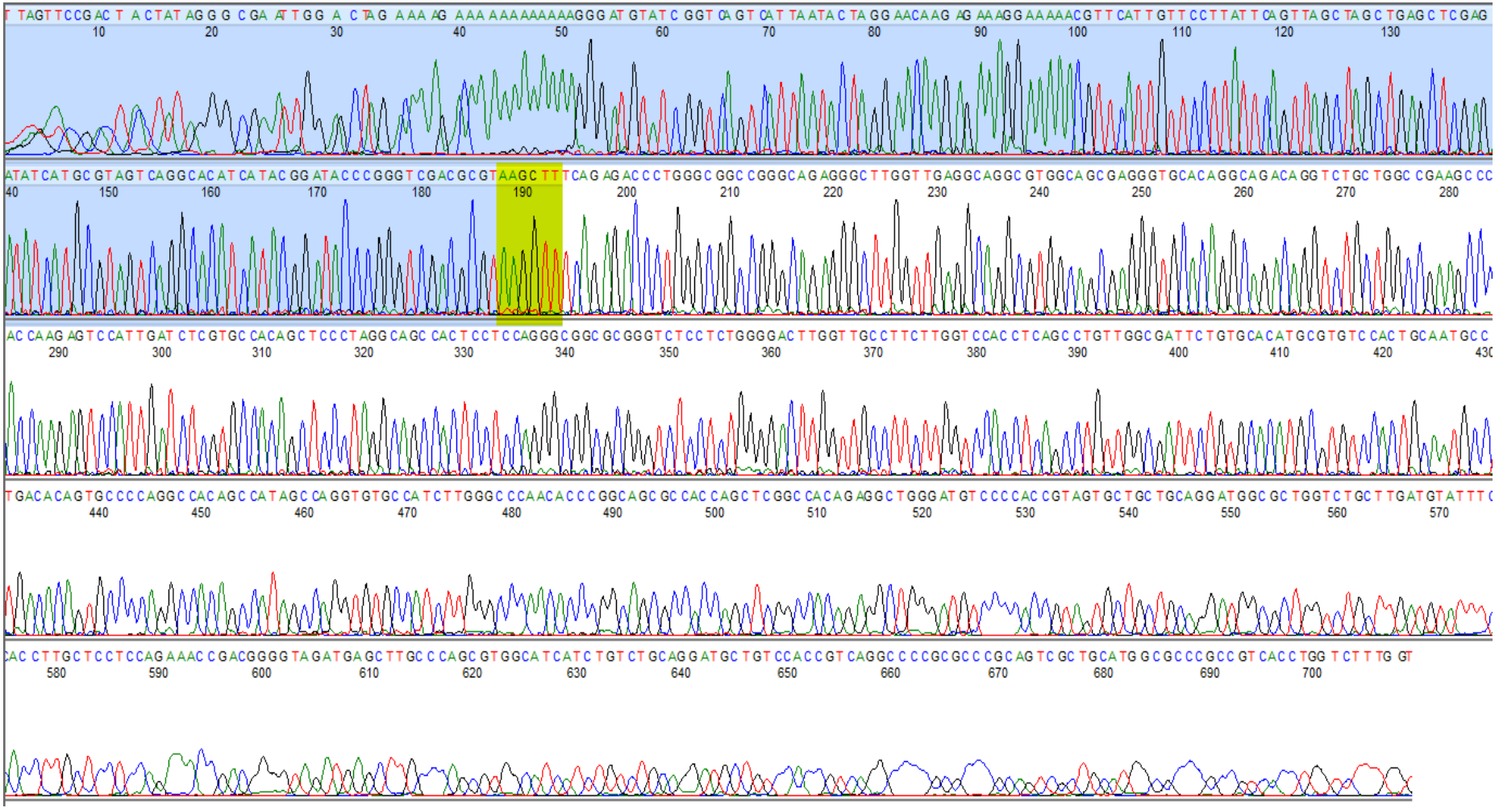

Sequencing results of pYX113-NTHL1 plasmid using M13F primer. The yellow highlighted part is HindIII enzyme digestion site.

Appendix II Chemicals, materials and reagents

General chemicals and reagents

4-(2-hydroxyethyl)-1-piperazineethanesulphonic acid (HEPES)	(Sigma-Aldrich, St. Louis, MO, USA)
Actinomycin D	(Sigma-Aldrich, St. Louis, MO, USA)
Ammonium persulphate	(Sigma-Aldrich, St. Louis, MO, USA)
Bovine serum albumin	(Sigma-Aldrich, St. Louis, MO, USA)
Bromophenol blue	(Sigma-Aldrich, St. Louis, MO, USA)
Calcium chloride	(Sigma-Aldrich, St. Louis, MO, USA)
Dextrose	(Sigma-Aldrich, St. Louis, MO, USA)
Dimethyl sulphoxide (culture grade)	(Sigma-Aldrich, St. Louis, MO, USA)
Disodium ethylenediaminetetraacetic acid dehydrate	(BDH, Leighton Buzzard, UK)
Ethanol	(Sigma-Aldrich, St. Louis, MO, USA)
Ethidium bromide	(Sigma-Aldrich, St. Louis, MO, USA)
Ethylene glycol tetraacetic acid	(Sigma-Aldrich, St. Louis, MO, USA)
Formaldehyde solution (37%)	(Sigma-Aldrich, St. Louis, MO, USA)
Galactose	(Sigma-Aldrich, St. Louis, MO, USA)
Glucose	(Sigma-Aldrich, St. Louis, MO, USA)
Glycerol	(USB Corp., Cleveland, Ohio, USA)
Glycine	(BDH, Leighton Buzzard, UK)
Hydrochloric acid	(Merck, Whitehouse Station, NJ, USA)
Hydrogen peroxide	(Sigma-Aldrich, St. Louis, MO, USA)
Isopropanol	(BDH, Leighton Buzzard, UK)
Lithium acetate	(Sigma-Aldrich, St. Louis, MO, USA)
Low melting point agarose	(Sigma-Aldrich, St. Louis, MO, USA)
Methylmethane sulphonate	(Sigma-Aldrich, St. Louis, MO, USA)
Phenol:Chloroform:Isoamyl Alcohol (25:24:1) solution	(USB Corp., Cleveland, Ohio, USA)
Phosphate Buffered Saline, pH 7.6	(Sigma-Aldrich, St. Louis, MO, USA)
Polyethylene glycol 3350	(USB Corp., Cleveland, Ohio, USA)
RNase A	(Sigma-Aldrich, St. Louis, MO, USA)
Sodium acetate	(Merck, Whitehouse Station, NJ, USA)
Sodium chloride	(BDH, Leighton Buzzard, UK)
Sodium citrate	(Sigma-Aldrich, St. Louis, MO, USA)
Sodium dodecyl sulphate	(Sigma-Aldrich, St. Louis, MO, USA)
Sodium hydroxide	(RDH, Spring Valley, CA, USA)
Sodium thiosulphate	(Sigma-Aldrich, St. Louis, MO, USA)
Standard agarose	(FMC Corporation, Philadelphia, PA, USA)
Tris(hydroxymethyl)aminomethane	(USB Corp., Cleveland, Ohio, USA)
Triton X-100	(Sigma-Aldrich, St. Louis, MO, USA)
Trypan blue solution (0.4% w/v)	(Sigma-Aldrich, St. Louis, MO, USA)

Tween 20	(Bio-Rad laboratories, Hercules, CA, USA)
β-mercaptoethanol	(Sigma-Aldrich, St. Louis, MO, USA)

RNA extraction and RT

Diethyl pyrocarbonate treated water	(Gibco, Carlsbad, CA, USA)
PureLink™ Micro-to-Midi™ Total RNA Purification Kit	(Invitrogen, Carlsbad, CA, USA)
RevertAid™ First Strand cDNA Synthesis Kit	(Fermentas, Ontario, Canada)
TRIZOL LS reagent	(Invitrogen, Carlsbad, CA, USA)

PCR

AmpliTaq Gold DNA polymerase	(Applied Biosystems, Carlsbad, CA, USA)
Deoxynucleotide triphosphates (dNTPs)	(Amersham biosciences, Uppsala, Sweden)
FastStart high fidelity enzyme	(Roche, Schweiz, Switzerland)
Phusion high-fidelity DNA polymerase	(Finnzymes, Espoo, Finland)

Real-time PCR

1X Universal PCR Master Mix	(Applied Biosystems, Carlsbad, CA, USA)
Maxima™ SYBR Green/ROX qPCR Master Mix (2X)	(Fermentas, Ontario, Canada)
Validated TaqMan® gene expression assays	(Applied Biosystems, Carlsbad, CA, USA)

Sequencing

BigDye® Terminator v3.1 ready reaction mix	(Applied Biosystems, Carlsbad, CA, USA)
Exonuclease I	(Fermentas, Ontario, Canada)
Hi-Di™ Formamide	(Applied Biosystems, Carlsbad, CA, USA)
Shrimp alkaline phosphatase	(Fermentas, Ontario, Canada)

Western blotting

Non-fat milk	(Anlene, Australia)
Novex sharp pre-stained protein standard	(Invitrogen, Carlsbad, CA, USA)
Polyvinylidene fluoride membranes	(Amersham biosciences, Uppsala, Sweden)
Protease inhibitors	(Roche, Schweiz, Switzerland)
Western Lightning Plus ECL	(Fermentas, Ontario, Canada)
Western Lightning® Plus–ECL, Enhanced Chemiluminescence Substrate	(Perkin Elmer, Waltham, Massachusetts, USA)

Antibodies

ABH2 antibody [hABH2-7]	(Abcam, Cambridge, MA, USA)
Actin (C-11) antibody	(Santa-Cruz biotechnology, Santa Cruz, CA, USA)
Anti-mouse IgG, HRP-linked antibody	(Cell Signaling Technology, Danvers, MA, USA)
Anti-rabbit IgG, HRP-linked antibody	(Cell Signaling Technology, Danvers, MA, USA)
B23 (H-106) antibody	(Santa-Cruz biotechnology, Santa Cruz, CA, USA)
human NTH1 MAb (Clone 208521), mouse IgG antibody	(R&D Systems, Minneapolis, MN, USA)
Normal Mouse IgG	(Millipore, Billerica, MA, USA)
Normal Rabbit IgG	(Millipore, Billerica, MA, USA)
NPM antibody	(Cell Signaling Technology, Danvers, MA, USA)
p53 (FL-393) antibody	(Santa-Cruz biotechnology, Santa Cruz, CA, USA)
PCNA antibody	(Cell Signaling Technology, Danvers, MA, USA)
Phospho-p53 (Ser15) antibody	(Cell Signaling Technology, Danvers, MA, USA)
Phospho-SAPK/JNK (Thr183/ Thy185) antibody	(Cell Signaling Technology, Danvers, MA, USA)
REV1 antibody	(Abcam, Cambridge, MA, USA)
SAPK/JNK (56G8) Rabbit mAb	(Cell Signaling Technology, Danvers, MA, USA)
β-Actin (C4) Antibody	(Santa-Cruz biotechnology, Santa Cruz, CA, USA)

Bacterial/Yeast culture

LB agar	(Sigma-Aldrich, St. Louis, MO, USA)
LB broth	(Sigma-Aldrich, St. Louis, MO, USA)
One Shot® TOP10 Chemically Competent *E. coli* cell	(Invitrogen, Carlsbad, CA, USA)
One-Shot® MAX Efficiency® DH5α™-T1R competent cells.	(Invitrogen, Carlsbad, CA, USA)
SOC broth	(Invitrogen, Carlsbad, CA, USA)
Yeast nitrogen base without amino acids	(Sigma-Aldrich, St. Louis, MO, USA)
Yeast peptone dextrose broth	(Sigma-Aldrich, St. Louis, MO, USA)
Yeast synthetic dropout medium without uracil	(Sigma-Aldrich, St. Louis, MO, USA)

Cell culture

Dulbecco's PBS solution	(Gibco, Carlsbad, CA, USA)
Fetal calf serum (heat-inactivated)	(Gibco, Carlsbad, CA, USA)
Minimum Essential Media (MEM) α medium	(Gibco, Carlsbad, CA, USA)
Trypsin-EDTA solution	(Gibco, Carlsbad, CA, USA)

Gene knoockdown

ALKBH2 Stealth RNAi™ siRNA (HSS133558)	(Invitrogen, Carlsbad, CA, USA)
Lipofectamine 2000 transfection reagent	(Invitrogen, Carlsbad, CA, USA)
pSilencer 2.0 vector	(Ambion, Carlsbad, CA, USA)

PDT drug

Photofrin	(Axcan Pharma, Quebec, Canada)

Other reagents

Ampicillin	(Sigma-Aldrich, St. Louis, MO, USA)
DNA sodium salt from salmon testes	(Sigma-Aldrich, St. Louis, MO, USA)
DNase/RNase-free distilled water	(Invitrogen, Carlsbad, CA, USA)
EcoRI	(Fermentas, Ontario, Canada)
HindIII	(Fermentas, Ontario, Canada)
T4 DNA ligase	(Fermentas, Ontario, Canada)
SYBR safe DNA gel stain	(Invitrogen, Carlsbad, CA, USA)
SYTOX Green I stain	(Invitrogen, Carlsbad, CA, USA)
GeneTailor™ site-directed mutagenesis system	(Invitrogen, Carlsbad, CA, USA)
QIAprep spin miniprep kit	(Qiagen, Hilden, Germany)

Appendix III Recipes of reagents and buffers

Reagents	Components	Purpose	Storage Temperature (°C)
E.coli transformation			
(1) 100 mg/mL Ampicillin	100 mg ampicillin powder dissolved in 1 mL MilliQ water and sterile filtered through a 0.22 µm filter.	Selecting the bacterial cells containing the introduced plasmid DNA.	-20
(2) LB agar	Agar 15 g/L, Sodium chloride (NaCl) 5 g/L, Tryptone (pancreatic digest of casein) 10 g/L and Yeast extract 5 g/L. ***LB agar plate:*** 35 g LB agar powder dissolved in 1 L MilliQ water and autoclaved for 15 minutes at 121°C. ***LB agar plate with 100 µg/mL ampicillin:*** 35 g LB agar powder dissolved in 999 mL MilliQ water and autoclaved for 15 minutes at 121°C. After the agar cooled down to 50°C, 1 mL ampicillin (100 µg/mL) added to the agar, mixed and pored onto the plates.	Culturing bacterial cells.	4
(3) LB broth	NaCl 5 g/L, Tryptone (pancreatic digest of casein) 10 g/L and Yeast extract 5 g/L. ***LB broth:*** 20 g LB broth powder dissolved in 1 L MilliQ water and autoclaved for 15 minutes at 121°C.	Culturing bacterial cells.	4

Reagents	Components	Purpose	Storage Temperature (°C)
(4) 0.1 M Calcium chloride ($CaCl_2$)	0.1 M calcium chloride ($CaCl_2$) powder made up to 50 mL with MilliQ water. ***0.1 M $CaCl_2$ plus 15% glycerol solution:*** 0.1 M $CaCl_2$ powder (Sigma) and 1.5 mL glycerol (100%) (BDH) made up to 10 mL with MilliQ water.	Preparing the cell membrane of bacterial cells to become	Room temperature
(5) SOC broth	2% w/v bacto-tryptone, 0.5% w/v bacto-yeast extract, 10 mM NaCl (0.584 g), 2.5 mM potassium chloride and 10 mM $MgCl_2$ and 20 mM glucose made up to 980 mL MilliQ water. The pH of the broth was adjusted to 7.0 with sodium hydroxide (NaOH) and the broth autoclaved for 15 minutes at 121°C. After the medium cooled down to 50°C, 20 mL was filtered for sterilisation, 50 mM glucose was added to the broth.	Recovering the heat shocked bacterial cells.	4
Yeast transformation			
(1) Yeast peptone dextrose (YPD) agar	65 g YPD agar powder (20 g/L Bacteriological peptone, 10 g/L Yeast extract, 20 g/L Glucose and 15 g/L Agar) made up to 1 L with distilled water. Autoclaved for 15 minutes at 121°C.	Culturing yeast cells.	4
(2) YPD broth	50 g YPD broth powder (20 g/L Bacteriological peptone, 10 g/L Yeast extract and 20 g/L Glucose) made up to 1 L with distilled water. Autoclaved for 15 minutes at 121°C.	Culturing yeast cells.	4

	Reagents	Components	Purpose	Storage Temperature (°C)
(3)	***10X TE buffer***	0.1 M Tris-HCl and 10 mM disodium ethylenediamine-tetraacetic acid (EDTA) dehydrate. The pH was adjusted to pH 7.5 with HCl and autoclaved for 15 minutes at 121°C.	Making the yeast cell chemical competent.	Room temperature
(4)	***10X Lithium acetate solution***	1 M LiOAc. The pH was adjusted to 7.5 with glacial acetic acid and autoclaved for 15 minutes at 121°C.	Making the yeast cell chemical competent.	Room temperature
(5)	***50% Polyethylene glycol (PEG) 3350 solution***	5 g PEG 3350 powder made up to 10 mL with sterilised distilled water. ***TE/LiOAc solution (Prepared fresh just prior to use):*** 1X TE buffer and 1X LiOAc solution. ***PEG/LiOAc solution (Prepared fresh just prior to use):*** 1X TE buffer, 1X LiOAc solution and 40% PEG 3350 solution.	Making the yeast cell chemical competent.	Room temperature
(6)	***10 mg/mL DNA sodium salt from salmon testes***	10 mg DNA sodium salt from salmon testes made up to 1 mL with sterilised distilled water.	Reducing yeast membrane binding to the introduced plasmid DNA.	-20
(8)	***Yeast SD (without uracil) agar***	6.7 g/L Yeast nitrogen base without amino acids, 1.92 g/L Yeast SD media supplement without uracil[a] and 20 g/L Agar made up to 960 mL with distilled water. Autoclaved for 15 minutes at 121°C. After the medium cooled down to 50°C, 40 mL filter sterilised 50% (w/v) Glucose solution was added.	Selecting the yeast cells containing the introduced plasmid DNA.	4

Reagents	Components	Purpose	Storage Temperature (°C)
(9) Yeast SD (without uracil) broth	6.7 g/L Yeast nitrogen base without amino acids and 1.92 g/L Yeast SD media supplement without uracil[a] made up to 950 mL with distilled water. Autoclaved for 15 minutes at 121°C and cooled down to 50°C. ***Yeast SD (without uracil) broth with glucose (YSDO medium):*** 50 mL filter sterilised 40% (w/v) Glucose solution was added. ***Yeast SD (without uracil) broth with galactose (induction medium):*** 50 mL filter sterilised 40% (w/v) Galactose solution was added.	Selecting the yeast cells containing the introduced plasmid DNA and expressing the target human gene.	4 or -20 in glycerol stock
Cell culture			
(1) Phosphate buffered saline (PBS) buffer	PBS, pH 7.4 was made up to 1 L of MilliQ water.	---	4
(2) Minimum Essential Medium Alpha (MEMα medium)	--- (Gibco).	---	4
(3) Complete MEMα medium	90% (v/v) MEMα medium and 10% (v/v) heat-inactivated foetal calf serum (FBS)	---	4

a Yeast SD media supplement without uracil containing 8 mg/L p-Aminobenzoic acid potassium salt, 18 mg/L Adenine hemisulphate, 380 mg/L Leucine and 76 mg/L of the following amino acids: Alanine, Arginine, hydrochloride, Asparagine monohydrate, Aspartic acid, Cysteine hydrochloride monohydrate, Glutamic acid monosodium salt, Glutamine, Glycine, Histidine, myo-Inositol, Isoleucine, Lysine monohydrochloride, Methionine, Phenylalanine, Proline, Serine, Threonine, Tryptophan, Tyrosine disodium salt and Valine.

Reagents	Components	Purpose	Storage Temperature (°C)
(4) 0.05% (v/v) Trypsin-EDTA solution	0.25% (w/v) Trypsin with tetrasodium EDTA solution (1X) was diluted with Dulbecco's PBS solution to a final concentration 0.05%.	---	-20
(5) Freezing medium	90% (v/v) complete MEMα medium and 10% (v/v) cell culture grade dimethyl sulphoxide at 0°C.	---	4
Alkaline comet assay			
(1) PBS buffer	Commercial PBS, pH 7.4 made up with 1 L of MilliQ water.	Wash cells and make buffers	4
(2) H_2O_2 (30%) solution	10 mM H_2O_2 stock solution was made by mixing 10 µL of 30% H_2O_2 solution with 10 mL PBS buffer.	Induce oxidative stress in cells as positive control.	4
(3) Lysis buffer	0.1 M disodium EDTA dehydrate, 10 mM Tris and 2.5 M NaCl made up with 1 L of MilliQ water. The pH was adjusted to 10 with concentrated NaOH. ***Working lysis buffer:*** 500 µL Triton X-100 per 50 mL lysis buffer was added immediately before use.	Denature the cellular proteins in lysis step.	4
(4) Alkaline electrophoresis buffer	0.3 M NaOH and 1 mM disodium EDTA dehydrate made up with 1 L of MilliQ water.	Denature DNA.	4
(5) Neutralising buffer	0.4 M Tris made up with 1 L of MilliQ water. The pH was adjusted to 7.5 with concentrated HCl.	Neutralise the alkaline buffers.	4

Reagents	Components	Purpose	Storage Temperature (°C)
Western blotting			
(1) Whole cell extraction buffer	20 mM 4-(2-hydroxyethyl)-1-piperazineethanesulfonic acid (HEPES), 1 mM EDTA, 1 mM ethylene glycol tetraacetic acid, 0.2 M NaCl, 0.5% Triton X-100, 10% Glycerol and one tablet per 10 mL protease inhibitors made up to 100 mL with MilliQ water.	Washing cells and dissolving samples	-20
(2) Sodium dodecyl sulphate sample buffer	62.5 mM Tris-HCl (pH 6.8), 1% β-mercaptoethanol, 10% glycerol, 1% soodium dodecyl sulphate and 0.001% bromophenol blue made up to 10 mL with MilliQ water.	Denaturing proteins	-20
(3) TBS buffer, pH 7.6	20 mM Tris and 137 mM NaCl made up to 1 L with MilliQ water. The pH was adjusted to 7.6 with concentrated HCl . ***TBS-Tween 20 (TBST) buffer:*** 0.1% (v/v) Tween 20 was added to 1 L TBS buffer.	Washing membrane.	4
(4) 1.5 M Tris-HCl, pH8.8	1.5 M Tris made up to 150 mL with MilliQ water. The pH was adjusted to 8.8 with concentrated HCl.	Setting polyacrylamide gel	4
(5) 0.5 M Tris-HCl, pH6.8	0.5 M Tris made up to 100 mL with MilliQ water. The pH was adjusted to 6.8 with concentrated HCl.	Setting polyacrylamide gel	4
(6) 10% Sodium dodecyl suphate solution	10 g SDS powder make up to 100 mL with MilliQ water.	Setting polyacrylamide gel	Room temperature
(7) 10% Ammonium persulphate solution	100 mg ammonium persulphate powder make up to 1 mL with MilliQ water.	Setting polyacrylamide gel	-20

Reagents	Components	Purpose	Storage Temperature (°C)
(8) Running buffer, pH8.3	25 mM Tris, 192 mM glycine and 0.1% (w/v) sodium dodecyl sulphate made up to 1 L with MilliQ water. The pH was adjusted to 8.3 with concentrated HCl.	Running gel	4
(9) Transfer buffer, pH 8.3	50 mM Tris, 384 mM glycine, 20% (v/v) methanol and 0.1% (w/v) sodium dodecyl sulphate made up to 1 L with MilliQ water. The pH was adjusted to 8.3 with HCl.	Transferring the proteins on gel to membrane	4
(10) Blocking buffer	5 g milk or 2 g bovine serum albumin made up to 100 mL with TBST buffer.	Blocking membrane	---
ChIP assay			
(1) 37% formaldehyde solution	--- (Sigma)	To cross-link DNA and proteins	Room temperature
(2) 25 M glycine solution	187.7 g glycine powder made up to 50 mL with MilliQ water.	To stop the cross-linking reaction	Room temperature
(3) PBS	Commercial PBS, pH 7.4 and made up with 1 L of MilliQ water.	To wash the cells	4
Commonly used reagents			
(1) 75% (v/v) ethanol	37.5 mL absolute ethanol make up to 50 mL with ribonuclease free water.	---	Room Temperature
(2) 95% (v/v) ethanol	47.5 mL absolute ethanol make up to 50 mL with ribonuclease free water.	---	Room Temperature

References

1. Auerbach, P., Bennett, R.A., Bailey, E.A., Krokan, H.E. & Demple, B. Mutagenic specificity of endogenously generated abasic sites in Saccharomyces cerevisiae chromosomal DNA. *Proc Natl Acad Sci U S A* **102**, 17711-6 (2005).

2. Madhusudan, S. & Middleton, M.R. The emerging role of DNA repair proteins as predictive, prognostic and therapeutic targets in cancer. *Cancer Treat Rev* **31**, 603-17 (2005).

3. Li, L. & Zou, L. Sensing, signaling, and responding to DNA damage: organization of the checkpoint pathways in mammalian cells. *J Cell Biochem* **94**, 298-306 (2005).

4. Nojima, K., Hochegger, H., Saberi, A., Fukushima, T., Kikuchi, K., Yoshimura, M., Orelli, B.J., Bishop, D.K., Hirano, S., Ohzeki, M., Ishiai, M., Yamamoto, K., Takata, M., Arakawa, H., Buerstedde, J.M., Yamazoe, M., Kawamoto, T., Araki, K., Takahashi, J.A., Hashimoto, N., Takeda, S. & Sonoda, E. Multiple repair pathways mediate tolerance to chemotherapeutic cross-linking agents in vertebrate cells. *Cancer Res* **65**, 11704-11 (2005).

5. Jackson, S.P. & Bartek, J. The DNA-damage response in human biology and disease. *Nature* **461**, 1071-8 (2009).

6. Sancar, A., Lindsey-Boltz, L.A., Unsal-Kacmaz, K. & Linn, S. Molecular mechanisms of mammalian DNA repair and the DNA damage checkpoints. *Annu Rev Biochem* **73**, 39-85 (2004).

7. Larsen, N.B., Rasmussen, M. & Rasmussen, L.J. Nuclear and mitochondrial DNA repair: similar pathways? *Mitochondrion* **5**, 89-108 (2005).

8. Fleck, O. & Nielsen, O. DNA repair. *J Cell Sci* **117**, 515-7 (2004).

9. Carr, A.M. & Hoekstra, M.F. The cellular responses to DNA damage. *Trends Cell Biol* **5**, 32-40 (1995).

10. Bernstein, C., Bernstein, H., Payne, C.M. & Garewal, H. DNA repair/pro-apoptotic dual-role proteins in five major DNA repair pathways: fail-safe protection against carcinogenesis. *Mutat Res* **511**, 145-78 (2002).

11. Meadows, K.L., Song, B. & Doetsch, P.W. Characterization of AP lyase activities of Saccharomyces cerevisiae Ntg1p and Ntg2p: implications for biological function. *Nucleic Acids Res* **31**, 5560-7 (2003).

12. Christmann, M., Tomicic, M.T., Roos, W.P. & Kaina, B. Mechanisms of human DNA repair: an update. *Toxicology* **193**, 3-34 (2003).

13. Mohrenweiser, H.W., Wilson, D.M., 3rd & Jones, I.M. Challenges and complexities in estimating both the functional impact and the disease risk associated with the extensive genetic variation in human DNA repair genes. *Mutat Res* **526**, 93-125 (2003).

14. Alseth, I., Korvald, H., Osman, F., Seeberg, E. & Bjoras, M. A general role of the DNA glycosylase Nth1 in the abasic sites cleavage step of base excision repair in Schizosaccharomyces pombe. *Nucleic Acids Res* **32**, 5119-25 (2004).

15. Barzilai, A. & Yamamoto, K. DNA damage responses to oxidative stress. *DNA Repair (Amst)* **3**, 1109-15 (2004).

16. Mishina, Y., Duguid, E.M. & He, C. Direct reversal of DNA alkylation damage. *Chem Rev* **106**, 215-32 (2006).

17. Mitra, S. & Kaina, B. Regulation of repair of alkylation damage in mammalian genomes. *Prog Nucleic Acid Res Mol Biol* **44**, 109-42 (1993).

18. Eker, A.P., Quayle, C., Chaves, I. & van der Horst, G.T. DNA repair in mammalian cells: Direct DNA damage reversal: elegant solutions for nasty problems. *Cell Mol Life Sci* **66**, 968-80 (2009).

19. Duncan, T., Trewick, S.C., Koivisto, P., Bates, P.A., Lindahl, T. & Sedgwick, B. Reversal of DNA alkylation damage by two human dioxygenases. *Proc Natl Acad Sci U S A* **99**, 16660-5 (2002).

20. Sedgwick, B. Repairing DNA-methylation damage. *Nat Rev Mol Cell Biol* **5**, 148-57 (2004).

21. Hoeijmakers, J.H. Genome maintenance mechanisms for preventing cancer. *Nature* **411**, 366-74 (2001).

22. Memisoglu, A. & Samson, L. Base excision repair in yeast and mammals. *Mutat Res* **451**, 39-51 (2000).

23. Guillet, M. & Boiteux, S. Origin of endogenous DNA abasic sites in Saccharomyces cerevisiae. *Mol Cell Biol* **23**, 8386-94 (2003).

24. Moldave, K., Mitra, S., McCullough, A.K., Lloyd, R.S. & Wilson, S.H. *BASE EXCISION REPAIR*, (ACADEMIC PRESS, San Diego, California., 2001).

25. Boiteux, S. & Guillet, M. Abasic sites in DNA: repair and biological consequences in Saccharomyces cerevisiae. *DNA Repair (Amst)* **3**, 1-12 (2004).

26. Nouspikel, T. DNA repair in mammalian cells : Nucleotide excision repair: variations on versatility. *Cell Mol Life Sci* **66**, 994-1009 (2009).

27. Shuck, S.C., Short, E.A. & Turchi, J.J. Eukaryotic nucleotide excision repair: from understanding mechanisms to influencing biology. *Cell Res* **18**, 64-72 (2008).

28. Araujo, S.J. & Wood, R.D. Protein complexes in nucleotide excision repair. *Mutat Res* **435**, 23-33 (1999).

29. Volker, M., Mone, M.J., Karmakar, P., van Hoffen, A., Schul, W., Vermeulen, W., Hoeijmakers, J.H., van Driel, R., van Zeeland, A.A. & Mullenders, L.H. Sequential assembly of the nucleotide excision repair factors in vivo. *Mol Cell* **8**, 213-24 (2001).

30. Svejstrup, J.Q. Mechanisms of transcription-coupled DNA repair. *Nat Rev Mol Cell Biol* **3**, 21-9 (2002).

31. Sharova, N.P. How does a cell repair damaged DNA? *Biochemistry (Mosc)* **70**, 275-91 (2005).

32. Kao, J., Rosenstein, B.S., Peters, S., Milano, M.T. & Kron, S.J. Cellular response to DNA damage. *Ann N Y Acad Sci* **1066**, 243-58 (2005).

33. Weterings, E. & Chen, D.J. The endless tale of non-homologous end-joining. *Cell Res* **18**, 114-24 (2008).

34. Sigurdsson, S., Van Komen, S., Petukhova, G. & Sung, P. Homologous DNA pairing by human recombination factors Rad51 and Rad54. *J Biol Chem* **277**, 42790-4 (2002).

35. Friedberg, E.C., Fischhaber, P.L. & Kisker, C. Error-prone DNA polymerases: novel structures and the benefits of infidelity. *Cell* **107**, 9-12 (2001).

36. Lehmann, A.R. Replication of UV-damaged DNA: new insights into links between DNA polymerases, mutagenesis and human disease. *Gene* **253**, 1-12 (2000).

37. Waters, L.S., Minesinger, B.K., Wiltrout, M.E., D'Souza, S., Woodruff, R.V. & Walker, G.C. Eukaryotic translesion polymerases and their roles and regulation in DNA damage tolerance. *Microbiol Mol Biol Rev* **73**, 134-54 (2009).

38. Masuda, Y., Piao, J. & Kamiya, K. DNA replication-coupled PCNA mono-ubiquitination and polymerase switching in a human in vitro system. *J Mol Biol* **396**, 487-500 (2010).

39. Sale, J.E., Batters, C., Edmunds, C.E., Phillips, L.G., Simpson, L.J. & Szuts, D. Timing matters: error-prone gap filling and translesion synthesis in immunoglobulin gene hypermutation. *Philos Trans R Soc Lond B Biol Sci* **364**, 595-603 (2009).

40. Martin, A. & Scharff, M.D. AID and mismatch repair in antibody diversification. *Nat Rev Immunol* **2**, 605-14 (2002).

41. Hsieh, P. & Yamane, K. DNA mismatch repair: molecular mechanism, cancer, and ageing. *Mech Ageing Dev* **129**, 391-407 (2008).

42. Li, G.M. Mechanisms and functions of DNA mismatch repair. *Cell Res* **18**, 85-98 (2008).

43. Resnick, M.A. & Cox, B.S. Yeast as an honorary mammal. *Mutat Res* **451**, 1-11 (2000).

44. Foury, F. Human genetic diseases: a cross-talk between man and yeast. *Gene* **195**, 1-10 (1997).

45. Taylor, E.M. & Lehmann, A.R. Conservation of eukaryotic DNA repair mechanisms. *Int J Radiat Biol* **74**, 277-86 (1998).

46. Gros, L., Saparbaev, M.K. & Laval, J. Enzymology of the repair of free radicals-induced DNA damage. *Oncogene* **21**, 8905-25 (2002).

47. Fry, R.C., Begley, T.J. & Samson, L.D. Genome-wide responses to DNA-damaging agents. *Annu Rev Microbiol* **59**, 357-77 (2005).

48. Kelley, M.R., Kow, Y.W. & Wilson, D.M., 3rd. Disparity between DNA base excision repair in yeast and mammals: translational implications. *Cancer Res* **63**, 549-54 (2003).

49. Michal, G. Biochemical pathways: an atlas of biochemistry and molecular biology. in *Nucleic acid metabolism, protein synthesis and cell cycle in eukarya* 137-57 (John Wiley, New York, 1999).

50. Pollard, T.D. & Earnshaw, W.C. Cell Biology. in *Cell cycle* 673-782 (Saunders, Philadelphia, 2002).

51. Tyson, J.J., Csikasz-Nagy, A. & Novak, B. The dynamics of cell cycle regulation. *Bioessays* **24**, 1095-109 (2002).

52. Park, M.T. & Lee, S.J. Cell cycle and cancer. *J Biochem Mol Biol* **36**, 60-5 (2003).

53. Vermeulen, K., Van Bockstaele, D.R. & Berneman, Z.N. The cell cycle: a review of regulation, deregulation and therapeutic targets in cancer. *Cell Prolif* **36**, 131-49 (2003).

54. Hartwell, L.H. & Weinert, T.A. Checkpoints: controls that ensure the order of cell cycle events. *Science* **246**, 629-34 (1989).

55. McDonald, E.R., 3rd & El-Deiry, W.S. Checkpoint genes in cancer. *Ann Med* **33**, 113-22 (2001).

56. Blagosklonny, M.V. & Pardee, A.B. The restriction point of the cell cycle. *Cell Cycle* **1**, 103-10 (2002).

57. group, N.P. (ed.) *Encyclopedia of life sciences*, 1-8 (Nature Publishing group, New York, 2002).

58. Pietenpol, J.A. & Stewart, Z.A. Cell cycle checkpoint signaling: cell cycle arrest versus apoptosis. *Toxicology* **181-182**, 475-81 (2002).

59. Laiho, M. & Latonen, L. Cell cycle control, DNA damage checkpoints and cancer. *Ann Med* **35**, 391-7 (2003).

60. Zhou, B.B. & Elledge, S.J. The DNA damage response: putting checkpoints in perspective. *Nature* **408**, 433-9 (2000).

61. Walworth, N.C. Cell-cycle checkpoint kinases: checking in on the cell cycle. *Curr Opin Cell Biol* **12**, 697-704 (2000).

62. Abraham, R.T. Cell cycle checkpoint signaling through the ATM and ATR kinases. *Genes Dev* **15**, 2177-96 (2001).

63. Bartek, J. & Lukas, J. Pathways governing G1/S transition and their response to DNA damage. *FEBS Lett* **490**, 117-22 (2001).

64. Bartek, J. & Lukas, J. Mammalian G1- and S-phase checkpoints in response to DNA damage. *Curr Opin Cell Biol* **13**, 738-47 (2001).

65. Stewart, Z.A. & Pietenpol, J.A. p53 Signaling and cell cycle checkpoints. *Chem Res Toxicol* **14**, 243-63 (2001).

66. Maeda, T., Chong, M.T., Espino, R.A., Chua, P.P., Cao, J.Q., Chomey, E.G., Luong, L. & Tron, V.A. Role of p21(Waf-1) in regulating the G1 and G2/M checkpoints in ultraviolet-irradiated keratinocytes. *J Invest Dermatol* **119**, 513-21 (2002).

67. Qin, J. & Li, L. Molecular anatomy of the DNA damage and replication checkpoints. *Radiat Res* **159**, 139-48 (2003).

68. Arima, Y., Hirota, T., Bronner, C., Mousli, M., Fujiwara, T., Niwa, S., Ishikawa, H. & Saya, H. Down-regulation of nuclear protein ICBP90 by p53/p21Cip1/WAF1-dependent DNA-damage checkpoint signals contributes to cell cycle arrest at G1/S transition. *Genes Cells* **9**, 131-42 (2004).

69. Kaufmann, W.K. Cell cycle checkpoints and DNA repair preserve the stability of the human genome. *Cancer Metastasis Rev* **14**, 31-41 (1995).

70. Xie, G., Habbersett, R.C., Jia, Y., Peterson, S.R., Lehnert, B.E., Bradbury, E.M. & D'Anna, J.A. Requirements for p53 and the ATM gene product in the regulation of G1/S and S phase checkpoints. *Oncogene* **16**, 721-36 (1998).

71. Mantel, C., Braun, S.E., Reid, S., Henegariu, O., Liu, L., Hangoc, G. & Broxmeyer, H.E. p21(cip-1/waf-1) deficiency causes deformed nuclear architecture, centriole overduplication, polyploidy, and relaxed microtubule damage checkpoints in human hematopoietic cells. *Blood* **93**, 1390-8 (1999).

72. O'Connell, M.J., Walworth, N.C. & Carr, A.M. The G2-phase DNA-damage checkpoint. *Trends Cell Biol* **10**, 296-303 (2000).

73. Taylor, W.R. & Stark, G.R. Regulation of the G2/M transition by p53. *Oncogene* **20**, 1803-15 (2001).

74. Maeda, T., Hanna, A.N., Sim, A.B., Chua, P.P., Chong, M.T. & Tron, V.A. GADD45 regulates G2/M arrest, DNA repair, and cell death in keratinocytes following ultraviolet exposure. *J Invest Dermatol* **119**, 22-6 (2002).

75. Yarden, R.I., Pardo-Reoyo, S., Sgagias, M., Cowan, K.H. & Brody, L.C. BRCA1 regulates the G2/M checkpoint by activating Chk1 kinase upon DNA damage. *Nat Genet* **30**, 285-9 (2002).

76. Griffin, C.S., Simpson, P.J., Wilson, C.R. & Thacker, J. Mammalian recombination-repair genes XRCC2 and XRCC3 promote correct chromosome segregation. *Nat Cell Biol* **2**, 757-61 (2000).

77. Watters, J.W. & McLeod, H.L. Recent advances in the pharmacogenetics of cancer chemotherapy. *Curr Opin Mol Ther* **4**, 565-71 (2002).

78. Pincheira, J., Bravo, M., Navarrete, M.H., Marcelain, K., Lopez-Saez, J.F. & de la Torre, C. Ataxia telangiectasia: G2 checkpoint and chromosomal damage in proliferating lymphocytes. *Mutagenesis* **16**, 419-22 (2001).

79. Dixon, H. & Norbury, C.J. Therapeutic exploitation of checkpoint defects in cancer cells lacking p53 function. *Cell Cycle* **1**, 362-8 (2002).

80. Vinson, R.K. & Hales, B.F. DNA repair during organogenesis. *Mutat Res* **509**, 79-91 (2002).

81. Bartek, J. & Lukas, J. Chk1 and Chk2 kinases in checkpoint control and cancer. *Cancer Cell* **3**, 421-9 (2003).

82. Yamane, K., Taylor, K. & Kinsella, T.J. Mismatch repair-mediated G2/M arrest by 6-thioguanine involves the ATR-Chk1 pathway. *Biochem Biophys Res Commun* **318**, 297-302 (2004).

83. Doherty, S.C., McKeown, S.R., McKelvey-Martin, V., Downes, C.S., Atala, A., Yoo, J.J., Simpson, D.A. & Kaufmann, W.K. Cell cycle checkpoint function in bladder cancer. *J Natl Cancer Inst* **95**, 1859-68 (2003).

84. Bhattacharyya, N., Chen, H.C., Grundfest-Broniatowski, S. & Banerjee, S. Alteration of hMSH2 and DNA polymerase beta genes in breast carcinomas and fibroadenomas. *Biochem Biophys Res Commun* **259**, 429-35 (1999).

85. Chen, H.C., Bhattacharyya, N., Wang, L., Recupero, A.J., Klein, E.A., Harter, M.L. & Banerjee, S. Defective DNA repair genes in a primary culture of human renal cell carcinoma. *J Cancer Res Clin Oncol* **126**, 185-90 (2000).

86. Ban, S., Shinohara, T., Hirai, Y., Moritaku, Y., Cologne, J.B. & MacPhee, D.G. Chromosomal instability in BRCA1- or BRCA2-defective human cancer cells detected by spontaneous micronucleus assay. *Mutat Res* **474**, 15-23 (2001).

87. Chahwan, C., Nakamura, T.M., Sivakumar, S., Russell, P. & Rhind, N. The fission yeast Rad32 (Mre11)-Rad50-Nbs1 complex is required for the S-phase DNA damage checkpoint. *Mol Cell Biol* **23**, 6564-73 (2003).

88. Chen, S., Tang, D., Xue, K., Xu, L., Ma, G., Hsu, Y. & Cho, S.S. DNA repair gene XRCC1 and XPD polymorphisms and risk of lung cancer in a Chinese population. *Carcinogenesis* **23**, 1321-5 (2002).

89. Baccarelli, A., Calista, D., Minghetti, P., Marinelli, B., Albetti, B., Tseng, T., Hedayati, M., Grossman, L., Landi, G., Struewing, J.P. & Landi, M.T. XPD gene polymorphism and host characteristics in the association with cutaneous malignant melanoma risk. *Br J Cancer* **90**, 497-502 (2004).

90. Cheng, L., Spitz, M.R., Hong, W.K. & Wei, Q. Reduced expression levels of nucleotide excision repair genes in lung cancer: a case-control analysis. *Carcinogenesis* **21**, 1527-30 (2000).

91. Venkitaraman, A.R. The breast cancer susceptibility gene, BRCA2: at the crossroads between DNA replication and recombination? *Philos Trans R Soc Lond B Biol Sci* **355**, 191-8 (2000).

92. Ishikawa, T., Ide, F., Qin, X., Zhang, S., Takahashi, Y., Sekiguchi, M., Tanaka, K. & Nakatsuru, Y. Importance of DNA repair in carcinogenesis: evidence from transgenic and gene targeting studies. *Mutat Res* **477**, 41-9 (2001).

93. Zhu, Q., Wani, G., Wani, M.A. & Wani, A.A. Human homologue of yeast Rad23 protein A interacts with p300/cyclic AMP-responsive element binding (CREB)-binding protein to down-regulate transcriptional activity of p53. *Cancer Res* **61**, 64-70 (2001).

94. Vilenchik, M.M. & Knudson, A.G. Endogenous DNA double-strand breaks: production, fidelity of repair, and induction of cancer. *Proc Natl Acad Sci U S A* **100**, 12871-6 (2003).

95. Masutani, C., Sugasawa, K., Yanagisawa, J., Sonoyama, T., Ui, M., Enomoto, T., Takio, K., Tanaka, K., van der Spek, P.J. & Bootsma, D. Purification and cloning of a nucleotide excision repair complex involving the xeroderma pigmentosum group C protein and a human homologue of yeast RAD23. *EMBO J* **13**, 1831-43 (1994).

96. Danesi, R., De Braud, F., Fogli, S., Di Paolo, A. & Del Tacca, M. Pharmacogenetic determinants of anti-cancer drug activity and toxicity. *Trends Pharmacol Sci* **22**, 420-6 (2001).

97. Burroughs, V.J., Maxey, R.W. & Levy, R.A. Racial and ethnic differences in response to medicines: towards individualized pharmaceutical treatment. *J Natl Med Assoc* **94**, 1-26 (2002).

98. McCarthy, J.J. Advances in pharmacogenomic research and development. *Mol Biotechnol* **25**, 275-82 (2003).

99. Donnelly, J.G. Pharmacogenetics in cancer chemotherapy: balancing toxicity and response. *Ther Drug Monit* **26**, 231-5 (2004).

100. Goode, E.L., Ulrich, C.M. & Potter, J.D. Polymorphisms in DNA repair genes and associations with cancer risk. *Cancer Epidemiol Biomarkers Prev* **11**, 1513-30 (2002).

101. Hu, J.J., Mohrenweiser, H.W., Bell, D.A., Leadon, S.A. & Miller, M.S. Symposium overview: genetic polymorphisms in DNA repair and cancer risk. *Toxicol Appl Pharmacol* **185**, 64-73 (2002).

102. Spurdle, A.B., Hopper, J.L., Chen, X., Dite, G.S., Cui, J., McCredie, M.R., Giles, G.G., Ellis-Steinborner, S., Venter, D.J., Newman, B., Southey, M.C. & Chenevix-Trench, G. The BRCA2 372 HH genotype is associated with risk of breast cancer in Australian women under age 60 years. *Cancer Epidemiol Biomarkers Prev* **11**, 413-6 (2002).

103. Le Marchand, L., Donlon, T., Lum-Jones, A., Seifried, A. & Wilkens, L.R. Association of the hOGG1 Ser326Cys polymorphism with lung cancer risk. *Cancer Epidemiol Biomarkers Prev* **11**, 409-12 (2002).

104. Winsey, S.L., Haldar, N.A., Marsh, H.P., Bunce, M., Marshall, S.E., Harris, A.L., Wojnarowska, F. & Welsh, K.I. A variant within the DNA repair gene XRCC3 is associated with the development of melanoma skin cancer. *Cancer Res* **60**, 5612-6 (2000).

105. Angele, S., Romestaing, P., Moullan, N., Vuillaume, M., Chapot, B., Friesen, M., Jongmans, W., Cox, D.G., Pisani, P., Gerard, J.P. & Hall, J. ATM haplotypes and cellular response to DNA damage: association with breast cancer risk and clinical radiosensitivity. *Cancer Res* **63**, 8717-25 (2003).

106. Ding, S.L., Sheu, L.F., Yu, J.C., Yang, T.L., Chen, B.F., Leu, F.J. & Shen, C.Y. Abnormality of the DNA double-strand-break checkpoint/repair genes, ATM, BRCA1 and TP53, in breast cancer is related to tumour grade. *Br J Cancer* **90**, 1995-2001 (2004).

107. Wang, G., Chuang, L., Zhang, X., Colton, S., Dombkowski, A., Reiners, J., Diakiw, A. & Xu, X.S. The initiative role of XPC protein in cisplatin DNA damaging treatment-mediated cell cycle regulation. *Nucleic Acids Res* **32**, 2231-40 (2004).

108. Arai, M., Sato, H., Kobayashi, H., Suganuma, M., Kawabe, T., Tomoda, H. & Omura, S. Selective inhibition of bleomycin-induced G2 cell cycle checkpoint by simaomicin alpha. *Biochem Biophys Res Commun* **317**, 817-22 (2004).

109. Labahn, J., Scharer, O.D., Long, A., Ezaz-Nikpay, K., Verdine, G.L. & Ellenberger, T.E. Structural basis for the excision repair of alkylation-damaged DNA. *Cell* **86**, 321-9 (1996).

110. Yamagata, Y., Kato, M., Odawara, K., Tokuno, Y., Nakashima, Y., Matsushima, N., Yasumura, K., Tomita, K., Ihara, K., Fujii, Y., Nakabeppu, Y., Sekiguchi, M. & Fujii, S. Three-dimensional structure of a DNA repair enzyme, 3-methyladenine DNA glycosylase II, from Escherichia coli. *Cell* **86**, 311-9 (1996).

111. Kuo, C.F., McRee, D.E., Fisher, C.L., O'Handley, S.F., Cunningham, R.P. & Tainer, J.A. Atomic structure of the DNA repair [4Fe-4S] enzyme endonuclease III. *Science* **258**, 434-40 (1992).

112. Nakabeppu, Y. & Sekiguchi, M. Regulatory mechanisms for induction of synthesis of repair enzymes in response to alkylating agents: ada protein acts as a transcriptional regulator. *Proc Natl Acad Sci U S A* **83**, 6297-301 (1986).

113. Shao, X. & Grishin, N.V. Common fold in helix-hairpin-helix proteins. *Nucleic Acids Res* **28**, 2643-50 (2000).

114. Liu, X. & Roy, R. Mutation at active site lysine 212 to arginine uncouples the glycosylase activity from the lyase activity of human endonuclease III. *Biochemistry* **40**, 13617-22 (2001).

115. Liu, X. & Roy, R. Truncation of amino-terminal tail stimulates activity of human endonuclease III (hNTH1). *J Mol Biol* **321**, 265-76 (2002).

116. Matsumoto, Y., Zhang, Q.M., Takao, M., Yasui, A. & Yonei, S. Escherichia coli Nth and human hNTH1 DNA glycosylases are involved in removal of 8-oxoguanine from 8-oxoguanine/guanine mispairs in DNA. *Nucleic Acids Res* **29**, 1975-81 (2001).

117. Marenstein, D.R., Chan, M.K., Altamirano, A., Basu, A.K., Boorstein, R.J., Cunningham, R.P. & Teebor, G.W. Substrate specificity of human endonuclease III (hNTH1). Effect of human APE1 on hNTH1 activity. *J Biol Chem* **278**, 9005-12 (2003).

118. Miyabe, I., Zhang, Q.M., Kino, K., Sugiyama, H., Takao, M., Yasui, A. & Yonei, S. Identification of 5-formyluracil DNA glycosylase activity of human hNTH1 protein. *Nucleic Acids Res* **30**, 3443-8 (2002).

119. Goto, M., Shinmura, K., Igarashi, H., Kobayashi, M., Konno, H., Yamada, H., Iwaizumi, M., Kageyama, S., Tsuneyoshi, T., Tsugane, S. & Sugimura, H. Altered expression of the human base excision repair gene NTH1 in gastric cancer. *Carcinogenesis* **30**, 1345-52 (2009).

120. Koketsu, S., Watanabe, T. & Nagawa, H. Expression of DNA repair protein: MYH, NTH1, and MTH1 in colorectal cancer. *Hepatogastroenterology* **51**, 638-42 (2004).

121. Jiang, Z., Hu, J., Li, X., Jiang, Y., Zhou, W. & Lu, D. Expression analyses of 27 DNA repair genes in astrocytoma by TaqMan low-density array. *Neurosci Lett* **409**, 112-7 (2006).

122. Eide, L., Bjoras, M., Pirovano, M., Alseth, I., Berdal, K.G. & Seeberg, E. Base excision of oxidative purine and pyrimidine DNA damage in Saccharomyces cerevisiae by a DNA glycosylase with sequence similarity to endonuclease III from Escherichia coli. *Proc Natl Acad Sci U S A* **93**, 10735-40 (1996).

123. Aspinwall, R., Rothwell, D.G., Roldan-Arjona, T., Anselmino, C., Ward, C.J., Cheadle, J.P., Sampson, J.R., Lindahl, T., Harris, P.C. & Hickson, I.D. Cloning and characterization of a functional human homolog of Escherichia coli endonuclease III. *Proc Natl Acad Sci U S A* **94**, 109-14 (1997).

124. Augeri, L., Lee, Y.M., Barton, A.B. & Doetsch, P.W. Purification, characterization, gene cloning, and expression of Saccharomyces cerevisiae redoxyendonuclease, a homolog of Escherichia coli endonuclease III. *Biochemistry* **36**, 721-9 (1997).

125. Polyak, K., Li, Y., Zhu, H., Lengauer, C., Willson, J.K., Markowitz, S.D., Trush, M.A., Kinzler, K.W. & Vogelstein, B. Somatic mutations of the mitochondrial genome in human colorectal tumours. *Nat Genet* **20**, 291-3 (1998).

126. You, H.J., Swanson, R.L., Harrington, C., Corbett, A.H., Jinks-Robertson, S., Senturker, S., Wallace, S.S., Boiteux, S., Dizdaroglu, M. & Doetsch, P.W. Saccharomyces cerevisiae Ntg1p and Ntg2p: broad specificity N-glycosylases for the repair of oxidative DNA damage in the nucleus and mitochondria. *Biochemistry* **38**, 11298-306 (1999).

127. Lieberman, H.B. DNA damage repair and response proteins as targets for cancer therapy. *Curr Med Chem* **15**, 360-7 (2008).

128. Ide, H. & Kotera, M. Human DNA glycosylases involved in the repair of oxidatively damaged DNA. *Biol Pharm Bull* **27**, 480-5 (2004).

129. Guay, D., Garand, C., Reddy, S., Schmutte, C. & Lebel, M. The human endonuclease III enzyme is a relevant target to potentiate cisplatin cytotoxicity in Y-box-binding protein-1 overexpressing tumor cells. *Cancer Sci* **99**, 762-9 (2008).

130. Cooley, N., Elder, R.H. & Povey, A.C. The effect of Msh2 knockdown on methylating agent induced toxicity in DNA glycosylase deficient cells. *Toxicology* **268**, 111-7 (2010).

131. Gillet, J.P. & Gottesman, M.M. Mechanisms of multidrug resistance in cancer. *Methods Mol Biol* **596**, 47-76 (2010).

132. Fukushima, T., Takeshima, H. & Kataoka, H. Anti-glioma therapy with temozolomide and status of the DNA-repair gene MGMT. *Anticancer Res* **29**, 4845-54 (2009).

133. Frosina, G. DNA repair and resistance of gliomas to chemotherapy and radiotherapy. *Mol Cancer Res* **7**, 989-99 (2009).

134. Jain, K.K. Personalized medicine. *Curr Opin Mol Ther* **4**, 548-58 (2002).

135. Efferth, T. & Volm, M. Pharmacogenetics for individualized cancer chemotherapy. *Pharmacol Ther* **107**, 155-76 (2005).

136. Gerson, S.L., Schupp, J., Liu, L., Pegg, A.E. & Srinivasen, S. Leukocyte O6-alkylguanine-DNA alkyltransferase from human donors is uniformly sensitive to O6-benzylguanine. *Clin Cancer Res* **5**, 521-4 (1999).

137. Moorehead, R.A., Armstrong, S.G., Wilson, B.C. & Singh, G. Cross-resistance to cisplatin in cells resistant to photofrin-mediated photodynamic therapy. *Cancer Res* **54**, 2556-9 (1994).

138. Woods, J.A., Traynor, N.J., Brancaleon, L. & Moseley, H. The effect of photofrin on DNA strand breaks and base oxidation in HaCaT keratinocytes: a comet assay study. *Photochem Photobiol* **79**, 105-13 (2004).

139. Saczko, J., Kulbacka, J., Chwilkowska, A., Drag-Zalesiniska, M., Wysocka, T., Lugowski, M. & Banas, T. The influence of photodynamic therapy on apoptosis in human melanoma cell line. *Folia Histochem Cytobiol* **43**, 129-32 (2005).

140. Saczko, J., Chwilkowska, A., Kulbacka, J., Berdowska, I., Zielinski, B., Drag-Zalesinska, M., Wysocka, T., Lugowski, M. & Banas, T. Photooxidative action in cancer and normal cells induced by the use of photofrin in photodynamic therapy. *Folia Biol (Praha)* **54**, 24-9 (2008).

141. Pass, H.I. Photodynamic therapy in oncology: mechanisms and clinical use. *J Natl Cancer Inst* **85**, 443-56 (1993).

142. Fritsch, C., Goerz, G. & Ruzicka, T. Photodynamic therapy in dermatology. *Arch Dermatol* **134**, 207-14 (1998).

143. Browning, A.C., Amoaku, W.M. & Dua, H.S. Treatment of age-related macular degeneration. *J R Soc Med* **97**, 166-9 (2004).

144. O'Connor, A.E., Gallagher, W.M. & Byrne, A.T. Porphyrin and nonporphyrin photosensitizers in oncology: preclinical and clinical advances in photodynamic therapy. *Photochem Photobiol* **85**, 1053-74 (2009).

145. Nyst, H.J., Tan, I.B., Stewart, F.A. & Balm, A.J. Is photodynamic therapy a good alternative to surgery and radiotherapy in the treatment of head and neck cancer? *Photodiagnosis Photodyn Ther* **6**, 3-11 (2009).

146. Zhao, S.P., Tao, Z.D., Xiao, J.Y., Peng, Y.Y., Yang, Y.H., Zeng, Q.S. & Liu, Z.W. Photoradiation therapy of animal tumors and nasopharyngeal carcinoma. *Ann Otol Rhinol Laryngol* **99**, 454-60 (1990).

147. Lou, P.J., Jager, H.R., Jones, L., Theodossy, T., Bown, S.G. & Hopper, C. Interstitial photodynamic therapy as salvage treatment for recurrent head and neck cancer. *Br J Cancer* **91**, 441-6 (2004).

148. Hornung, R., Walt, H., Crompton, N.E., Keefe, K.A., Jentsch, B., Perewusnyk, G., Haller, U. & Kochli, O.R. m-THPC-mediated photodynamic therapy (PDT) does not induce resistance to chemotherapy, radiotherapy or PDT on human breast cancer cells in vitro. *Photochem Photobiol* **68**, 569-74 (1998).

149. Calzavara-Pinton, P.G., Venturini, M. & Sala, R. Photodynamic therapy: update 2006. Part 1: Photochemistry and photobiology. *J Eur Acad Dermatol Venereol* **21**, 293-302 (2007).

150. Moan, J. & Peng, Q. An outline of the history of PDT in *Photodynamic Therapy* (ed. Patrice, T.) 1-18 (RSC Publishing London 2003).

151. Hasan, T., Ortel, B., Moor, A.C. & Pogue, B.W. Photodynamic Therapy of Cancer. in *Cancer Medicine 6* (eds. Kufe, D.W. et al.) (BC Decker Inc., Hamilton (Canada), 2003).

152. Triesscheijn, M., Baas, P., Schellens, J.H. & Stewart, F.A. Photodynamic therapy in oncology. *Oncologist* **11**, 1034-44 (2006).

153. Pervaiz, S. Reactive oxygen-dependent production of novel photochemotherapeutic agents. *FASEB J* **15**, 612-7 (2001).

154. Ris, H.B., Altermatt, H.J., Stewart, C.M., Schaffner, T., Wang, Q., Lim, C.K., Bonnett, R. & Althaus, U. Photodynamic therapy with m-tetrahydroxyphenylchlorin in vivo: optimization of the therapeutic index. *Int J Cancer* **55**, 245-9 (1993).

155. Morlet, L., Vonarx-Coinsmann, V., Lenz, P., Foultier, M.T., de Brito, L.X., Stewart, C. & Patrice, T. Correlation between meta(tetrahydroxyphenyl)chlorin (m-THPC) biodistribution and photodynamic effects in mice. *J Photochem Photobiol B* **28**, 25-32 (1995).

156. Veenhuizen, R.B., Ruevekamp, M.C., Oppelaar, H., Helmerhorst, T.J., Kenemans, P. & Stewart, F.A. Foscan-mediated photodynamic therapy for a peritoneal-cancer model: drug distribution and efficacy studies. *Int J Cancer* **73**, 230-5 (1997).

157. Mansfield, R., Bown, S. & McEwan, J. Photodynamic therapy: shedding light on restenosis. *Heart* **86**, 612-8 (2001).

158. Dougherty, T.J., Gomer, C.J., Henderson, B.W., Jori, G., Kessel, D., Korbelik, M., Moan, J. & Peng, Q. Photodynamic therapy. *J Natl Cancer Inst* **90**, 889-905 (1998).

159. Oleinick, N.L. & Evans, H.H. The photobiology of photodynamic therapy: cellular targets and mechanisms. *Radiat Res* **150**, S146-56 (1998).

160. Moor, A.C. Signaling pathways in cell death and survival after photodynamic therapy. *J Photochem Photobiol B* **57**, 1-13 (2000).

161. Callahan, D.E., Forte, T.M., Afzal, S.M., Deen, D.F., Kahl, S.B., Bjornstad, K.A., Bauer, W.F. & Blakely, E.A. Boronated protoporphyrin (BOPP): localization in lysosomes of the human glioma cell line SF-767 with uptake modulated by lipoprotein levels. *Int J Radiat Oncol Biol Phys* **45**, 761-71 (1999).

162. Lei, W., Xie, J., Hou, Y., Jiang, G., Zhang, H., Wang, P., Wang, X. & Zhang, B. Mitochondria-targeting properties and photodynamic activities of porphyrin derivatives bearing cationic pendant. *J Photochem Photobiol B* **98**, 167-71 (2010).

163. Guan, H., Liu, X., Peng, W., Cao, R., Ma, Y., Chen, H. & Xu, A. Beta-carboline derivatives: novel photosensitizers that intercalate into DNA to cause direct DNA damage in photodynamic therapy. *Biochem Biophys Res Commun* **342**, 894-901 (2006).

164. Allison, R.R., Downie, G.H., Cuenca, R., Hu, X.H., Childs, C.J. & Sibata, C.H. Photosensitizers in clinical PDT. *Photodiagnosis and Photodynamic Therapy* **1**, 27-42 (2004).

165. Huang, Z. A review of progress in clinical photodynamic therapy. *Technol Cancer Res Treat* **4**, 283-93 (2005).

166. Ferrario, A., Von Tiehl, K., Wong, S., Luna, M. & Gomer, C.J. Cyclooxygenase-2 inhibitor treatment enhances photodynamic therapy-mediated tumor response. *Cancer Res* **62**, 3956-61 (2002).

167. Biel, M. Advances in photodynamic therapy for the treatment of head and neck cancers. *Lasers Surg Med* **38**, 349-55 (2006).

168. DiProspero, L., Singh, G., Wilson, B.C. & Rainbow, A.J. Cross-resistance to photofrin-mediated photodynamic therapy and UV light and recovery from photodynamic therapy damage in Rif-8A mouse fibrosarcoma cells measured using viral capacity. *J Photochem Photobiol B* **38**, 143-51 (1997).

169. Wen, P.Y. & Kesari, S. Malignant gliomas in adults. *N Engl J Med* **359**, 492-507 (2008).

170. de Groot, J. & Milano, V. Improving the prognosis for patients with glioblastoma: the rationale for targeting Src. *J Neurooncol* **95**, 151-63 (2009).

171. Colman, H. & Aldape, K. Molecular predictors in glioblastoma: toward personalized therapy. *Arch Neurol* **65**, 877-83 (2008).

172. Pardridge, W.M. Blood-brain barrier drug targeting: the future of brain drug development. *Mol Interv* **3**, 90-105, 51 (2003).

173. Gerstner, E.R. & Fine, R.L. Increased permeability of the blood-brain barrier to chemotherapy in metastatic brain tumors: establishing a treatment paradigm. *J Clin Oncol* **25**, 2306-12 (2007).

174. Adams, K., Rainbow, A.J., Wilson, B.C. & Singh, G. In vivo resistance to photofrin-mediated photodynamic therapy in radiation-induced fibrosarcoma cells resistant to in vitro Photofrin-mediated photodynamic therapy. *J Photochem Photobiol B* **49**, 136-41 (1999).

175. Manyak, M.J. & Ogan, K. Photodynamic therapy for refractory superficial bladder cancer: long-term clinical outcomes of single treatment using intravesical diffusion medium. *J Endourol* **17**, 633-9 (2003).

176. Wilson, J.J., Jones, H., Burock, M., Smith, D., Fraker, D.L., Metz, J., Glatstein, E. & Hahn, S.M. Patterns of recurrence in patients treated with photodynamic therapy for intraperitoneal carcinomatosis and sarcomatosis. *Int J Oncol* **24**, 711-7 (2004).

177. Ferrario, A., Rucker, N., Wong, S., Luna, M. & Gomer, C.J. Survivin, a member of the inhibitor of apoptosis family, is induced by photodynamic therapy and is a target for improving treatment response. *Cancer Res* **67**, 4989-95 (2007).

178. Wenig, B.L., Kurtzman, D.M., Grossweiner, L.I., Mafee, M.F., Harris, D.M., Lobraico, R.V., Prycz, R.A. & Appelbaum, E.L. Photodynamic therapy in the treatment of squamous cell carcinoma of the head and neck. *Arch Otolaryngol Head Neck Surg* **116**, 1267-70 (1990).

179. Stylli, S.S., Howes, M., MacGregor, L., Rajendra, P. & Kaye, A.H. Photodynamic therapy of brain tumours: evaluation of porphyrin uptake versus clinical outcome. *J Clin Neurosci* **11**, 584-96 (2004).

180. Rigual, N.R., Thankappan, K., Cooper, M., Sullivan, M.A., Dougherty, T., Popat, S.R., Loree, T.R., Biel, M.A. & Henderson, B. Photodynamic therapy for head and neck dysplasia and cancer. *Arch Otolaryngol Head Neck Surg* **135**, 784-8 (2009).

181. Golab, J., Nowis, D., Skrzycki, M., Czeczot, H., Baranczyk-Kuzma, A., Wilczynski, G.M., Makowski, M., Mroz, P., Kozar, K., Kaminski, R., Jalili, A., Kopec, M., Grzela, T. & Jakobisiak, M. Antitumor effects of photodynamic therapy are potentiated by 2-methoxyestradiol. A superoxide dismutase inhibitor. *J Biol Chem* **278**, 407-14 (2003).

182. Nowis, D., Legat, M., Grzela, T., Niderla, J., Wilczek, E., Wilczynski, G.M., Glodkowska, E., Mrowka, P., Issat, T., Dulak, J., Jozkowicz, A., Was, H., Adamek, M., Wrzosek, A., Nazarewski, S., Makowski, M., Stoklosa, T., Jakobisiak, M. & Golab, J. Heme oxygenase-1 protects tumor cells against photodynamic therapy-mediated cytotoxicity. *Oncogene* **25**, 3365-74 (2006).

183. Saczko, J., Kulbacka, J., Chwilkowsa, A., Pola, A., Lugowski, M., Marcinkowska, A., Malarska, A. & Banas, T. Cytosolic superoxide dismutase activity after photodynamic therapy, intracellular distribution of Photofrin II and hypericin, and P-glycoprotein localization in human colon adenocarcinoma. *Folia Histochem Cytobiol* **45**, 93-8 (2007).

184. Usuda, J., Hirata, T., Ichinose, S., Ishizumi, T., Inoue, T., Ohtani, K., Maehara, S., Yamada, M., Tsutsui, H., Okunaka, T., Kato, H. & Ikeda, N. Tailor-made approach to photodynamic therapy in the treatment of cancer based on Bcl-2 photodamage. *Int J Oncol* **33**, 689-96 (2008).

185. Makowski, M., Grzela, T., Niderla, J., M, L.A., Mroz, P., Kopee, M., Legat, M., Strusinska, K., Koziak, K., Nowis, D., Mrowka, P., Wasik, M., Jakobisiak, M. & Golab, J. Inhibition of cyclooxygenase-2 indirectly potentiates antitumor effects of photodynamic therapy in mice. *Clin Cancer Res* **9**, 5417-22 (2003).

186. Luna, M., Wong, S., Ferrario, A. & Gomer, C.J. Cyclooxygenase-2 expression induced by photofrin photodynamic therapy involves the p38 MAPK pathway. *Photochem Photobiol* **84**, 509-14 (2008).

187. Gomer, C.J., Ferrario, A., Luna, M., Rucker, N. & Wong, S. Photodynamic therapy: combined modality approaches targeting the tumor microenvironment. *Lasers Surg Med* **38**, 516-21 (2006).

188. deCarvalho, A.C., Zhang, X., Roberts, C., Jiang, F., Kalkanis, S.N., Hong, X., Lu, M. & Chopp, M. Subclinical photodynamic therapy treatment modifies the brain microenvironment and promotes glioma growth. *Glia* **55**, 1053-60 (2007).

189. Zheng, X., Jiang, F., Katakowski, M., Zhang, X., Jiang, H., Zhang, Z.G. & Chopp, M. Sensitization of cerebral tissue in nude mice with photodynamic therapy induces ADAM17/TACE and promotes glioma cell invasion. *Cancer Lett* **265**, 177-87 (2008).

190. Wong, T.W., Tracy, E., Oseroff, A.R. & Baumann, H. Photodynamic therapy mediates immediate loss of cellular responsiveness to cytokines and growth factors. *Cancer Res* **63**, 3812-8 (2003).

191. Gilljam, K.M., Feyzi, E., Aas, P.A., Sousa, M.M., Muller, R., Vagbo, C.B., Catterall, T.C., Liabakk, N.B., Slupphaug, G., Drablos, F., Krokan, H.E. & Otterlei, M. Identification of a novel, widespread, and functionally important PCNA-binding motif. *J Cell Biol* **186**, 645-54 (2009).

192. Yi, C., Yang, C.G. & He, C. A Non-Heme Iron-Mediated Chemical Demethylation in DNA and RNA. *Acc Chem Res* (2009).

193. Yang, C.G., Yi, C., Duguid, E.M., Sullivan, C.T., Jian, X., Rice, P.A. & He, C. Crystal structures of DNA/RNA repair enzymes AlkB and ABH2 bound to dsDNA. *Nature* **452**, 961-5 (2008).

194. Falnes, P.O., Klungland, A. & Alseth, I. Repair of methyl lesions in DNA and RNA by oxidative demethylation. *Neuroscience* **145**, 1222-32 (2007).

195. Chen, G., Yuan, S.S., Liu, W., Xu, Y., Trujillo, K., Song, B., Cong, F., Goff, S.P., Wu, Y., Arlinghaus, R., Baltimore, D., Gasser, P.J., Park, M.S., Sung, P. & Lee, E.Y. Radiation-induced assembly of Rad51 and Rad52 recombination complex requires ATM and c-Abl. *J Biol Chem* **274**, 12748-52 (1999).

196. Symington, L.S. Role of RAD52 epistasis group genes in homologous recombination and double-strand break repair. *Microbiol Mol Biol Rev* **66**, 630-70, table of contents (2002).

197. Evans, H.H., Horng, M.F., Ricanati, M., Deahl, J.T. & Oleinick, N.L. Mutagenicity of photodynamic therapy as compared to UVC and ionizing radiation in human and murine lymphoblast cell lines. *Photochem Photobiol* **66**, 690-6 (1997).

198. Fritz, G. Human APE/Ref-1 protein. *Int J Biochem Cell Biol* **32**, 925-9 (2000).

199. Tada-Oikawa, S., Oikawa, S., Hirayama, J., Hirakawa, K. & Kawanishi, S. DNA damage and apoptosis induced by photosensitization of 5,10,15,20-tetrakis (N-methyl-4-pyridyl)-21H,23H-porphyrin via singlet oxygen generation. *Photochem Photobiol* **85**, 1391-9 (2009).

200. Conlon, K.A. & Berrios, M. Site-directed photoproteolysis of 8-oxoguanine DNA glycosylase 1 (OGG1) by specific porphyrin-protein probe conjugates: a strategy to improve the effectiveness of photodynamic therapy for cancer. *J Photochem Photobiol B* **87**, 9-17 (2007).

201. Yang, Z.Z., Li, M.X., Zhang, Y.S., Xiang, D.B., Dai, N., Zeng, L.L., Li, Z.P., Wang, G. & Wang, D. Knock down of the dual functional protein apurinic /apyrimidinic endonuclease 1 enhances the killing effect of hematoporphrphyrin derivative-mediated photodynamic therapy on non-small cell lung cancer cells in vitro and in a xenograft model. *Cancer Sci* **101**, 180-7 (2010).

202. Petermann, E., Keil, C. & Oei, S.L. Roles of DNA ligase III and XRCC1 in regulating the switch between short patch and long patch BER. *DNA Repair (Amst)* **5**, 544-55 (2006).

203. Yoo, H., Li, L., Sacks, P.G., Thompson, L.H., Becker, F.F. & Chan, J.Y. Alterations in expression and structure of the DNA repair gene XRCC1. *Biochem Biophys Res Commun* **186**, 900-10 (1992).

204. Chang-Claude, J., Ambrosone, C.B., Lilla, C., Kropp, S., Helmbold, I., von Fournier, D., Haase, W., Sautter-Bihl, M.L., Wenz, F., Schmezer, P. & Popanda, O. Genetic polymorphisms in DNA repair and damage response genes and late normal tissue complications of radiotherapy for breast cancer. *Br J Cancer* **100**, 1680-6 (2009).

205. Azria, D., Ozsahin, M., Kramar, A., Peters, S., Atencio, D.P., Crompton, N.E., Mornex, F., Pelegrin, A., Dubois, J.B., Mirimanoff, R.O. & Rosenstein, B.S. Single nucleotide polymorphisms, apoptosis, and the development of severe late adverse effects after radiotherapy. *Clin Cancer Res* **14**, 6284-8 (2008).

206. Dworaczek, H. & Xiao, W. Xeroderma pigmentosum: a glimpse into nucleotide excision repair, genetic instability, and cancer. *Crit Rev Oncog* **13**, 159-77 (2007).

207. Lindenbaum, Y., Dickson, D., Rosenbaum, P., Kraemer, K., Robbins, I. & Rapin, I. Xeroderma pigmentosum/cockayne syndrome complex: first neuropathological study and review of eight other cases. *Eur J Paediatr Neurol* **5**, 225-42 (2001).

208. Finlan, L.E., Kernohan, N.M., Thomson, G., Beattie, P.E., Hupp, T.R. & Ibbotson, S.H. Differential effects of 5-aminolaevulinic acid photodynamic therapy and psoralen + ultraviolet A therapy on p53 phosphorylation in normal human skin in vivo. *Br J Dermatol* **153**, 1001-10 (2005).

209. Vogelstein, B., Lane, D. & Levine, A.J. Surfing the p53 network. *Nature* **408**, 307-10 (2000).

210. Woods, D.B. & Vousden, K.H. Regulation of p53 function. *Exp Cell Res* **264**, 56-66 (2001).

211. Donehower, L.A., Godley, L.A., Aldaz, C.M., Pyle, R., Shi, Y.P., Pinkel, D., Gray, J., Bradley, A., Medina, D. & Varmus, H.E. Deficiency of p53 accelerates mammary tumorigenesis in Wnt-1 transgenic mice and promotes chromosomal instability. *Genes Dev* **9**, 882-95 (1995).

212. Harvey, M., Vogel, H., Lee, E.Y., Bradley, A. & Donehower, L.A. Mice deficient in both p53 and Rb develop tumors primarily of endocrine origin. *Cancer Res* **55**, 1146-51 (1995).

213. Chumakov, P.M. Versatile functions of p53 protein in multicellular organisms. *Biochemistry (Mosc)* **72**, 1399-421 (2007).

214. Brown, L., Boswell, S., Raj, L. & Lee, S.W. Transcriptional targets of p53 that regulate cellular proliferation. *Crit Rev Eukaryot Gene Expr* **17**, 73-85 (2007).

215. Riley, T., Sontag, E., Chen, P. & Levine, A. Transcriptional control of human p53-regulated genes. *Nat Rev Mol Cell Biol* **9**, 402-12 (2008).

216. Gatz, S.A. & Wiesmuller, L. p53 in recombination and repair. *Cell Death Differ* **13**, 1003-16 (2006).

217. Demonacos, C. & La Thangue, N.B. Drug discovery and the p53 family. *Prog Cell Cycle Res* **5**, 375-82 (2003).

218. Feng, Z., Hu, W., Rajagopal, G. & Levine, A.J. The tumor suppressor p53: cancer and aging. *Cell Cycle* **7**, 842-7 (2008).

219. Tong, Z., Singh, G. & Rainbow, A.J. The role of the p53 tumor suppressor in the response of human cells to photofrin-mediated photodynamic therapy. *Photochem Photobiol* **71**, 201-10 (2000).

220. Fisher, A.M., Ferrario, A., Rucker, N., Zhang, S. & Gomer, C.J. Photodynamic therapy sensitivity is not altered in human tumor cells after abrogation of p53 function. *Cancer Res* **59**, 331-5 (1999).

221. Kannabiran, C., Morris, G.F. & Mathews, M.B. Dual action of the adenovirus E1A 243R oncoprotein on the human proliferating cell nuclear antigen promoter: repression of transcriptional activation by p53. *Oncogene* **18**, 7825-33 (1999).

222. Banks, D., Wu, M., Higa, L.A., Gavrilova, N., Quan, J., Ye, T., Kobayashi, R., Sun, H. & Zhang, H. L2DTL/CDT2 and PCNA interact with p53 and regulate p53 polyubiquitination and protein stability through MDM2 and CUL4A/DDB1 complexes. *Cell Cycle* **5**, 1719-29 (2006).

223. Moldovan, G.L., Pfander, B. & Jentsch, S. PCNA, the maestro of the replication fork. *Cell* **129**, 665-79 (2007).

224. Akramiene, D., Aleksandraviciene, C., Grazeliene, G., Zalinkevicius, R., Suziedelis, K., Didziapetriene, J., Simonsen, U., Stankevicius, E. & Kevelaitis, E. Potentiating effect of beta-glucans on photodynamic therapy of implanted cancer cells in mice. *Tohoku J Exp Med* **220**, 299-306 (2010).

225. Uehara, M., Inokuchi, T., Sano, K., Sekine, J. & Ikeda, H. Cell kinetics of mouse tumour subjected to photodynamic therapy--evaluation by proliferating cell nuclear antigen immunohistochemistry. *Oral Oncol* **35**, 93-7 (1999).

226. Uehara, M., Inokuchi, T., Tobita, T., Ohba, S. & Asahina, I. Expression of heat shock protein 47 in the fibrous tissue adjacent to mouse tumour subjected to photodynamic therapy. *Oral Oncol* **43**, 804-10 (2007).

227. Dhanasekaran, D.N. & Reddy, E.P. JNK signaling in apoptosis. *Oncogene* **27**, 6245-51 (2008).

228. Wu, G.S. The functional interactions between the p53 and MAPK signaling pathways. *Cancer Biol Ther* **3**, 156-61 (2004).

229. Tafolla, E., Wang, S., Wong, B., Leong, J. & Kapila, Y.L. JNK1 and JNK2 oppositely regulate p53 in signaling linked to apoptosis triggered by an altered fibronectin matrix: JNK links FAK and p53. *J Biol Chem* **280**, 19992-9 (2005).

230. Hayakawa, J., Depatie, C., Ohmichi, M. & Mercola, D. The activation of c-Jun NH2-terminal kinase (JNK) by DNA-damaging agents serves to promote drug resistance via activating transcription factor 2 (ATF2)-dependent enhanced DNA repair. *J Biol Chem* **278**, 20582-92 (2003).

231. Topisirovic, I., Gutierrez, G.J., Chen, M., Appella, E., Borden, K.L. & Ronai, Z.A. Control of p53 multimerization by Ubc13 is JNK-regulated. *Proc Natl Acad Sci U S A* **106**, 12676-81 (2009).

232. Christmann, M., Tomicic, M.T., Aasland, D. & Kaina, B. A role for UV-light-induced c-Fos: Stimulation of nucleotide excision repair and protection against sustained JNK activation and apoptosis. *Carcinogenesis* **28**, 183-90 (2007).

233. Hsieh, Y.J., Wu, C.C., Chang, C.J. & Yu, J.S. Subcellular localization of Photofrin determines the death phenotype of human epidermoid carcinoma A431 cells triggered by photodynamic therapy: when plasma membranes are the main targets. *J Cell Physiol* **194**, 363-75 (2003).

234. Assefa, Z., Vantieghem, A., Declercq, W., Vandenabeele, P., Vandenheede, J.R., Merlevede, W., de Witte, P. & Agostinis, P. The activation of the c-Jun N-terminal kinase and p38 mitogen-activated protein kinase signaling pathways protects HeLa cells from apoptosis following photodynamic therapy with hypericin. *J Biol Chem* **274**, 8788-96 (1999).

235. Okuwaki, M. The structure and functions of NPM1/Nucleophsmin/B23, a multifunctional nucleolar acidic protein. *J Biochem* **143**, 441-8 (2008).

236. Wu, M.H., Chang, J.H. & Yung, B.Y. Resistance to UV-induced cell-killing in nucleophosmin/B23 over-expressed NIH 3T3 fibroblasts: enhancement of DNA repair and up-regulation of PCNA in association with nucleophosmin/B23 over-expression. *Carcinogenesis* **23**, 93-100 (2002).

237. Latonen, L. & Laiho, M. Cellular UV damage responses--functions of tumor suppressor p53. *Biochim Biophys Acta* **1755**, 71-89 (2005).

238. Colombo, E., Marine, J.C., Danovi, D., Falini, B. & Pelicci, P.G. Nucleophosmin regulates the stability and transcriptional activity of p53. *Nat Cell Biol* **4**, 529-33 (2002).

239. Chan, H.J., Weng, J.J. & Yung, B.Y. Nucleophosmin/B23-binding peptide inhibits tumor growth and up-regulates transcriptional activity of p53. *Biochem Biophys Res Commun* **333**, 396-403 (2005).

240. Kurki, S., Peltonen, K., Latonen, L., Kiviharju, T.M., Ojala, P.M., Meek, D. & Laiho, M. Nucleolar protein NPM interacts with HDM2 and protects tumor suppressor protein p53 from HDM2-mediated degradation. *Cancer Cell* **5**, 465-75 (2004).

241. Bertwistle, D., Sugimoto, M. & Sherr, C.J. Physical and functional interactions of the Arf tumor suppressor protein with nucleophosmin/B23. *Mol Cell Biol* **24**, 985-96 (2004).

242. Li, J., Zhang, X., Sejas, D.P., Bagby, G.C. & Pang, Q. Hypoxia-induced nucleophosmin protects cell death through inhibition of p53. *J Biol Chem* **279**, 41275-9 (2004).

243. Bobola, M.S., Blank, A., Berger, M.S., Stevens, B.A. & Silber, J.R. Apurinic/apyrimidinic endonuclease activity is elevated in human adult gliomas. *Clin Cancer Res* **7**, 3510-8 (2001).

244. Wyatt, M.D. & Pittman, D.L. Methylating agents and DNA repair responses: Methylated bases and sources of strand breaks. *Chem Res Toxicol* **19**, 1580-94 (2006).

245. Konat, G.W. H2O2-induced higher order chromatin degradation: a novel mechanism of oxidative genotoxicity. *J Biosci* **28**, 57-60 (2003).

246. Wu, D.Y., Ugozzoli, L., Pal, B.K., Qian, J. & Wallace, R.B. The effect of temperature and oligonucleotide primer length on the specificity and efficiency of amplification by the polymerase chain reaction. *DNA Cell Biol* **10**, 233-8 (1991).

247. Gietz, R.D. & Schiestl, R.H. Applications of high efficiency lithium acetate transformation of intact yeast cells using single-stranded nucleic acids as carrier. *Yeast* **7**, 253-63 (1991).

248. Hill, J., Donald, K.A. & Griffiths, D.E. DMSO-enhanced whole cell yeast transformation. *Nucleic Acids Res* **19**, 5791 (1991).

249. Gietz, D., St Jean, A., Woods, R.A. & Schiestl, R.H. Improved method for high efficiency transformation of intact yeast cells. *Nucleic Acids Res* **20**, 1425 (1992).

250. West, R.W., Jr., Yocum, R.R. & Ptashne, M. Saccharomyces cerevisiae GAL1-GAL10 divergent promoter region: location and function of the upstream activating sequence UASG. *Mol Cell Biol* **4**, 2467-78 (1984).

251. Giniger, E., Varnum, S.M. & Ptashne, M. Specific DNA binding of GAL4, a positive regulatory protein of yeast. *Cell* **40**, 767-74 (1985).

252. Lundin, C., North, M., Erixon, K., Walters, K., Jenssen, D., Goldman, A.S. & Helleday, T. Methyl methanesulfonate (MMS) produces heat-labile DNA damage but no detectable in vivo DNA double-strand breaks. *Nucleic Acids Res* **33**, 3799-811 (2005).

253. Haase, S.B. & Reed, S.I. Improved flow cytometric analysis of the budding yeast cell cycle. *Cell Cycle* **1**, 132-6 (2002).

254. Roth, B.L., Poot, M., Yue, S.T. & Millard, P.J. Bacterial viability and antibiotic susceptibility testing with SYTOX green nucleic acid stain. *Appl Environ Microbiol* **63**, 2421-31 (1997).

255. Rieseberg, M., Kasper, C., Reardon, K.F. & Scheper, T. Flow cytometry in biotechnology. *Appl Microbiol Biotechnol* **56**, 350-60 (2001).

256. Krokan, H.E., Standal, R. & Slupphaug, G. DNA glycosylases in the base excision repair of DNA. *Biochem J* **325 (Pt 1)**, 1-16 (1997).

257. Bruner, S.D., Norman, D.P. & Verdine, G.L. Structural basis for recognition and repair of the endogenous mutagen 8-oxoguanine in DNA. *Nature* **403**, 859-66 (2000).

258. Savas, S., Kim, D.Y., Ahmad, M.F., Shariff, M. & Ozcelik, H. Identifying functional genetic variants in DNA repair pathway using protein conservation analysis. *Cancer Epidemiol Biomarkers Prev* **13**, 801-7 (2004).

259. Cooper, G.M. & Hausman, R.E. *The cell : a molecular approach*, xx, 713 p. (ASM Press ; Sinauer Associates, Washington, D.C. Sunderland, Mass., 2004).

260. Eide, L., Luna, L., Gustad, E.C., Henderson, P.T., Essigmann, J.M., Demple, B. & Seeberg, E. Human endonuclease III acts preferentially on DNA damage opposite guanine residues in DNA. *Biochemistry* **40**, 6653-9 (2001).

261. Robertson, A.B., Klungland, A., Rognes, T. & Leiros, I. DNA repair in mammalian cells: Base excision repair: the long and short of it. *Cell Mol Life Sci* **66**, 981-93 (2009).

262. Porro, D. & Srienc, F. Tracking of individual cell cohorts in asynchronous Saccharomyces cerevisiae populations. *Biotechnol Prog* **11**, 342-7 (1995).

263. Hampsey, M. A review of phenotypes in Saccharomyces cerevisiae. *Yeast* **13**, 1099-133 (1997).

264. Chang, Y.F., Imam, J.S. & Wilkinson, M.F. The nonsense-mediated decay RNA surveillance pathway. *Annu Rev Biochem* **76**, 51-74 (2007).

265. Hanna, M., Chow, B.L., Morey, N.J., Jinks-Robertson, S., Doetsch, P.W. & Xiao, W. Involvement of two endonuclease III homologs in the base excision repair pathway for the processing of DNA alkylation damage in Saccharomyces cerevisiae. *DNA Repair (Amst)* **3**, 51-9 (2004).

266. Yang, N., Chaudhry, M.A. & Wallace, S.S. Base excision repair by hNTH1 and hOGG1: a two edged sword in the processing of DNA damage in gamma-irradiated human cells. *DNA Repair (Amst)* **5**, 43-51 (2006).

267. Chang, M., Bellaoui, M., Boone, C. & Brown, G.W. A genome-wide screen for methyl methanesulfonate-sensitive mutants reveals genes required for S phase progression in the presence of DNA damage. *Proc Natl Acad Sci U S A* **99**, 16934-9 (2002).

268. Hu, J., de Souza-Pinto, N.C., Haraguchi, K., Hogue, B.A., Jaruga, P., Greenberg, M.M., Dizdaroglu, M. & Bohr, V.A. Repair of formamidopyrimidines in DNA involves different glycosylases: role of the OGG1, NTH1, and NEIL1 enzymes. *J Biol Chem* **280**, 40544-51 (2005).

269. Luna, L., Bjoras, M., Hoff, E., Rognes, T. & Seeberg, E. Cell-cycle regulation, intracellular sorting and induced overexpression of the human NTH1 DNA glycosylase involved in removal of formamidopyrimidine residues from DNA. *Mutat Res* **460**, 95-104 (2000).

270. Ocampo-Hafalla, M.T., Altamirano, A., Basu, A.K., Chan, M.K., Ocampo, J.E., Cummings, A., Jr., Boorstein, R.J., Cunningham, R.P. & Teebor, G.W. Repair of thymine glycol by hNth1 and hNeil1 is modulated by base pairing and cis-trans epimerization. *DNA Repair (Amst)* **5**, 444-54 (2006).

271. Melo, R.G., Leitao, A.C. & Padula, M. Role of OGG1 and NTG2 in the repair of oxidative DNA damage and mutagenesis induced by hydrogen peroxide in Saccharomyces cerevisiae: relationships with transition metals iron and copper. *Yeast* **21**, 991-1003 (2004).

272. Flattery-O'Brien, J.A. & Dawes, I.W. Hydrogen peroxide causes RAD9-dependent cell cycle arrest in G2 in Saccharomyces cerevisiae whereas menadione causes G1 arrest independent of RAD9 function. *J Biol Chem* **273**, 8564-71 (1998).

273. Clopton, D.A. & Saltman, P. Low-level oxidative stress causes cell-cycle specific arrest in cultured cells. *Biochem Biophys Res Commun* **210**, 189-96 (1995).

274. Wharton, W. Cell cycle constraints on peroxide- and radiation-induced inhibitory checkpoints. *Cancer Res* **55**, 5069-74 (1995).

275. Lam, K. & Timmerman, H. Yeast as a screening tool. *Drug Discov Today* **2**, 187-92 (2005).

276. Hilt, W. Targets of programmed destruction: a primer to regulatory proteolysis in yeast. *Cell Mol Life Sci* **61**, 1615-32 (2004).

277. Tsukuda, T., Fleming, A.B., Nickoloff, J.A. & Osley, M.A. Chromatin remodelling at a DNA double-strand break site in Saccharomyces cerevisiae. *Nature* **438**, 379-83 (2005).

278. Aggarwal, M. & Brosh, R.M., Jr. Genetic studies of human DNA repair proteins using yeast as a model system. *J Vis Exp* (2010).

279. Parsons, A.B., Geyer, R., Hughes, T.R. & Boone, C. Yeast genomics and proteomics in drug discovery and target validation. *Prog Cell Cycle Res* **5**, 159-66 (2003).

280. Botstein, D., Chervitz, S.A. & Cherry, J.M. Yeast as a model organism. *Science* **277**, 1259-60 (1997).

281. Kataoka, T., Powers, S., Cameron, S., Fasano, O., Goldfarb, M., Broach, J. & Wigler, M. Functional homology of mammalian and yeast RAS genes. *Cell* **40**, 19-26 (1985).

282. Baudin, A., Ozier-Kalogeropoulos, O., Denouel, A., Lacroute, F. & Cullin, C. A simple and efficient method for direct gene deletion in Saccharomyces cerevisiae. *Nucleic Acids Res* **21**, 3329-30 (1993).

283. Damia, G. & D'Incalci, M. Targeting DNA repair as a promising approach in cancer therapy. *Eur J Cancer* **43**, 1791-801 (2007).

284. Zhu, Y., Hu, J., Hu, Y. & Liu, W. Targeting DNA repair pathways: a novel approach to reduce cancer therapeutic resistance. *Cancer Treat Rev* **35**, 590-6 (2009).

285. Bernstein, M. & Berger, M.S. *Neuro-oncology : the essentials*, xvii, 477 p. (Thieme, New York, 2008).

286. Nowis, D., Makowski, M., Stoklosa, T., Legat, M., Issat, T. & Golab, J. Direct tumor damage mechanisms of photodynamic therapy. *Acta Biochim Pol* **52**, 339-52 (2005).

287. Au, C.M., Luk, S.K., Jackson, C.J., Ng, H.K., Yow, C.M. & To, S.S. Differential effects of photofrin, 5-aminolevulinic acid and calphostin C on glioma cells. *J Photochem Photobiol B* **85**, 92-101 (2006).

288. Dhawan, A., Bajpayee, M. & Parmar, D. Comet assay: a reliable tool for the assessment of DNA damage in different models. *Cell Biol Toxicol* **25**, 5-32 (2009).

289. Collins, A.R., Oscoz, A.A., Brunborg, G., Gaivao, I., Giovannelli, L., Kruszewski, M., Smith, C.C. & Stetina, R. The comet assay: topical issues. *Mutagenesis* **23**, 143-51 (2008).

290. Speit, G. & Hartmann, A. The comet assay (single-cell gel test). A sensitive genotoxicity test for the detection of DNA damage and repair. *Methods Mol Biol* **113**, 203-12 (1999).

291. Olive, P.L. DNA damage and repair in individual cells: applications of the comet assay in radiobiology. *Int J Radiat Biol* **75**, 395-405 (1999).

292. Tice, R.R., Agurell, E., Anderson, D., Burlinson, B., Hartmann, A., Kobayashi, H., Miyamae, Y., Rojas, E., Ryu, J.C. & Sasaki, Y.F. Single cell gel/comet assay: guidelines for in vitro and in vivo genetic toxicology testing. *Environ Mol Mutagen* **35**, 206-21 (2000).

293. Collins, A.R. The comet assay for DNA damage and repair: principles, applications, and limitations. *Mol Biotechnol* **26**, 249-61 (2004).

294. Collins, A.R. The comet assay. Principles, applications, and limitations. *Methods Mol Biol* **203**, 163-77 (2002).

295. Moller, P. Assessment of reference values for DNA damage detected by the comet assay in human blood cell DNA. *Mutat Res* **612**, 84-104 (2006).

296. Collins, A.R., Dobson, V.L., Dusinska, M., Kennedy, G. & Stetina, R. The comet assay: what can it really tell us? *Mutat Res* **375**, 183-93 (1997).

297. Collins, A.R., Duthie, S.J. & Dobson, V.L. Direct enzymic detection of endogenous oxidative base damage in human lymphocyte DNA. *Carcinogenesis* **14**, 1733-5 (1993).

298. Chomczynski, P. & Sacchi, N. Single-step method of RNA isolation by acid guanidinium thiocyanate-phenol-chloroform extraction. *Anal Biochem* **162**, 156-9 (1987).

299. Giulietti, A., Overbergh, L., Valckx, D., Decallonne, B., Bouillon, R. & Mathieu, C. An overview of real-time quantitative PCR: applications to quantify cytokine gene expression. *Methods* **25**, 386-401 (2001).

300. Kricka, L.J. Stains, labels and detection strategies for nucleic acids assays. *Ann Clin Biochem* **39**, 114-29 (2002).

301. Schefe, J.H., Lehmann, K.E., Buschmann, I.R., Unger, T. & Funke-Kaiser, H. Quantitative real-time RT-PCR data analysis: current concepts and the novel "gene expression's CT difference" formula. *J Mol Med* **84**, 901-10 (2006).

302. Arya, M., Shergill, I.S., Williamson, M., Gommersall, L., Arya, N. & Patel, H.R. Basic principles of real-time quantitative PCR. *Expert Rev Mol Diagn* **5**, 209-19 (2005).

303. Dorak, M.T. Real-time PCR. xxvi, 333 p. (Taylor & Francis, New York, NY, 2006).

304. Uprichard, S.L. The therapeutic potential of RNA interference. *FEBS Lett* **579**, 5996-6007 (2005).

305. Aagaard, L. & Rossi, J.J. RNAi therapeutics: principles, prospects and challenges. *Adv Drug Deliv Rev* **59**, 75-86 (2007).

306. Zhang, J. & Hua, Z.C. Targeted gene silencing by small interfering RNA-based knock-down technology. *Curr Pharm Biotechnol* **5**, 1-7 (2004).

307. Paul, C.P., Good, P.D., Winer, I. & Engelke, D.R. Effective expression of small interfering RNA in human cells. *Nat Biotechnol* **20**, 505-8 (2002).

308. Lu, P.Y., Xie, F. & Woodle, M.C. In vivo application of RNA interference: from functional genomics to therapeutics. *Adv Genet* **54**, 117-42 (2005).

309. Ren, B. & Dynlacht, B.D. Use of chromatin immunoprecipitation assays in genome-wide location analysis of mammalian transcription factors. *Methods Enzymol* **376**, 304-15 (2004).

310. Lutfalla, G. & Uze, G. Performing quantitative reverse-transcribed polymerase chain reaction experiments. *Methods Enzymol* **410**, 386-400 (2006).

311. Cheadle, C., Fan, J., Cho-Chung, Y.S., Werner, T., Ray, J., Do, L., Gorospe, M. & Becker, K.G. Stability regulation of mRNA and the control of gene expression. *Ann N Y Acad Sci* **1058**, 196-204 (2005).

312. Atwater, J.A., Wisdom, R. & Verma, I.M. Regulated mRNA stability. *Annu Rev Genet* **24**, 519-41 (1990).

313. Sobell, H.M. Actinomycin and DNA transcription. *Proc Natl Acad Sci U S A* **82**, 5328-31 (1985).

314. Zhao, X., Aldini, G., Johnson, E.J., Rasmussen, H., Kraemer, K., Woolf, H., Musaeus, N., Krinsky, N.I., Russell, R.M. & Yeum, K.J. Modification of lymphocyte DNA damage by carotenoid supplementation in postmenopausal women. *Am J Clin Nutr* **83**, 163-9 (2006).

315. Zhao, H., Traganos, F. & Darzynkiewicz, Z. Phosphorylation of p53 on Ser15 during cell cycle caused by Topo I and Topo II inhibitors in relation to ATM and Chk2 activation. *Cell Cycle* **7**, 3048-55 (2008).

316. Filion, T.M., Qiao, M., Ghule, P.N., Mandeville, M., van Wijnen, A.J., Stein, J.L., Lian, J.B., Altieri, D.C. & Stein, G.S. Survival responses of human embryonic stem cells to DNA damage. *J Cell Physiol* **220**, 586-92 (2009).

317. Xu, Y., Zhou, Z., Yang, H. & Zhang, Z. Raman spectroscopic study of microcosmic photodamage of the space structure of DNA sensitized by Yangzhou haematoporphyrin derivative and Photofrin II. *J Photochem Photobiol B* **52**, 30-4 (1999).

318. Egyeki, M., Toth, K., Waldeck, W., Schmezer, P., Langowski, J. & Csik, G. DNA damaging capability of hematoporphyrin towards DNAs of various accessibilities. *J Photochem Photobiol B* **84**, 119-27 (2006).

319. Penning, L.C., Lagerberg, J.W., VanDierendonck, J.H., Cornelisse, C.J., Dubbelman, T.M. & VanSteveninck, J. The role of DNA damage and inhibition of poly(ADP-ribosyl)ation in loss of clonogenicity of murine L929 fibroblasts, caused by photodynamically induced oxidative stress. *Cancer Res* **54**, 5561-7 (1994).

320. Gupta, S., Dwarakanath, B.S., Muralidhar, K. & Jain, V. Cellular uptake, localization and photodynamic effects of haematoporphyrin derivative in human glioma and squamous carcinoma cell lines. *J Photochem Photobiol B* **69**, 107-20 (2003).

321. McNair, F.I., Marples, B., West, C.M. & Moore, J.V. A comet assay of DNA damage and repair in K562 cells after photodynamic therapy using haematoporphyrin derivative, methylene blue and meso-tetrahydroxyphenylchlorin. *Br J Cancer* **75**, 1721-9 (1997).

322. Kvam, E., Stokke, T., Moan, J. & Steen, H.B. Plateau distributions of DNA fragment lengths produced by extended light exposure of extranuclear photosensitizers in human cells. *Nucleic Acids Res* **20**, 6687-93 (1992).

323. Moan, J., Berg, K. & Kvam, E. Effects of photodynamic treatment on DNA and DNA-related cell functions. in *Photodynamic therapy of neoplastic disease* (ed. Kessel, D.) 197-209 (CRC Press, Boston, 1990).

324. Rousset, N., Keminon, E., Eleouet, S., Le Neel, T., Auget, J.L., Vonarx, V., Carre, J., Lajat, Y. & Patrice, T. Use of alkaline Comet assay to assess DNA repair after m-THPC-PDT. *J Photochem Photobiol B* **56**, 118-31 (2000).

325. Saczko, J., Mazurkiewicz, M., Chwilkowska, A., Kulbacka, J., Kramer, G., Lugowski, M., Snietura, M. & Banas, T. Intracellular distribution of Photofrin in malignant and normal endothelial cell lines. *Folia Biol (Praha)* **53**, 7-12 (2007).

326. Evensen, J.F. & Moan, J. Photodynamic action and chromosomal damage: a comparison of haematoporphyrin derivative (HpD) and light with X-irradiation. *Br J Cancer* **45**, 456-65 (1982).

327. Prakash, S., Johnson, R.E. & Prakash, L. Eukaryotic translesion synthesis DNA polymerases: specificity of structure and function. *Annu Rev Biochem* **74**, 317-53 (2005).

328. Lee, D.H., Jin, S.G., Cai, S., Chen, Y., Pfeifer, G.P. & O'Connor, T.R. Repair of methylation damage in DNA and RNA by mammalian AlkB homologues. *J Biol Chem* **280**, 39448-59 (2005).

329. Ringvoll, J., Moen, M.N., Nordstrand, L.M., Meira, L.B., Pang, B., Bekkelund, A., Dedon, P.C., Bjelland, S., Samson, L.D., Falnes, P.O. & Klungland, A. AlkB homologue 2-mediated repair of ethenoadenine lesions in mammalian DNA. *Cancer Res* **68**, 4142-9 (2008).

330. Cetica, V., Genitori, L., Giunti, L., Sanzo, M., Bernini, G., Massimino, M. & Sardi, I. Pediatric brain tumors: mutations of two dioxygenases (hABH2 and hABH3) that directly repair alkylation damage. *J Neurooncol* **94**, 195-201 (2009).

331. Fisher, A.M., Danenberg, K., Banerjee, D., Bertino, J.R., Danenberg, P. & Gomer, C.J. Increased photosensitivity in HL60 cells expressing wild-type p53. *Photochem Photobiol* **66**, 265-70 (1997).

332. Fisher, A.M., Rucker, N., Wong, S. & Gomer, C.J. Differential photosensitivity in wild-type and mutant p53 human colon carcinoma cell lines. *J Photochem Photobiol B* **42**, 104-7 (1998).

333. Xie, Y., Wei, Z.B., Zhang, Z., Wen, W. & Huang, G.W. Effect of 5-ALA-PDT on VEGF and PCNA expression in human NPC-bearing nude mice. *Oncol Rep* **22**, 1365-71 (2009).

334. Almeida, R.D., Manadas, B.J., Carvalho, A.P. & Duarte, C.B. Intracellular signaling mechanisms in photodynamic therapy. *Biochim Biophys Acta* **1704**, 59-86 (2004).

335. Chan, P.S., Koon, H.K., Wu, Z.G., Wong, R.N., Lung, M.L., Chang, C.K. & Mak, N.K. Role of p38 MAPKs in hypericin photodynamic therapy-induced apoptosis of nasopharyngeal carcinoma cells. *Photochem Photobiol* **85**, 1207-17 (2009).

336. Tong, Z., Singh, G., Valerie, K. & Rainbow, A.J. Activation of the stress-activated JNK and p38 MAP kinases in human cells by Photofrin-mediated photodynamic therapy. *J Photochem Photobiol B* **71**, 77-85 (2003).

337. Weyergang, A., Kaalhus, O. & Berg, K. Photodynamic therapy with an endocytically located photosensitizer cause a rapid activation of the mitogen-activated protein kinases extracellular signal-regulated kinase, p38, and c-Jun NH2 terminal kinase with opposing effects on cell survival. *Mol Cancer Ther* **7**, 1740-50 (2008).

338. Fritz, G. & Kaina, B. Late activation of stress kinases (SAPK/JNK) by genotoxins requires the DNA repair proteins DNA-PKcs and CSB. *Mol Biol Cell* **17**, 851-61 (2006).

339. Shimada, K., Nakamura, M., Anai, S., De Velasco, M., Tanaka, M., Tsujikawa, K., Ouji, Y. & Konishi, N. A novel human AlkB homologue, ALKBH8, contributes to human bladder cancer progression. *Cancer Res* **69**, 3157-64 (2009).

340. Xu, Y., Porntadavity, S. & St Clair, D.K. Transcriptional regulation of the human manganese superoxide dismutase gene: the role of specificity protein 1 (Sp1) and activating protein-2 (AP-2). *Biochem J* **362**, 401-12 (2002).

341. Dhar, S.K., Lynn, B.C., Daosukho, C. & St Clair, D.K. Identification of nucleophosmin as an NF-kappaB co-activator for the induction of the human SOD2 gene. *J Biol Chem* **279**, 28209-19 (2004).

342. Dhar, S.K., Xu, Y., Chen, Y. & St Clair, D.K. Specificity protein 1-dependent p53-mediated suppression of human manganese superoxide dismutase gene expression. *J Biol Chem* **281**, 21698-709 (2006).

343. Hoeijmakers, J.H. DNA damage, aging, and cancer. *N Engl J Med* **361**, 1475-85 (2009).

344. Kuptsova, N., Kopecky, K.J., Godwin, J., Anderson, J., Hoque, A., Willman, C.L., Slovak, M.L. & Ambrosone, C.B. Polymorphisms in DNA repair genes and therapeutic outcomes of AML patients from SWOG clinical trials. *Blood* **109**, 3936-44 (2007).

345. McKean-Cowdin, R., Barnholtz-Sloan, J., Inskip, P.D., Ruder, A.M., Butler, M., Rajaraman, P., Razavi, P., Patoka, J., Wiencke, J.K., Bondy, M.L. & Wrensch, M. Associations between polymorphisms in DNA repair genes and glioblastoma. *Cancer Epidemiol Biomarkers Prev* **18**, 1118-26 (2009).

346. Clarkson, S.G. & Wood, R.D. Polymorphisms in the human XPD (ERCC2) gene, DNA repair capacity and cancer susceptibility: an appraisal. *DNA Repair (Amst)* **4**, 1068-74 (2005).

347. Michiels, S., Danoy, P., Dessen, P., Bera, A., Boulet, T., Bouchardy, C., Lathrop, M., Sarasin, A. & Benhamou, S. Polymorphism discovery in 62 DNA repair genes and haplotype associations with risks for lung and head and neck cancers. *Carcinogenesis* **28**, 1731-9 (2007).

348. Henriette Tanja, L., Guchelaar, H.J. & Gelderblom, H. Pharmacogenetics in chemotherapy of colorectal cancer. *Best Pract Res Clin Gastroenterol* **23**, 257-73 (2009).

349. Monzo, M., Navarro, A., Ferrer, G. & Artells, R. Pharmacogenomics: a tool for improving cancer chemotherapy. *Clin Transl Oncol* **10**, 628-37 (2008).

350. Camps, C., Sarries, C., Roig, B., Sanchez, J.J., Queralt, C., Sancho, E., Martinez, N., Taron, M. & Rosell, R. Assessment of nucleotide excision repair XPD polymorphisms in the peripheral blood of gemcitabine/cisplatin-treated advanced non-small-cell lung cancer patients. *Clin Lung Cancer* **4**, 237-41 (2003).

351. Consortium, I.H. A haplotype map of the human genome. *Nature* **437**, 1299-320 (2005).

352. Rajaraman, P., Hutchinson, A., Wichner, S., Black, P.M., Fine, H.A., Loeffler, J.S., Selker, R.G., Shapiro, W.R., Rothman, N., Linet, M.S. & Inskip, P.D. DNA repair gene polymorphisms and risk of adult meningioma, glioma, and acoustic neuroma. *Neuro Oncol* **12**, 37-48 (2010).

353. Liu, Y., Shete, S., Etzel, C.J., Scheurer, M., Alexiou, G., Armstrong, G., Tsavachidis, S., Liang, F.W., Gilbert, M., Aldape, K., Armstrong, T., Houlston, R., Hosking, F., Robertson, L., Xiao, Y., Wiencke, J., Wrensch, M., Andersson, U., Melin, B.S. & Bondy, M. Polymorphisms of LIG4, BTBD2, HMGA2, and RTEL1 genes involved in the double-strand break repair pathway predict glioblastoma survival. *J Clin Oncol* **28**, 2467-74 (2010).

354. Savas, S., Taylor, I.W., Wrana, J.L. & Ozcelik, H. Functional nonsynonymous single nucleotide polymorphisms from the TGF-beta protein interaction network. *Physiol Genomics* **29**, 109-17 (2007).

355. Cargill, M., Altshuler, D., Ireland, J., Sklar, P., Ardlie, K., Patil, N., Shaw, N., Lane, C.R., Lim, E.P., Kalyanaraman, N., Nemesh, J., Ziaugra, L., Friedland, L., Rolfe, A., Warrington, J., Lipshutz, R., Daley, G.Q. & Lander, E.S. Characterization of single-nucleotide polymorphisms in coding regions of human genes. *Nat Genet* **22**, 231-8 (1999).

356. Ramensky, V., Bork, P. & Sunyaev, S. Human non-synonymous SNPs: server and survey. *Nucleic Acids Res* **30**, 3894-900 (2002).

357. Ryan, M., Diekhans, M., Lien, S., Liu, Y. & Karchin, R. LS-SNP/PDB: annotated non-synonymous SNPs mapped to Protein Data Bank structures. *Bioinformatics* **25**, 1431-2 (2009).

358. Bauer-Mehren, A., Furlong, L.I., Rautschka, M. & Sanz, F. From SNPs to pathways: integration of functional effect of sequence variations on models of cell signalling pathways. *BMC Bioinformatics* **10 Suppl 8**, S6 (2009).

359. Bromberg, Y. & Rost, B. Correlating protein function and stability through the analysis of single amino acid substitutions. *BMC Bioinformatics* **10 Suppl 8**, S8 (2009).

360. Hall, I. Candidate gene studies in respiratory disease: avoiding the pitfalls. *Thorax* **57**, 377-8 (2002).

361. Berquist, B.R., Singh, D.K., Fan, J., Kim, D., Gillenwater, E., Kulkarni, A., Bohr, V.A., Ackerman, E.J., Tomkinson, A.E. & Wilson, D.M., 3rd. Functional capacity of XRCC1 protein variants identified in DNA repair-deficient Chinese hamster ovary cell lines and the human population. *Nucleic Acids Res* (2010).

362. Jeong, H., Herskowitz, I., Kroetz, D.L. & Rine, J. Function-altering SNPs in the human multidrug transporter gene ABCB1 identified using a Saccharomyces-based assay. *PLoS Genet* **3**, e39 (2007).

363. Warbrick, E. A functional analysis of PCNA-binding peptides derived from protein sequence, interaction screening and rational design. *Oncogene* **25**, 2850-9 (2006).

364. Ooi, S.L., Pan, X., Peyser, B.D., Ye, P., Meluh, P.B., Yuan, D.S., Irizarry, R.A., Bader, J.S., Spencer, F.A. & Boeke, J.D. Global synthetic-lethality analysis and yeast functional profiling. *Trends Genet* **22**, 56-63 (2006).

365. Takahashi, M., Shimodaira, H., Andreutti-Zaugg, C., Iggo, R., Kolodner, R.D. & Ishioka, C. Functional analysis of human MLH1 variants using yeast and in vitro mismatch repair assays. *Cancer Res* **67**, 4595-604 (2007).

366. Blumenthal, R.D., Leone, E., Goldenberg, D.M., Rodriguez, M. & Modrak, D. An in vitro model to optimize dose scheduling of multimodal radioimmunotherapy and chemotherapy: effects of p53 expression. *Int J Cancer* **108**, 293-300 (2004).

367. Redmond, K.M., Wilson, T.R., Johnston, P.G. & Longley, D.B. Resistance mechanisms to cancer chemotherapy. *Front Biosci* **13**, 5138-54 (2008).

368. Helleday, T. Homologous recombination in cancer development, treatment and development of drug resistance. *Carcinogenesis* **31**, 955-60 (2010).

369. Plummer, R., Jones, C., Middleton, M., Wilson, R., Evans, J., Olsen, A., Curtin, N., Boddy, A., McHugh, P., Newell, D., Harris, A., Johnson, P., Steinfeldt, H., Dewji, R., Wang, D., Robson, L. & Calvert, H. Phase I study of the poly(ADP-ribose) polymerase inhibitor, AG014699, in combination with temozolomide in patients with advanced solid tumors. *Clin Cancer Res* **14**, 7917-23 (2008).

370. McHugh, P.J., Spanswick, V.J. & Hartley, J.A. Repair of DNA interstrand crosslinks: molecular mechanisms and clinical relevance. *Lancet Oncol* **2**, 483-90 (2001).

371. Helleday, T., Petermann, E., Lundin, C., Hodgson, B. & Sharma, R.A. DNA repair pathways as targets for cancer therapy. *Nat Rev Cancer* **8**, 193-204 (2008).

372. Liu, X., Wang, Y., Benaissa, S., Matsuda, A., Kantarjian, H., Estrov, Z. & Plunkett, W. Homologous recombination as a resistance mechanism to replication-induced double-strand breaks caused by the anti-leukemia agent, CNDAC. *Blood* **116**, 1737-46 (2010).

373. Eljamel, M.S., Goodman, C. & Moseley, H. ALA and Photofrin fluorescence-guided resection and repetitive PDT in glioblastoma multiforme: a single centre Phase III randomised controlled trial. *Lasers Med Sci* **23**, 361-7 (2008).

374. Korbelik, M. & Cecic, I. Complement activation cascade and its regulation: relevance for the response of solid tumors to photodynamic therapy. *J Photochem Photobiol B* **93**, 53-9 (2008).

375. Liu, W., Baer, M.R., Bowman, M.J., Pera, P., Zheng, X., Morgan, J., Pandey, R.A. & Oseroff, A.R. The tyrosine kinase inhibitor imatinib mesylate enhances the efficacy of photodynamic therapy by inhibiting ABCG2. *Clin Cancer Res* **13**, 2463-70 (2007).

376. Moan, J., Berg, K., Kvam, E., Western, A., Malik, Z., Ruck, A. & Schneckenburger, H. Intracellular localization of photosensitizers. *Ciba Found Symp* **146**, 95-107; discussion 107-11 (1989).

377. Haylett, A.K., Ward, T.H. & Moore, J.V. DNA damage and repair in Gorlin syndrome and normal fibroblasts after aminolevulinic acid photodynamic therapy: a comet assay study. *Photochem Photobiol* **78**, 337-41 (2003).

378. Daniels, D.S., Woo, T.T., Luu, K.X., Noll, D.M., Clarke, N.D., Pegg, A.E. & Tainer, J.A. DNA binding and nucleotide flipping by the human DNA repair protein AGT. *Nat Struct Mol Biol* **11**, 714-20 (2004).

379. Ragg, S., Xu-Welliver, M., Bailey, J., D'Souza, M., Cooper, R., Chandra, S., Seshadri, R., Pegg, A.E. & Williams, D.A. Direct reversal of DNA damage by mutant methyltransferase protein protects mice against dose-intensified chemotherapy and leads to in vivo selection of hematopoietic stem cells. *Cancer Res* **60**, 5187-95 (2000).

380. van Nifterik, K.A., van den Berg, J., van der Meide, W.F., Ameziane, N., Wedekind, L.E., Steenbergen, R.D., Leenstra, S., Lafleur, M.V., Slotman, B.J., Stalpers, L.J. & Sminia, P. Absence of the MGMT protein as well as methylation of the MGMT promoter predict the sensitivity for temozolomide. *Br J Cancer* **103**, 29-35 (2010).

381. Verbeek, B., Southgate, T.D., Gilham, D.E. & Margison, G.P. O6-Methylguanine-DNA methyltransferase inactivation and chemotherapy. *Br Med Bull* **85**, 17-33 (2008).

382. Sedgwick, B., Robins, P. & Lindahl, T. Direct removal of alkylation damage from DNA by AlkB and related DNA dioxygenases. *Methods Enzymol* **408**, 108-20 (2006).

383. Lane, D.P. Cancer. p53, guardian of the genome. *Nature* **358**, 15-6 (1992).

384. Guimaraes, D.P. & Hainaut, P. TP53: a key gene in human cancer. *Biochimie* **84**, 83-93 (2002).

385. Zawacka-Pankau, J., Krachulec, J., Grulkowski, I., Bielawski, K.P. & Selivanova, G. The p53-mediated cytotoxicity of photodynamic therapy of cancer: recent advances. *Toxicol Appl Pharmacol* **232**, 487-97 (2008).

386. Foroutan, B., Ali Ruf, A., Jerwood, D. & Anderson, D. In vitro studies of DNA damage and its repair in cells from NHL patients with different p53 mutant protein status, resistant (p53(+)) and sensitive (p53(-)) to cancer chemotherapy. *J Pharmacol Toxicol Methods* **55**, 58-64 (2007).

387. Batista, L.F., Roos, W.P., Kaina, B. & Menck, C.F. p53 mutant human glioma cells are sensitive to UV-C-induced apoptosis due to impaired cyclobutane pyrimidine dimer removal. *Mol Cancer Res* **7**, 237-46 (2009).

388. Naumann, S.C., Roos, W.P., Jost, E., Belohlavek, C., Lennerz, V., Schmidt, C.W., Christmann, M. & Kaina, B. Temozolomide- and fotemustine-induced apoptosis in human malignant melanoma cells: response related to MGMT, MMR, DSBs, and p53. *Br J Cancer* **100**, 322-33 (2009).

389. Batista, L.F., Roos, W.P., Christmann, M., Menck, C.F. & Kaina, B. Differential sensitivity of malignant glioma cells to methylating and chloroethylating anticancer drugs: p53 determines the switch by regulating xpc, ddb2, and DNA double-strand breaks. *Cancer Res* **67**, 11886-95 (2007).

390. Barberi-Heyob, M., Vedrine, P.O., Merlin, J.L., Millon, R., Abecassis, J., Poupon, M.F. & Guillemin, F. Wild-type p53 gene transfer into mutated p53 HT29 cells improves sensitivity to photodynamic therapy via induction of apoptosis. *Int J Oncol* **24**, 951-8 (2004).

391. Oren, M. Regulation of the p53 tumor suppressor protein. *J Biol Chem* **274**, 36031-4 (1999).

392. Vilborg, A., Wilhelm, M.T. & Wiman, K.G. Regulation of tumor suppressor p53 at the RNA level. *J Mol Med* **88**, 645-52 (2010).

393. Palaniswamy, V., Moraes, K.C., Wilusz, C.J. & Wilusz, J. Nucleophosmin is selectively deposited on mRNA during polyadenylation. *Nat Struct Mol Biol* **13**, 429-35 (2006).

394. Marenstein, D.R., Ocampo, M.T., Chan, M.K., Altamirano, A., Basu, A.K., Boorstein, R.J., Cunningham, R.P. & Teebor, G.W. Stimulation of human endonuclease III by Y box-binding protein 1 (DNA-binding protein B). Interaction between a base excision repair enzyme and a transcription factor. *J Biol Chem* **276**, 21242-9 (2001).

395. Sanchez-Perez, I. DNA repair inhibitors in cancer treatment. *Clin Transl Oncol* **8**, 642-6 (2006).

396. Burdak-Rothkamm, S. & Prise, K.M. New molecular targets in radiotherapy: DNA damage signalling and repair in targeted and non-targeted cells. *Eur J Pharmacol* **625**, 151-5 (2009).